



University Library

Author/Filing Title BETHELL

Class Mark T

Please note that fines are charged on ALL
overdue items.

FOR REFERENCE ONLY

0402803345



Remote measurement
of temperature using
laser induced luminescence


By
Alison Bethell
B.Eng.(hons)

A Doctoral Thesis

Submitted in partial fulfilment of the requirements for the award of
Doctor of Philosophy of Loughborough University

October 2002

© A. Bethell F.(2002)

 Loughborough University Open Access Library
Date 02 03
Class
Acc No. 0E0285334

Abstract

A technique is required to measure the temperature of rotating compressor wheels at speeds of up to 80,000rpm and within the range 100°C to 250°C. Present available methods such as emissivity cannot be used due to the substantial interference from surrounding objects, nor can thermocouples due to their affect on the airflow within the compressor. Laser induced fluorescence (LIF) has been used successfully on rotating objects, but at speeds much less than the speeds which are required for implementation on a running compressor. Previous work with LIF has related the decay time of the fluorescence with temperature, this cannot be accurately implemented at high speeds due to the short amount of time that fluorescence is available to the detector, and as such a short amount of the decay curve is collected.

The fluorescent peak positions and intensities are to be used for temperature measurement in this project. Numerous materials have been considered from which two materials showed great potential for this technique, they were Ruby and Yttrium Oxysulphide Praseodymium doped ($Y_2O_2:Pr$). Ruby has been used previously for temperature measurement, but not from rotating objects. It is shown here that this material can be used to measure temperature remotely. $Y_2O_2:Pr$ has not been used previously for temperature measurement, it has been shown in this work to have a strong relationship with temperature.

The attachment of the material to the compressor wheel has required the creation of a fluorescent paint, a technique which is presently used, and plasma coating, a technique which has not been considered previously. For Ruby powder the paint technique did not produce strong fluorescence. For $Y_2O_2:Pr$ the paint technique worked well producing a strong fluorescence signal and was shown to withstand repeated heating and cooling over a 7 hour period. The plasma coating technique produced a strong reliable fluorescence signal.

Software has been developed using LabView to enable the required information to be extracted from the spectrum and a temperature reading given out in real time.

Acknowledgements

This work has been carried out in the Mechanical Engineering Department of Loughborough University under the supervision of Dr. John Tyrer. I would like to thank all the academic and technical staff of the Mechanical Engineering department who have helped me during this work. In particular Dick Potter and Steve Hammond in the electronics workshop who have designed and built the triggering system for my rig. Dr. Dave Worrall from the Chemistry department for his help and technical input. Holset Engineering for support, advice and financial support of this work. Friends and colleagues who have helped me over the past years.

But in particular I would like to thank my Husband for his immense support, as well as his help with the programming, without whom I would not be at this stage today.

Contents

1	Introduction	1
1.1	Compressors and turbines	3
1.2	Overview of the project	4
2	Literature Survey	7
2.1	Temperature Measurement	7
2.1.1	Temperature sensitive paints	8
2.1.2	Radiation thermometry	9
2.1.3	Fibre optic thermometers	12
2.1.4	Luminescence techniques	12
2.1.5	Summary of temperature measurement techniques	14
2.2	Luminescence	16
2.2.1	Temperature measurement	17
2.3	Pressure measurement	25
2.4	Luminescent materials available	28
2.4.1	Acridine Yellow	28
2.4.2	Ruby	29
2.4.3	Sapphire	36
2.4.4	Phosphors	37
2.4.5	Summary of the luminescent materials available	41
2.5	Measurement from a rotating disc	45
2.5.1	Optical Affects	46
2.5.2	Materials used	47
2.5.3	Measurement within Turbine Engines	48
2.5.4	Conclusion	49
2.6	Coatings	50
2.6.1	Techniques used for temperature sensitive coatings	50
2.6.2	Adhesive techniques	52
2.6.3	Other coating techniques	53
2.6.4	Surface preparation	57
2.6.5	Summary of coating techniques	58
2.7	Data analysis	60
2.7.1	Smoothing techniques	61
2.7.2	Curve fitting	62
2.7.3	Software	63
2.7.4	Selection of data analysis techniques	64
3	Study of fluorescent materials	65
3.1	Acridine Yellow	66
3.2	Brilliant Sulphoflavine	70
3.3	Panacryl Brilliant Flavine	73
3.4	Sapphire	74
3.5	Ruby	76

3.5.1	Testing of pressure sensitivity	79
3.5.2	Ruby conclusion	81
3.6	Yttrium Oxysulphide Praseodymium doped	81
4	Data analysis	86
4.1	Smoothing techniques	86
4.1.1	Averaging and subtracting the background	87
4.1.2	Using known smoothing techniques	88
4.2	Ruby spectrum analysis	91
4.2.1	Solid Ruby	92
4.2.2	Ruby paint coated	106
4.2.3	Ruby plasma coated	106
4.2.4	Summary of Ruby as a temperature sensor	112
5	Creating a fluorescent coating	114
5.1	Coating techniques using Ruby	114
5.1.1	Adhesive Techniques	115
5.1.2	Plasma coating	121
5.1.3	Comparing the Ruby coatings	134
5.2	Summary of coating techniques	136
6	Yttrium Oxysulphide Praseodymium doped	138
6.1	$Y_2O_3S:Pr$ decay-time temperature relationship	139
6.2	$Y_2O_3S:Pr$ spectrum temperature relationship	141
6.3	Creating a fluorescent coating using $Y_2O_3S:Pr$	143
6.3.1	The relationship of the coating with temperature	144
6.4	$Y_2O_3S:Pr$ powder temperature sensitivity	156
6.5	Summary	165
7	Spin Testing	167
7.1	High speed detection	167
7.2	Ruby	169
7.2.1	Simulation of 80,000rpm	170
7.2.2	Low speed testing	171
7.2.3	High speed test using Ruby coating	172
7.3	Yttrium Oxysulphide Praseodymium doped	174
7.3.1	Experimental arrangement	174
7.3.2	Experimental results	179
7.3.3	Conclusion on spinning $Y_2O_3S:Pr$	182
7.4	Summary of spinning	183
8	Conclusion	185
8.1	Further Work	189

9 Appendix	191
9.1 Equipment specification	191
9.1.1 General	191
9.1.2 For ruby experimentation	191
9.1.3 For $Y_2O_3S:Pr$ experimentation	192
9.2 Material Specification	193
9.3 Theory	194
9.3.1 Radiation	194
9.3.2 Luminescence	195
9.3.3 Ruby	197
9.4 Coatings	200
9.4.1 Safety	200
9.4.2 Plasma coatings	201
9.5 Luminescent Materials	202
9.6 Calculations	209
9.6.1 Thermodynamic calculations	209
9.6.2 Ruby energy calculations	209
9.6.3 Ruby timing calculations	210
9.6.4 $Y_2O_3S:Pr$ timing calculations	210
9.6.5 Fiber optic	212
9.7 Programming	212
9.7.1 Determining the reliability of the equations	213
9.7.2 Summing the spectrum and finding the average	219
9.7.3 LabView program to determine temperature from spectrum in real time	223
9.8 Equations	236
9.8.1 Lorentzian	236
9.8.2 Gaussian ¹⁸¹	236
9.8.3 Voight ¹⁸¹	236
9.8.4 Pearson VII ¹⁸¹	237
9.8.5 Munro ⁶	237
9.8.6 Stern-Volmer	238
9.9 References	239

Glossary

Term	Definition
Absorption	Absorption occurs when a molecule absorbs a photon of light, this light energy can then be translated into rotational, vibrational or electronic modes, which is dependent upon the wavelength of the light absorbed.
Brittleness	Tendency of a material to fracture without apparent plastic deformation.
Compressor, centrifugal	An air compressor in where the pressure rise occurs by the centrifugal forces created by a rotating impeller.
Decay-time	The time for the excited state concentration to decay to 1/e (about 37%) of the initial value.
Delay-time	The period between absorption and start of emission.
Emission	The liberation of electrons from the surface of a substance.
Emission spectrum	The electromagnetic spectrum produced when emission occurs. Excitation is at a constant wavelength and the wavelength for viewing emission is varied.
Excitation spectrum	The emission is viewed at a constant wavelength and the excitation wavelength is varied. This resembles an absorption spectrum.
Fluorescence	Light emission from a material with decay time $<10^{-8}$ sec
Fourier transform	The expression of a function as a summation of sinusoidal components.
Incandescence	The emission of visible radiation at high temperatures.
Laser	A source of ultraviolet, visible, or infrared radiation which produces light amplification by stimulated emission of radiation.
Lifetime	Also known as Decay-time
Luminescence	The general term for fluorescence and phosphorescence
Moving average	Takes the average of a certain number of data points to create a trend.
Phosphor	A substance which emits luminescence at temperatures below that where incandescence would occur.
Phosphorescence	Light emission from a material with decay time $>10^{-8}$ sec
Photobleaching	The lack of fluorescence emission from the excited molecule to a chemical reaction with its surroundings or due to break up.
Photodegradation	The process of decomposition under exposure to a radiant energy, such as light.
Plasma	A gas made up of charged particles. Usually plasmas are neutral but not necessarily so.
Plasma Spraying	Propelling molten coating material against the base metal by use of a hot ionised gas torch.
Plasmas	Electrically conductive gasses which are composed of neutral particles, ionised particles and electrons but which taken as a whole are electrically neutral.
Plastic Deformation	The changes in dimensions of items caused by stress that are relaxed after stress
Q-switched laser	A state that allows the laser to run at very low losses, increasing the Quality factor of the cavity allowing the build up of very short very intense laser pulse.
Quenching	Quenching in terms of fluorescence is a process that decreases the intensity of the fluorescence.
Thermoluminescence	Thermoluminescence is the process in which a material emits light when being heated.

Definition of terms

Term	Definition
BaClF:Sm ²⁺	Barium Chlorofluoride activated by Divalent Samarium
Cr	Chromium
Dy	Dysprosium
Eu	Europium
Gd	Gadolinium
La	Lanthanum
La ₂ O ₂ S:Eu	Europium-doped Lanthanum Oxysulphide
La ₂ O ₂ S:Eu	Lanthanum Oxysulphide Europium doped
LaF ₃ :Dy	Lanthanum Fluorine Dysprosium doped
LuPO ₄ :Dy	Lutetium Polonium Dysprosium doped
Mg ₄ (F)GeO ₆ :Mn	Manganese-doped Magnesium Fluorogermanate
Nd	Neodymium
Tb	Terbium
Ti	Titanium
Tm	Thulium
Y	Yttrium
Y ₂ O ₂ S	Yttrium oxysulphide
Y ₂ O ₂ S:Eu	Yttrium oxysulphide Europium doped
Y ₂ O ₂ S:Yb	Yttrium oxysulphide Ytterbium doped
Y ₂ O ₂ S:Tb	Yttrium oxysulphide Terbium doped
Y ₂ O ₃	Yttrium Oxide
Y ₂ O ₃ :Eu	Yttrium oxide Europium doped
Y ₂ O ₃ :Gd	Yttrium oxide Gadolinium doped
Y ₂ O ₃ S:Pr	Yttrium oxysulphide Praseodymium doped
Y ₂ SiO ₅ :Ce	Yttrium Silicate Cerium doped
Y ₃ (Al,Ga) ₅ O ₁₂ :Ce	Yttrium Gallium Garnet
Y ₃ Al ₅ O ₁₂ :Ce also known as YAG:Ce	Yttrium Aluminium Garnet Cerium doped
Y ₃ AlO ₃ :Ce	Yttrium Aluminium Perovskite Cerium doped
YAG	Yttrium Aluminium Garnet
YAG:Dy	Yttrium Aluminium Garnet Dysprosium doped
YAG:Nd	Yttrium Aluminium Garnet Neodymium doped
YAG:Sm	Yttrium Aluminium Garnet Samarium doped
YVO ₄ :Dy	Dysprosium-doped Yttrium Vanadate
YVO ₄ :Eu	Yttrium Vanadate Europium doped
ZnTPP	Tetraphenylporphyrin

1 Introduction

The measurement of temperature using contact techniques when high speeds of rotation are present is complex. Conventional techniques are difficult and sometimes impractical to implement. The measurement of the temperature of moving objects through a non-contact technique is important to enable the design of a system to be improved. This technique has particular benefits to the engine industry, where it is important that techniques used do not affect the normal running conditions, as this can cause localised temperature changes. The traditional methods of measuring temperature involve either attaching probes to the surface or touching the surface with a probe. Recent developments have led to the introduction of infrared techniques, laser induced fluorescence and thermoluminescence.

Must have requirements	Ideal requirements
Measure temperature in the range 100°C to 250°C	Measure temperature in the range 20°C to 300°C
Will cause very little disturbance to the normal running conditions	Have a self referencing technique
Can be used to measure temperature on the tips of the blades	Can be set up on site
Can be used at speeds from 40,000rpm up to 80,000rpm, on wheels of diameter 140mm. Equivalent to 0.6km/sec	Invasive
Does not use infrared techniques	Accuracy of $\pm 1^\circ\text{C}$
Can be measured in real time	Take reading on each rotation
Temperature measurement is localised to area of interest and is not affected by surrounding objects	Can take temperature readings at more than one point
Can be implemented in a standard test cell	
Withstand pressure changes of 4bar	
Easy to implement in industry	
Record the temperature readings for analysis later	

Table 1-1 The project specification

Holset Engineering, a manufacturer of turbomachinery requires a non-contact method of detecting the temperature on a rotating compressor wheel. This involvement with industry has meant that the project has constantly been in touch with the needs of industry in this area. The stresses in the compressor wheel during operation are related to temperature, and therefore being able to measure temperature will enable the stress to be

determined. This allows the areas of weakness to be determined and allow for redesigning of the compressor wheel.

The temperature range that the compressor wheel is expected to achieve in normal running conditions is 100°C to 250°C, this is therefore the temperature range of interest for this project. It is the temperature at the tip of the blades that is of interest, in the first instance. Speeds of up to 80,000rpm are possible and the diameter of the compressor wheel can be up to 140mm. The temperature reading will be used to improve the software implemented for designing the compressor and therefore help to improve the efficiency and help determine the maximum running conditions. Emmissivity based temperature measurement techniques have been tested previously by Holset and have been shown to be unsuccessful for this problem. The requirements of Holset Engineering for their temperature measuring system are summarised in Table 1-1.

Within the compressor the temperature is directly related to the efficiency of the compressor, being able to measure the temperature accurately will mean that the efficiency of the compressor can also be measured ¹. This temperature range is of extreme importance to the engine industry as a whole, as it is well known that the strength of aluminium starts to decay rapidly above temperatures of 200°C ². Thus measuring the temperature of the compressor wheel will allow the strength of the material to be determined. This will enable Holset to determine whether the engine can be pushed further, or whether different designs are feasible.

Thermoluminescence and emissivity methods are similar in that they both use a reaction of the object to temperature to determine its temperature. The advantage of thermoluminescence is that the wavelength used is unique to the coating, whereas with emissivity surrounding surfaces are also emitting similar wavelengths which cause interference. Thermoluminescence is used for both temperature and pressure measurements. Phosphors can be used for measuring temperature in the range -200°C to 1900°C dependent upon the phosphors. Although phosphors are available to measure temperature in the temperature range, very few are available for the range 25°C to 300°C. The pressure sensitivity of the majority of the phosphors is outside the pressure range within the compressor.

1.1 Compressors and turbines

Compressors are devices used to increase the pressure of a fluid or gas using as minimal an amount of input power as possible. Greater efficiency and an increase in compression ratio from compressors are being sought, this leads to an increase in operating temperature and therefore in stress levels in the compressor³. The pressure of a gas or vapour may be increased either by decreasing its volume or by importing to it a high kinetic energy which is converted into pressure energy in a diffuser⁴. The use of inducer guide vanes increases the fluids angular momentum without increasing its radius of rotation.

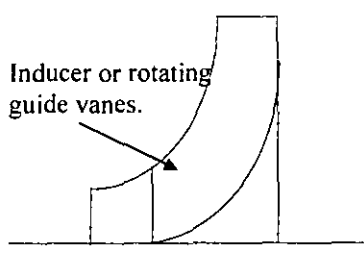


Figure 1-1 The Compressor Wheel

The compressor process is carried out in a compressor stage which comprises four elements⁵.

- The inlet casing - whose function is to accelerate the fluid to the impeller inlet.
- The impeller - in which the energy transfer occurs, resulting in a rise of fluid kinetic energy and pressure.
- The diffuser - whose function is to transform the high kinetic energy of the fluid at the impeller outlet into pressure.
- The outlet casing - which comprises of a fluid collector known as a volute or scroll and a conical outlet diffuser which further transforms fluid kinetic energy into pressure.

Advances in turbine design means that turbines can run at much higher temperatures. Knowing the temperature of the compressor wheel will enable it to be run at much higher speeds, and therefore increase the efficiency of the compressor. Temperatures, at which the superalloys are used at present, will struggle, the movement is towards ceramic

materials. This leads to temperature measurement problems as existing techniques such as thermocouples, blackbody and emissivity can no longer be used.

1.2 Overview of the project

A brief overview of the project is given here and how all the processes are brought together. Different methods of temperature measurement available were first of all investigated. This showed that attached electronics were not feasible due to their method of attachment and size which would affect the airflow around the compressor. To transfer the data, from the rotating object, slip rings are required; this can be difficult to implement with many sensors. Radiation techniques were not a possibility due to the amount of interference from the surrounding casing. It was determined that luminescence is the best method to use, as it gives a reading that is unique to the coated area, and does not affect the normal operating conditions. Ideally a non-invasive technique would be preferable though this is not possible as radiation techniques cannot be used, and aluminium is not known to fluoresce. Therefore the least invasive technique is used which is the addition of a luminescent coating.

The main technique used for temperature measurement is the decay time technique. This technique is not viable at the speeds which are being considered here, as it requires the decay time to change significantly during the time available, and for the detection system to be fast enough to be able to detect the changes accurately enough. When spinning at 80,000rpm, the edge of the compressor wheel, which is the fastest point of interest to be measured, will be moving at 0.6km/sec. This will require a decay period of less than 20 μ sec, for the majority of the fluorescence to be collected and for the detection system to be able to detect the change over this time period. Short decay times can also become rotation rate dependent, so at this speed a decay time greater than 1.7msec would be required to avoid this.

The feasibility of the fluorescence technique using peak position or intensity is to be examined through experimental means. A suitable luminescent material is to be selected, this requires an absorption wavelength at an easily available high intensity wavelength.

The emission peak is to be temperature dependent, easily separated from the excitation wavelength and to have a short decay period. The collection of the luminescence by a fibre optic is to be considered, as is the selection of a suitable detector and analysis software. Materials which are known to show a luminescent temperature sensitivity also tend to show a pressure sensitivity. The pressure that is expected within the compressor is up to 4bar, it is therefore important that the luminescence does not show a pressure dependence over this pressure range.

This led to the selection of luminescent materials for the temperature range 25°C to 300°C, but in particular 100°C to 250°C. The initial selection was Ruby as this has the possibility of being self calibrated which would remove the need for calibration of each separate sample. The major disadvantage of this material is its long decay period of 3msec. This means that when spinning at high speeds only a small proportion of the fluorescence is collected by the detector.

The main advantage of Ruby is the two peaks separated by about 2nm, both of which change with temperature. A number of variables can be used to determine the temperature and so produce a more reliable reading. Ruby is also pressure dependent, though previous research shows that this can be accounted for⁶. The ratio between the two peaks can be used for temperature measurement. This value is independent of coating quality, excitation intensity and variation on position of excitation, and can therefore be used as a self-calibration method.

Different ways of attaching the substance to the aluminium wheel were considered. This requires obtaining the Ruby in a powder form so that the material can be coated as finely as possible to the wheel. Creating a Ruby paint by mixing Ruby powder and adhesive together was considered in the first instance. This was found to bond well to the wheel and withstand the conditions within the compressor housing. The use of the adhesive reduced the amount of fluorescence received by the detector. Plasma coating was then used, this melts the Ruby and uses an air stream to project the particles onto the wheel. This method of coating produced much stronger fluorescence but is much more difficult to apply.

A material with a much shorter decay time was required, the Phosphor Yttrium Oxysulphide was therefore considered as this has a much shorter decay time of 7 μ sec. Its intensity reduces with temperature, it also has a number of wavelengths at which it fluoresces that can be used for self-referencing.

To implement the technique on a rotating object means that a fully gated system is required. The system requires a compact light source and spectrometer, as the equipment will have to be easily moved so that it can be used on different test rigs. A technique of attaching the material to the wheel also has to be derived. The creation of fluorescent paint was considered along with plasma coating. The ideal light source is a Q switched laser as this emits short high energy pulses, a pulse length of less than 20 μ sec would be required. The light would then be transmitted to the compressor via optical fibres, a different optical fibre would be used to transmit the luminescence back to the spectrometer for detection.

To enable the fluorescence spectrum to be related to temperature, data analysis had to be undertaken and this involved determining the type of peak so that the peak's details are determined. These are then used to create a relationship between temperature and the spectrum. The use of different smoothing techniques was considered this included Fourier Analysis and Moving Average.

The finished product is a temperature sensitive coating, whose luminescent spectrum can be collected in real time and after data processing can be used to determine temperature in less than 1 second.

2 Literature Survey

2.1 Temperature Measurement

There are many ways of measuring temperature. The two main temperature sensors available are radiation thermometry and thermocouples, though these do have disadvantages for our project. Thermocouples are surface mounted which disturbs the airflow, the heat transfer characteristics and the temperature at the point at which it is attached, but they have a high failure rate. Thin film thermocouples have negligible affect on temperature but do not adhere well under adverse operating conditions. Radiation thermometry gives erroneous readings in the presence of intense background radiation and they only work for temperatures above 700°C. These techniques also do not work well with low emissivity values and aluminium is well known for its low emissivity, and oxidation of the aluminium at temperatures around 300°C can also affect the emissivity values⁷.

Temperature measurement does not always give true temperature readings, this is often due to non-equilibrium conditions. A temperature sensor, even if well designed, will not always indicate the temperature it is supposed to be measuring, as there is often a delay while the sensor reacts to the change in temperature. Uncertainty of temperature measurement within a high-speed compressor environment is made up of many variables that include; detection period, sensor reaction speed, and temperature noise from surrounding objects and sensor placement.

Electrical means of measuring temperature are intrusive and can be affected by external factors such as static electricity, ionised air, humidity and being dropped. Infrared techniques can be inaccurate due to interference from the surroundings. Liquid crystal thermography has a limited range from -25°C to 250°C, and their individual active temperature range is constricted⁸. It was noted by Bize et al⁹ that when using liquid crystals for temperature measurement the wavelength recorded would change depending upon the viewing angle.

In the aerospace industry, where scaled down models are used in wind tunnels for surface pressure testing, pressure sensitive paints are used. The paints used for these experiments must meet the following requirements¹⁰:

- Sensitive to very small changes in temperature.
- Be robust, and adhere to the surface and withstand the temperature and pressure ranges it faces.
- Be able to be polished to the required surface smoothness.
- Easy to apply to large surface areas.
- Be removable without damaging the finish of the surface to which it is applied.

As thermoluminescent materials are insulators there will always be a delay in temperature from the surface temperature of the object to the surface of the thermoluminescent coating. Light based systems are faster than most other systems of temperature measurement, as they tend to have smaller mass, if any, and therefore react much quicker to temperature change which is an important advantage on high speed applications.

Non-contact techniques are much more favourable compared with contact techniques as these will produce less interference with the running of the normal running conditions of the compressor. Non-invasive techniques would be the preferred technique to use as this would not cause any changes whatsoever to the running of the compressor. A non-contact method of measuring temperature is required to ensure that this causes the least amount of change on the normal running conditions of the compressor.

2.1.1 Temperature sensitive paints

There are two types of temperature sensitive paints available. The first will melt or change colour at a certain temperature, these are generally used to warn of over heating. The other will gradually change colour as the temperature rises. They do not produce an accurate reading but do work at temperatures well above 1000°C¹¹, they are used more as a guide to give a general temperature reading.

The reliability is affected by the length of time the paint is being heated for. If a surface is gradually heated to the required temperature then colour change can occur at lower temperatures. The accuracy of this technique depends greatly upon the properties of the paint and the measurement system used. Inaccuracies can occur due to chemical and physical properties, detector noise, and changes in the signal received from the coating due to contamination or shift in the object. Although these cannot be eliminated they can be minimised or compensated for. Short exposure time will decrease the inaccuracies from the chemical and physical properties. Monitoring of the input intensity will account for fluctuations in the light source, control of the equipment temperature will reduce the detector noise. Using a non-intensity based technique can eliminate errors caused through shift in the object or degradation of the coating or through a referencing technique, this will also help to reduce errors produced through the apparatus used. They tend to be able to be used only once as the colour change tends to be non-reversible.

2.1.2 *Radiation thermometry*

Radiation thermometry is a non-contact method of measuring the surface temperature of an object from the thermal electromagnetic radiation emitted. They can be used for taking spot, line or area temperature measurements. This technique is also known by; emissivity, pyrometers, infrared thermometers, fibre optic thermometers, thermal imaging radiometers. Low emissivity leads to an underestimate of temperature in this technique.

There are three main problems in trying to determine the temperature from the signal in this technique:

1. The value of emissivity varies in different materials, and is generally unknown. It depends upon surface roughness, contamination, oxidation, angle, polarisation, and wavelength.
2. Reflective fluxes from the surroundings is a big problem especially when in hot surroundings, or with materials with high reflectance. The surrounding can be taken into consideration in complex calculations that tend to rely on estimates or secondary measurements and can therefore be inaccurate¹².
3. Absorption by the gases between the surface and the detector can affect the result¹².

The paper by Zhang et al¹³ describes more completely the application of these relationships and the various experimental methods.

To measure temperature using the optical pyrometry technique requires the intensity of the thermal radiation from the sample to be measured and compared to a known variable source. High optical background, such as infrared from surrounding surfaces, stops this technique from being used and the emissivity of the sample must be known for this technique.

By using a pulsed laser beam onto the object the emitted and reflective fluxes can be separated. The emitted flux will pulse with the laser and the reflective flux will be a constant¹². A two colour technique has also been developed which allows much lower temperatures to be measured using optical pyrometry. Two measurements are taken at two different wavelengths the ratio of the signals can be used to determine the temperature. Temperatures as low as 340°K have been measured using the two colour technique and 300°K using the pulsing technique.

There are a number of different types of infrared thermometers available¹⁴. Total radiation types are sensitive to all wavelengths, the transmission of the materials used can reduce the wavelength ranges seen. They are simple, reliable and relatively inexpensive and have been in use for many years. Partial radiation types are sensitive to wavelengths shorter than a cut-off set by the detection optics. Filter types, which are sensitive to a band of wavelengths, are determined by the inclusion of a filter in the optical system. The partial radiation and filtered radiation types can offer greater precision. There is also the use of two thermometers to produce a ratio type, the two thermometers having different sensitivities. These are placed within the same housing and can reduce emissivity errors or those associated with partial obstruction of the target.

Spectral radiation from an object changes with wavelength and temperature. Limiting the detector to a waveband whose upper limit is around that of the peak spectral radiation will provide optimal performance. The errors due to inexact knowledge of the emissivity or incorrect filling of the field of view, are much reduced in partial radiation thermometers than total radiation thermometers.

These techniques are currently implemented in a number of industries such as glass, steel and semiconductor chip manufacture. Their main advantage is that nothing needs to be attached to the item being measured. Radiation thermometers can measure temperature in the range -50°C to $3,000^{\circ}\text{C}$ with $\pm 0.1\%$ ¹⁵. They are designed to focus on specific wavelengths dependent upon the material being measured. An infrared thermometer must have an unobstructed line of sight to be successful. As with other optical means of optical temperature measurement fibre optics can be used.

The main disadvantage of the infrared technique is the interference of radiation from surrounding objects. Filters can be used to remove known interference as long as it does not clash with wavelengths being measured. Interference from the surrounding environment can be taken into consideration by using the equation below ¹⁴.

$$Q = \varepsilon f(T_s) + (1 - \varepsilon) f(T_F)$$

Equation 2-1

where;

- ε = emissivity of object
- T_s = temperature of object
- T_F = temperature of surroundings
- Q = radiation received by the thermometer

The surrounding temperature can be measured using a second sensor such as a thermocouple or another infrared sensor.

When measuring the surface temperature within a hot environment errors can be reduced by painting the surface to be measured black. This will reduce the amount of radiation reflected by the surface. The use of windows to view the surface can absorb infrared radiation and so affect the readings of infrared detectors.

Generally radiation thermometry is more effective and simpler to implement for high temperature measurement. As infrared techniques are emissivity dependent they can be used for temperatures above 0°C , this means that they are also dependent upon the surface condition. Surface finish needs to be considered, as does degradation of the surface due to coating with debris and oxidation. Painting the surface black can help to

provide uniform emissivity¹⁶. For implementation on a rotating object, the object will have to be imaged allowing the temperature of the same spot to be measured each time.

These techniques also do not work well with low emissivity values and aluminium is well known for its low emissivity, and oxidation of the aluminium at temperatures around 300°C can also affect the emissivity values¹⁷.

2.1.3 Fibre optic thermometers

Fibre optic probes can be used for measuring environmental temperature, whether it is liquid or gas. Most are a slight variation from radiation thermometers. They are characterised by those that use the fibre as the transducer¹⁸ and those that use the optical change in a secondary material¹⁹.

Those using the fibre use the increase in scattering coefficients of liquid core fibres with temperature or by implementing the Raman effect. These tend to be more expensive than the use of a secondary material due to the light sources and signal processing that is required.

Those that use the characteristics of a material have involved the use of the change in absorption characteristics with temperature²⁰. A temperature sensing material is placed at one end of the fibre, the other end is attached to a measuring system that collects the radiation that has passed down the fibre, this information is then processed into a temperature reading. This technique is not viable for surface temperature measurement from a rotating object.

2.1.4 Luminescence techniques

The use of the luminescence method as a temperature sensor is based on one of the following: Intensity change with temperature, shift in wavelength of the luminescence peak, change in shape of luminescence peak, decay time changing with temperature.

Delay between excitation and emission changing with temperature. The main advantage of this technique is that it is a non-intrusive, non-contact means of measuring temperature.

Using the technique of fluorescence or absorption shifts can require expensive and sometimes delicate optics. The lifetime technique does not require such expensive equipment but the sensitivity to temperature can be less²¹. In some cases, to overcome each of these disadvantages, the intensity ratio of two peaks can be used. A combination of techniques can be used to make the technique more accurate and reliable.

Dissolving a fluorescent material into a host can affect the molecular structure and therefore the temperature dependence. This will need to be a consideration of the coating techniques used and the material that is selected, as mixing the material with an adhesive may change the temperature relationship of the material. Choosing a field of view that is similar to the shape being measured will help to fill the field of view and therefore increase the accuracy of the measurement.

When using the decay time technique with magnesium fluorogermanate activated with tetravalent for temperature measurement of measuring the decay time after the excitation source had ceased. It was determined by Wickersham et al²² that to achieve a reproducibility of $\pm 1^\circ\text{C}$ it was required to measure the lifetime to an accuracy of microseconds out of a total life time of several milliseconds.

It is possible that to cover a broad temperature range accurately more than one phosphor may be required, or two different emission lines from one phosphor, which react to different temperature ranges to cover the whole temperature. This technique has been used successfully by Wagenaar et al to measure the temperature of flowing single particles at speeds of up to 10m/sec²³.

The angle of incidence of the emission wavelength onto a filter is important, because if this angle is increased the peak wavelength shifts to shorter wavelengths. An increase in temperature causes a shift to longer wavelengths, this shift is dependent upon temperature and the filter. This implies that care has to be taken in the arrangement and that the repeatability of a set of readings will not be able to be repeated accurately. Many

of the differences gained will be due to the alignment of the optics and the apparatus used. The system will therefore have to be calibrated each time it is used.

The fluctuation of the speed of the turbine will affect the consistency of the point being monitored. This will also affect the calibration when intensity based techniques are being employed. Pulse jitters, and trigger error of the laser are also factors, though these are minimal especially with modern equipment.

2.1.5 Summary of temperature measurement techniques

A number of techniques for temperature measurement have been considered in this chapter. Those which are of most interest are the non-contact techniques; temperature sensitive paints, luminescence, radiation thermometry, and fibre optic thermometry.

Ideally for measurement within a compressor a non-invasive radiation based technique would be chosen but this is not possible due to interference from the surrounding material. When using this technique the emission from the material is dependent upon the surface quality and the exact composite of the alloy. It can also be affected by any gasses within the atmosphere between the surface and the point of collection. These techniques also do not work well with low emissivity values and aluminium is well known for its low emissivity. Oxidation of the aluminium at temperatures around 300°C can also affect the emissivity values²⁴.

The attachment of electronic measuring devices to the rotating surface will affect the operating conditions of the compressor thus affecting the temperature of the blade. This will not give a true running condition of the compressor wheel. The method of attachment can also cause localised stresses on the blade, which in turn could affect the temperature of the blade. It is also difficult to add multiple sensors due to the use of slip rings to transmit the data from the rotating object.

Temperature sensitive paints are available but these indicate that a certain temperature has been reached rather than giving a continuous temperature reading, and are therefore

not suitable for this application. Fibre optic, temperature sensitive probes are used in measuring environmental temperature such as air temperature, or fluid temperature. These are used successfully in industry but cannot be used for temperature measurement of moving surfaces, though they implement the luminescence technique.

Considering the options of measuring temperature outlined in this chapter, it has been decided to look further into luminescence as a possible technique for measuring the temperature of a rotating surface. The advantage of luminescence over the other techniques is that it is a non-contact technique, which is unique to the coated area, and is the least intrusive technique available. As this technique is non-intrusive it will cause little affect to the air flow within the compressor and therefore the operating conditions of the compressor. The temperature range that can be measured is dependent upon the luminescent material chosen.

2.2 Luminescence

Luminescence is the property that some materials have of being able to absorb light of a specific wavelength and then convert some of this absorbed energy into light of a longer wavelength. This change in wavelength is due to strain within the molecular structure. Anything that changes this molecular structure will affect the luminescence. The main factors being impurities, thermal treatment, stress, UV rays, particle size, infrared stimulation and pressure. Luminescence is generally as a result of the introduction of an impurity into a host lattice through heat treatment ²⁵.

There are two forms of luminescence; phosphorescence and fluorescence. The differences between the two is that phosphorescence occurs at a lower energy state (longer wavelength) and is red shifted which makes it easier to distinguish from the energy source. Phosphorescence has a longer delay time, also known as delayed fluorescence, and a longer lifetime, this means that when the exciting wavelength is removed the emission can still be seen. With fluorescence the time delay between absorption and emission is only a fraction of a second so when the exciting wavelength is removed the emission apparently stops. The choice of whether to select a material that emits phosphorescence or fluorescence will depend if steady or unsteady conditions are being measured.

Thermoluminescence is the light emitted during heating or cooling of a sample that has absorbed energy from radiation. The heat present during thermoluminescence is only a moderator and cannot by itself cause the luminescence. An extra stimulant of an optical type is required to produce the luminescence. The amount of oxygen in the atmosphere can affect the thermoluminescence spectrum ²⁶, as oxygen can act as a quencher. Pressure sensitive luminescent materials require oxygen, whereas temperature sensitive materials do not ⁴⁶. Thermoluminescent samples are insulators, this means that there is always a delay between the actual temperature of the environment and the temperature of the luminescent material, the delay depends upon material thickness and conductivity of the material.

The emission is affected by environmental conditions that can cause a decrease in intensity, duration of emission or width of the bands, this process is known as quenching. There are four main types of quenching; temperature, oxygen, concentration and impurity. When quenching occurs the energy inputted into the system through the excitation wavelength is removed through photon coupling between molecules.

The intensity of the emission is directly proportional to the intensity of the excitation wavelength. An increase in temperature will cause a decrease in intensity. The luminescence intensity is proportional to the molar absorptivity. It is possible that a material can absorb too much energy, emptying the ground state of available electrons, therefore the fluorescence decreases at high concentrations.

When changes in temperature pressure and other variables occur simultaneously intensity based techniques would produce a more reliable technique than those based around the shift in position of the maximum fluorescence²⁷.

The efficiency of a material is determined by the energy emitted by the material to the energy absorbed. This can be temperature dependent in some materials and gives the opportunity for temperature measurement.

2.2.1 Temperature measurement

When using the luminescence technique as a temperature sensor there are two basic methods available. Those using an optical fibre itself as the transducer, and those that use an optical effect in a material.

2.2.1.1 Measurement using emission peak properties

The shape of the emission peak as well as its position can be related to temperature for some luminescent materials. Some materials will emit one peak, others will emit many peaks.

2.2.1.1.1 Intensity based techniques

The intensity of some of the peaks found in the fluorescence spectra decrease with temperature. This tends to follow a trend so that the peak intensity can be used to determine the temperature of the material.

An advantage of this technique is that it can be used in 2D measurements. The disadvantage of this technique is that the intensity is dependent on a number of factors. These are the excitation source power, condition of the coating, the structure of the material, and changes in the fibres and detector. Ratiometric techniques remove some of these errors and provide a signal independent temperature measurement technique. It is inexpensive, and expensive optics and electronics can be protected from the environment.

Thermographic paints are readily available, Ervin et al ⁸ have used these on a curved surface over a temperature range 24°C to 55°C using the ratio technique. They have compared the temperatures given by a thermocouple to those given by the phosphor, a difference of 1.2°C was recorded using a resolution of 0.3nm.

It can be that the intensity of some peaks increase with temperature while others decrease with temperature, in the same phosphor. This was so with the material Zinc(II) Tetraphenylporphyrin (ZnTPP). This is explained by the increase from delayed fluorescence which is due to thermal activation, and the decreasing peak is phosphorescence²⁸.

2.2.1.1.2 The ratio technique

The ratio technique involves using the ratio of two intensities of output wavelengths from a single excitation wavelength as described by Goss et al ²⁹. The two beams are both dependent upon the same environmental changes, such as losses through the fibre, and variations in the excitation source. It provides an accurate self-referenced measuring system. The variable that is dependent upon the change in temperature here is the

intensity of the variable wavelength. The ratio of the intensity of these two emission wavelengths gives a linear relationship to temperature.

The technique could either use one peak that does not change and one that does, or two peaks that change at different rates, or more than two peaks to get an even more reliable result. It is possible that this technique will have wavelengths that are temperature sensitive at different temperatures. This would therefore enable the temperature profile of the turbine blade to be monitored more accurately during heating and cooling. This may require different excitation wavelengths to be used.

The rare earth ion Dysprosium (Dy) introduced into a YAG crystal has been determined to be an ideal fluorescent species for thermometry. Dy:YAG has been proved to be sensitive to temperatures up to 1526°C²⁹ and was used with an excitation wavelength of 355nm from a Nd:YAG laser. For optical thermometers pink Ruby laser rod has also been used with the excitation wavelength gained from two green LED's with peak emission at 565nm³⁰, Ruby has a wide absorption band centring at around 555nm.

The emission signals are very repeatable and therefore the main errors occur due to the electrical equipment, and the initial calibration. Errors occur due to background and detector noise. Fluctuations are also possible due to the presence of wavelength dependent effects in the optical system which collects and conveys the phosphor's fluorescence³¹.

As well as using the value for the intensity to determine the ratio value it is possible to also use the integral over a certain bandwidth²⁷.

2.2.1.1.3 Shift in wavelength

The wavelength at which a material emits luminescence can change with temperature, the luminescent peaks will shift to longer wavelengths with an increase in temperature.

It is thought that any variable that causes a change in density, for example pressure, will also produce a shift in the fluorescence and absorption wavelengths. Munro et al have shown that it is possible to measure temperature and pressure simultaneously.

2.2.1.2 Time dependent techniques

The length of time that the emission occurs is known as the decay time. This can decrease with increase in temperature. The time between stimulation and emission is known as the delay time. This can also be temperature related.

2.2.1.2.1 Decay-time technique

The use of the decay-time technique has proven to be extremely reliable for the measurement of temperature. It is possible to achieve high accuracy in temperature measurement even with poor signal-to-noise ratio³². Allison et al noted³³ that it is this property of the fluorescence that shows the most dramatic change with temperature.

The advantages of this technique are its insensitivity to ambient light, paint thickness and surface curvature. A pulse laser is used as the excitation source. Although large variations in paint thickness can reduce response times, this is roughly proportional to the square of the paint thickness.

The main disadvantage in implementing this technique on to a rotating object is that the decay-time must be such that it will change significantly in the time in which it passes through the detection optics. For short decay times this measurement must occur quick enough to enable very small changes in the decay time to be recorded accurately. This technique is not viable for a 2D approach because the decay-time is so rapid that it is not possible to obtain the necessary images over the measurement area to compute the decay-times³⁴.

The lifetime can be affected by collision broadening, natural lifetime, non-radiative transition in solids³⁵. It is not affected by inhomogenous broadening in magnetic fields,

and the statistical strain broadening so long as the adiabatic condition holds³⁵. The velocity of ions in crystals is too low for Doppler broadening to be significant³⁵.

Phase-modulation spectroscopy involves the measurement of the phase delay and amplitude modulation index of the fluorescence emission with respect to a periodically modulated excited source. In time decay spectroscopy this technique has been used at frequencies of 200MHz³⁶. Phase-modulation can discriminate lifetime differences from different molecules that photon counting techniques cannot resolve.

The intensity of the light emitted falls rapidly with time, this can be related by the intensity of the radiation emitted $I(t)$, at a time t after termination of the exciting pulse, the initial intensity I_0 , and where τ is the decay-time characteristic of the medium.

$$I(t) = I_0 e^{-t/\tau}$$

Equation 2-2

Neodymium (Nd) is one dopant that has been used with this technique, and was successful for temperatures up to 130°C³⁷, though temperatures up to 350°C are thought possible. This dye has three absorption bands, 750nm, 805nm, 860nm, the strongest being 805nm.

Other compounds used include Barium Chlorofluoride activated by Divalent Samarium (BaClF:Sm^{2+})³. This has a high quantum efficiency and narrow band emissions. This compound was excited at 417nm, and temperatures of up to 350°C were attained. $\text{La}_2\text{O}_2\text{S:Eu}$ has also been used for temperatures up to 300°C, with excitation wavelengths of 337nm produced by a N_2 laser³¹.

Work undertaken by Allison et al states that a disadvantage of the decay-time technique is that the measurement is dependent upon the speed on the surface from which the measurement is being taken. When the target's surface speed is comparable to or greater than the inverse of the phosphor's characteristic decay-time, the calibration of intensity-based methods becomes rotation-rate dependent³¹. A wheel spinning at 80,000rpm and with measurements taken at a diameter 140mm a decay time greater than 1.7msec would

be required. Advantages are it is less susceptible to the effects of electronic drift, ground loops and other forms of interference which produce uncertainty in dc measurements ³¹.

The use of this technique will produce a very reliable reading as it is the structure of the dye itself that produces the results. This will require testing of the dye at high temperatures in case of breakdown within the structure due to the temperature. Ruby has been used with this technique for temperatures up to 600°C ³⁸.

2.2.1.2.2 *Delayed fluorescence*

The time between the substance being excited and fluorescence being seen varies with temperature. This factor can also be used for temperature measurement ³⁹. It is the triplet lifetime which decreases with the increase of temperature. This leads to an increased rate of delayed fluorescence. This technique is not widely used for temperature measurement.

Acridine Yellow and trehalose ^{21,39} glass combination have been used with this technique. The reduced diffusion rates in the glass prevents quenching from competing with the decay process. The combination of an activated decay route, and direct decay of the triplet state determines the triplet state lifetime at a given temperature. There is a very high temperature sensitivity due to the slow phosphorescence rate and the large energy barrier compared to other materials used.

2.2.1.2.3 *Absorption changes*

The absorption spectrum of the dye changes with temperature, this can be monitored using techniques readily available. Here the excitation spectrum is monitored at a given emission wavelength, while the temperature changes.

One compound that has been used with this technique is LuPO₄:Dy ⁴⁰, where a Nd:YAG laser was used at 266nm. It was noticed that the absorption lines do not appreciably broaden or shift.

2.2.1.2.4 Summary of the luminescence techniques available

The use of luminescence as a means of measuring temperature has been widely used for both environment and surface temperature measurement. There are two main techniques used for determining the temperature from the luminescence, using the peak shape, or using the decay time of the fluorescence.

Using the intensity of the emission peaks by themselves is not a reliable method as intensity of the peak is dependent upon a number of factors such as coating and laser energy. Using the ratio of peaks is a possibility, as this will remove non-temperature factors. The main advantage of intensity based measurement is that it the possibility for use as 2D measurement rather than single spot measurement. The ratio technique can be implemented through the use of two excitation sources at different wavelengths if the material can be stimulated at two wavelengths. This would require the intensity of the excitation sources to be measured, and the emission to be at two distinguishable wavelengths. It could also add extra expense to the final solution. Alternatively if a material emits more than one wavelength from the same excitation source then the ratio of the peaks can be used. This has the advantage of reducing the amount of equipment and measurements required thus creating a more reliable solution.

Using the shift in wavelength provides a technique that is independent upon changes such as the coating and the laser energy. Depending upon the material, the position of the wavelength may also change with pressure. This will have to be considered when selecting the material as the pressure within the compressor will change during operation, though this could be compensated for within the calculations but would introduce more error. As with the intensity technique it has the possibility for 2D measurement.

The decay-time of the luminescence has been shown to provide a strong relationship with temperature for a number of materials. This technique has the advantage of being independent upon coating and other environmental conditions. To implement this technique under the required conditions, a decay time less than 20 μ sec would be required. This technique can only be used for single spot measurement due to the short decay times.

From the above techniques it is the intensity ratio technique and shift in wavelength which is to be followed further. The main reason for this is that they will allow the technique to be developed into a 2D profile. The very short lifetime required for the decay time technique at high speeds would mean that large changes in temperature would result in only small changes in the lifetime, decreasing the accuracy of the system. The very short lifetime also makes it very difficult to be able to collect the lifetime data ³⁴. Using the ratio of intensities and the peak positions provides the opportunity for self-referencing which would remove any differences in the coating and effects due to external influences such as optical collection. A self-referencing technique will also remove the requirement of extra equipment making the system cheaper and easier to implement in industry.

2.3 Pressure measurement

Changes in pressure are present within compressors, pressures from atmospheric up to 4bar are present within the compressors that the temperature measurement system is to be used. Luminescent techniques can also be pressure sensitive as well as temperature sensitive. It is therefore important that the technique or material chosen is not pressure sensitive or that the pressure sensitivity can be accounted for.

Pressure sensitive paints have mainly been used in wind tunnels but more recently have been used in low speed flows and on rotating machinery. It has been shown that pressure measurements can be made using the luminescent technique. The advantage of pressure sensitive paints is that they give global surface measurements with spatial resolution much greater than those available from pressure taps⁴¹. The pressure sensitive paints are limited only by optical access and can therefore be used in places where pressure taps are impossible to install. The use of pressure is relatively simple and non-intrusive.

The problems associated with pressure sensitive paints are summarised below.

- Oxygen must be able to dissolve into and diffuse through the paint in order to quench the phosphor. This imposes limitation on the response, which for rapid pressure transitions could be significant.
- The majority of paints in use are for pressures close to atmospheric (0.5 to 2bar).
- Available paints do not include a reference phosphor, which is not pressure sensitive. This means that a reference luminescence value must be measured for every point on the object to be examined.
- All pressure sensitive paints undergo some photochemical decomposition. This is most severe when using ultraviolet excitation wavelengths or when the paint is subjected to high operating temperatures.
- The relative luminescence of all pressure sensitive paints are temperature dependent.
- Interference to the luminescent signal can also occur due to reflections from one surface to another.
- The use of a binder can affect the temperature sensitivity and limit time response of the paint.

A reliable, non-intrusive, rapid method of recording surface pressure measurements has many applications within the aerospace and automation industries. Using coatings designed for stationary objects cannot always be transferred onto moving models as loss of sensitivity and resolution can occur due to the increase in absolute pressure. As with the use of luminescent coatings for temperature measurement, the accuracy depends upon

the measurement system and the properties of the paint. The use of pressure sensitive paints has proved to be a promising tool for measuring surface pressure distributions⁴².

The response of the paint is inversely proportional to the absolute pressure in the air⁴³. The fluorescence of the phosphor used is quenched by oxygen. If the oxygen concentration in the air is constant the effect of luminescence quenching may be used for measurement of air pressure⁴⁴. Small pressure changes cause a small change in the total luminescence level, the changes due to temperature can obscure the changes due to pressure in a low speed flow. The intensity of the luminescence seen after excitation, by a suitable wavelength, is inversely proportional to the partial pressure of oxygen.

The quenching competes more effectively with slower phosphorescence than the faster fluorescence and is therefore more sensitive to pressure changes and also to changes in temperature as the quenching rate increases with temperature. The Stern-Volmer¹ constant is determined by recording the luminescence intensity as a function of pressure under controlled conditions. The use of lifetime measurements rather than intensity based measurements have the advantage that they are independent of coating thickness and illumination and therefore a reference measurement is not required. For intensity based methods a reference point is required at each measurement point. The reasons behind temperature dependence of the pressure paints can be explained by two factors⁴⁵. The oxygen solubility of the paint decreases with temperature, this causes a decrease in the Stern-Volmer equation. The rate of the quenching reaction of the phosphor increases with temperature and would increase the Stern-Volmer constant. It can occur that these two factors can compensate each other giving a paint that is temperature independent.

Another technique is to use rate decay of the fluorescence⁴⁶ rather than intensity as the fluorescence parameter measured. The advantages of this are the insensitivity to ambient light, paint thickness and surface curvature. A pulse laser is used as the excitation source. Large variations in paint thickness can reduce response time, which is roughly proportional to the square of the paint thickness. The time response of pressure sensitive paints results from the finite diffusion times of oxygen through the binder layers⁴⁷. Thickness of around $2\mu\text{m}$ will determine a response time of around 5msec.

¹ See Appendix- 9.8 Equations

The pressure spectra at room temperature of a material reflect the electronic structure⁴⁸. Poor reflectivity in the lower energy range, such as that observed with FeS₂, indicates an insulator while strong reflectivity, CoS₂ shows it to be metallic. As the pressure increases, the peaks which occur in FeS₂ and CoS₂ shift to higher energy levels. This shift indicates an increase in the distance between the energy band levels with an increase in pressure, and also indicates that the binding energy increases. Non-elastic deformation can occur at high pressures, this can cause errors in pressure measurements when coating techniques are used.

To find a phosphor that has low photodegradation, good quantum efficiency, satisfactory quenching, suitable finish and low temperature sensitivity is almost impossible. It is therefore seen that at the present time it is most suitable to measure the temperature in situ, and make the corresponding calibration. At low speeds pressure differences of 0.02psid have been measured at low speeds. Pressure ranges of 200mbar to 1000mbar have been recorded with accuracies of ± 2 mbar. Pressure sensitive paints can be reused as the affect of the pressure disappears once the pressure is removed.

It is possible to create one coating that can measure temperature and pressure simultaneously. The temperature sensitive phosphor must not be quenched by oxygen, the factor that causes pressure dependence. Ideally, these two phosphors would be excited by the same wavelength, emitting peaks that are far enough apart to be distinguished, but close together so that they can be detected using the same device with a high enough resolution. The ratio of the intensity of the fluorescence of the two phosphors must be independent of paint thickness, and not undergo photodegradation.

It is possible to remove the pressure dependence of a coating by using an impermeable glue such as PVA to place a barrier between the paint and the atmosphere⁴⁶. This will stop the pressure sensitivity of the paint by eliminating the oxygen, thus creating a local temperature sensor. Oxygen does slowly leak through the PVA barrier, and therefore cannot be used as an accurate means of measuring temperature over long periods. It could therefore be possible to measure both the temperature and the pressure at a point on a compressor blade simultaneously.

2.4 Luminescent materials available

The requirements of the temperature sensitive material is that it must have a high temperature coefficient, low pressure coefficient, high intensity, small linewidth, and little background. Research has been carried out to see if materials were known to be temperature sensitive over the 20 to 300°C range. It was found that various researchers had studied a number of materials. There are many fluorescent materials that have been shown to produce temperature sensitive fluorescence, a list of materials studied in this work is summarised in Appendix 9.5. Temperatures ranging from -200°C to 1,500°C have been achieved using the luminescence technique and at speeds of up to 13,000rpm.

From this range of materials there are a few that stand out as possibilities for use with our system which are Acridine Yellow, Ruby, Sapphire, Lanthanum and Yttrium. These have been selected for further study due to the fact that they are known to have a temperature sensitivity in the range 100°C to 300°C, have proven to produce accurate temperature measurement, or have been used on rotating machinery before.

2.4.1 Acridine Yellow

Acridine Yellow has been used in experiments by J.C. Fister et al^{21,39}, where they considered a temperature range of -50°C to 50°C. They considered both lifetime and ratio techniques. It was found by Fister et al that Acridine Yellow has a very high temperature sensitivity of the delayed fluorescence lifetime compared to Ruby and Neodymium.

The luminescence spectrum has two peaks, one being fluorescent at 500nm the other phosphorescent at 630nm. The peak at 500nm was proven to change with temperature whereas the 630nm peak is independent of temperature. The two peaks can be used together to determine temperature, meaning a self-referencing technique can be used.

A time-dependent blue shift could be seen in the fluorescence spectrum, it was also found that the intensity ratio decreased with time. It was determined that due to high

temperature sensitivity of Acridine Yellow it could be used to give a temperature reading to the nearest degree, in the range -50°C to $+50^{\circ}\text{C}$.

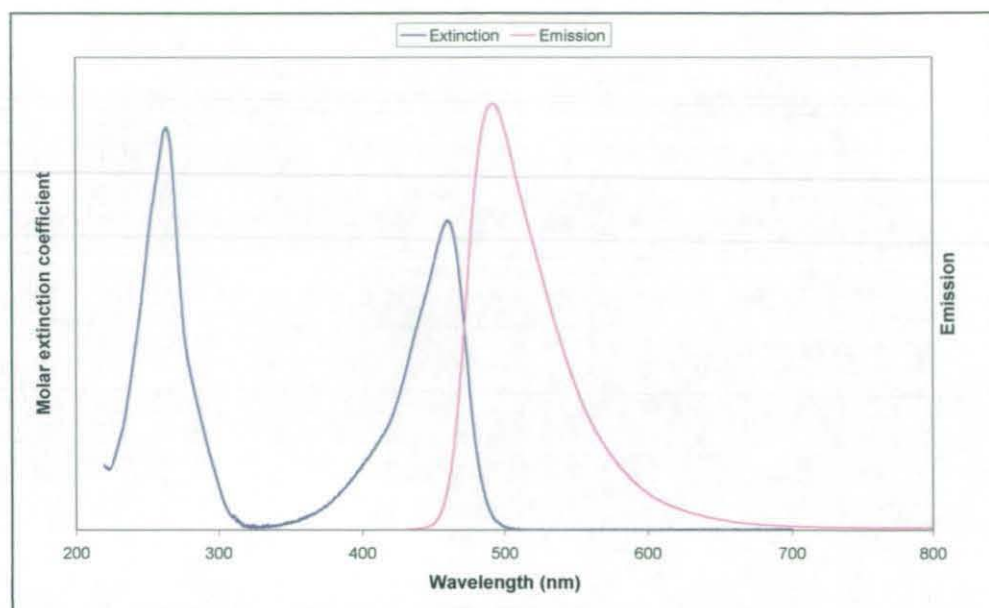


Figure 2-1 The Extinction and Emission spectra of Acridine Yellow⁴⁹.

2.4.2 *Ruby*

Ruby works well as a fluorescent material as it has an unusually broad and well located pump absorption band⁵⁰. It has been used in laser applications for a number of years, it was in fact used in the first optical MASER⁵¹. Its properties are well known and defined and it is easily obtainable as synthetic Ruby is grown for use in the laser industry.

It can make very efficient use of the broadband radiation from standard flash lamps. It emits with a very narrow linewidth with a long lifetime and has a fluorescent quantum efficiency very close to 1. The Ruby emission is exponential in profile, examination of the pulse showed that during the first millisecond the output is not smooth. It was also determined that the emission consists of a sequence of sharp narrow pulses. Under stable conditions this spiking appeared to damp out.

Ruby has been used for temperatures in the range -200°C to 500°C , though most previous work has concentrated on the range -200°C to 170°C . The Ruby mainly used in previous work has generally had a Chromium content of 0.05%, which is the same as the Ruby used in lasers. It has been determined that above 500°C the efficiency of Ruby drops significantly causing a decrease in the intensity and the lifetime^{19,52}. At temperatures lower than -200°C re-absorption was found to be a problem which affected the fluorescence spectrum¹⁹.

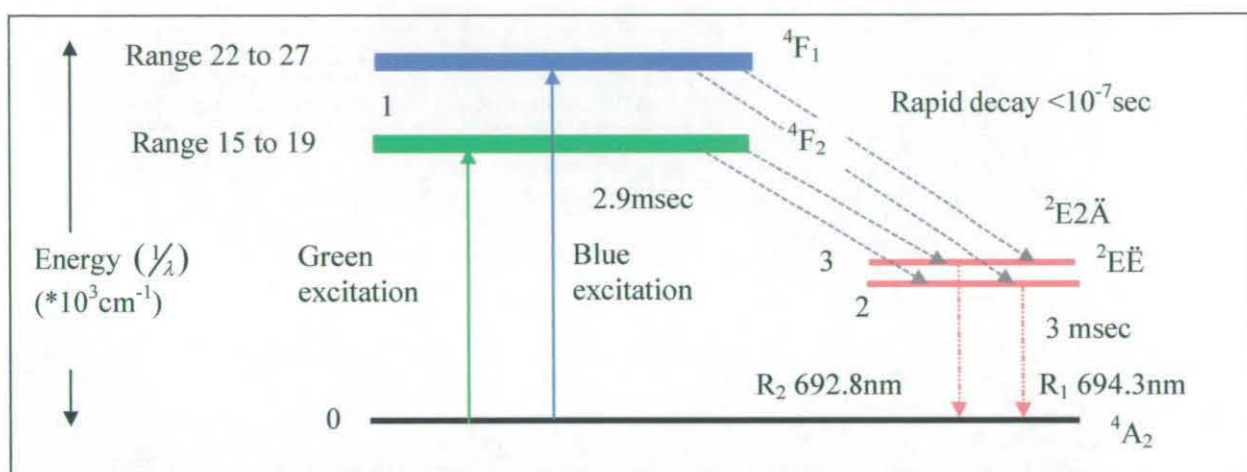


Figure 2-2 The energy-levels of ruby.

Synthetic rubies have an afterglow of 3.5 msec, in natural rubies the luminescence is quenched by the presence of iron and so a much shorter duration of afterglow can be seen.

Crushed Ruby was used by Ghasemlooy et al⁵³ in producing a cheap temperature probe and in this study it was determined that crushing the Ruby did not affect the fluorescence. Crushed Ruby has the advantage of not requiring expensive polishing of the surface and enables low quality Ruby material to be used. The crushed Ruby can be used as a mass of miniature prisms, causing random scattering of the excitation wavelength as it passes through the Ruby. This scattering produces an increase in the path length of the excitation wavelength and therefore an increase in the absorption of the light. When using fine Ruby crystals it can be assumed that there is no pressure difference acting on the material.

Temperature affects both the coefficient of absorption throughout the spectrum and the position of the lines and bands in the absorption spectrum⁵⁴. It is the red side that is affected the most by temperature, the blue transmission was nearly cut out at higher temperatures. There is a shift in the absorption band in the green from 548nm to 566nm. This creates a broadening of the absorption band as the temperature increases. Throughout most of the spectrum there is a large increase in the absorption as the temperature increases, but in the blue-green area the absorption decreases.

2.4.2.1 Temperature measurement using Ruby

The bandwidth, peak position, intensity and the decay time all change with temperature. The bandwidth increases, peak position shifts toward higher wavelengths, the two peaks shift at different rates causing a separation of the two peaks. The intensity decreases with temperature, becoming more rapid after 200°C, and the decay time decreases also. The loss in intensity from the peaks is redistributed to higher and lower wavelengths on either side of the peak, therefore a constant fluorescence output is kept but only to 500°K³⁰.

At low concentrations of chromium, <0.1%, the luminescence spectrum is dominated by two strong lines R₁ and R₂⁵⁵. Increasing the chromium level above this lines are found at 750nm. At -200°C the lines R₁ and R₂ are the weaker, with the peak at 750nm being dominant. At 25°C the lines R₁ and R₂ are the strongest though the 750nm peak is still strong. Above 520°C the fluorescence quantum efficiency of Ruby drops dramatically and the lifetime also becomes much shorter¹⁹.

Large and small temperature probes were compared by Hu et al¹⁹. It was determined that the smaller probe had a shorter fluorescence lifetime than the larger probe especially at temperatures below -70°C. This suggests that the fluorescent light is reabsorbed and re-excited in the larger probe. The relationship between the luminescence of Ruby and temperature has been studied by a number of groups, the definitions determined are detailed below.

The relationship between temperature and peak wavelength was defined by Abella and Cummins⁵⁶ as;

$$\lambda(T) = 6943.25 + 0.068(T - 20)$$

Equation 2-3

With temperature being in degrees Celsius and wavelengths being in angstroms.

A relationship determined by K.S. Gibson⁵⁴, for the absorption spectrum is shown below.

$$\lambda = a + be^{kT}$$

Equation 2-4

$$\lambda = 6900 + 22e^{0.01637T}$$

Equation 2-5

$$\lambda = 6900 + 23e^{0.0157T}$$

Equation 2-6

Where a, b, k are constants, wavelength is in angstroms and temperature in degrees Celsius. The differences in the constants from the two data sets could be explained by the accuracy of the detection equipment used.

It was determined that temperature sensitivity in the high temperature region is higher and therefore temperature can be determined to within a degree or even a fraction of a degree within 0.1 cm^{-1} discrepancy⁵⁷ in the peak position.

It has been determined by Munro et al that in the temperature range 20°C to 200°C the relative intensity of the two peaks varies very little with temperature but above this temperature the intensity decreased rapidly to only 80% of the initial value at 270°C .

The linewidths of R_1 and R_2 increase exponentially with temperature and at different rates. It is thought that under increasing pressure the two linewidths decrease slightly, this finding was surrounded by uncertainty in the pressure coefficient describing the change hence the reason for doubt.

Gaussian and Lorentzian functions¹¹ can be used to represent the basic trend of the emission from Ruby, though as the temperature increases the representation becomes less and less similar to the actual trend. Combining the Gaussian and Lorentzian function creates a third function the Voigt function, this can be adjusted to give a good profile of the Ruby spectrum in the R_1 and R_2 region. The Gaussian trend is due to strain broadening due to the random crystal field distortion⁵⁸, and can generally be taken to be temperature independent. The Lorentzian contribution is from two-photon relaxation and thermal broadening. Munro et al⁶ considered this in detail.

In summary, it is determined that wavelength will increase with an increase in temperature, the decay time will decrease, and the intensity will decrease.

2.4.2.2 *Pressure measurement using Ruby*

At room temperature and under hydrostatic pressure the R_1 line has a red shift, while the separation between R_1 and R_2 stays almost constant⁵⁹. In pure uniaxial strain measurements the separation between R_1 and R_2 increases for Ruby strained along the a-axis and decreases when strained along the c-axis. The affects on the peak R_2 cancel and the overall change in fluorescence wavelength is due to the volume change as in hydrostatic compression. It was concluded that R_1 is sensitive to inhomogeneous strain and R_2 is sensitive to all pressure.

It was shown that the shift of R_1 depends upon the direction of the applied stress, where R_2 has little dependence on the direction of the stress⁶⁰. This was agreed by Gupta⁶¹ et al who also stated that the R_1 line is dependent upon nonhydrostatic stresses where R_2 is independent on nonhydrostatic stresses. It was also noted by Eggert et al⁶² that the R_1 line broadens more radically than the R_2 line. Chai et al⁵⁹ determined that if R_1 was used for measuring pressure, a difference of 3Gpa could occur between from underestimating c-axis and overestimating a-axis. This indicated that the R_2 line is most useful in pressure measurement.

¹¹ See Appendix - 9.8 Equations for definition

Further experimentation by Chai et al⁵⁹ showed that in the pressure region 2GPa to 12GPa, the predicted separation and actual separation agreed well for the c-normal samples. With the a-normal samples this was only so up to 6GPa. The best fit to the c-normal data gave a relationship between pressure and separation as $0.241 \pm 0.012 \text{ \AA/GPa}$. This compares well to the relationship determined by Feher et al⁶³ of $0.273 \pm 0.015 \text{ \AA/GPa}$. No line broadening was noted by Gupta et al though they noted an increase in R line separation with increased compression along the a-axis.

Nonhydrostatic pressure tends to create broader lines, this is largely due to the pressure gradients⁶². In areas of sparse Ruby coverage substantial line narrowing occurred compared to areas of heavy Ruby coverage. This showed that in the presence of pressure gradients small sampling areas are advised. At high pressures there is a large difference in the R_1 line frequency between nonhydrostatic and quasihydrostatic pressures. Under hydrostatic pressure the two R lines shift equally⁶¹.

It was seen by Piermarini et al⁶⁴ that the spectral line broadening was greater than expected for simple pressure variations. They determined that this was due to local uniaxial components of the stress which affect both the frequency of the emitted light and the hydrostatic component. In a later paper⁶⁵ they determined there is a linear pressure dependence up to about 23kbar of $\pm 0.003 \text{ cm}^{-1} \text{ kbar}^{-1}$. It was also determined that as well as line shift, line shape was also an important factor in the analysis. Findings from Ruby under nonhydrostatic stress show that R_1 and R_2 linewidths increase rapidly. This is due to the non-uniformity of the pressure on the sample.

Without detailed knowledge of the crystal orientation and the stress type it is difficult to use R_1 for pressure measurement. The R_2 line shift is dependent only upon the density compression and is therefore independent of crystal orientation and stress type.

Previous use of the changes in the R line with pressure has involved pressure ranges much higher than that inside the compressor housing. Looking at two of these studies it can be seen that in the range of 0 to 195kbar the accuracy was $\pm 0.016 \text{ kbar \AA}^{-1}$. At an even higher pressure range 0.06 to 1Mbar the accuracy was low as 6% in terms of pressure.

The pressure range that is present within the compressor housing is ambient to 4bar (400kPa). As the pressure change is insignificant compared to the pressure ranges that

have been considered it is thought that the small changes in pressure will not significantly affect the Ruby spectrum.

2.4.2.3 *Temperature and pressure measurements with Ruby*

Munro et al⁶ have modelled the Ruby spectrum using a combination of Gaussian and Lorentzian. From this the positions and widths of the two peaks R_1 and R_2 can be determined which can be used to measure both temperature and pressure. The defined model is shown below.

$$R(x) = c_1 R_1(x) + c_2 R_2(x) + \rho(x)$$

Equation 2-7

where;

$R(x)$ = net intensity at the position x
 c_1 & c_2 = amplitude factors for the R_1 & R_2 peaks
 $\rho(x)$ = background factor

$$R_k(x) = C_L(k)L(A_k, B_k, x) + (1 - C_L(k))G(A_k, B_k, x)$$

Equation 2-8

where;

$C_L(k)$ = relative amplitude factor $0 \leq C_L(k) \leq 1$

$$L(A, B, x) = \frac{B^2}{B^2 + 4(A - x)^2}$$

$$G(A, B, x) = \exp\left(\frac{\ln(1/2)(A - x)^2}{(B/2)^2}\right)$$

Equation 2-9

where;

A_k = peak position for peak R_k
 B_k = full width at half maximum (FWHM) for the Lorentzian contribution
 B_k = full width at half maximum (FWHM) for the Gaussian contribution

The peak position and the amplitude factors are functions of both temperature and pressure.

2.4.3 Sapphire

Sapphire is a material with chromium host with an added dopant, the dopant added determines the colour of the sapphire which can be yellow, green, blue or pink. Naturally occurring Sapphire is blue in colour while Sapphire that is used in lasers is pink in colour, which comes from its Titanium (Ti) dopant.

Using the decay time for temperature measurement with Sapphire can give a resolution of 1°C over the temperature range 20 to 450°C ⁶⁶. The lifetime of Cr doped Sapphire is similar to that of Ruby, at room temperature it is 3msec, and at 450°C it goes down to 0.5msec ⁶⁷. The absorption and emission spectra can be seen in Figure 2-3.

When being used for temperature measurement Sapphire tends to be used as a fibre optic temperature sensor. Sapphire has been used to measure temperature to an accuracy of $\pm 0.01^{\circ}\text{C}$ within the temperature range -200°C to $4,000^{\circ}\text{C}$ ⁶⁸. The technique is implemented on a temperature sensitive probe, where the purpose of the Sapphire is to collect narrow band radiation from the surface to be measured which is transmitted to a fibre optic. Using a Cr doped fibre optic Shen et al ⁶⁷ have determined a technique where both lifetime and intensity can be used in the same detector to produce a temperature range of 20 to 1800°C .

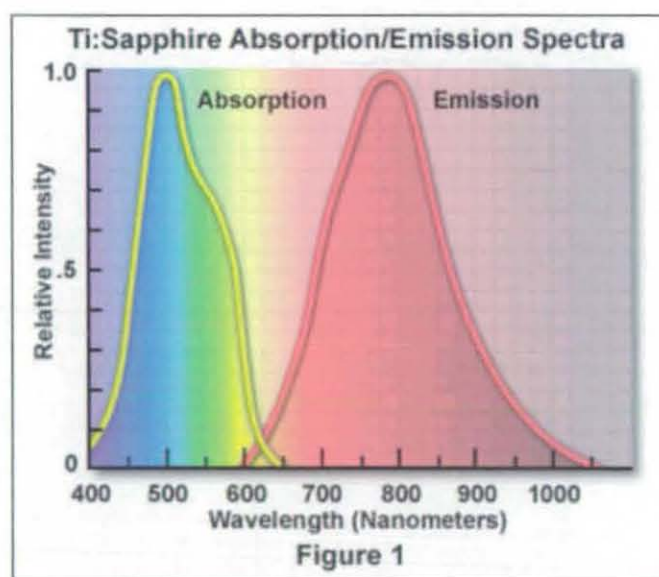


Figure 2-3 The absorption and emission spectrum for Ti:Sapphire ⁶⁹

The disadvantage of Sapphire is that it only emits a single broad band peak which means that it cannot be self referenced. Although it has been used to measure a wide range of temperatures accurately this has been done using a high quality piece of material in controlled conditions. As the material has to be ground to achieve a coating then the quality of the material would be seriously disadvantaged. Given the fact that it is known to produce such accurate temperature readings the fluorescence spectrum will be considered for temperature measurement from a surface.

2.4.4 Phosphors

Thermographic phosphors are mainly ceramics which consist of rare earths, phosphates, or oxysulfides, where a different rare earth doped into the structure⁸. They are chemically stable, durable metal oxides. These are very efficient and have lifetimes ranging from nano-seconds up to seconds. Their uses include lamps, colour TV. There are two main phosphors that have been used for temperature measurement, these are Lanthanum (La) and Yttrium (Y) bases which are both rare-earth doped group III metals. To achieve the fluorescent spectra the main dopants that have been used are Eu, Dy, Tb, and Gd. These materials together with their dopants are discussed below.

2.4.4.1 Lanthanum

Lanthanum as a metal is soft, ductile and is one of the most reactive of the rare-earth metals⁷⁰. It has been used for both intensity and decay time techniques, it has a short decay period, which means that it is a suitable material to use on a spinning object.

Coating techniques that have been used include the settling technique³⁴, this technique is used in coating cathode ray tubes, this produces a very fragile coating and a protective layer have to be placed over the top. Work undertaken by Fonger & Struck 1970⁷² shows that the intensities of the different wavelength emissions from $\text{La}_2\text{O}_3\text{:Eu}$ are affected differently by temperature.

The material $\text{LaF}_3:\text{Dy}^{+3}$ produces a poor accuracy, and little is known about the luminescence of the material so it has been decided not to continue with this material. $\text{La}_2\text{O}_2\text{S}:\text{Eu}$ shows good potential though a disadvantage of this material is that it requires ultra violet to excite it which is a difficult wavelength to range to work in as it does not transmit easily through optics.

Material	Technique	Temperature	Excitation	Emission	Decay period @room temp	Ref
$\text{LaF}_3:\text{Dy}^{+3}$	Ratiometric	25 → 1225°C ± 10 → 50°C				29
$\text{La}_2\text{O}_2\text{S}:\text{Eu}$	Intensity, lifetime	-70 → 300°C ±0.3°C	337, 355	512, 537 does not change until above 150°C, 620	0.02 → 0.12 msec	71, 72, 73, 67, 72, 31, 74

Table 2-1 The uses of Lanthanum based phosphors for temperature measurement
iii

2.4.4.2 Yttrium

Research based on Yttrium based coatings has looked at the use of temperature to anneal the coating to increase the intensity of the emission^{75,76}. A number of Yttrium based materials has shown a relationship between temperature and their fluorescent spectrum, these are shown in Table 2-2. Yttrium oxysulphide ($\text{Y}_2\text{O}_2\text{S}$) itself emits an intense output with a short decay period⁷⁷, the dopant, and the level of dopant within the material can affect this output.

The concentration of the dopant can affect the intensity of fluorescence. For $\text{Y}_2\text{O}_3:\text{Eu}$ to achieve maximum fluorescence the dopant was found to be in the region 25 to 35 atomic percent⁷⁸. The dopant level can also affect the sensitivity of the phosphor's sensitivity to temperature. Ranson et al⁷⁸ have tested for this affect and have found the temperature range and sensitivity remains constant for a dopant level of 25 to 35 atomic percent (a%).

ⁱⁱⁱ See Appendix - 9.5 Luminescent Materials for more detailed table

Of the materials in Table 2-2 those which show possibility for use in this application are $Y_2O_3:Gd$ because it is sensitive within the required temperature range, has a short lifetime, and could use the ratio technique. $Yag:Dy$ also shows possibility, as it is sensitive to temperature in the required range, and has a short lifetime. It has only been considered for temperature measurement using the decay time technique so it is not known whether its peak could be used for temperature measurement.

Material	Technique	Temperature	Excitation	Emission	Decay period @room temp	Ref
$Y_2O_2S:Eu$	Decay time	60 → 150°C	254, 337 250 → 400	624 400 → 700		79, 72, 80
$Y_2O_2S:Tb$	Intensity, Decay time	200 → 500°C		545nm	300nsec to 1msec	74
$Y_2O_3:Eu$	Intensity, Decay time	500 → 1200°C	254, 355, 337, 467, 538	611	500µsec 300nsec to 1msec	81, 82, 78, 83, 84, 74, 76
$Y_2O_3:Gd$	Intensity, Decay time	48 → 465°C		418nm peak has max at 105°C 549nm peak has max at 160°C	300nsec to 1msec	74
$Y_2O_3S:Pr^{3+}$	Linewidth	-270 → -70°C				85
YAG:Dy	Intensity	27 → 1427°C	355	467, 496, 514		29
YAG:Nd	Decay time Blackbody	50 → 900°C ±3°C	810	1064		13
YAG:Sm	Frequency shift	700°C				86
YVO ₄ :Dy	Decay time	290 → 450°C		574		73
YVO ₄ :Eu	Decay time	300 → 760°C	337, 355	618	500µsec	81, 82, 83, 87, 88

Table 2-2 Yttrium based phosphors for temperature measurement^{IV}

Work undertaken by Fonger & Struck 1970⁷² shows that the intensities of the different wavelength emissions from $Y_2O_2S:Eu$ are affected differently by temperature. Though there is little affect with temperature below 25°C. $Y_2O_2S:Eu$ has been found to have an upper threshold limit of 100µJ, at which the phosphor saturates⁸⁰. It is therefore important that the laser energy is kept below this.

The Yttrium phosphors have been coated onto surfaces using a number of techniques. $Y_2O_2S:Eu$ has been successfully coated onto a surface creating a luminescent paint using an epoxy to powder ratio of 1:1 by weight⁸⁰. $Y_2O_3:Eu$ has been coated using electron-

^{IV} See Appendix - 9.5 Luminescent Materials for more detailed table

beam deposition, which has been shown to give strong emission after coating, when compared to the powder before coating⁸¹, though during running this decayed and epoxy based coating survived much longer.

Material	Excitation	Emission	Decay period to 10% @room temp	Efficiency
Y ₂ O ₂ S:Eu	320nm broad	619nm multiple peaks	0.85 msec	14%
Y ₂ O ₂ S:Eu,Yb	0.8μm, 1μm 1.55μm	560nm or 900nm excitation dependent, multiple peaks	Process dependent	Excitation dependent
Y ₂ O ₂ S:Tb	280nm	545nm multiple peaks	1.5 msec	
Y ₂ O ₃ :Eu	480nm	610nm	1.7 msec	
Y ₂ O ₃ S:Pr	310nm	513nm multiple peaks	7 μsec	14%
Y ₂ SiO ₅ :Ce	370nm	400nm broad	120 μsec	6%
Y ₃ (Al,Ga) ₅ O ₁₂ :Ce	365nm broad	530nm broad	250 nsec	
Y ₃ Al ₅ O ₁₂ :Ce otherwise known as YAG:Ce	360nm broad	530nm broad	70 nsec	
Y ₃ AlO ₃ :Ce	300nm broad	370nm broad	25 nsec	
YVO ₄ :Eu	330nm broad	617nm multiple peaks	1 msec	
YVO ₄ :Eu	330nm broad	478nm	220 μsec	

Table 2-3 The specification for Yttrium based phosphors available from Applied Scintillation Technologies.⁸⁹

Consideration into the availability of the phosphors was considered as well as similar materials and these are detailed in Table 2-3. Of these materials there is one that could be used for temperature measurement which, is Y₂O₃S:Pr due to its very short lifetime and multiple peak emission.

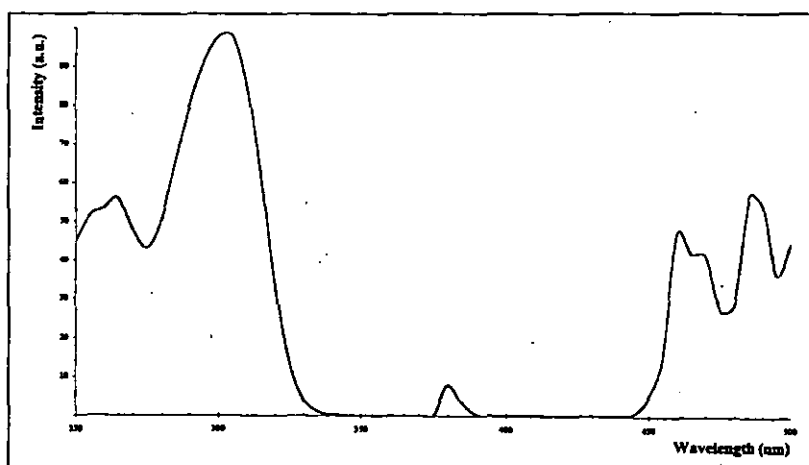


Figure 2-4 The absorption spectra of Yttrium oxysulphide praseodymium doped⁸⁹.

Praseodymium has been used as a dopant in many rare-earths, and is known to emit strong fluorescence. Although little work has been undertaken for its use as a temperature sensor, its short decay times makes it an ideal candidate for high speed applications.

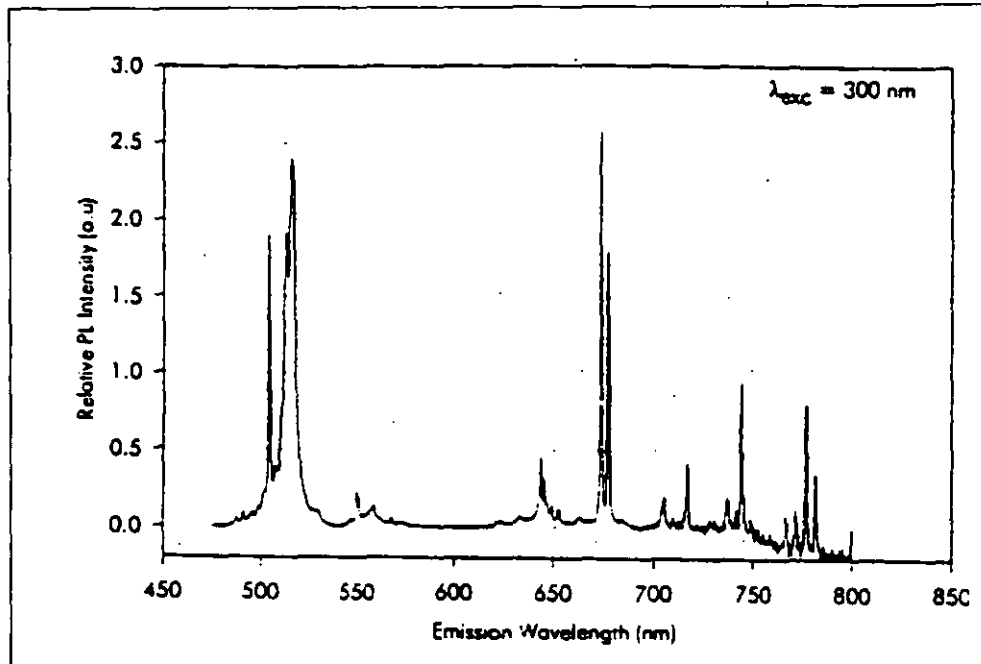


Figure 2-5 The emission absorption spectra of Yttrium oxysulphide praseodymium doped⁸⁹.

From the many Yttrium based phosphors that are available, those which show potential for use in this project are $Y_2O_3S:Pr$, $Y_2O_3:Gd$, and $Yag:Dy$. These have been selected due to their short lifetime, emission spectrum, and their known temperature dependence within the required temperature range.

2.4.5 *Summary of the luminescent materials available*

From the research into finding possible luminescent materials there is a wide selection of possible materials. Of these there is a number that have been considered extensively by others. These are Ruby, $Y_2O_3:Eu$, $YVO_4:Eu$ and $La_2O_2S:Eu$. A summary of the materials considered to be the most promising is shown in Table 2-4. The materials have been rated on their properties to determine which to continue with.

Ideally a material would be known to produce a strong temperature relationship in the range 100°C to 300°C, to remove the need for calibration of a material. It should have multiple peaks and use peak intensity, peak position or peak width for temperature measurement to enable it to be self referenced and to allow for 2D temperature mapping to be considered in the future. It should have a decay period of less than 20µsec to allow the maximum fluorescence intensity to be collected while spinning. It should be easily obtainable so that it is possible for industry to be able to purchase the material. It should be excited in the visible as it is easier and cheaper than ultra violet radiation to use. Using a point system for the number of criteria that each material matches it can be seen that there are a limited number of materials that could be considered for use, these are discussed here.

Material	Known to be temperature sensitive in range 100 → 300°C	Uses peak sensitivity for temperature measurement	Decay period less than 20µsec	Multiple peaks	Easily obtainable	Visible excitation wavelength	Score
Acridine Yellow	No	Yes	?	Yes	Yes	Yes	4.5
La ₂ O ₂ S:Eu	Yes	Yes	No	Yes	No	No	3
LaF ₃ :Dy ⁺³	Yes	Yes	?	?	No	?	3.5
Ruby	Yes	Yes	No	Yes	Yes	Yes	5
Sapphire	Yes	Yes	No	No	Yes	Yes	4
Y ₂ O ₂ S:Eu	No	No	No	Yes	Yes	Yes	3
Y ₂ O ₂ S:Tb	No	Yes	Yes	No	Yes	?	3.5
Y ₂ O ₂ S:Yb	?	?	?	Yes	Yes	No	3.5
Y ₂ O ₃ :Eu	No	Yes	Yes	No	Yes	No	4
Y ₂ O ₃ :Gd	?	Yes	?	?	No	?	3
Y ₂ O ₃ S:Pr	No	Yes	Yes	Yes	Yes	No	4
Y ₂ SiO ₅ :Ce	?	?	Yes	No	Yes	No	3
Y ₃ (Al,Ga) ₅ O ₁₂ :Ce	?	?	Yes	No	Yes	No	3
Y ₃ Al ₅ O ₁₂ :Ce	?	?	Yes	No	Yes	No	3
Y ₃ AlO ₃ :Ce	?	?	Yes	No	Yes	No	3
YAG:Dy	Yes	Yes	No	Yes	No	?	3.5
YAG:Nd	Yes	No	?	No	No	No	1.5
YAG:Sm	Yes	Yes	?	No	No	?	2
YVO ₄ :Dy	No	No	?	No	No	?	1
YVO ₄ :Eu	No	No	No	No	No	No	0

Table 2-4 Summary of the materials considered.

Work undertaken by Fister et al with Acridine Yellow shows that it can give a temperature accuracy to 1°C. It emits at two wavelengths, though one of which is

phosphorescent which may not be of use for high speed temperature measurement. Work into the temperature sensitivity of Acridine Yellow above 50°C is to be carried out to see if this material is suitable for this work.

Ruby gives two strong sharp fluorescent peaks. This means that it can be used with the ratio technique, the position of the peaks also changes with temperature. The number of effects with temperature means that it can provide more accurate means of temperature measurement than one single reading. It has been used previously to achieve an accuracy of less than $\pm 1^\circ\text{C}$. Its major problem is its long decay period, this will mean that only a small portion of the luminescence will be available for collection. As Ruby has a high efficiency it is thought that Ruby would still be a viable solution.

Although Sapphire has a very similar chemical structure to Ruby its emission is a broad single peak. It has been shown to produce temperature readings to an accuracy of $\pm 0.01^\circ\text{C}$. This has been achieved using a high quality piece of material in controlled conditions. As the material has to be ground to achieve a coating then the quality of the material would be seriously disadvantaged. Given the fact that it is known to produce such accurate temperature readings the fluorescence spectrum will be considered for temperature measurement from a surface.

Yttrium Oxide Europium doped ($\text{Y}_2\text{O}_3:\text{Eu}$) has been studied extensively and has not been found to be temperature sensitive within the range 100°C to 300°C. It is stated by Noel et al ⁷⁴ that this material is usable for temperature measurement above 550°C, when carrying out experiments from room temperature up to 900°C. It is therefore not viable to continue with this material.

Yttrium Oxysulphide Praseodymium doped ($\text{Y}_2\text{O}_3\text{S}:\text{Pr}$) is a material that has little investigation for its temperature sensitivity. It has a short lifetime which is particularly important for this application, and emits strongly at a number of wavelengths. Yttrium based materials are known to create good fluorescent coatings and have been implemented well for temperature measurement. It is therefore considered worth looking into whether $\text{Y}_2\text{O}_3\text{S}:\text{Pr}$ shows a temperature sensitivity within the required temperature range

This gives four materials to be looked into further; Acridine Yellow, Ruby, Sapphire and $Y_2O_3S:Pr$. Although Ruby has a long decay time, its relationship with both temperature and pressure is well known. It is also an efficient material which is easily obtainable. It has been used successfully on many occasions previously as a temperature sensor for environmental conditions rather than surface measurement. Yttrium Praseodymium doped has not been used as a temperature sensor but shows great potential for use on high speed objects due to its short decay period and high efficiency. Yttrium Oxysulphide doped with various elements has been shown to be temperature sensitive from $-70^{\circ}C$ up to $1200^{\circ}C$.

2.5 Measurement from a rotating disc

Fluorescent materials have been used to measure the temperature of a rotating turbine wheel ^{73,74,81,90,33}. Reading the luminescence spectrum from an object that is rotating at high speeds produces many obstacles. The main one being, collecting sufficient light to enable the luminescent peaks to be determined from the background. The other major problem is the forces and environmental conditions endured by the coating when subjected to the high speeds of rotation, causing the coating to break up and come away from the disc.

Temperatures of up to 670°C and speeds of up to 13,200 rpm have been achieved ⁷³ using the decay time luminescent technique. Using the decay time technique means that the delay period has to be short, at a speed of 13,200 rpm a decay time of about 200µsec is required to enable one full decay period to be recorded ⁷³. Using longer decay periods relates in a drop in the accuracy of the temperature reading. The phosphors used to achieve this temperature range are La₂O₂S:Eu, YVO₄:Dy and Mg₄(F)GeO₆:Mn ^V. Temperatures were found to be within 4% of the readings given by thermocouples. For temperatures up to 1,200°C Yttrium Oxide (Y₂O₃) has been used.

It has been reported that there is a difference in the temperature measured using luminescence and thermocouples when used on a rotating object ⁹¹. This difference is said to increase at higher rotational speeds. It has been evaluated by using infrared techniques and the results showed that the temperature shift was possibly due to disturbance errors which affected the thermocouples rather than affects due to the thermochromic liquid crystal.

The error in the thermocouple reading can be explained. For a rotating body at a constant temperature, the heat transfer coefficient and hence the surface heat flux increases as the rotational speed increases. The thermal disturbance error created by an embedded thermocouple will increase with rotational speed ⁹¹. Measurements that use fibre optics will usually require at least two fibres because of the narrow field of view.

^V More details of these materials can be seen in the Appendix – 9.5 Luminescent Materials

To enable temperature to be measured on rotating surfaces using an infrared camera, a software package has been developed ⁹². A thermal profile is produced by projecting a line on to a rotating object. The line is scanned with a known frequency, stored, and used later for analysis. This is possible with speeds of up to 300rpm, giving an accuracy of $\pm 5^{\circ}\text{C}$ over a temperature range of 50°C to $1,000^{\circ}\text{C}$.

The fluctuation of the speed of the turbine will affect the consistency of the point being monitored and this will also affect the calibration when intensity based techniques are being employed. Pulse jitter, phase-delay and trigger error of the laser are also factors affecting the timing system. The resolution can be improved by using a thin delivery fibre in conjunction with a focusing lens to produce a smaller spot size. It will be important not to view too small an area or local fluctuations and errors in the fluorescence will affect the overall result required.

2.5.1 *Optical Affects*

Doppler shifting is a technique used for measuring the vibration of a rotating object. In this technique a laser beam is reflected from the rotating surface and the movement is recorded through the change in wavelength detected. With our situation the light we are interested in, is being generated from the moving object.

$$V_s = 2\pi NZ.\text{Cos}(Y)$$
$$f_r = \frac{4\pi}{\lambda} Na.\text{Cos}(Y)$$

Equation 2-10 Doppler shift

Where;

V_s = Speckle pattern velocity

F_r = Mean frequency shift

Y = Angle between disc velocity and the incident beam

Z = Distance between the detector and the laser spot on the disc

N = rev/min

A = Radial position of the spot on the disc

It has been stated by Allison et al ³¹ that the decay-time of fluorescence is only rotation-rate dependent when the surface speed is comparable to, or greater than, the inverse of the phosphors characteristic decay time.

$$\text{Intensity is a factor of speed if surface speed} \geq \frac{1}{\text{decay time}}$$

Equation 2-11

When running at speeds of 80,000rpm a decay time of greater than 1.7msec is required, at 40,000rpm this increases to 3.4msec, when considering the surface speed in metres per second.

2.5.2 Materials used

Materials that have been used for temperature measurement on rotating objects are summarised in Table 2-5. The decay time is the technique that has been most widely used for measuring the temperature from rotating objects. At higher speeds less of the decay time is seen which reduces the accuracy of the measurements. The decay time techniques is more widely used as this is seen as being more accurate because this is not affected by changes in laser intensity, coating quality and other factors which intensity measurements can be affected by.

Material	Technique	Temperature range	How used	Ref:
La ₂ O ₂ S:Eu	Decay time	100 → 300°C	Turbine wheel 13,200rpm	73, 31, 93
La ₀ F ₃ :Dy ⁺³	Decay time, intensity	-70 → 230°C	2,000rpm	93
Liquid crystal			7,500rpm	91
Mg ₄ (F)GeO ₆ :Mn	Decay time	450 → 730°C	Turbine wheel 13,200rpm	73
Y ₂ O ₂ :Eu	Decay time	650 → 1200°C	10,568rpm	71
YVO ₄ :Dy		290 → 450°C	Turbine wheel 13,200rpm	73
YVO ₄ :Eu	Decay time Intensity ratio	149 → 677°C	10,568rpm	73, 71, 43

Table 2-5 Materials that have been used for temperature measurements from spinning objects.

2.5.3 *Measurement within Turbine Engines*

Within the turbomachinery industry there are many areas where temperature measurement is an important variable in order to determine accurately. Such areas are turbine and compressor blades, housing, and air flow. Rolls-Royce⁹⁴ have researched into temperature measurement in gas turbines. They feel that to accurately characterize engine component efficiency to $\pm 0.5\%$ the engine gas path temperature must be measured to accuracies ranging from $\pm 2^\circ\text{C}$ to 0.25°C . They have considered the use of different types of thermocouples for use in the temperature range -20°C to 60°C .

Research has been carried out on the measurement of temperature on the first stage rotor blades and stator blades, of the turbine^{73,74,83}. These blades are positioned just behind the burner so are the most difficult part of the turbine to measure due to them being the hottest and reflecting the blackbody radiation from the fuel. It is important the coating used will withstand the temperature, speed and the erosive environment.

Decay-time measurements were implemented to determine the temperature⁷³. The disk was run at 4 different speeds each with different ambient temperatures, these are stated here 6,600rpm 149°C , 9,330rpm 316°C , 1,140rpm 482°C , 13,200rpm 677°C . To measure more than one point on the disk a mirror was used to direct the laser beam.

It was thought by Lutz et al that the use of spectral analysis of the fluorescence is less precise than decay-time techniques. The decay-time technique is already implemented onto moving objects. To measure this range of temperatures three different phosphors were used.

Lutz et al only used 22% of the available decay-time to determine the temperature, which relates to 60% of the intensity. This is due to distortion of the results through a slight tilt in the flat-field data later in the decay period. The results were found to be comparable with a thermocouple within 4% ($\pm 12^\circ\text{C}$ @ 300°C).

2.5.4 *Conclusion*

The luminescence technique of temperature measurement has been used previously for speeds up to 13,000 rpm. Both decay time and intensity based techniques have been used. At 80,00rpm decay times of about 20 μ sec or less are required to collect all the fluorescence emitted by the material. With such low decay times the intensity based technique will not be speed dependent. The main materials that have been used are Yttrium and Lanthanum based phosphors.

2.6 Coatings

There are many different methods of producing coatings available. Coatings are widely used to protect, strengthen, and to alter surfaces and their properties. This has been so for many years and much work has been undertaken to develop these techniques. Thin coatings mean smaller thermal gradients that increase the accuracy of the temperature reading from the thermographic coating. The texture of the surface required is dependent upon the type of coating technique used.

2.6.1 Techniques used for temperature sensitive coatings

The durability of thin film and bonded powder, otherwise known as thick film, coatings have been tested in a gas turbine engine by McClean et al⁸⁷ and Ranson et al⁷⁸. It was found that there was five times more loss for the bonded powder than the thin film coating and that the thin film coating will last for ten times longer. Both techniques showed good repeatability for the decay-time temperature measurement technique. The huge losses of material from the bonded coatings result in short operation times and a loss in accuracy. The thin film coating was produced through radio frequency sputtering. McClean et al⁸⁷ achieved the first successful thin film coating for use in the turbine environment.

Allison et al³³ have used radio frequency sputtering and electron-beam-deposition for creating coatings, the two techniques produce similar results. They found that regardless of the method used for bonding the phosphor to the surface, a significant increase in the efficiency can be achieved through post-annealing, after which efficiencies of 30 to 60% of the pure powder can be achieved. The authors have not stated a reason for this, though it is thought that the post-annealing has removed impurities within the material which could have caused quenching.

Electrodeposition is used for coating metallic surfaces onto components although this technique can produce thin coats. The use of electron-beam-deposition has been used to coat thermographic phosphors onto turbine blades. This was found to produce less than 0.7% of the brightness of the powder before deposition⁸³. Previous work by Noel et al has shown that thermographic phosphors bonded to nonpassivated areas either did not bond well or tended to come off after exposure to an oxidising atmosphere. They stated that this was due to the fact that the thermographic phosphor thin coating is porous to oxygen, the metal therefore oxidises and the oxide spalls when the metal cools taking the phosphor with it. This technique requires the phosphor to be hot or cold-pressed into a disk shape and mounted in the vacuum chamber.

The room temperature photoluminescent spectra for bonded films were more intense than that received from the thin film coating. Lifetime measurements were able to be taken for ten hours at 1,200°C with the thin film coating compared to one hour for bonded coatings at the same temperature. The post-growth process of annealing is an important part in the creation of thermographic thin film coatings. This allows the dopant ions to reposition themselves within the atomic structure and producing the intense fine emission lines associated with the phosphors, though the emission was still found to be less than the powder by two orders of magnitude.

Sputter coating has been tested by Noel et al⁷⁴ for fluorescent materials, a coating of 1µm was found to produce low fluorescence, which is thought to be due to the small thickness of the coating. They also considered the use of electron-beam depositions⁸¹ and again found that the signal gained from the coating was far too weak for use when spinning.

A settling technique that is used in the production of cathode ray tubes has been used by Chyu and Bizzark³⁴ to produce a fluorescent coating. The phosphor is suspended in a fluid and is allowed to settle onto the surface of the object. This technique produced a very fragile coating that had to be protected with a thin silicone layer. To obtain a fluorescence uniformity of ±5% from this technique a coating density of 10mg/cm² was required. This produces a coating thickness of 100µm.

2.6.2 *Adhesive techniques*

This technique is the most widely used for creating temperature and pressure sensitive luminescent coatings. In general temperature and pressure sensitive paints are created by dissolving a luminescent substance into a polymer solution. This can then be applied through brushing, spraying or dipping. The solvent evaporates leaving a thin smooth coating behind.

The size of the particles determines the levelling of the coating. Higher particle packing densities are less likely to produce the orange peel affect, will have fewer voids, and are less likely to shrink during curing. The larger particles are more likely to fall out of the spray cloud. Below a film thickness of 100 μ m the gravitational forces play no significant role in film formation. The addition of paint to a surface can modify the aerodynamics of that surface. The use of a binder reduces the efficiency due to light absorption and scattering.

The properties and thickness of the binder layer can drastically reduce the response time of the coating. The faster response coatings tend to be soft and tacky, these coatings affect the aerodynamic drag characteristics of the model and their lack of endurance limits their application⁹⁵. Harder coatings which may be able to survive rugged test environments such as rotating machinery, tend to have slower response times⁹⁵.

Solvent based coatings create a film formation due to evaporation of the solvent. The crystalline melting temperature is an important factor in selecting a binder. It affects the physical and chemical stability of the coating during storage, and the development of internal stresses during film life. For optical usages other factors need to be taken into consideration. These include, the adhesive should not fluoresce at the same wavelength as the fluorescent material when excited at the excitation wavelength of the fluorescent material. The adhesive will transmit both the excitation and the fluorescence wavelength. Careful selection of the adhesive will is therefore required to consider these factors.

Binders that have been tested by Noel et al⁷⁴ are sodium and potassium silicate, silicone resin-silicate-organic solvent mixture from Sperex Corporation, and water-reacting

powdered-refractory binder. The sodium and potassium silicate was found to survive up to 1,040°C, its expansion coefficient is not compatible with all substrates. The Sperex binder also survives up to 1,040°C depending upon its thickness, it is also flexible which means that its coefficient of expansion does not have to be matched to the substrate. The water-reacting binder is also useful up to 1,040°C though it produces a thick coating.

The type and amount of solvent used can adjust the characteristics of a solvent-based coating. The mechanical properties are dependent upon the average molecular weight; it has been established that this should be between 20,000 and 200,000 for a commercial polymer⁹⁶. This will ensure that it will have a good impact resistance and tensile strength.

2.6.3 *Other coating techniques*

The groups of surface coating that are available are chemical, electro-deposition, physical vapour deposition, chemical vapour deposition, thermal spraying, welding, and cladding. The properties of the coating are closely linked to its microstructure.

Coloured anodized aluminium is a strong, light and coloured coating. The oxide coating consists of a very large number of regular parallel sided pores stretching from the outer layer to the non-porous thin barrier with the aluminium surface. The colour is introduced into the oxide layer through absorption. The anodized sample is immersed into a suitable dye, which is absorbed into the pores of the oxide film.

Ion assisted deposition (IAD) is a dynamic process applied to conventional thin films producing hard, environmentally and wavelength stable coatings⁹⁷. It is used for creating optical films, particularly for neutral beamsplitters, colour display filters, hot and cold mirrors, fibre optic WDM filters and colour selective filters. This technique is good for low temperature coatings for plastics, it has low film stresses, and its spectral characteristics are stable up to 300°C.

Ion beam sputter deposition coatings produce films that have extremely low losses and defects ⁹⁷. It is used for creating high quality laser coatings such as anti-reflection coatings, laser protection filters, and polarisers. They have high damage threshold levels, environmental and spectral stability, low absorption and scatter, and low losses.

Thermal spraying, which involves the heating of the coating material and propelling it onto the material to be coated. Heating techniques involve the use of either chemical flame heating, or electrical heating, and can be summerized by four main types; flame spraying, arc spraying, detonation spraying, and plasma spraying. The thickness of the coating varies between the techniques; this can be between 0.1mm to 6mm.

The flame spraying technique is mostly used in commercial processes. The material to be coated is heated by the flame which can cause distortion. It is not suitable for some ceramic materials, as the melting point of the material is too high for the flame. Arc spraying can reach higher temperatures than the flame technique⁹⁸, which means a more dense coating is achieved. The running costs are lower but the initial capital cost is higher. The molten particles are usually blown by an air blast against the material to be coated, which must be conductive. The detonation process is the most expensive of this type of coating. It produces very dense coatings, which have Excellent adhesion ⁹⁸. One disadvantage is it has more geometrical limitations than the other techniques. In plasma coatings the material to be coated is not heated, which allows for low melting point materials to be coated with high melting point materials. The coatings produced are usually dense and adherent.

Powder coatings have been developed over the last 30 years. The coatings now being both environmentally friendly and cost effective when compared to solvent and wet techniques, though the technique does still have some weaknesses such as the orange peel affect, inconsistent transfer efficiency, and the coating of difficult to reach areas.

2.6.3.1 Plasma coating

Plasma spraying is a deposition process that comes into the category of thermal spraying. It has an advantage over other thermal techniques in that it does not heat the surface

being coated to the melting temperature of the coating material. This means that materials can be coated with materials with a higher melting point. The main advantages of a plasma coating are its resistance to wear and corrosion, it can be used for any different materials, and the coating produced has a high density. Three processes are required to achieve the coating⁹⁸;

- Heating the material to be sprayed so that it is almost molten.
- Projecting the molten material onto the base material.
- The projected material adheres to the material to give the required coating.

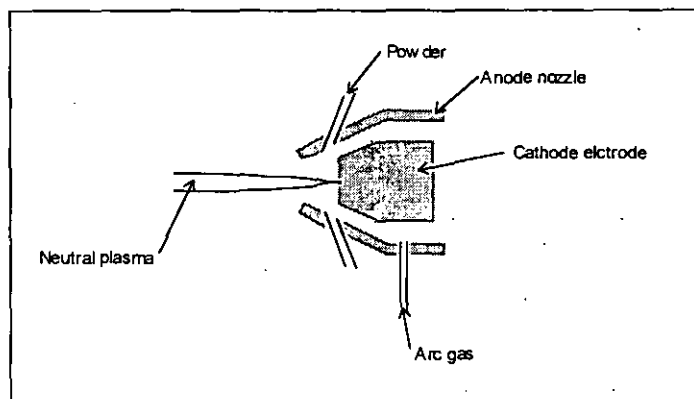


Figure 2-6 The plasma nozzle

A plasma arc is formed from a high current arc which is used to heat the injected gas, creating a high temperature plasma. This occurs due to the gas becoming ionised and collisions between electrons and ions generate radiant energy.

Plasma coatings are formed by injecting a powder into a direct current plasma jet, the particles are then melted and are directed onto the substrate by the jet, as the particles spread and solidify they form a coating. The coating itself depends upon the coating material microstructure and the formation of the coating. Factors related to the formation of the coating include the temperature, size and velocity of the particles as they hit the surface. Unmelted particles hitting the surface tend to bounce off the substrate.

In general, materials with high porosity are more brittle, have lower strength, and lower electrical and thermal conductivity. This is the same with coatings applied to materials. Though it is not always the case as finely distributed porosity can improve the thermal shock resistance of brittle materials⁹⁹. The elastic modulus and the thermal conductivity of the coating tends to be much lower than that of the bulk material¹⁰⁰, this can be explained by the number of pores parallel to the substrate created by the rapid cooling.

These pores reduce the actual contact between substrate and coating. In thermal conductivity the conductivity occurs only across the points of true contact. The pores have been shown to be removed through laser remelting of the coating¹⁰¹.

To achieve reproducible coatings the spray parameters need to be controlled, as well as the powder used being chemically uniform to enable reproducible melting to be achieved. Controlling the atmosphere in which the nozzle is located produces a more dense coating than undertaking the process in normal atmospheric conditions. A chamber is fitted around the nozzle and this is brought down to a vacuum pressure and then filled with argon to a pressure of 40mBar. The lack of oxygen in the atmosphere prevents the sprayed particles from becoming oxidised allowing for a better bond.

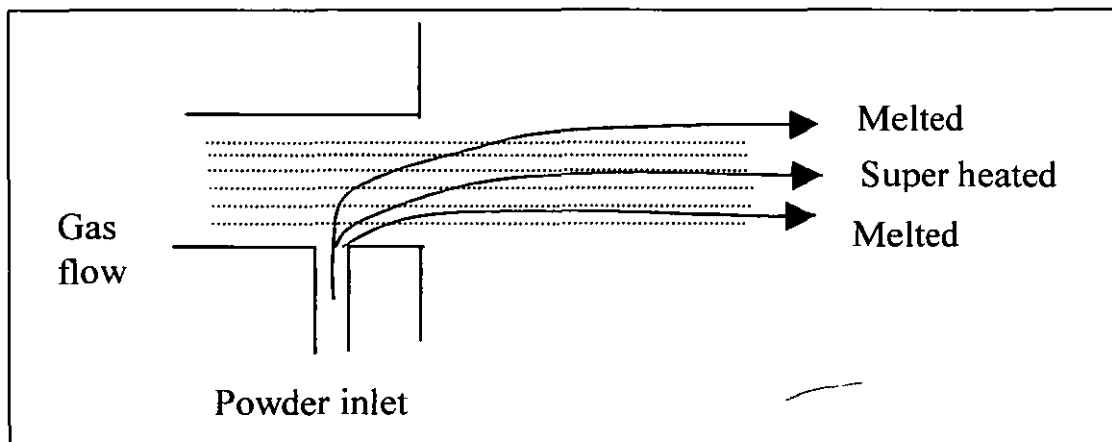


Figure 2-7 The outlet flow of gas from the plasma nozzle, and the powder injection

A high current arc is generated within the head that heats the injected gas creating a high temperature plasma. The powder is injected into the plasma jet; this melts the powder and propels it onto the surface. For the most efficient heating it is not necessary for a powder particle to pass through the arc core as it can be heated to a higher temperature by passing longitudinally through one of the recombination zones⁹⁸. To obtain a situation where the particles are melted to the same stage similar trajectory paths are required for all particles. Since the trajectories are dependent on gas flow and particle size, successful plasma spraying requires a close size range of powder. For a given flow rate, smaller particles attain a much higher velocity, high velocity is associated with low contamination and good deposit characteristics.

Using this technique means that a bonding agent is not required, except possibly between the surface to be coated and the fluorescent material depending on the material to which the coating is being added. The fine coating means that it will respond quickly to changes in temperature and will not affect the local temperature of the blade, and the surrounding airflow. The coating produced is well bonded and has a high density. Thickness of the coat can vary from 0.003mm to 2.5mm but normally occur within the range 0.1mm and 0.6mm.

Coating of $\text{Al}_2\text{O}_3\text{-TiO}_2$ has been produced by Chuanxian et al¹⁰² using the plasma coating technique. A fully automated low pressure plasma system for coating turbine blades and vanes has been designed and built by Meyer and Muehlberger¹⁰³. This was undertaken for general coating of parts rather than for the coating of luminescent material.

The disadvantages of this technique are, coatings can only be achieved in a direct line of sight, and high temperatures are involved, it is therefore not suitable for materials with low melting points.

2.6.4 *Surface preparation*

It is important that good adhesion is achieved, for the coating to adhere well to the material surface good surface preparation is required This can be done through blast cleaning which both cleans the surface and gives it microscopic roughness that helps the adhesive to adhere. Other surface preparation techniques include ultrasonic cleaning, solvents, or non-abrasive brushes.

The selection of which surface preparation technique to use depends upon the material to be coated, what is to be coated, and cost. The substances that may have to be removed from a surface include dirt, dust, chemicals, oils, grease, polishing media, tarnish films, corrosion products and machining swarf and fluids such as coolant. Possible techniques are shown in Table 2-6.

Method	Purpose	Notes
Wire brushing	Removal of loose rust and paint, millscale.	
Flame cleaning	Removal of loose rust and paint, millscale.	Especially use full in damp conditions.
Grit blasting	Removal of rust and millscale to the highest levels of cleanness.	Produces a rough surface that can help the adhesion of the coating.
Solvent degreasing	Dissolution of oils and greases by drip or vapour.	
Alkaline degreasing	Chemical removal of degenerated oils and greases.	
Pickling	Chemical dissolution of oxide and scale.	
Etching	Selective chemical dissolution giving roughened/patterned surface	Improve adhesion of subsequent coating; may be decorative.

Table 2-6 Surface cleaning techniques available

2.6.5 *Summary of coating techniques*

The coating-surface treatment used should not impair the fluorescent properties of the fluorescent material, or the mechanical or aerodynamic properties of the compressor blade. It must be able to coat the area of interest uniformly, this could be a complex shape or hard to reach area. The thickness of the coating produced will depend upon the technique used. A thin coating is preferable as this will react quickly to changes in the surface temperature, giving a true temperature reading. If the material has a low thermal conductivity then the top surface of the coating will be slow to react to the actual temperature of the blade, thus giving a temperature reading that is more closely related to the temperature of the air rather than that of the blade. A thin coating will also cause little affect to the aerodynamic properties of the compressor wheel.

A widely used and tested technique is the production of a luminescent paint, this has been successfully used for both temperature and pressure measurements. It does not require any specialist equipment or personnel to produce the coating, which makes it a cheap method easily implemented in industry. It uses the material efficiently and can produce very smooth, reliable and repeatable coatings. The selection of an adhesive that will not affect the excitation or emission wavelengths, and will withstand the temperature and forces within the compressor, is the challenge.

The requirements of the adhesive are; it must have a high thermal conductivity property, it must withstand temperatures of 300°C, it must have a thermal expansion coefficient similar to that of the aluminium so that excessive heating does not cause the paint to crack, and it must not affect the excitation and emission wavelengths. Adhesives that are possible for this technique include silicone based adhesives and two component epoxies. Mbond 600 is used at present for attachment of thermocouples at Holset so this is known to withstand the required temperatures, and has a high thermal conductivity. Sodium and potassium silicate, silicone resin-silicate-organic solvent, and water-reacting powdered-refractory binder are binders that have been used by Noel et al⁷⁴ for creating luminescent coatings at high temperatures.

The other techniques discussed required expensive equipment to create the coatings along with skilled personnel. These tend to produce a much thinner and even coating than the paint technique. Anodization requires extra chemicals to produce the coating, electrodeposition can only be used for metallic materials. Sputtering and deposition techniques show a possibility but cannot be easily created due to the equipment available. The final type is thermal spraying, all of these except plasma coating, tend to heat the surface being coated to high temperatures. As aluminium melts at a relatively low temperature of 600°C these techniques are not possible.

Plasma coating heats the coating away from the surface and therefore does not heat the surface to high temperatures. The coatings produced using this technique are thin and dense. It also does not require any bonding agent as the melted particles of the material embed into the surface and melt together. This means that any excitation wavelength is only absorbed by the fluorescent material, and also removes the absorption of the emission wavelength by the bonding agent thus producing a more efficient coating.

2.7 Data analysis

It is important that the data is shown in a clear manner and should not be mis-leading. A lot initial analysis can be done manually through looking at the data and therefore comparing data on different scales can be confusing and mis-leading. Showing a small picture of data can lead the viewer to come to a different conclusion than the showing of a broader picture. For example showing a small section of a relationship between two functions can lead the viewer to a conclusion of a linear relationship, though increasing the range would show a logarithmic relationship.

A discussion ¹⁰⁴ with a member of the mathematical department at Loughborough University determined that although a great deal of research has gone into curve fitting of single peaks very little work has been done on curve fitting of twin peaks. Within the field of chemistry a lot of work is done on analysis of materials using fluorescence techniques to determine content. Rather than fitting an equation to a peak a database is kept of all the elements and their particular peak, an unknown peak is then compared to those in the database.

Database referencing is widely used in the field of Chemistry. The ratio of peaks, shape of peak, and position of peaks are stored. This information is then compared to the spectrum under study to determine the compound of the material. This has the possibility for use, though it will depend upon the nature of the luminescent material selected.

The amount of scatter seen is a function of a number of parameters, including; number of averages taken, stability of furnace, noise on the detector, non-optimisation of the optics, and experiment arrangement. It is possible to use the data taken at room temperature as a reference image and to ratio all the other readings against this to determine the temperature. This technique eliminates differences from one experiment to another.

Data analysis must be used carefully as techniques such as smoothing can hide the magnitude of experimental error, meaning the errors are ignored rather than confronted and reduced or removed. Important bits of information can also be lost.

2.7.1 *Smoothing techniques*

The smoothing techniques are a form of averaging of the data. The data is averaged throughout the spectrum. This has the advantage of the data being independent of any other results the peaks not being distorted through the addition of a number spectra. If the temperature is changing rapidly it allows for the temperature readings to follow this trend where through averaging a number of readings the average temperature is just gained. Many of these techniques can be found in commercially available software.

Taking the average of a set of data will reduce fluctuations from one reading to another, though it is possible to distort the data by changing the shape of the peaks slightly. This is a simple technique which can be used quickly and when coupled with subtracting the background it can produce reliable results. Detector noise is a constant that cannot be removed through image averaging.

Smoothing functions are a form of averaging where instead of a number of sets of data being analysed the data is averaged throughout the spectrum. This has the advantage of the data being independent of any other results, the peaks not being distorted through the addition of a number of spectra. If the temperature is changing rapidly it allows for the temperature readings to follow this trend where through averaging a number of readings the average temperature is just gained.

Hanning
$$e_i = \frac{d_{i-1}}{4} + \frac{d_i}{2} + \frac{d_{i+1}}{4}$$
 except for first and last values

Running Means
$$e_i = \frac{d_{i-1}}{3} + \frac{d_i}{3} + \frac{d_{i+1}}{3}$$
 except for first and last values

The Fourier transform technique can be used to smooth the spectrum. Using this technique the different frequencies involved in the format of the spectra can be separated and removed if required. This allows the high and low frequency noise to be removed. Such as the high frequency electronic noise and the low frequency background noise detected in a spectrum.

2.7.2 *Curve fitting*

This allows the shape of the peaks to be defined and therefore temperature. Previous work by Munro et al⁶ has defined an equation that fits the shape of the peaks. From this the shape of the peak can be determined.

Least squares curve fitting procedure is generally used for fitting a curve to the profile. The initial parameters are altered to gain a good fit. In order to start the curve fit iteration estimates are required of the peak positions, height, and half height bandwidth.

It is possible that even when an equation is produced it will provide a meaningful fit¹⁰⁵. It was stated by Vandeginste et al¹⁰⁵ that if the bands do not conform to a few basic conditions then the results can be inaccurate even when they appear precise. Often when curve fitting a base line is required, incorrectly chosen it can provide an extra source of error. If a profile has only two inflection points but three peaks then many solutions are possible¹⁰⁶. It is therefore important to be careful about attaching physical meaning to values obtained from curve fitting¹⁰⁷. A combination of Gaussian and Lorentzian profiles for peak fitting in the infrared are shown by Vandeginste et al¹⁰⁸.

As a general rule reliable curve fitting of two overlapping bands of unknown band shape is only possible when separation of the peak maxim is larger than their average width at half height. Selecting the incorrect baseline or ignoring it completely can also introduce errors into the process. It is thought that the eye is one of the most powerful tools for determining the peak as it can distinguish what is noise¹⁰⁹ within the profile. It has been stated by Jones¹¹⁰ that if a computer produces weak components through curve fitting that are not evident to the eye, they should be treated with caution.

When using the equation determined by Pitha et al¹⁰⁷ an accuracy of 0.5% was gained by Vandeginste et al for the area, when the number of inflection points is twice the number of peaks. It appeared that the accuracy of the initial value of the peak position was an important factor in achieving the accuracy. When the number of inflection points is less than twice the number of peaks the exact number of bands must be known or derived from the curve fit procedure.

2.7.3 *Software*

There are a number of mathematical based software packages available commercially. There are also free packages available on the internet. The free packages tend to have been developed by a researcher for a very specific purpose and so are not easily useable for this, though they can be useful for initial analysis of data. The commercially available packages are extremely powerful and some can be programmed to do a number of different functions. The functions can vary from one package to another, such as smoothing techniques which can give different results even though they are described as being the same function. This needs to be considered when taking relationships from one package to another.

GaussIX is a computer program developed by Egger et al for analysis of gamma-ray spectra. Using a correlation technique it can identify the centre of a peak. A smoothing operation is present, which will help in defining weak peaks. The program normally fits a Gaussian function and uses a linear background. Work has also been carried out by Hult et al¹¹¹, Akkila et al¹¹² and Kakanis et al¹¹³ on single and multiple peak fitting and background fitting.

Software that has been considered for use are Mathematica, Matlab, Maple, and LabView which are programming languages which can be used as powerful analysis tools. Initial analysis is more easily undertaken using application software such as Excel, and PeakAlyze, these incorporate limited programming capabilities.

LabView was chosen for use because this is an easy to use programming package, where intense knowledge of a programming language is not required. Complicated programs can still be designed and run using this package, which can also be used to control and receive information from external devices. The spectrometer used for collecting data for the Yttrium powder is also compatible with the LabView language.

Excel was chosen for use for data analysis because it is widely available, can be used for many different forms of data analysis, and can be programmed to enable analysis to be done much quicker. It also provides a clear method of displaying the results so the eye

can view these easily. Some of the data analysis tools used from Excel included data fitting, histogram, and smoothing.

PeakAlyze is a package used in fitting shapes to curves. The standard peak shapes such as Lorentzian and Gaussian are available within the package or the equation for a peak shape could be entered. The variables can be set so that only values within certain ranges are acceptable. For example if you were looking at ratio, the value can be set so that the peak shape is only determined with a ratio value within the range zero to one. Start values for the variables can also be set so that time taken to produce a fit can be decreased dramatically.

2.7.4 *Selection of data analysis techniques*

The analysis technique used will depend greatly on the material selected and its relationship to temperature. The use of smoothing techniques will be considered to determine whether this will improve the reliability of the data. Curve fitting techniques will be considered to locate the peak and determine its shape. The use of peak fitting programs have the advantage of being able to locate hidden peaks, and interpolate between points. Excel and PeakAlyze will be used to determine the peak shape and its parameters and their relationship with temperature. Once the relationship has been determined the method of determining the temperature in real-time will be considered. For this LabView program would be the easiest as this has the ability to import data from a remote source and analyse it.

3 Study of fluorescent materials

The fluorescent properties of a number of materials were considered for temperature measurement over the range 100°C to 300°C. Their relationship with temperature and their feasibility for use as a remote temperature sensor is discussed in this chapter. The materials studied were chosen due to the requirements set-out in chapter 2.4.5 Summary of the luminescent materials available.

The materials considered were Acridine Yellow, Brilliant Sulphoflavine, Panacryl Brilliant Flavine, Ruby, Sapphire and Yttrium Oxysulphide Praseodymium doped. It was the non-organic materials that proved to be the best for this technique. Of these materials those whose fluorescence spectrum have been considered previously for temperature sensitivity are Acridine Yellow by Fister et al, Ruby by many authors^{VI}, and Sapphire which is used as a fibre optic temperature probe. It has been noted that the linewidths of Yttrium Oxysulphide Praseodymium doped are affected by temperature by Okuno et al.

The interest in the temperature sensitivity of Ruby has been involving solid crystals of Ruby. It has been investigated for the stability of laser output, it has also been used as a means of measuring temperature, which involves using a Ruby crystal in a fibre optic probe. Ruby has shown to be temperature sensitive over the temperature range -200°C to 500°C. The work here is to see if Ruby can be used to create a temperature sensitive coating whose fluorescent spectrum can be read remotely.

Sapphire has a similar structure to Ruby and although its temperature sensitivity is not as well documented as Ruby it is used by industry as a fibre optic temperature probe. The work here is to see if its fluorescence spectrum can be used as a remote means of measuring temperature.

The work undertaken on Acridine Yellow has been in using the fluorescence decay period for temperature measurement in the range -50°C to 50°C, where it has been

^{VI} See 2.4 Luminescent materials available

dissolved into a glass. The work here is to see if the fluorescent spectrum shows a temperature relationship up to 300°C.

Yttrium Oxysulphide Praseodymium doped has been shown to be affected by temperature within the range -270°C to -70°C. The work undertaken here is to see if the fluorescence spectrum has a temperature sensitivity in the temperature range 200°C to 300°C.

Other materials considered are Panacryl and Brilliant Sulphoflavine, these have not been used before for thermoluminescent techniques. Their absorption and fluorescent spectra are known from previous luminescent experiments.

3.1 Acridine Yellow

The organic substance Acridine Yellow has been tested for temperature relationship in both an ethanol based solution and as a coating. The coating was produced using a lacquer^{VII} with the Acridine Yellow powder mixed into it. The lacquer has been tested for fluorescence at the same excitation wavelength as used for Acridine Yellow and was found not to fluoresce, nor to absorb the excitation or emission wavelength. The program used for the fitting of the peak shape was PeakAlyze.

It is documented that the fluorescence spectrum of Acridine Yellow only emits one peak^{VIII} in the wavelength range that is studied here. Therefore the peak fitting has been undertaken assuming that this is true, as the peak achieved through experimentation shows no signs of a shoulder which would indicate a second peak.

Assuming a linear relationship between intensity and temperature, and that the same trend continues, Acridine Yellow could be used for temperature prediction up to 175°C

^{VII} Lacquer used was Rustins Transparent lacquer.

^{VIII} See 2.4 Luminescent materials available

under these conditions. The intensity of the fluorescence is very much dependent upon the intensity of the light source, quantity of material and the collection optics. Using the maximum point as the peak position and intensity of the fluorescence spectrum shows a good relationship with the peak intensity found with the peak fitting program. With the peak position this is much more scattered, though follows a similar trend for the lacquer base. This shows that selecting the maximum value for determining temperature has a possibility, and this would remove the need for curve fitting programs, would be simple to implement, and reduce the amount of processing time required. Although under these conditions temperatures above 200°C could not be obtained, the use of a higher power laser could increase the temperature range.

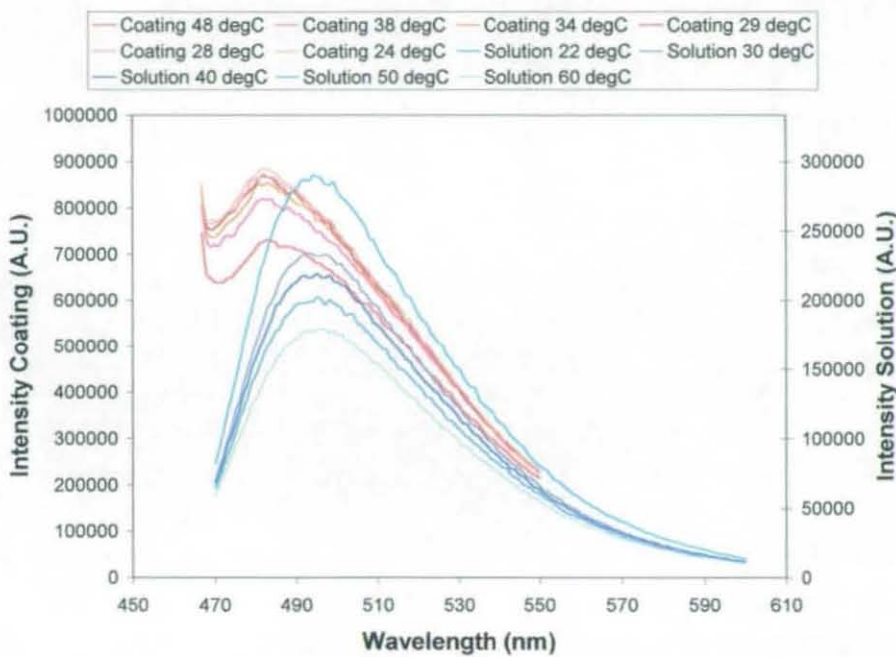


Figure 3-1 The fluorescence spectrum of Acridine Yellow in ethanol solution, and as a lacquer based coating.

The experiments undertaken for the solution and lacquer bases used different fluorometers to record the spectrum, which could account for the differences in the spectrum. Another possibility for the differences in the spectrum is that the host material affected the fluorescence from the Acridine Yellow, as it is known that the solution that a luminescent material is placed into can affect the absorption, emission and efficiency^{114,115}. The background reading indicates that a peak at 500nm is expected, as that seen with the solution. It can therefore be determined that this reading is correct and that the shift in wavelength seen with the lacquer is either due to the equipment or due to

the lacquer having an effect on the fluorescence. The equipment has been checked and it has been found that this is the cause in the change in wavelength.

The shape of the peak was asymmetrical and could be fitted by the equation for asymmetrical skewed Gaussian peaks^{IX}. The asymmetrical value of the peak decreases with increase in temperature, this means that the peak is moving towards a symmetrical Gaussian peak. This change in the asymmetrical value cannot be due to the decrease in intensity of the peak nor the broadening of the peak, as the asymmetric value is independent of these. This affect is more noticeable in the ethanol based sample than the more scattered data from the lacquer based sample. As the temperature of the substance is the only changing factor in these experiments, this change in peak property must be due to the change in temperature. As this value is independent of peak height it is independent of fluctuations in intensity and therefore is a reliable value that can be used for measuring temperature.

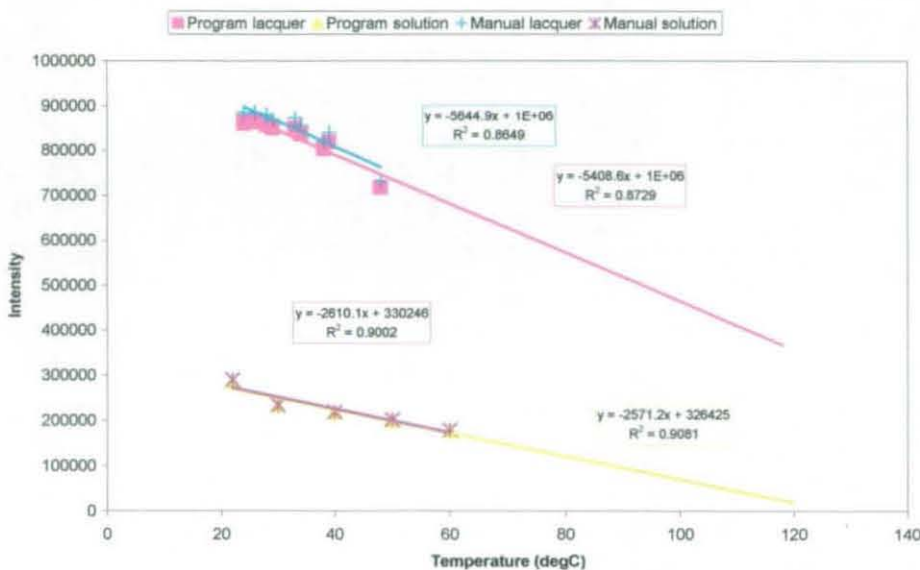


Figure 3-2 The Difference between finding the peak intensity of the fluorescent peak through using a peak fitting program (program data) and using the point of maximum intensity (manual data).

The increase in the temperature changes the lattice structure of the material thus causing a shift in peak wavelength to higher wavelengths with increase in temperature. This also

^{IX} See Appendix - 9.8 Equations

contributes to the broadening of the peak. It is thought that this is also the contributing factor to the change in the asymmetric factor of the peak.

Relationship of temperature with	Solution	Lacquer
Intensity	$y = -2571.2x + 326425$ $R^2 = 0.9081$	$y = -5408.6x + 1E+06$ $R^2 = 0.8729$
Asymmetrical factor	$y = -0.0009x + 0.6136$ $R^2 = 0.928$	$y = -0.0007x + 0.4479$ $R^2 = 0.0449$
Peak Position	$y = 0.0244x + 494.1$ $R^2 = 0.8665$	$y = 0.0829x + 480.71$ $R^2 = 0.7263$
Peak Width	$y = 0.0886x + 50.641$ $R^2 = 0.9649$	$y = 0.0891x + 69.445$ $R^2 = 0.1096$
Intensity : Width	$y = -54.058x + 6304.5$ $R^2 = 0.925$	$y = -83.571x + 14181$ $R^2 = 0.7668$
Peak intensity : Background intensity	$y = -0.0471x + 19.415$ $R^2 = 0.9658$	$y = -0.0137x + 4.0244$ $R^2 = 0.875$
Area	$y = -144743x + 2E+07$ $R^2 = 0.8916$	$y = -695998x + 8E+07$ $R^2 = 0.4868$

Table 3-1 The affect of temperature on the luminescent peak of Acridine Yellow, using peak fitting program to determine peak shape and position.

The peak position, peak width, and the intensity ratio between peak intensity and background have all been studied for temperature sensitivity. Their relationships can be seen in Table 3-1. This shows that the ethanol host produces much greater reliability than the lacquer host. The use of a different adhesive host may produce a strong relationship between temperature and fluorescence such as that shown by the ethanol host. This would require consideration of a number of adhesives to determine the ideal host. The ethanol solution shows that peak shape has a strong relationship with temperature.

The affect of the excitation wavelength is shown in Figure 3-3. As it can be seen that to gain the highest intensity it is important to select the correct wavelength. The wavelength used for excitation will also affect the peak position of the emission. This material was excited at different wavelengths to see how much an effect the excitation wavelength has on the emission from the material. This shows that the selection of wavelength is critical to get the most efficient result, and that the wavelength 458nm produces the most intense fluorescence with a peak at around 485nm. This is lower than the fluorescence wavelength that Fister et al saw. It is known that the wavelength of maximum absorption is 461nm. Using this wavelength to excite the dye rather than the 458nm used in the experiment would only produce a 6% increase in intensity.

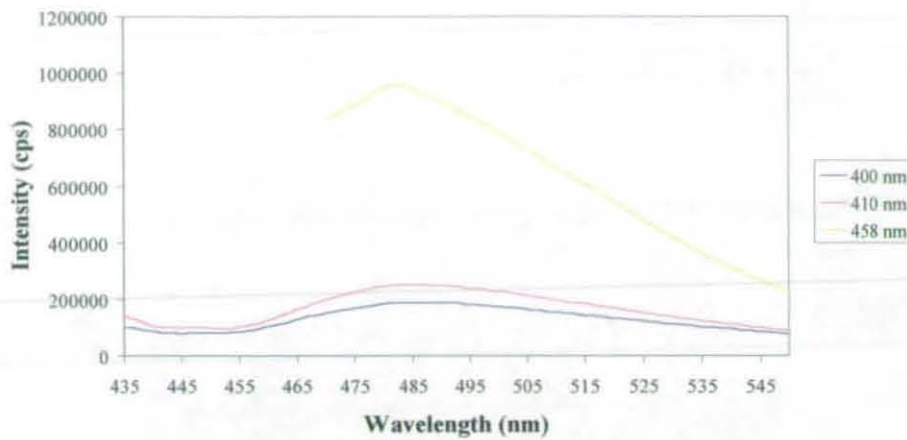


Figure 3-3 The effect of excitation wavelength on the fluorescence spectra.

The work undertaken here shows that the fluorescence spectrum from Acridine Yellow can be used as a means of measuring temperature. Under the conditions here it could not be used for measuring temperatures above 175°C, and temperatures up to 300°C are required by Holset. Increase in the laser energy and the material density could increase the temperature range of the material making it viable for this application. It is shown that the peak shape can be used to measure temperature as well as the peak position and peak temperature. The selection of the right host adhesive could increase the sensitivity of the paint to temperature. This would need to be considered if this material is to be looked into further. Given the one peak it is not an ideal candidate for the application to enable self-referencing so therefore will not be considered further.

3.2 Brilliant Sulphoflavine

The fluorescence spectrum for Brilliant Sulphoflavine has been studied for change with temperature in both an ethanol solution and a bonded coating. The peak was found to be asymmetric in profile, following the same profile as Acridine Yellow fluorescence. As with the experimentation carried out with Acridine Yellow two sets of equipment were used for the solution and the coating.

There is a shift in wavelength between the two bases of at least 100nm, compared to a separation of 20nm for Acridine Yellow and Panacryl. The separation of the peaks can therefore be considered to be due to the lacquer because if it was the equipment this would be constant with the other two materials. The fluorescence from a fluorescent material is very dependent on its environment, and this would explain the differences seen with Brilliant Sulphoflavine between the ethanol and lacquer bases. This indicates that optical centres have been affected by the host materials causing different energy transfers and as such different wavelengths to be emitted.

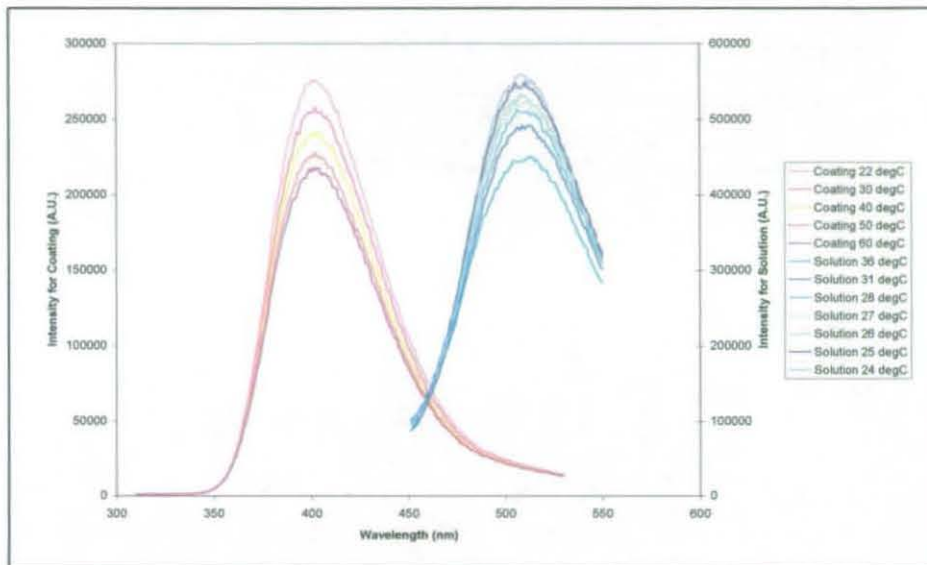


Figure 3-4 Spectra from Brilliant Sulphoflavine for lacquer based coating and for solution.

It was found that the wavelength of the peak position obtained from the solution based sample, only shifted by 0.2nm over a temperature change of 40°C. The bonded sample wavelength of the peak position increased with temperature, the data from which was erratic and could not be used as a definite relationship.

The asymmetric peak shape factor of Brilliant Sulphoflavine was found not to be affected by temperature. The width of the peaks increased much steeper than the Acridine Yellow peak. A good relationship with temperature and width was determined for both samples. A good relationship between area under the peak and temperature was determined for both manual and program determined data.

The decrease in intensity with temperature was much steeper with the bonded coating than with the solution. Assuming the variation in the intensity is linearly related to temperature and that the same trend continue to higher temperatures, it can be predicted using the equation in Table 3-2. Temperatures up to about 200°C can be determined with the ethanol solution, or 90°C using the coating technique, under these conditions.

Relationship of temperature with	Solution	Lacquer
Intensity	$y = -1501.9x + 303372$ $R^2 = 0.9777$	$y = -8163.4x + 739216$ $R^2 = 0.9566$
Asymmetrical factor	$y = 1E-05x^2 - 0.001x + 0.4118$ $R^2 = 0.9052$	$y = 0.0008x^2 - 0.0462x + 0.8189$ $R^2 = 0.848$
Peak Position	$y = -0.0052x + 402.72$ $R^2 = 0.8754$	$y = 0.0602x + 509.63$ $R^2 = 0.2556$
Peak Width	$y = 0.0268x + 62.991$ $R^2 = 0.9163$	$y = 0.412x + 69.979$ $R^2 = 0.9035$
Intensity : Width	$y = -25.056x + 4802$ $R^2 = 0.9749$	$y = -129.38x + 9896.9$ $R^2 = 0.9472$
Peak intensity : Background intensity	$y = -3.1706x + 228.29$ $R^2 = 0.8247$	$y = -0.101x + 9.8626$ $R^2 = 0.7772$
Area	$y = -107672x + 2E+07$ $R^2 = 0.9936$	$y = -497086x + 5E+07$ $R^2 = 0.9574$

Table 3-2 The affect of temperature on the luminescent peak of Brilliant Sulphoflavine, using peak fitting program to determine peak shape and position.

The change in wavelength between the two bases would not be considered to be a problem provided this was constant between batches. This material shows a relationship with temperature, though this relationship is not thought to be viable above temperatures of 200°C, under these conditions. Consideration of the optical system would be required to determine if stronger fluorescence could be obtained should this material be considered further. Given the single peak fluorescence this material is not an ideal candidate though the peak does have a number of functions that are temperature dependent. Due to the single peak emission this peak will not be considered further, as this will not allow for self-referencing of the signal.

3.3 Panacryl Brilliant Flavine

The temperature profile of Panacryl Brilliant Flavine was considered for both the solution based sample and a coated sample. These two followed the same relationship between peak width and temperature.

The spectrum gained for Panacryl in the lacquer showed two peaks. When fitting with the peak fitting program the first, smaller, peak could not be fitted. The data to the left of the saddle was therefore omitted from the fitting program. The tail of this smaller peak could have affected the type of peak that the fluorescence peak followed.

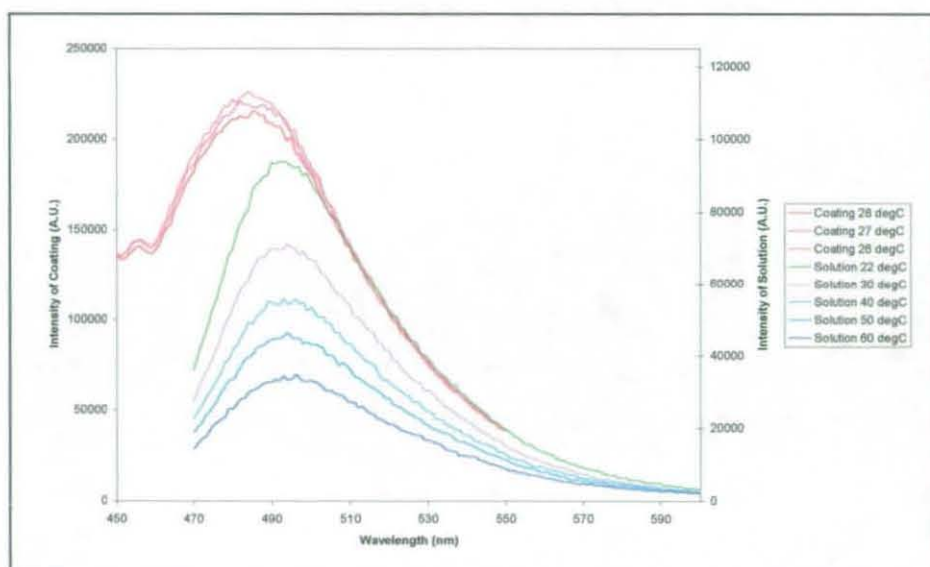


Figure 3-5 The fluorescence spectra for the lacquer based coating and ethanol based solution.

The coating followed a Munro^X profile, which is based on a combination of Lorentzian and Gaussian profiles, rather than the asymmetrical profile that the fluorescence peaks of the other two organic materials followed. The peak was also found to be fitted well by the Person VI^X profile. The position and intensity values from the Person fit followed very closely the values obtained from the Munro fit. The solution based sample followed an asymmetric profile. This shows that the first peak has affected the shape of the second.

^X See Appendix - 9.8 Equations

A change in fluorescence intensity was detected by the human eye, until the temperature of 94°C was reached where no fluorescence was seen, for the lacquer based sample. Using the data from the peak fitting of the solution based sample it is predicted that temperatures of about 100°C could be reached.

The lacquer based sample did not produce a reliable method for measuring temperature. This is due to interference from another peak during the fitting of a peak to the data causing an error in the fit, though it was found that the peak position, width and ratio between peak intensity and background each provided a temperature relationship. The width of the Munro peak was determined by adding the widths for the Lorentzian and Gaussian terms. Each of the width terms were also multiplied by their ratio term and added to improve the temperature relationship^{XI}. This did show a big improvement in the temperature relationship.

The solution provided a good relationship between temperature and the peak profile. With this material the asymmetric peak shape factor increased with increase with temperature. It is predicted though that only temperatures of 100°C could be reached so this material will not be considered further, as temperatures up to 300°C are required.

3.4 Sapphire

Pink Sapphire has a similar molecular structure as Ruby. Sapphire produces a single peak at 710nm with a much broader bandwidth than Ruby. According to background work pink Sapphire emits at 800nm⁶⁹. It is thought that this shift in wavelength was due to the chromium content in the Sapphire.

An interesting point to note is that on initial heating, the intensity of the emission wavelength increased from what it had been at room temperature and then decreased. Materials are only sensitive to environmental changes over certain ranges. The data here

^{XI} See Appendix - 9.8 Equations

indicates that at lower temperatures Sapphire has a different relationship with temperature than at higher temperatures. With Ruby it is known that below about 20°C the intensity increases with an increase in temperature, while above 20°C the intensity decreases with increase in temperature¹¹⁶. It is possibly this situation which is occurring here but at a slightly higher temperature than for Ruby.

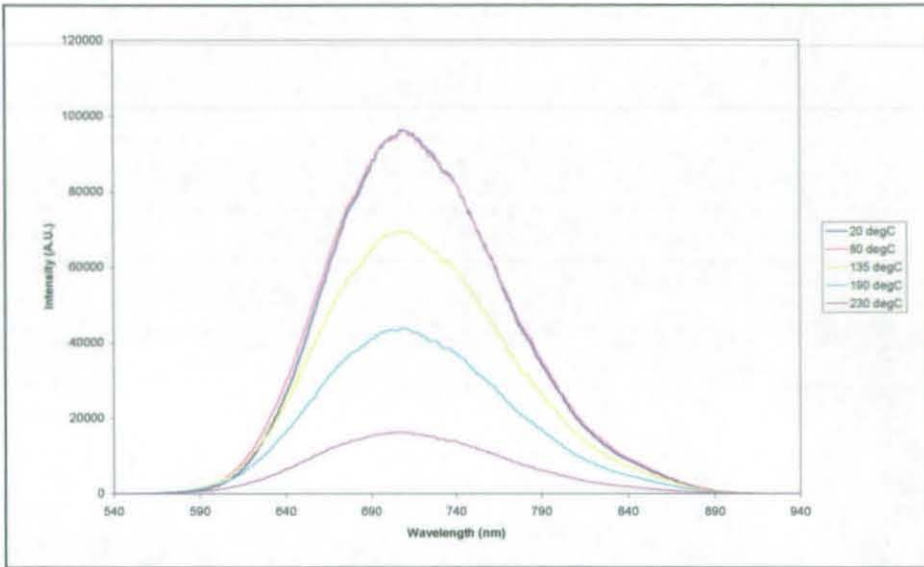


Figure 3-6 The fluorescence spectra of a piece of synthetic Sapphire.

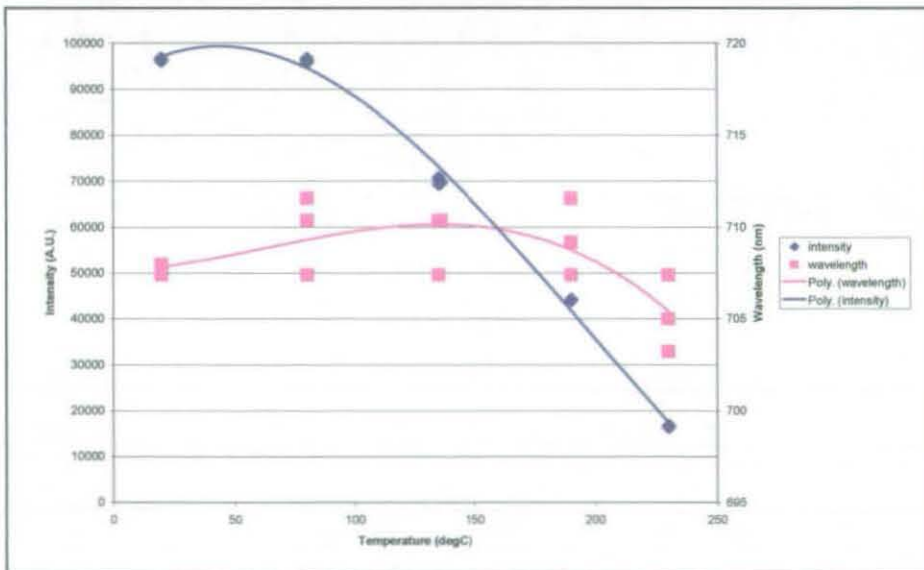


Figure 3-7 The affect of temperature on the peak wavelength and intensity.

The peak position could also not be used for temperature measurement over the temperature range 100°C to 175°C, which is part of the temperature range which Holset require to be measured. It was decided not to continue with any further work with

Sapphire as it has only a single peak, it did not emit a stable temperature relationship, and it seems that the chromium content affects the emission greatly, which could cause problems with batch continuity.

3.5 Ruby

Ruby has been studied for temperature measurement, background indicated that there is a number of wavelengths that can be used to excited Ruby Of these 532nm was chosen as this is easily obtainable from a frequency doubled Nd:Yag laser, this is also easily obtainable as a pulsed source. The laser used in these experiments is a Q-switched diode pumped solid state laser LCS-DTL-112QT, it has a pulse duration of 10nsec with a pulse energy of $1.5\mu\text{J}$. The spectrometer used is a Solar T II, whos detector uses software written by Cronin electronics to collect, display and save the spectrum. The spectrometer has a resolution of 0.1nm, and a 40% grating efficiency.

The experimentation was carried out with the Ruby sample placed in a furnace with the furnace door replaced with a door with a quartz window in it which will withstand the temperatures, this will allow the fluorescence readings to be taken without removing the sample from the furnace. An average of ten reading was used for the work in this section.

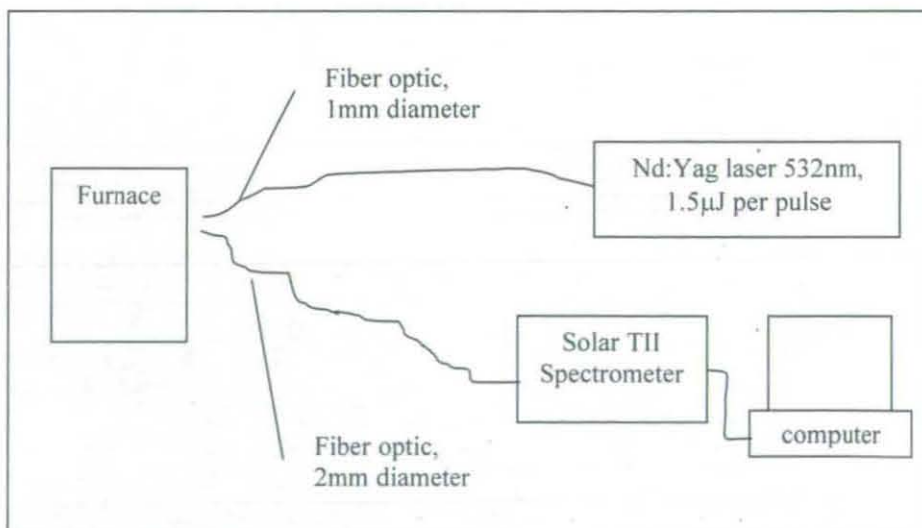


Figure 3-8 The experimentation arrangement

From the spectrum it can easily be seen that there is a strong affect of temperature on the intensity and the peak positions. The peak positions are determined by using the maximum value in that area of the spectrum. The peak position and intensity relationships with temperature can be seen in the charts below. These show that intensities and the ratio of the intensity produce a good relationship with temperature up to 300°C. The peak positions also show a strong relationship with temperature up to 300°C, but the separation of the peaks does not show a relationship with temperature.

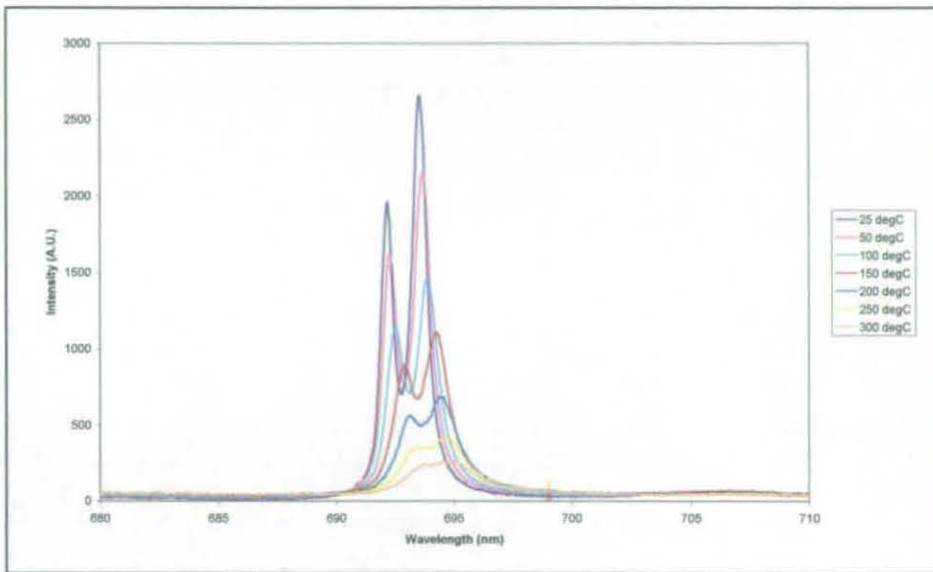


Figure 3-9 The fluorescence of solid Ruby

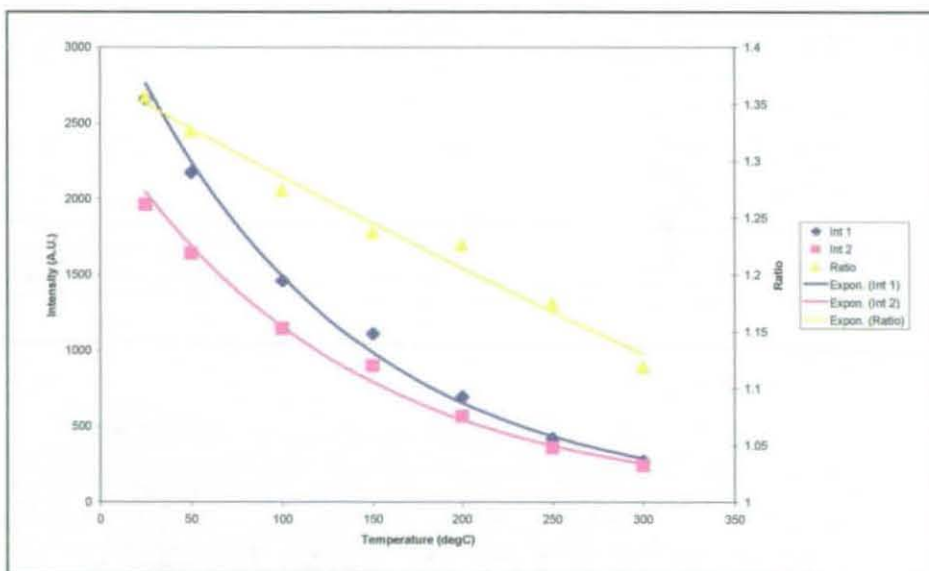


Figure 3-10 The affect of temperature on the peak intensities.

It is difficult to accurately determine the peak position due to noise within the spectrum. It is therefore necessary that curve-fitting processes are undertaken to determine peak positions. If slight changes in the Ruby spectra occur from one reading to the next then use of averaging techniques will change the shape of the peak, and therefore each reading should be treated separately. A combination of Gaussian and Lorentzian peak descriptions have been used previously and have shown to give close fits of the spectra and so allowing the peak positions to be determined.

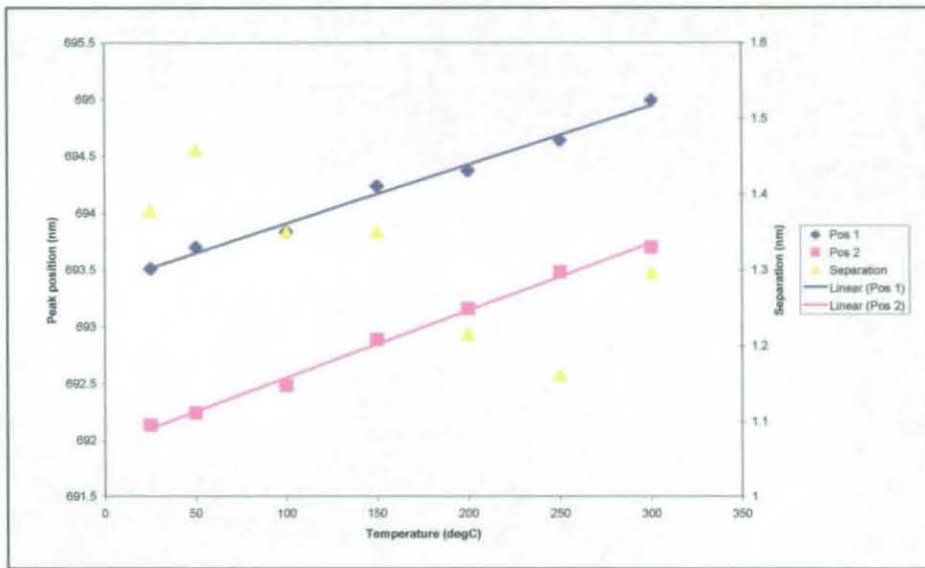


Figure 3-11 The affect of temperature on the peak positions.

As well as the two main peaks two much smaller peaks can also be seen with high intensity peaks. The two extra peaks occur at around 710nm, at which Ruby is known to emit. The peaks also decrease with increasing temperature, and tend to disappear at higher temperatures.

Ruby shows a good relationship between temperature and its fluorescent spectrum. The affect of pressure on the fluorescence is therefore considered below. Further work will continue on the creation of the coating and the analysis of the spectrum.

3.5.1 Testing of pressure sensitivity

It is known that fluorescent materials sensitive to temperature can also be sensitive to pressure. As the pressure will be changing within the compressor it is important to understand how this may affect the fluorescence spectra.

A pressure container has been designed that will allow samples to be pressurised up to 4Bar as this is the expected pressure range achieved within the compressor housing. This will allow the affects of pressure on the materials to be determined. The lab temperature remained constant throughout the experimentation so any changes in the spectrum is not due to changes in temperature.

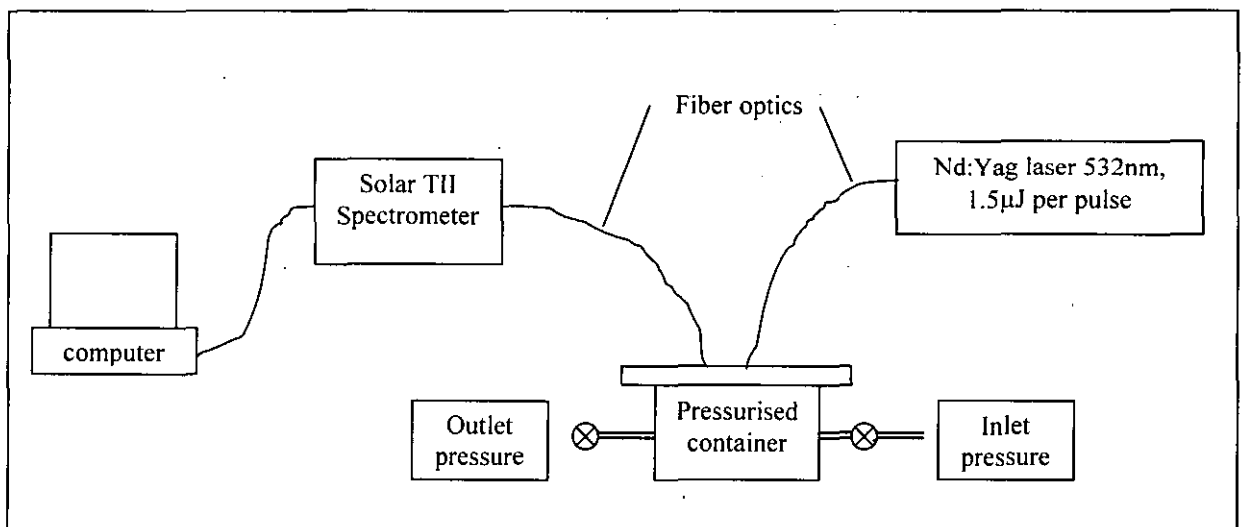


Figure 3-12 The experimentation arrangement

A Ruby rod has been tested for pressure dependency at room temperature within the pressure range 1 to 4Bar. This showed that the intensity decreased with an increase in pressure, the positions of the peaks decreased slightly with pressure. This change in the peak shape was compared to that of a piece of Ruby held at constant temperature, to determine if this change in peak shape is within the normal shift, Table 3-3.

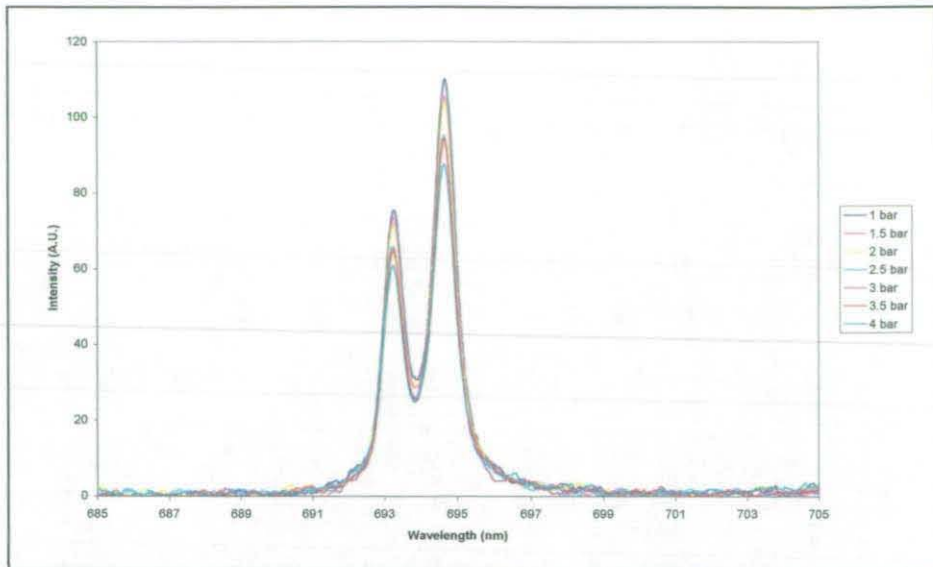


Figure 3-13 The fluorescence spectrum for Solid Ruby at pressures up to 4 Bar.

	Non-smoothed		Smoothed	
	Pressure	@ 27°C	Pressure	@ 27°C
Intensity Peak 1	23.8	17.3	22.5	5.35
% decrease	20%	0.26%	20%	0.30%
Position Peak 1	0.108	0.627	0.054	0.626
Intensity Peak 2	16.28	20.87	14.5	9.99
% decrease	19%	0.72%	20%	0.85%
Position Peak 2	0.135	0.627	0.027	0.627
Intensity ratio	0.066	0.018	0.023	0.013
Peak separation	0.108	0.003	0	0.003

Table 3-3 Comparing the change in spectrum at pressure with that at a stable temperature.

It can be seen that for an increase in pressure there is a corresponding decrease in intensity. Considering the smoothed data there is no shift in the separation of the peak positions with pressure. For the non-smoothed data, although the peak positions are within the shift noted at the stable temperature, the change in the peak separation is above that of the stable temperature data. This difference in separation could be due to noise within the data rather than a true pressure dependence given that the smoothed data produces no change in peak separation over the given pressure range.

For the smoothed pressure data the peak height can be related to pressure through the following equations;

Intensity of peak 1;

$$\% \text{ decrease in intensity} = 0.0646 \times \text{pressure} - 0.0589$$

Intensity of peak 2;

$$\% \text{ decrease in intensity} = 0.0635 \times \text{pressure} - 0.064$$

3.5.2 Ruby conclusion

Ruby emits two main bands, both of which show to be temperature dependent. As each peak has a different relationship with temperature it is possible to create a self referencing signal, and will therefore remove errors due to influences such as signal noise, and environmental changes. Ruby has also shown to not be affected by the pressure range that is present within the compressor. It has also been shown to be sensitive to temperatures up to 300°C. Ruby is therefore a prime candidate for a luminescent temperature measuring coating.

3.6 Yttrium Oxysulphide Praseodymium doped

Praseodymium doped Yttrium Oxysulphide ($\text{Y}_2\text{O}_3\text{S:Pr}$) has been tested for its temperature sensitivity. This phosphor has been chosen because of its very short lifetime, which will allow most of the fluorescence to be detected during the pass of the compressor wheel. It also has a number of emission peaks, which allows for the possibility of self-referencing the reading. The wavelength used to excite the material is 266nm, which can be obtained from a frequency quadrupled Nd:YAG laser. The equipment used in this work is a Spectron SL284 quadrupled Nd:YAG, which has a pulse energy of 6mJ and a pulse duration of 9nsec.

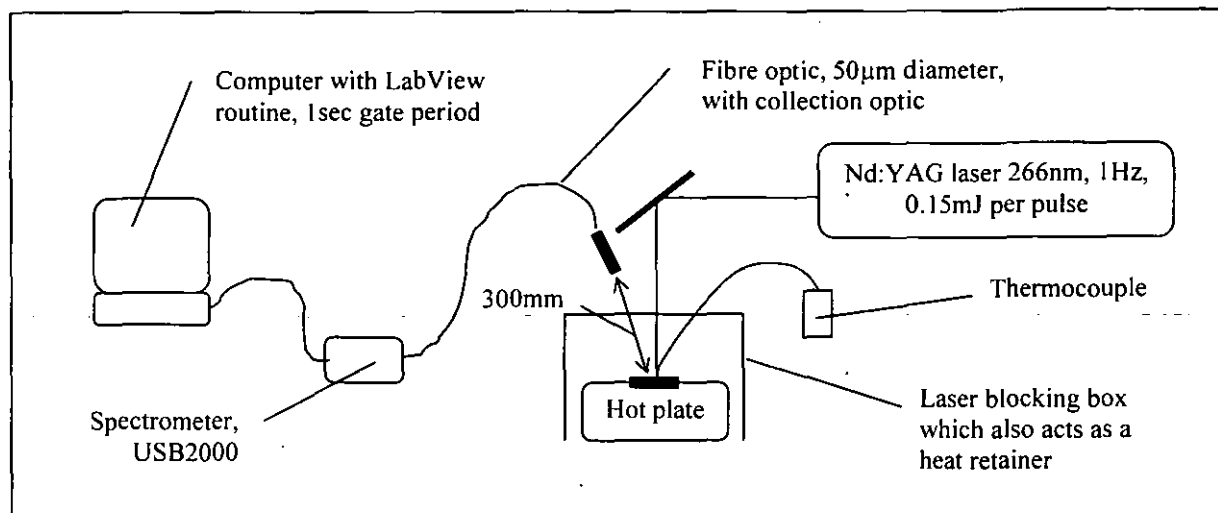


Figure 3-14 The experimentation arrangement

$\text{Y}_2\text{O}_3\text{S:Pr}$ was obtained only in powder form, the experiments were therefore carried out with $\text{Y}_2\text{O}_3\text{S:Pr}$ mixed with adhesive to create a paint, which was coated onto a piece of aluminium. The sample was heated using a hot plate since to the location of the laser prevented the use of a furnace. The powder was placed into a shallow bottomed container with a thermocouple located in the powder. The coating had a thermocouple attached to the centre of the coating.

The spectrum recorded shows that there is a strong relationship between temperature and fluorescence intensity. The intensity of the larger peak at lower temperatures is off the scale of the spectrometer which is why the broad top peak is seen. From the spectrum four main peaks can be seen at 500nm, 510nm, 660nm, 670nm, it is these that are initially studied for temperature dependence. The peak position and intensities have been considered for temperature relationship. The peak intensities show a strong relationship with temperature, Figure 3-16. All the peaks show strong temperature relationship up to 300°C, especially the more intense peaks at 500nm, and 510nm.

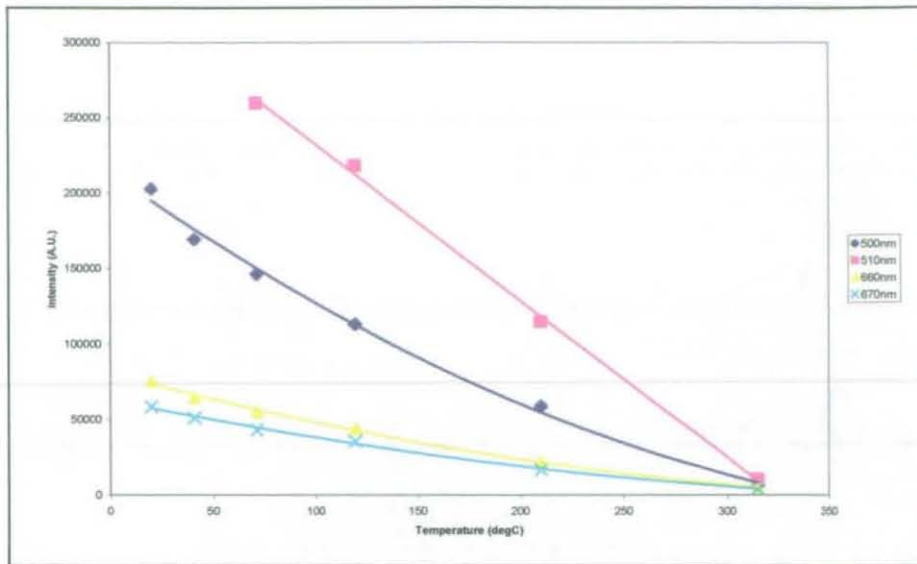


Figure 3-15 The fluorescence of Yttrium Oxysulphide Praseodymium doped.

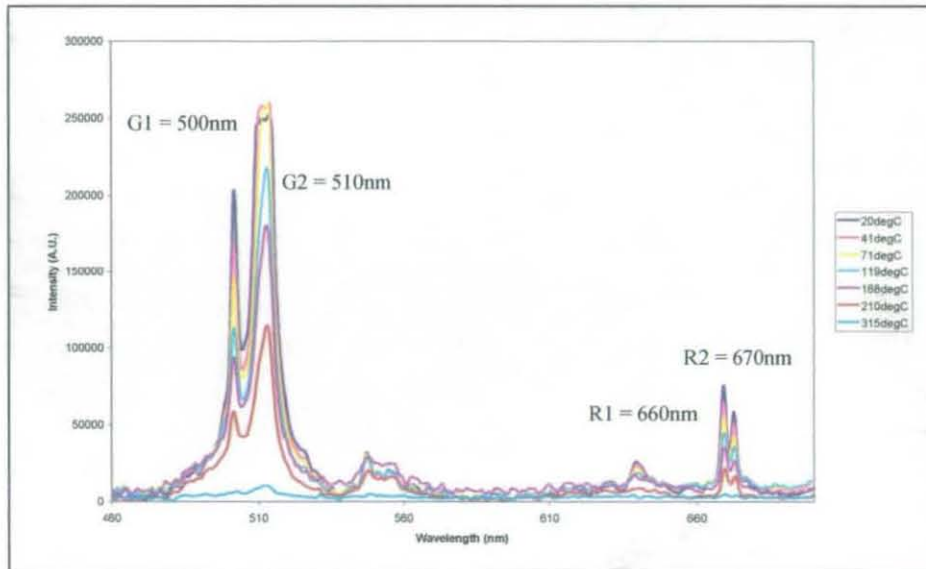


Figure 3-16 The affect of temperature on the intensity.

Some of the peak positions and the peak separations showed a strong relationship with temperature, and others did not, Figure 3-17.

A summary of the peak position relationships with temperature can be seen in Table 3-4. From the data in the table two peak position relationships show a strong relationship with temperature, R2-G2 and G2-G1 as they show a small temperature shift with a 1nm shift. A small temperature shift with wavelength means that a smaller uncertainty in temperature measurement can be achieved than a larger temperature shift. The

relationship R1-G1 shows little shift in wavelength with temperature and can therefore be used as reference value.

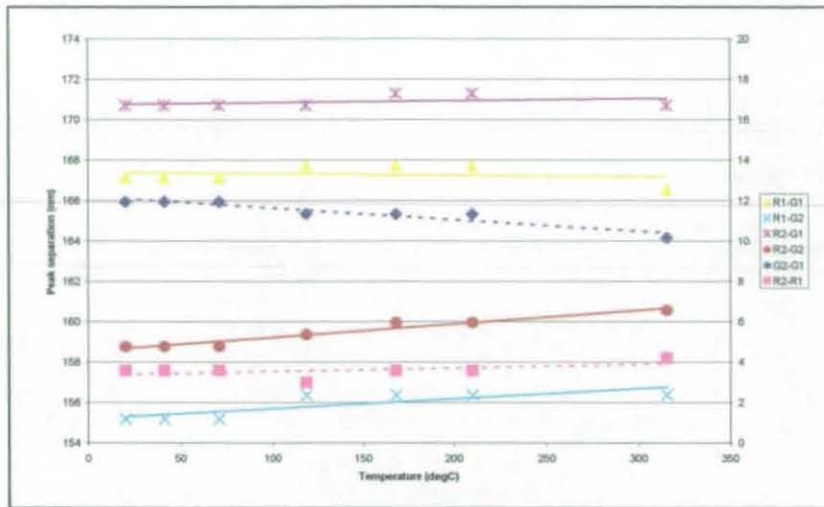


Figure 3-17 The affect of temperature on peak position

Function	Shift of 1nm relates to ^{XII}	Change of 1°C relates to	R ²
R2-G2	147°C	0.0068 nm	0.9464
G2	400°C	0.0025 nm	0.9021
G2-G1	172°C	0.0058 nm	0.8914
R2	233°C	0.0043 nm	0.6614
G1	303°C	0.0033 nm	0.6614
R1-G2	200°C	0.0050 nm	0.6614
R1	400°C	0.0025 nm	0.5778
R2-R1	556°C	0.0018 nm	0.2931
R2-G1	1000°C	0.0010 nm	0.1253
R1-G1	1250°C	0.0008 nm	0.0342

Table 3-4 The relationship between the Y₂O₃S:Pr emission spectrum and temperature

Curve fitting will allow the peak positions and thus the temperature relationship to be fitted more accurately. The use of peak separation will allow a technique to be developed that would be independent upon coating quality and optical alignment. This material shows a strong possibility of use as a temperature sensor and will be considered further. The disadvantage of this material is that it requires UV excitation which is absorbed by most materials and therefore the use of fibre optics to transmit the excitation wavelength to the compressor would be expensive.

^{XII} Spectral resolution 1.03nm

This material shows a relationship with temperature up to 300°C, emits more than one fluorescence peak, and produces relationships with temperature and none changes with temperature, which means that it can be self-referenced. It has a very short lifetime of 7μsec which means that the majority of the fluorescence can be collected in one rotation.

4 Data analysis

This section looks at some of the data analysis techniques that are available for extracting the required data from the spectrum. This has been undertaken using the data collected from Ruby.

4.1 Smoothing techniques

Different techniques for smoothing have been considered. These include subtracting the background, averaging, and the use of the Hanning, Running Mean, and Exponential smoothing functions.

Subtracting the background and averaging does not significantly reduce the noise, but is essential for the standardisation of the data. If this was not considered then a high background would give a very different set of results for intensity than a low background. This difference would not be taken into consideration by the ratio of two intensities.

The Hanning, Running Mean, and Exponential smoothing functions are similar operations using averaging of adjacent values in the spectrum techniques. The Hanning and Running Mean techniques reduce the amplitude of the noise but at higher temperature, after 5 smoothing operations, these do not smooth the higher temperature spectra. It is at the higher temperatures that the use of a smoothing technique is most critical. The exponential smoothing function (Excel) shifts the peaks and decreases their intensity, the noise has been reduced greatly using this technique.

Fourier analysis has been shown to be able to remove the low level frequencies of the background and the high level frequencies of the electrical noise successfully. To determine the range of frequencies that were required to be removed, different frequencies were removed and the ratio between the intensities of the maximum and minimum positions were compared. This data was then curve fitted using the Munro equation.

4.1.1 *Averaging and subtracting the background*

The accumulation of a number of spectra could cause distortion in the overall spectra. It could be possible that when recording the spectrum we will be summing together slightly different spectrums due to the decay in intensity from the initial pulse. This could produce a rather more broad curve than expected and therefore at higher temperatures more reliable readings will be gained from a single pulse.

Finding the average of tens sets of data does not significantly reduces the noise, which indicates that the noise is a constant associated with the detector. Subtracting a background reading from the fluorescence spectrum makes a huge difference to the clarity of the peaks at high temperature.

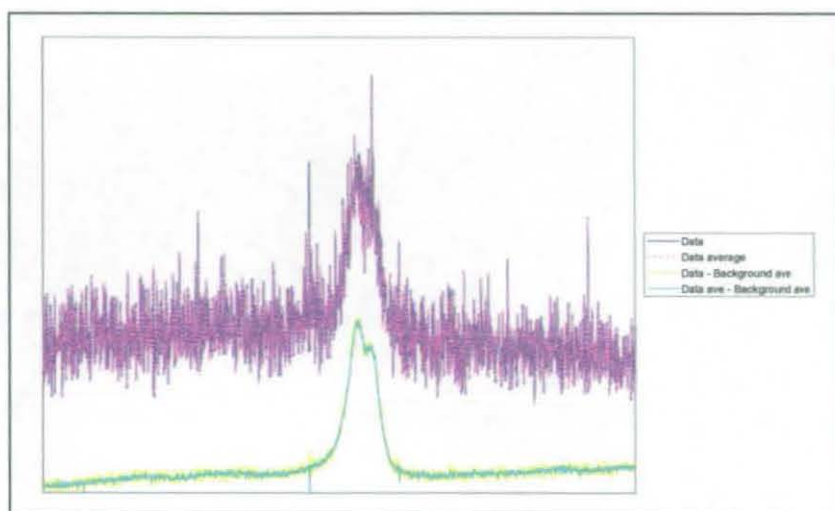


Figure 4-1 The difference in the noise levels can be seen to be reduced through background subtraction, data taken at 250°C.

The subtraction of the background also gives a stable base from which to work when using the intensity of the peaks for temperature measurement.

4.1.2 Using known smoothing techniques

The moving average technique and Hanning technique of smoothing have been considered for peak analysis. It can be seen that these techniques produce very similar results. With the raw data it is mainly the sharp peaks noise that is removed. It makes very little difference to the background subtracted data, though increasing the moving average range produces a very smooth curve at the expense of shifting the peaks.

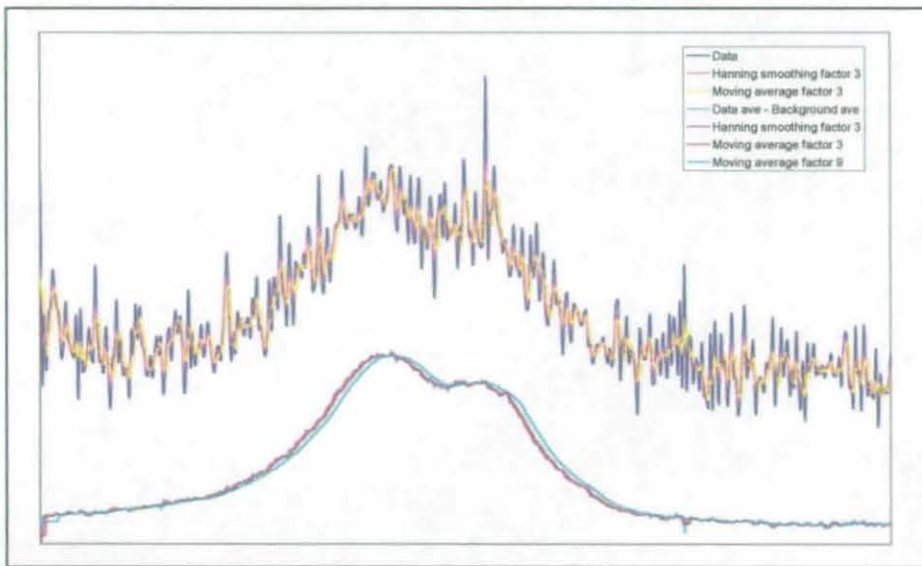


Figure 4-2 The affect of the smoothing techniques on raw data and background subtracted data.

These technique show possibility for use with the data, mainly for removing any sharp noise peaks that may occur around the peaks and thus affect the peak fitting routine.

4.1.2.1 Fourier Transform

The Fourier Transform technique can be used to remove the high and low frequencies, this enables the high frequencies such as electrical noise, and low frequencies such as background to be removed. To remove the electrical noise it is important that the whole spectrum is analysed rather than just the area around the peaks as the noise can be determined more accurately.

Removing too much noise produced just one peak, it is important that the correct amount of noise is removed so that the most defined peaks are shown without distorting the shape of the peaks.

To determine which frequencies should be removed to both reduce the noise and keep the shape of the peaks, a number of Fourier transforms have been taken on the same data. The data has had different high and low frequencies removed, peaks have been fitted to the resulting data. The height, width and position of these peaks are then being used to determine whether they still fit the shape of a Ruby peak as defined by Munro et al and if the data can still be related to temperature. It is found that not all of the Fourier transform data fit the Munro et al definition.

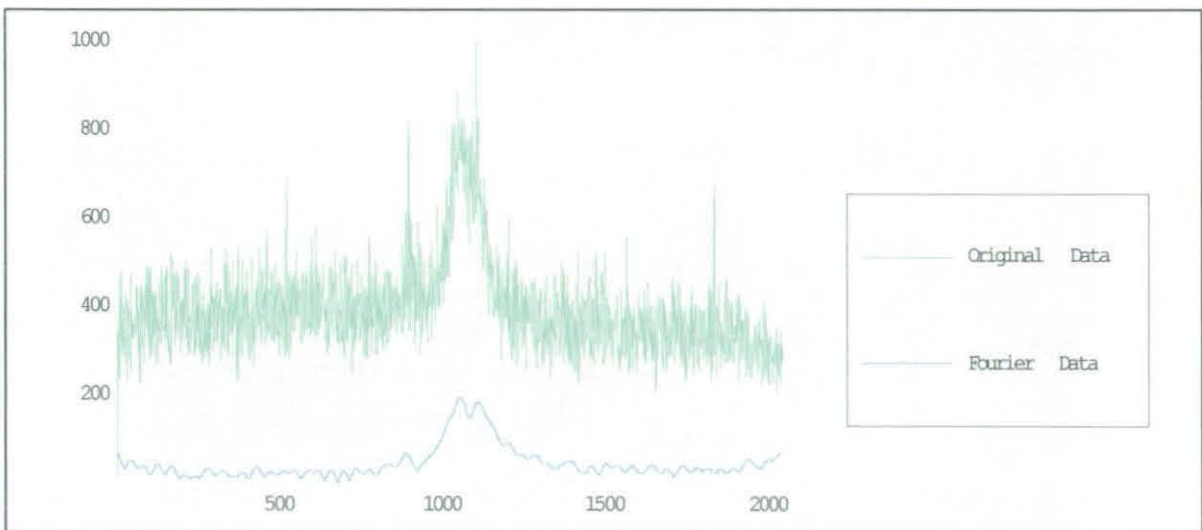


Figure 4-3 The smoothing affect of Fourier analysis on the spectrum, using data taken at 250°C.

It was found that using the range of frequencies between 2 and 70 provided a high ratio between the intensities for both temperatures of 25°C and 250°C. It was thought that a high ratio will mean that the peaks are more distinct and therefore easier to define. Curve fitting the Fourier analysed data showed that the Munro equation did not fit the data. This showed that the Fourier analysis has changed the shape of the spectra through the removal of a single, or a group of, frequencies. It was therefore important to determine which frequencies were required to define the Ruby spectra, if this technique is to be used.

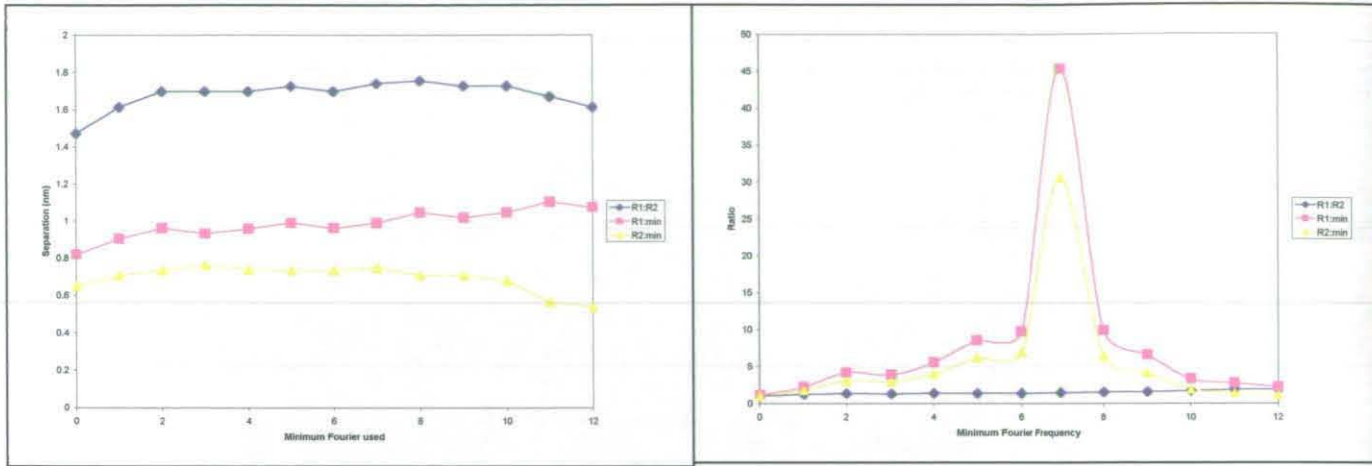


Figure 4-4 The affect of the lower frequency removal on the peaks.

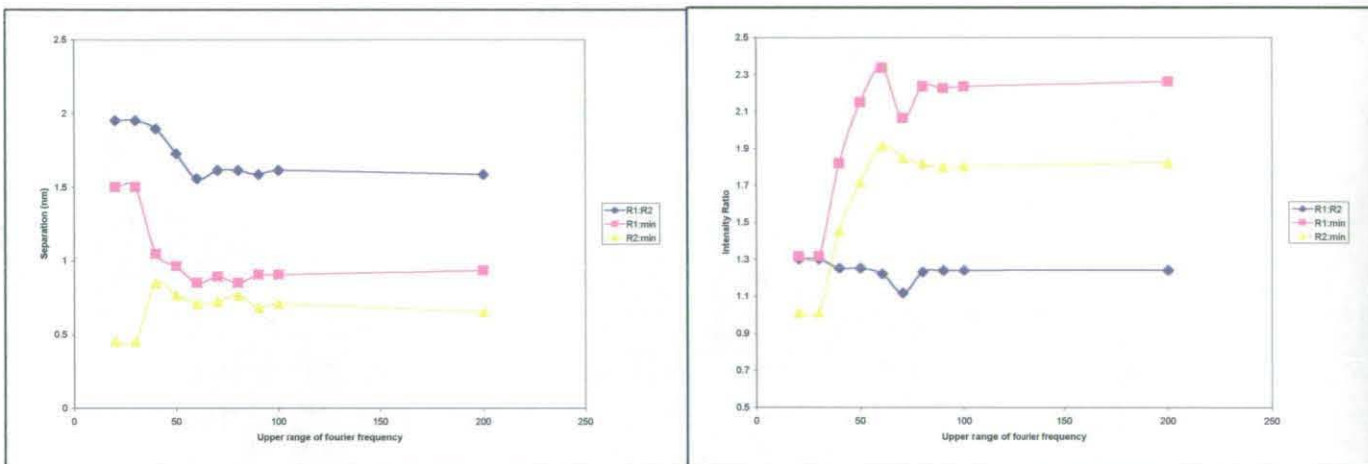


Figure 4-5 The affect of the higher frequency removal on the peaks.

When considering the peak position and the intensity rather than the peak shape then it was determined that the removal of the lower frequencies affected the position and height of the saddle between the two peaks and not the actual peaks themselves. At the higher frequencies removing frequencies less than 70 affected the separation and ratio of the intensities of the two peaks.

The use of Fourier analysis shows a possibility that will enable the peaks to be more defined at higher temperatures. This technique can also be implemented by using a data filter on the data as it is recorded and therefore does not require extra software processing during data analysis.

The work here shows that to produce consistent data the background should be subtracted from the raw data. This also works as a smoothing technique by removing most of the high frequency detector noise. Smoothing techniques can be used once the background noise has been subtracted. Fourier analysis can be used but this requires careful selection of the frequencies to remove so was not to affect the peak shape. The techniques to be used further are background subtraction, averaging of data over a number of readings, and the Moving Average technique.

4.2 Ruby spectrum analysis

This section looks at the temperature sensitivity of both solid Ruby and coatings using Ruby powder. The results of the peak position are compared to the known trends defined by Munro et al and Abella and Cummins. The trends determined compare well to these known trends. The temperature range of interest is 100°C to 300°C, particularly the range 150°C to 250°C.

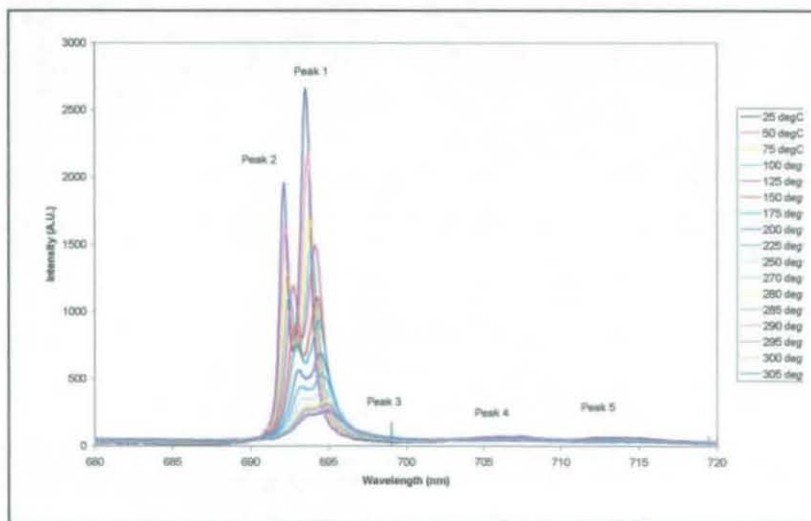


Figure 4-6 The spectrum of solid Ruby.

The possibility of still being able to measure the average temperature accurately when large fluctuations in temperature occur while taking the reading has been considered. This has shown that the average temperature can be recorded for difference in temperature of 30°C.

The spectrum of Ruby, Figure 4-6, has two peaks at around 690nm, which are the main ones used for temperature measurement. Two wider peaks can be seen at around 710nm, and a fifth was determined through peak fitting at around 700nm.

4.2.1 *Solid Ruby*

A number of sets of spectrum have been recorded at temperatures ranging from 25°C to 330°C. The gate period for each data set varied from 700msec to 10msec. At each temperature step ten separate spectrum have been recorded, as well as ten sets of background readings. The data set that has been used for comparison here is the data taken with a 500msec gate period.

4.2.1.1 *Fitting of Munro peak shape*

Munro et al have determined that the shape of the Ruby peaks are similar in profile to a Voight profile^{XIII}. It is this profile determined by Munro et al that has been used here to extract information from the fluorescence peaks obtained from experimentation. Previous work has suggested that the peak width, height and position of Ruby, are all related to temperature. The exact relationship has been shown by previous work to be dependent upon the Chromium content of the Ruby.

The Munro peak shape was fitted using the PeakAlyze program with the Munro equation entered into the program. Initial values were inputted determined from previous fits, sometimes requiring a number of fits before a close fit was determined.

The parameters that have been shown to be related to temperature previously are; amplitude, peak position, Gaussian and Lorentzian widths. These have been considered

^{XIII} See Appendix - 9.8 Equations

as well as the ratio of the amplitudes, peak separation and ratio of the Gaussian and Lorentzian widths. It is shown that the peak positions, and the separation of the peaks are related to temperature.

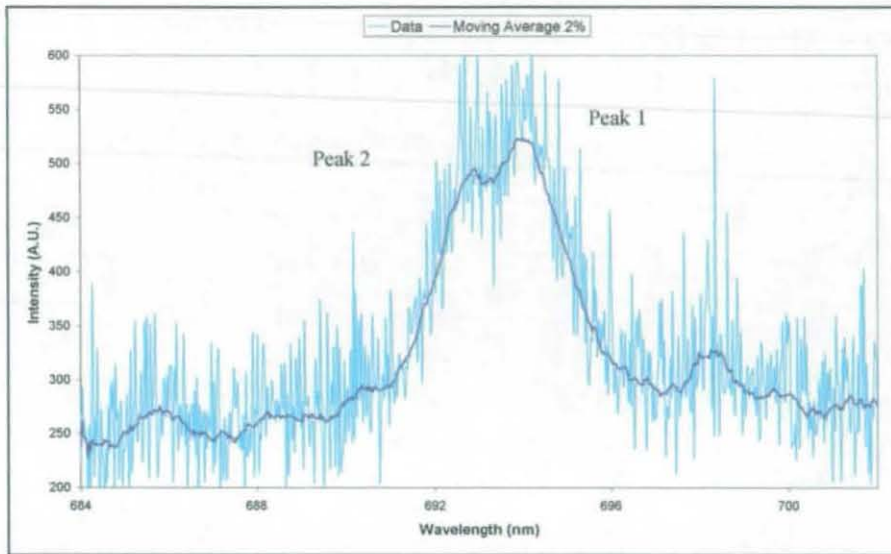


Figure 4-7 The difference between smoothed and non-smoothed data at 250°C

4.2.1.1.1 *Non-smoothed data*

Using the peak fitting program PeakAlyze, the Munro peak shape was fitted to the whole spectrum without any smoothing operations. The values determined for each for the functions of the peak shape were recorded and a temperature relationship found the fit using Excel. The best equations determined from this process are shown below along with their R^2 value, a summary of the whole set of fits is shown in the appendix.

Using the intensity of the peaks;

$$\text{Peak 1; } y = -815.99\text{Ln}(\text{temp}) + 4811.4 \quad R^2 = 0.97$$

$$\text{Peak 2 } y = -570.73\text{Ln}(\text{temp}) + 3330.6 \quad R^2 = 0.98$$

Using the position of the peaks;

$$\text{Peak 1; } y = 164.28 * \text{temp} - 114033 \quad R^2 = 0.98$$

$$\text{Peak 2 } y = 178.72 * \text{temp} - 123434 \quad R^2 = 0.98$$

Using the separation of the peaks;

$$y = 0.0005 * \text{temp} + 3.4528 \quad R^2 = 0.97$$

Equation 4-1 Set of equations showing the relationship between temperature and the fluorescence spectrum of Ruby. Peak details determined from the Munro equation.

These equations were determined for data within the temperature range 25°C to 300°C. This shows that the peak amplitude and position can both be related to temperature, as well as the peak separation. The use of the peak amplitude is not ideal as the intensity of the fluorescence varies depending upon the optical arrangement of the experiment. The peak position is the best function to use as this is totally independent from the optical arrangement as it is due to the internal molecular structure of the material.

The equations determined for finding the temperature from the position of the peaks are shown on page 94. It was determined that taking a reference reading at a known temperature at the start of the experiment was required and the reference temperature was best taken at the mid point of the temperature range. This will enable any fluctuations in the sample or detection equipment that may cause differences in the position readings to be eliminated. These equations were produced for the temperature range 25°C to 200°C.

$$\text{For Peak 1; } T = \left(\frac{P_1 - P_{1ref}}{0.006} \right) + T_{ref} \quad \text{Equation 4-2}$$

$$\text{For Peak 2; } T = \left(\frac{P_2 - P_{2ref}}{0.0055} \right) + T_{ref} \quad \text{Equation 4-3}$$

$$\text{For Peak 1 - Peak 2; } T = \left(\frac{D - 3.4528}{0.0005} \right) \quad \text{Equation 4-4}$$

Where;

T = temperature (°C)

P_1 & P_2 = positions of peaks 1 & 2

D = separation of peak positions

T_{ref} = temperature at which the reference was taken

P_{1ref} & P_{2ref} = positions of peaks 1 & 2 at the reference temperature

As the equation for the separation of the peaks is independent of any fluctuations in the detector it is thought that this would provide the best means of determining temperature. With the Solar T II spectrometer the grating is altered using a micrometer stage, this enables a wider range of wavelengths to be detected compared to a stationary grating as the resolution of the spectrometer is such that only a range of 55nm can be detected at one instant. A variation in the micrometer setting of 0.01mm means a shift in wavelength

of 0.4nm, which in turn relates to a temperature shift of 66°C this means that the wavelength of the peak positions is dependent upon the accuracy of the reading of the micrometer position. If this is also moved without knowing then errors will occur in the peak wavelength value.

The use of the peak separation in fact proved to be the worst of the three equations, with large errors between the actual temperature and the determined temperature, see Figure 4-8. The use of the reference value removes the error due to the grating setting and making each set of readings independent of the grating.

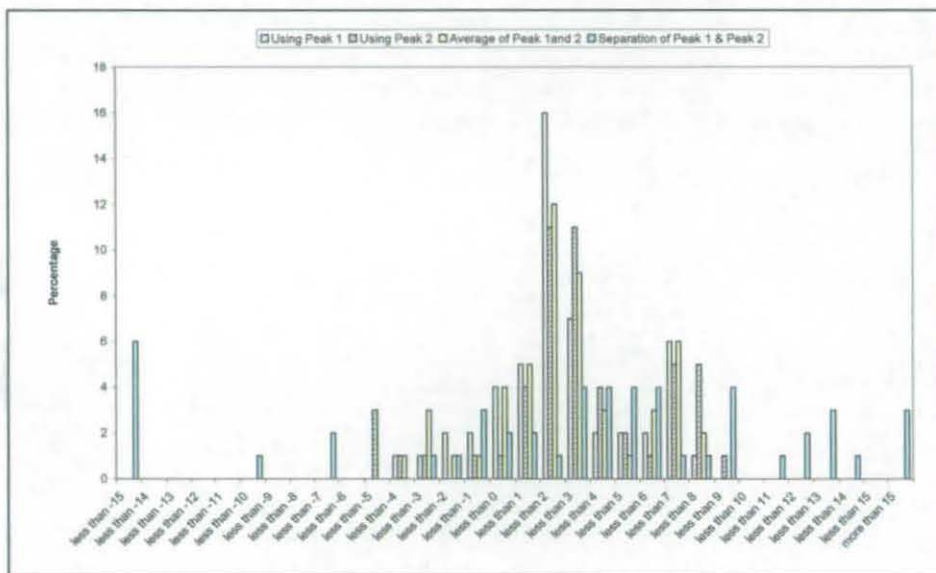


Figure 4-8 The distribution of the percentage error for the temperature range 125°C to 270°C.

When fitting these equations to known data it was observed that above 250°C the data became scattered, and therefore large differences between the actual and measured data occurred. It was therefore determined that these equations were only suitable for up to 250°C. Considering this temperature range the temperature could be measured to an accuracy of -14% to +7%. Reducing the temperature range to 125°C to 270°C the accuracy of the fit could be improved to -5% to +7%. There is little difference in the accuracy of the fits between the positions of peak 1 and peak 2. Using peak 1 only produces a slightly better fit than the others, see Figure 4-8. The secondary peak at 'less than 7' in Figure 4-8 can all be accounted for by the difference at 125°C. It therefore shows that for the temperature range 150°C to 270°C a very accurate temperature measurement can be made.

To improve the accuracy of the fit, the difference between the temperatures achieved from the two peaks was considered. If the two temperature readings were not within 5°C then it was considered an error had occurred and the data was in error and was to be ignored. This technique did not decrease the error as it was found that if an error occurred then it tended to be due to a shift from both peaks rather than just one. As both peaks shift then the difference in the temperature values does not increase significantly.

4.2.1.1.2 *Smoothed spectrum*

Smoothing techniques have the advantage of being able to remove noise from the spectrum enabling the peaks to be more defined. The use of smoothing techniques can affect the shape of the peaks. As it is the peak shape that gives the temperature relationship it is thought that smoothing of the data should not be undertaken. The work here is to determine whether smoothing operations can be used to help define the peaks from the background without affecting the relationship with temperature. The same data set that was used for the non-smoothing analysis has been used here.

The data has been smoothed using the Moving Average technique, as defined in the PeakAlyze program. Smoothing has been used to reduce the high frequency noise, to help in the fitting of the data at higher temperature where the peaks are close to the noise level, Figure 4-7.

Using the intensity of the peaks;

$$\text{Peak 1; } y = 0.0305 \cdot \text{temp}^2 - 14.702 \cdot \text{temp} + 2137.6 \quad R^2 = 0.93$$

$$\text{Peak 2 } y = 0.0187 \cdot \text{temp}^2 - 9.6172 \cdot \text{temp} + 1414.6 \quad R^2 = 0.96$$

Using the position of the peaks;

$$\text{Peak 1; } y = 0.0064 \cdot \text{temp} + 694.09 \quad R^2 = 0.98$$

$$\text{Peak 2 } y = 0.0057 \cdot \text{temp} + 692.66 \quad R^2 = 0.97$$

Using the separation of the peaks;

$$\text{Peaks 1\&3 } y = -0.0068 \cdot \text{temp} + 5.9955 \quad R^2 = 0.97$$

$$\text{Peaks 2\&3 } y = -0.0062 \cdot \text{temp} + 7.4305 \quad R^2 = 0.96$$

Using the ratio of the peak intensities;

$$\text{Peaks 1\&3 } y = 55.036e^{-0.0107 \cdot \text{temp}} \quad R^2 = 0.93$$

$$\text{Peaks 2\&3 } y = 34.989e^{-0.0103 \cdot \text{temp}} \quad R^2 = 0.94$$

Equation 4-5 Set of equations showing the relationship between temperature and the fluorescence spectrum of Ruby. Spectrum is smoothed and the peak details are then determined from the Munro equation.

These equations have been determined over the temperature range 25°C to 300°C. Through smoothing a third peak at a longer wavelength has become obvious. This peak can be used to reference the other two peaks, as it did not shift with temperature. The separation between the third peak and the other two can be related to temperature, which gives a more reliable relationship than using the separation between the first two peaks. It is the position of peaks 1 and 2 that have been found to produce the best fit with temperature and produced the following equations;

For Peak 1;
$$T = \left(\frac{P_1 - P_{1ref}}{0.0064} \right) + T_{ref}$$
 Equation 4-6

For Peak 2;
$$T = \left(\frac{P_2 - P_{2ref}}{0.0057} \right) + T_{ref}$$
 Equation 4-7

For Peak 1 – Peak 3;
$$T = \left(\frac{D_1 - 5.9955}{-0.0068} \right)$$
 Equation 4-8

For Peak 2 – Peak 3;
$$T = \left(\frac{D_2 - 7.4305}{-0.0062} \right)$$
 Equation 4-9

Where;

$T = \text{temperature } (^{\circ}\text{C})$

$P_1 \ \& \ P_2 = \text{positions of peaks 1 \& 2}$

$D_1 \ \& \ D_2 = \text{separation of peak 1 \& 2 from peak 3}$

$T_{ref} = \text{temperature at which the reference was taken}$

$P_{1ref} \ \& \ P_{2ref} = \text{positions of peaks 1 \& 2 at the reference temperature}$

The third peak was only found on 40% of the spectra, the separation of peaks 1 and 2 from the third peak can therefore not be used reliably. It was found though that if the third peak existed, the separation could be used as a check with the determined temperature in the range 100°C to 250°C as this produced more accurate relationship with temperature than using just the peak positions. There is very little difference in the accuracy of the results determined from the peak positions. Using the average of the temperature determined from peaks one and two produced the most accurate result, see Figure 4-9.

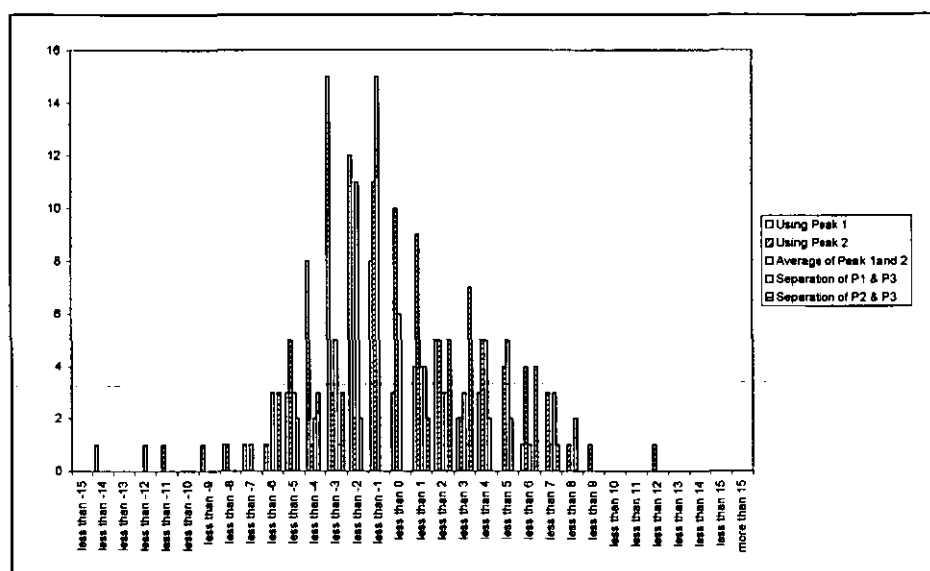


Figure 4-9 The distribution of the percentage error for the temperature range 125°C to 270°C.

4.2.1.1.3 Summary of Munro fitted data

There is very little difference between the accuracy of the fits determined by the smoothed and non-smoothed data. For both methods it is determined that the temperature range 125 to 270°C gives the most accurate results, this incorporates the range of interest which is 150°C to 250°C. For the non-smoothed data an accuracy of -5% to +7% is achieved, from the temperature determined from peak 1. With the smoothed data an accuracy of -7% to +6% is achieved from using the average temperature determined from the two peaks. Although there is a slight difference in the two error ranges this is not significant enough to say that the non-smoothed data is better. This is well within the accuracy quoted by Munro et al of $\pm 10\%$. The error is the difference between the actual temperature value and the temperature reading, this difference is then determined as a percentage of the temperature value.

At this point there is no preference between using smoothed or non-smoothed data to determine the temperature from the spectrum by fitting the Munro peak profile. Comparing the trends determined here with the trend determined by Munro et al and Abella & Cummins it is seen that the smoothed data produces a trend which is similar. The non-smoothed data produces a shift of peak 2 away from peak 1. For the

measurement of temperature this difference for the non-smoothed data is not a problem as long as this is constant from one data set to another.

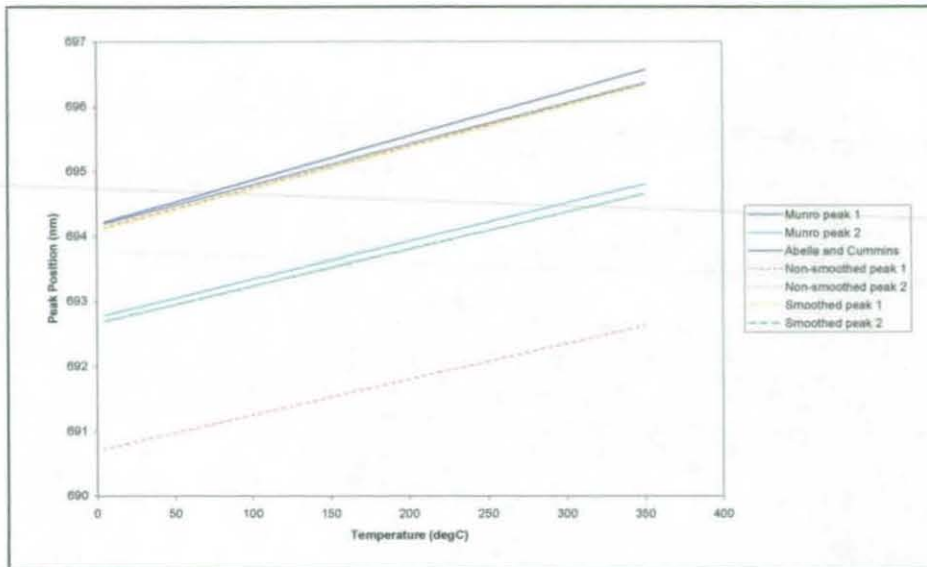


Figure 4-10 Comparing the equations determined using Munro peak profile to determine peak positions.

4.2.1.2 Using automated software to extract peak details from the spectrum

As it is the peak position and amplitude that is of interest and not the peak width, the use of the LabView routine, 'peak find', can be used. The use of the LabView routine will enable the automated extraction of data from the spectrum, this will involve the use of the peak find routine in LabView. This data was then entered into an Excel workbook where a macro has been written to remove data that is not of interest to the temperature measurement. With the work undertaken with fitting of the Munro profile to the data it was determined that the peak positions and intensities of peaks 1 and 2 provided the best fit. As there was little difference in the correlation between the smoothed and non-smoothed data from Munro peak shape fitting, especially for the peak position, no smoothing operation was undertaken.

Using the LabView routine, the peak width and threshold are set, the width refers to the number of data points that are used in the determination of whether a peak exists. The minimum number of data points which can be used is three, the maximum which can be used successfully is the half peak width at half height. For noisy data it is not recommended to use the value of three to reduce the amount of noise which is detected. If the width value is either too large or too small for the data set then errors can occur. Using the threshold value will also reduce the noise detection. The threshold value is the minimum height that a peak can be. If this value is set too low then too many noise peaks will be detected, if set too high then the lower peak will not be detected at higher temperatures. If low threshold values are set then a large number of peaks is detected, this means that double peaks are sometimes produced, the Excel macro has been designed to remove these double peaks ^{XIV}.

4.2.1.2.1 Analysis of the data using LabView peak find routine

A number of data sets have been used here to allow the reliability of data from one set to another to be determined. It is the data set that has been used in the sections 4.2.1.1.1 Non-smoothed data, and 4.2.1.1.2 Smoothed spectrum which is discussed in most detail here. The background was determined at each temperature stage and subtracted from the fluorescence spectra. It was confirmed by these data sets that the position and intensity of peak 1 and peak 2 provided a strong relationship with temperature.

At 200°C the peak width at half height of peak 1 and peak 2 is 18nm and 9nm respectively. LabView works in terms of data points, a half width in terms of data points of 666 and 333. The separation of the peaks is around 1.4nm, which in terms of data points is 52. The initial band widths which were considered are 3 to 30, to avoid too much overlap of the peaks while fitting. It is shown that widths 25 to 30 give the best fits for use with temperature analysis. It is also shown that the threshold affects the results considerably.

LabView gives the peak position and peak intensity, this information was then organised into wavelength bands, which refer to the positions of the peaks of interest. This data was

^{XIV} See Appendix – 9.7 Programming

then organised so that if more than one peak occurred in the wavelength band then that data was eliminated. This was done as with low threshold levels and low widths noise is detected as peaks. This noise is seen as many narrow band width peaks, this deletion will then show that this is not a good set of parameters to use to determine the peaks of interest. This organization of the peaks was done through a macro written in Excel. The fitting of the data is done through an Excel macro, using the linear regression function.

The best results from fitting the peak parameters from this data set with temperature are shown below, the results from the other data sets and the remaining results from this set can be seen in the appendix. The choice of best fit is determined by considering both the R^2 value, the temperature range to which it fitted, and the number of data points that resulted in the fit. An ideal fit would cover the temperature range 25 to 300°C, have an R^2 value greater than 0.9. and have a high number of data points. The number of data points will vary from one data set to another due to the number of readings taken

Peak 1 position, threshold set as 200		
25 → 300°C	$y=0.0055*\text{temp}+694.42$	$R^2= 0.98$
25 → 270°C	$y=0.0056*\text{temp}+694.40$	$R^2= 0.99$
Peak 2 position, threshold set as 200		
25 → 300°C	$y=0.0065*\text{temp}+692.92$	$R^2= 0.97$
25 → 200°C	$y=0.0062*\text{temp}+692.95$	$R^2= 0.99$
Ratio of the intensities of Peak 1&2, threshold set as 200		
25 → 270°C	$y=0.00064*\text{temp}+0.71$	$R^2= 0.92$
Ratio of the intensities of Peak 2&3, threshold set as 100		
25 → 250°C	$y=-0.13*\text{temp}+19.49$	$R^2= 0.98$

Equation 4-10 Set of equations showing the relationship between temperature and the fluorescence spectrum of Ruby. The peak details are determined using the peak find routine in LabView.

As with the Munro peak shape data it is the peak position that gives the most reliable fit. It is therefore these that are considered. For this data set the equations determined with a threshold of 200, and a width value of 30, have been considered. This threshold level has the most number of points in the fit. Setting low threshold values and small widths means a lot of background noise is detected. This can affect the results by causing double peaks, two peaks very close together, this is a problem as it is not known which is the true peak. The Excel macro is therefore used to remove these double peaks. This deletion of peaks is why the count is low for low thresholds and much higher at higher thresholds.

For Peak 1;
$$T = \left(\frac{P_1 - P_{1ref}}{0.0056} \right) + T_{ref}$$
 Equation 4-11

For Peak 2;
$$T = \left(\frac{P_2 - P_{2ref}}{0.0064} \right) + T_{ref}$$
 Equation 4-12

Where;

T = temperature (°C)

P_1 & P_2 = positions of peaks 1 & 2

T_{ref} = temperature at which the reference was taken

P_{1ref} & P_{2ref} = positions of peaks 1 & 2 at the reference temperature

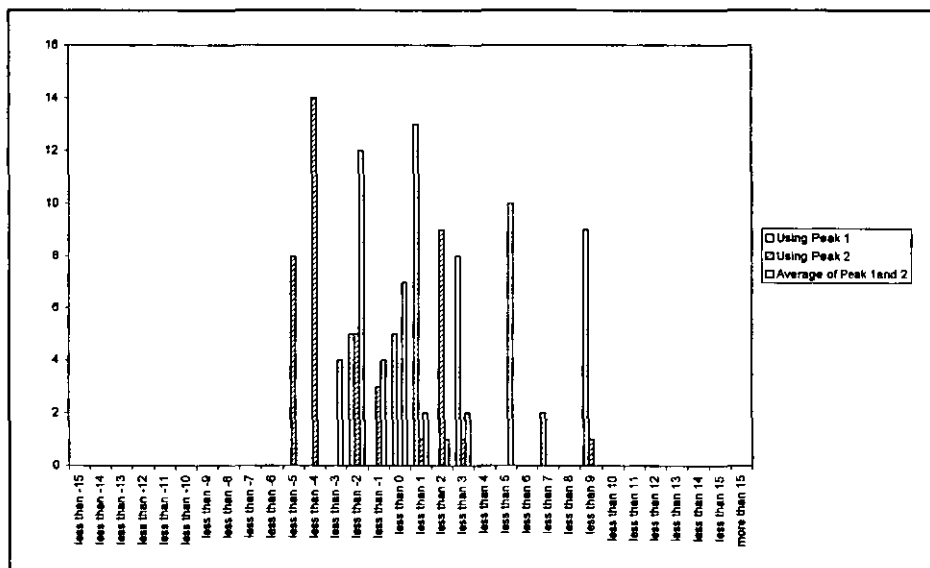


Figure 4-11 The distribution of the percentage error for the temperature range 125°C to 225°C.

The equations determined here compare well to the equation derived from the fitting of the Munro peak shape to the peaks. For the temperature range 125°C to 225°C an accuracy of -3% to +5% is achieved when the average of the two temperature values are considered. For the range 25°C to 225°C an accuracy of ±9% is achieved using the temperature value from the position of peak 1.

4.2.1.2.2 Averaging of peaks

The affect of the summation of a number of peaks at different temperatures has been considered. This is to ensure that if a rapidly changing surface temperature is encountered then a relevant temperature can be measured from the fluorescence spectra recorded. Temperature differences of up to 30°C were considered, the accuracy between the average measured temperature and the calculated temperature was found to vary greatly with temperature. The average temperature value from the values determined by positions of peak 1 and peak 2 was used. For a temperature range of 65°C to 270°C an accuracy of $\pm 12\%$ was achieved, though this was greatly improved over the temperature range 90°C to 240°C where an accuracy of -3 to $+8\%$ was achieved. This shows that this is within the error expected to be achieved from the averaging over a wide temperature range, within that achieved from stable temperature spectrum.

4.2.1.2.3 Affect of gate period on the fit

The five different data sets were taken with different gate periods to determine whether the time period has an affect on the spectrum reading obtained. This is an important consideration, as when spinning the gate period would be determined by the speed of the object. The readings were taken on two separate days.

On each day the readings were taken one after another with only the gate period changing. Therefore any changes noted will only be from the change in the gate period.

The data has been considered using a linear relationship between temperature and the function. The peak parameters set in LabView affect the values for the equation $y=mx+c$, it is therefore important to determine a set of values that produces a strong relationship with temperature. As expected the intensities of peak 1 and peak 2 show a strong relationship with gate period.

4.2.1.3 Summary of Ruby Rod data

The relationships created have been compared to known relationships derived by ‘Munro et al’ and ‘Abella and Cummins’, and these have been found to compare well. The equations determined for each fit is shown in the relevant section. Different techniques for the fitting of peaks have been considered, as well as the consideration of the affects of averaging over a wide temperature region and for stability.

Analysis Type	% error				
	20→300°C	20→250°C	20→250°C	125→270°C	125→225°C
Munro et al accuracy	±10% (20%)				
Munro Non-smoothed		-14 to +7% (21%)		-5% to +7% (12%)	
Munro Smoothed				-6% to +7% (13%)	
LabView Non-smoothed			±9% (18%)		-3% to +5% (8%)

Table 4-1 The accuracy’s achieved from the same data set using different fitting techniques.

The wavelength of the peak positions was found to change slightly over prolonged heating periods. This change was not related to time and can therefore only be accounted for by slight changes in the molecular structure. The temperature remained constant and neither the optical components nor the sample was moved.

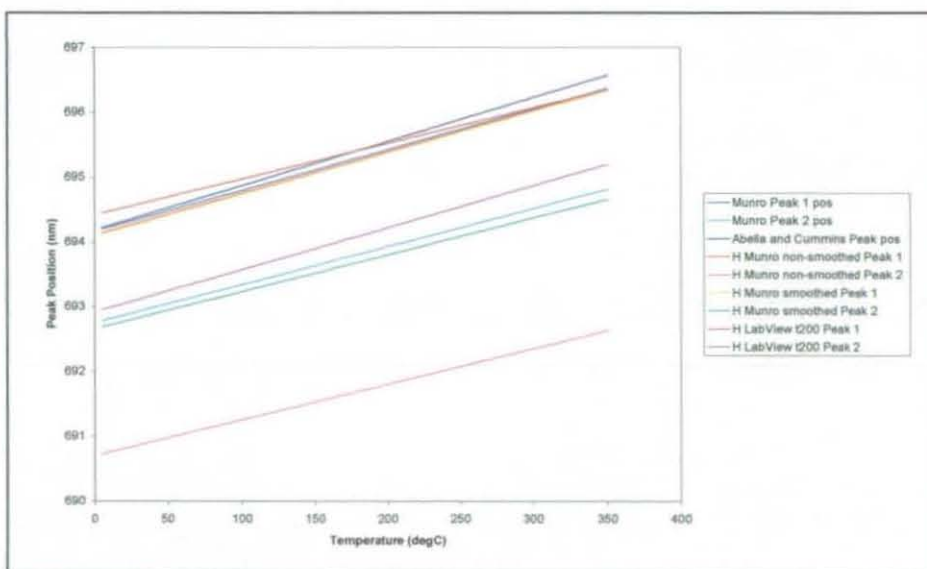


Figure 4-12 Comparison between determined relationships and known relationships.

The equations determined have been compared, the accuracy of fit has been found for data taken with a 500msec gate period, Figure 3-12. To improve the accuracy of the fit the difference in temperature determined from the two separate peak positions has been considered. If the separation was less than 2, 5, or 10°C the average of the two peaks was used, if outside of these ranges it was considered to be an error measurement. This was not found to increase the accuracy of the fit. The accuracy of the results is less than the estimated accuracy of fit determined by Munro et al of 10%. It is determined that the use of the peak find LabView routine threshold set as 200 and width as 30, provides the best fit using the position of peak 1. For this position 50% of the predicted temperatures are within 3% of the measured temperature.

Peak function used	Method	Maximum Temperature °C	Accuracy %	% of data fitted
Position Peak 1	LabView	272	4.81	100
Position Peak 2	Munro smoothed	300	5.22	100
Average of position of Peak 1 and Peak 2	Munro non-smoothed	300	5.30	100
Average of position of Peak 1 and Peak 2	LabView	272	5.31	100
Average of position of Peak 1 and Peak 2, where values are within $\pm 10^\circ\text{C}$	Munro smoothed	300	5.32	89
Position Peak 1	Munro non-smoothed	300	5.38	100
Average of position of Peak 1 and Peak 2	Munro smoothed	300	5.38	100
Average of position of Peak 1 and Peak 2, where values are within $\pm 5^\circ\text{C}$	Munro non-smoothed	300	5.57	76
Position Peak 2	Munro non-smoothed	300	5.59	100
Average of position of Peak 1 and Peak 2	Munro smoothed	250	5.76	100
Average of position of Peak 1 and Peak 2, where values are within $\pm 10^\circ\text{C}$	Munro non-smoothed	300	5.77	84
Average of position of Peak 1 and Peak 2, where values are within $\pm 10^\circ\text{C}$	LabView	270	5.84	87
Position Peak 1	Munro smoothed	300	5.86	100
Position Peak 2	Munro smoothed	250	6.05	100
Position Peak 2	LabView	270	6.54	100
Position Peak 2	Munro non-smoothed	200	6.58	100
Average of position of Peak 1 and Peak 2	Munro non-smoothed	200	6.66	100
Average of position of Peak 1 and Peak 2, where values are within $\pm 10^\circ\text{C}$	Munro non-smoothed	200	6.66	80
Average of position of Peak 1 and Peak 2, where values are within $\pm 5^\circ\text{C}$	Munro non-smoothed	200	6.66	80
Position Peak 1	Munro non-smoothed	200	6.75	100
Average of position of Peak 1 and Peak 2, where values are within $\pm 2^\circ\text{C}$	Munro non-smoothed	200	6.85	77

Table 4-2 Comparison of the spectrum fitting results from the position of Peak 1 and Peak 2, for the Ruby rod data.

4.2.2 *Ruby paint coated*

The paint coating has been shown to be able to withstand temperatures of 250°C for long periods, while temperatures of 300°C could only be sustained for short periods of around five minutes, because after long periods the coating becomes brittle and starts to detach itself from the aluminium.

Using the Munro equation to fit the data the accuracy obtained is very poor, and the trend differs greatly from that obtained from the Ruby rod. Less than 10% of the data is within $\pm 10\%$ of the actual temperature reading. This technique is shown not to be a useful technique of temperature measurement and so little analysis has been undertaken on the analysis of the paint coating technique.

4.2.3 *Ruby plasma coated*

The coating of Ruby to an aluminium surface using plasma coating has been considered. The coating has been shown to withstand the conditions within the compressor environment. It is the fluorescence relationship with temperature of the coating being tested here.

The whole spectrum has been used while fitting the Ruby peaks. The peak-fitting program PeakAlyze was used to fit the Munro equation to the peaks. Two data sets have been analysed here, one with a 100msec detector gate period and the other with a 2msec detector gate period. The long gate period of 100msec was chosen to enable a reliable temperature relationship to be determined. The much shorter gate period of 2msec was chosen as this is similar to the time period that the detector would be exposed to Ruby fluorescence whilst spinning at 80,000rpm, corresponding to one complete resolution of the rotating compressor disc.

4.2.3.1 Taking readings with 100msec gate period.

4.2.3.1.1 Using the Munro profile

From the analysis of the data it could be seen that lower temperatures gave a slightly different trend to higher temperatures. The spectrum achieved for this data set can be seen in Figure 4-13, at temperatures below 275°C readings were taken every 25°C, above this they were taken every 5°C. At each temperature stage 10 separate spectrum were recorded which have been used to create the relationships below, Equation 4-13.

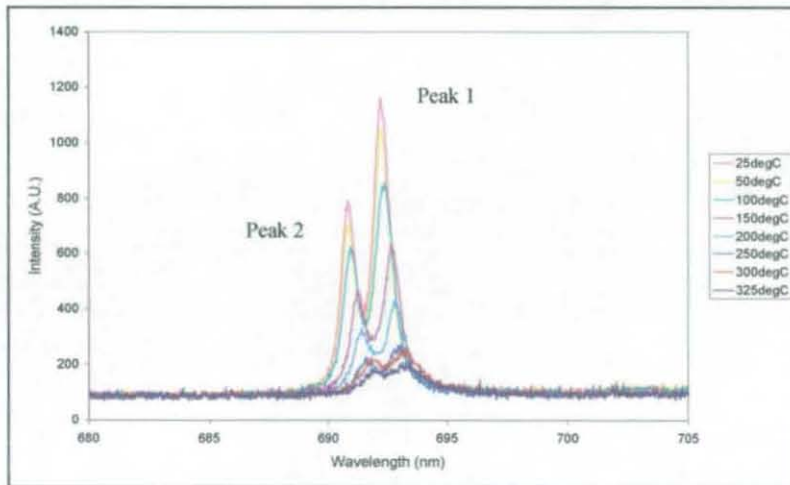


Figure 4-13 The luminescence spectrum of plasma coated Ruby, before smoothing.

Peak 1, intensity		
25 → 275°C	$y = -2.3315 * \text{temp} + 753.95$	$R^2 = 0.94$
Peak 2, intensity		
25 → 275°C	$y = -1.2397 * \text{temp} + 398.14$	$R^2 = 0.94$
Peak 1, position		
25 → 275°C	$y = 0.0038 * \text{temp} + 694.15$	$R^2 = 0.96$
Peak 2, position		
25 → 275°C	$y = 0.0039 * \text{temp} + 692.66$	$R^2 = 0.96$
150 → 275°C	$y = 0.0034 * \text{temp} + 692.78$	$R^2 = 0.99$

Equation 4-13 Set of equations showing the relationship between temperature and the fluorescence spectrum of Ruby. The peak details are determined using the Munro equation.

The data on each peak was determined using PeakAlyze. The peaks in each spectrum were smoothed using the moving average function in PeakAlyze which was set to 1%. Peaks 1 and 2 were found to follow the Munro profile^{xv}, while Peaks 4 and 5 were Lorentzian^{xv} in shape. To determine the correlation between the peak shape and temperature Excel was used.

Secondary peaks, peaks 4 and 5, were fitted using a Lorentzian profile rather than the Munro profile that was used to fit the main peaks. This was because the Munro profile was found not to fit the peak shape of the secondary peaks. These peaks did not show any relationship to temperature.

4.2.3.1.2 *The use of the LabView routine*

The peak profiles were also determined using LabView. This gives a linear relationship with temperature for the peak positions and intensities. It showed that a wide width in the fitting process gave a good fit for the peak positions while the intensities required a much smaller width to determine a good temperature relationship. This gave a fit similar to that obtained from the curve fitting data. This shows that this technique can be used for determining the temperature in real time from a fluorescence spectrum.

Relationship	Peak 1 intensity	Peak 2 intensity	Peak 1 position	Peak 2 position
Threshold	50	50	50	50
Average				
Number of data points	280	312	283	312
m	-2.96	-1.86	0.0039	0.0043
b	1022	679	693.17	691.71
R ²	0.95	0.95	0.96	0.98
Best fit				
Width	11	11	25	25
Number of data points	214	218	312	383
m	-3.02	-1.92	0.0039	0.0043
b	1037	695	693.16	691.72
R ²	0.95	0.96	0.98	0.98
temp min	23	23	23	23
temp max	320	325	325	325

Table 4-3 The difference in the peak position relationship with temperature between the high and low temperature regions.

^{xv} See Appendix - 9.8 Equations

4.2.3.2 Taking readings with 2msec gate period.

For this data set only the higher temperature range was considered as this is the temperature range that is of most interest. It is also this range that is going to be difficult to detect due to the decrease in the intensity that occurs at higher temperatures.

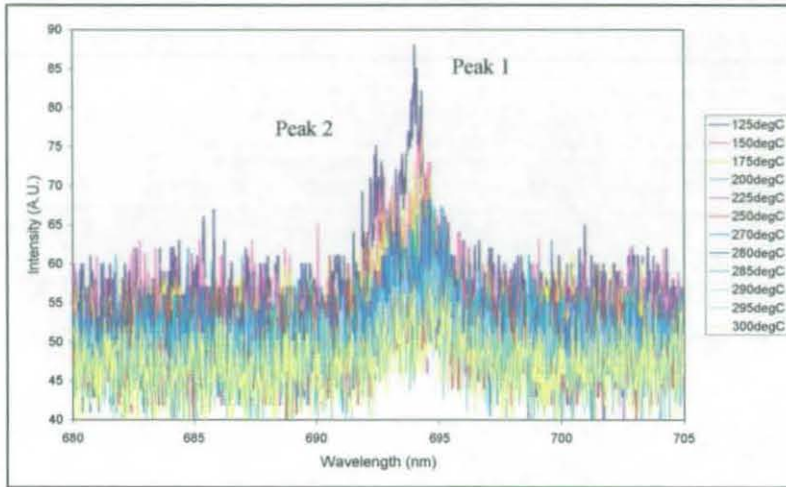


Figure 4-14 Spectrum taken with 2msecgate period.

4.2.3.2.1 Using the Munro profile without smoothing

This shows that a poor relationship with temperature is produced. The position of peak 1 gives the best relationship with temperature for the whole range studied, 125°C to 300°C. For the narrower temperature range the position of peak 1 gives a good relationship with temperature though it is its amplitude that gives the best temperature relationship.

Peak 1, intensity

$$125 \rightarrow 200^{\circ}\text{C} \quad y = -0.1659 * \text{temp} + 43.649 \quad R^2 = 0.91$$

Peak 1, position

$$125 \rightarrow 300^{\circ}\text{C} \quad y = 0.0043 * \text{temp} + 693.89 \quad R^2 = 0.83$$

Equation 4-14 Set of equations showing the relationship between temperature and the fluorescence spectrum of Ruby. The peak details are determined using the Munro equation without smoothing.

4.2.3.2.2 *Using the Munro profile after smoothing*

The positions of the peaks were erratic as with the non-smoothed data. The temperature relation to the positions followed an exponential trend rather than the linear trend that is expected. The peak positions did not produce a good fit with the single equation gained from the two peaks producing over 50% of the error between temperature read and temperature gained the equation being over $\pm 10^\circ\text{C}$. This was the case for the temperature range 125°C to 300°C , and 125°C to 250°C .

Peak 1, intensity

$$125 \rightarrow 300^\circ\text{C} \quad y = -0.0493 * \text{temp} + 20.729 \quad R^2 = 0.81$$

$$125 \rightarrow 300^\circ\text{C} \quad y = -0.0895 * \text{temp} + 27.093 \quad R^2 = 0.92$$

Peak 1, position

$$125 \rightarrow 300^\circ\text{C} \quad y = 0.0047 * \text{temp} + 693.83 \quad R^2 = 0.84$$

Equation 4-15 Set of equations showing the relationship between temperature and the fluorescence spectrum of Ruby. The peak details are determined using the Munro equation after smoothing.

The separation of the peaks could not be used for defining temperature. It was decided not to continue using this data set for temperature calibration. This change of fit of peak position could be due to the small amplitude of the peaks of this data set that makes peak fitting difficult.

4.2.3.2.3 *LabView fitted*

As it is only the peak position and amplitude that give a relationship with temperature the use of peak shape fitting is not required. The peak details of data taken using a 2msec gate period are therefore fitted using LabView to determine if this can be used. With this data set it is noted that to gain the best fit for peak 1 and peak 2, different widths are required. The results from the fitting of the peak positions with temperature are shown in Equation 4-16.

Peak 1, intensity,
125 → 300°C $y = -0.081 * \text{temp} + 32.79$ $R^2 = 0.88$

Peak 1, position
125 → 300°C $y = 0.0045 * \text{temp} + 693.05$ $R^2 = 0.93$

Equation 4-16 Set of equations showing the relationship between temperature and the fluorescence spectrum of Ruby. The peak details are determined using the LabView peak fit routine, threshold is set to 10.

The peak height of peak 2 became too small to be able to be detected above the background noise hence the smaller temperature range that is shown. This decrease in peak height is due to the decrease in intensity caused by heating. The equation used to determine the temperature from the peak position is shown below.

For Peak 1;
$$T = \left(\frac{P_1 - P_{1ref}}{0.0045} \right) + T_{ref}$$
 Equation 4-17

For Peak 2;
$$T = \left(\frac{P_2 - P_{2ref}}{0.0067} \right) + T_{ref}$$
 Equation 4-18

Where;

T = temperature (°C)

P_1 & P_2 = positions of peaks 1 & 2

D = separation of peak positions

T_{ref} = temperature at which the reference was taken

P_{1ref} & P_{2ref} = positions of peaks 1 & 2 at the reference temperature

The equation for peak 1 gives an accuracy of -11% to +15% whereas the equation for peak 2 gives an accuracy of -6 % to +12%. This poor accuracy is due to the small amplitude to the peaks thus making the fitting of the peaks difficult. A longer gate period would increase this accuracy as can be seen through the data taken with 100msec.

4.2.3.3 Summary of plasma coating technique

The plasma coated Ruby gives a relationship similar to that of the solid Ruby. The use of the smoothing technique changes the relationship very slightly, which indicates that the peaks can still be easily determined without many data smoothing operations having to

be undertaken even with low levels of light. Comparing the fits for position of Peak 1 for the different data operations, shows that there is very little difference between the fits. The difference in the constant would not affect the data, as a reference point is taken and used to create an equation that is independent of this value. The taking of the reference value eliminates errors due to the misalignment of the grating in the spectrometer.

	100msec Munro non-smoothed	2msec Munro non-smoothed	2msec Munro smoothed	2msec LabView
m	0.0038	0.0043	0.0043	0.0045
b	694.15	693.89	693.83	693.05
R ²	0.96	0.83	0.80	0.93

Table 4-4 Comparing the results from the different data operations for Peak 1 of plasma coated Ruby.

4.2.4 *Summary of Ruby as a temperature sensor*

This shows that Plasma coating of Ruby can be used to define temperature though this is dependent upon the quality of the signal received by the detector. Due to the poor signal to noise ratio the data has to be smoothed before fitting to enable it to be able to be used for temperature prediction.

Ruby in form	Analysis Type	% error				
		20→300°C	20→250°C	25→270°C	125→270°C	125→225°C
Solid	Munro et al accuracy	±10% (20%)				
Rod	Munro Non-smoothed		-14 to +7% (21%)		-5% to +7% (12%)	
Rod	Munro Smoothed				-6% to +7% (13%)	
Rod	LabView Non-smoothed		±9% (18%)			-3% to +5% (8%)
Paint	Munro Smoothed & Non-smoothed	Less than 10% within ±10%				
Paint	LabView					
Plasma coated	LabView Non-smoothed			±4% (8%)		

Table 4-5 The accuracy's achieved from the same data set using different fitting techniques.

The temperature of the Ruby rod can be predicted to an accuracy of $\pm 5^{\circ}\text{C}$, for non-smoothed data in the temperature range 25°C to 225°C . The smoothed plasma coated Ruby can be predicted to an accuracy of $\pm 4^{\circ}\text{C}$ in the temperature range 25°C to 270°C .

	Rod	Paint Coating	Plasma Coating
m	0.0052	0.0031	0.0039
b	694.54	694.86	693.16
R ²	1	1	0.98

Table 4-6 Comparing the relationships for peak 1 from LabView fitted data for each type of Ruby, data taken with a gate period of 100msec

This improvement in accuracy from solid Ruby to plasma coated Ruby could be due to the Ruby rod, as when the fluorescence is reflected back through the sample Raman scattering could occur thus broadening the peak slightly. This would then mean that the peaks could not be fitted as accurately as the plasma coated Ruby where the fluorescence has not been scattered through the material. It could also be due to an improvement in the data analysis technique used, and the optical collection of the fluorescence. Another explanation could be that the heating of the powder to achieve the coating could have had an annealing affect removing impurities from the material.

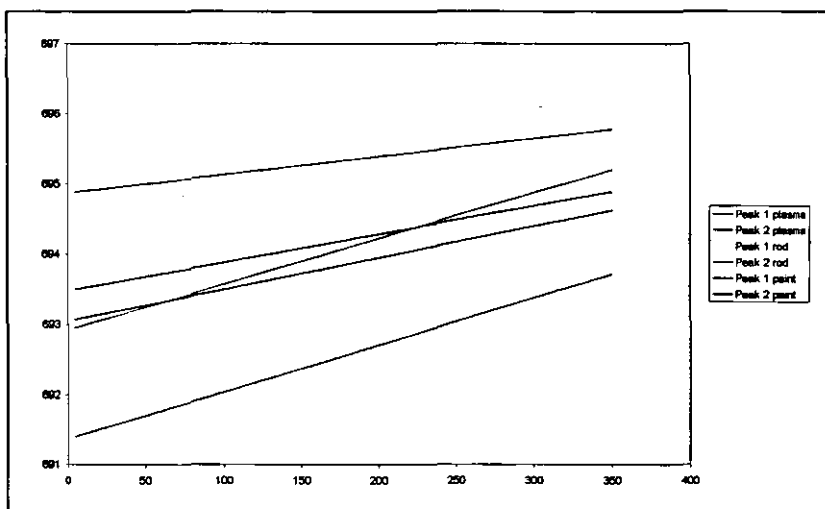


Figure 4-15 The difference between temperature and peak position of the different Ruby, peaks fitted using LabView.

The plasma-coated Ruby and the Ruby rod are both linearly related to temperature but the slope of the relationship varies. Although the plasma Ruby gives the better fit for the individual peaks in the lower temperature range, the Ruby rod gives the more accurate temperature prediction when the two peak positions are placed in the same equation.

5 Creating a fluorescent coating

The chosen fluorescent material has to be attached to the wheel, as the addition of the fluorescent material to the wheel material during manufacture is not a possibility. If the fluorescent material was added to the wheel material then there would not be enough material to create a strong fluorescent signal at the point of interest. A coating will have to withstand the temperatures and centrifugal forces that are present within a compressor. It is important that a wheel is well balanced when spinning. The addition of a coating can be compensated for by careful removal of material from the back of the object or by adding weight to the opposite side of the object. For the compressor wheel the removal of material is the most favourable method.

The coating should be uniform to achieve consistent spectrum readings. This uniformity of coating and low mass are essential attributes of a temperature sensitive luminescent coating. Thermal properties of the coating need to be considered for if the coating is too thick then a true temperature reading of the surface will not be achieved. This is due to the insulating properties of the thermoluminescent materials.

Two techniques of creating coating will be considered, the well used adhesive technique, and the previously unconsidered Plasma coating technique. Of these coating techniques Plasma coating produced the best coating, though this technique requires specialist equipment to produce the coating. The creating of a fluorescent paint produced good results and is easy to create.

5.1 Coating techniques using Ruby

Different techniques for coating fluorescent materials onto a spinning disc were considered. Ruby was used as the main material for testing of the coatings, as this was the most widely used of the materials in this work. Although Ruby was been studied previously for temperature measurement it was not clear if it had been made into a coating. It is therefore an experimental issue whether we can produce a coating that will

give a strong fluorescent signal and withstand the centrifugal forces present. The techniques tested were governed by those techniques that were easily available.

The techniques considered have included, air brushing, mixing the Ruby with the glue and painting onto the surface, adding Ruby powder to a layer of glue, and plasma coating. Mixing the Ruby and glue into a paint produces the most even coverage of the adhesive techniques. Plasma coating produced the best coating in both luminescent, thickness and smoothness. Both the paint technique and the plasma technique can be used to create a fluorescent coating.

5.1.1 Adhesive Techniques

Using adhesive is a simple technique of producing a coating. An adhesive that withstands temperatures of 350°C is required. An adhesive of the name Mbond 600 has been used as this is known to withstand these temperatures as it is used for attaching thermocouples to surfaces. This adhesive has been tested for luminescent properties when excited at 532nm, the wavelength used for exciting of Ruby. No fluorescence was noted when excited at this wavelength.

One of the disadvantages of placing the fluorescent material into a solution such as an adhesive is that scattering of both the excitation light and the fluorescence occurs thus reducing the intensity received by the detector.

5.1.1.1 Coarse powder

Initial thoughts were to use a fine layer of adhesive and pressing the material onto the adhesive. This is a very basic technique where a Ruby rod was crushed into a number of small fragments and these attached to the compressor wheel using an adhesive. This was tested optically and within the compressor. The sizes of these particles were between 3mm and 0.5mm in diameter.

A wheel with a blade coated with crystals was spun in the compressor at Holset Engineering at speeds up to 90,000rpm for 10minutes. During this test temperatures of 130°C were achieved. Fragments of diameters up to 1mm remained attached to the wheel. This showed that this is a possibility for small fragments though these do affect the shape of the blade and will therefore affect the airflow. Optical testing showed that a strong fluorescent signal could be obtained.

Although this was successful in terms of fluorescence due to its high density of material of the particles, this was not an ideal situation for spinning. The larger particles would not withstand the centrifugal forces produced in the running of a compressor. Due to the size of the particles the air flow through the compressor would also be affected, which will cause changes in the running conditions compared to normal running and therefore could not produce a reliable method of temperature measurement.

5.1.1.2 *Fine powder*

The particle size of the Ruby powder^{XVI} used in these experiments was measured using a Malvern Mastersizer particle sizer and was found to be around 10µm in diameter. The adhesive used was Mbond 600, an adhesive known to withstand the temperatures present in the compressor as this is used for attaching thermocouples. The adhesive has been tested for transmission of the excitation and fluorescence wavelengths, and for fluorescence due to excitation at 532nm. It was found not to fluoresce and to transmit both the excitation and fluorescence wavelengths.

The creating of a fluorescent paint was initially considered, as this is the technique mainly used in previous fluorescent coatings. Although the addition of the material into a solution would reduce fluorescence intensity due to scattering it is thought that this would be more than compensated for by the volume of material that can be mixed into the adhesive.

^{XVI} Sourced by Holset Engineering

A coated compressor wheel was spun at Holset Engineering at speeds of up to 79,000rpm to determine its durability within the compressor environment, as speeds of up to 80,000rpm are required to be achieved. The coatings were not damaged and the fluorescence signal from the coating was not affected.

To get the best bonding the correct proportion of Ruby to glue needed to be achieved, hence different mixes of powder and adhesive were tested, Table 5-1, as if too little material is present a weak luminescent signal will be achieved. Too much powder and the adhesive bond will not be strong enough and the coating will not stay attached to the wheel during spinning. These were then coated onto a piece of aluminium and excited, the fluorescence recorded, and then heated to 300°C. The optical tests were to ensure that the coating would produce a measurable signal and that this still produces a relationship with temperature after heating. The samples were also tested for repeatability of fluorescence signal.

paint	Ratio		Time made
	Powder	Glue	
1	1	1	12.20
2	4	3	12.25
3	1	2	12.27
4	2	1	Would not mix

Table 5-1 The make up of the samples, the ratio is in terms of volume.

The coatings were compared for how well they bonded to the aluminium, the intensity of the fluorescence signal, and whether time between making the paint and coating the aluminium had an affect on the fluorescence. The coatings were compared at room temperature before heating, after heating at 200°C and 300°C. A piece of aluminium was coated with the different coatings, at different time intervals since this would enable all the samples to be compared under the same conditions. Once the paint was made it was stored in an air tight container. Before coating, the paint was stirred in the pot to enable an even density of material.

It can be seen that there is a linear relationship between density of powder in the paint and intensity as would be expected, see Figure 5-1. At room temperature a decrease in powder in the paint of 15% would cause a 15% decrease in fluorescence intensity, though if the paint is left for 25 hours before painting the decrease in intensity would

increase to 35%. This chart also shows that the intensity of the paint decreases with time between creating the paint and creating the coating.

Paint	Coating	Time between making paint and creating coating
1	A	0
	D	3 ½ hours
	G	21 hours 10 minutes
	J	25 hours 40 minutes
2	B	0
	E	3 ½ hours
	H	21 hours 10 minutes
	K	25 hours 40 minutes
3	C	0
	F	3 ½ hours
	I	21 hours 10 minutes
	L	25 hours 40 minutes

Table 5-2 The making of the coatings.

The sample was placed in a pre-heated furnace for half an hour at 200°C, after heating to 200°C all the coating changed colour from being white to a cream, coating 2 began to crack and became brittle. Again a notable decrease in the ratio of peak 1 and peak 2^{xvii} for paint 3 is seen with time. The interesting point here is that intensities of peaks 1 and 2 increase for paints 1 and 2 with an increase in time between creation of paint and coating, where before heating these decreased with time. The peaks positions and separation of the peaks are not affected by time.

Due to the change in the coatings due to heating, the sample was then only placed for 10 minutes in the pre-heated furnace at 300°C. The ratios of the peaks intensities for each of the paints follows the same trend with time. It is now noted that a slight change in the peak separation with time taken to create the coating, for paints 2 and 3.

The sample was then reheated to 300°C for half an hour. After this amount of time all the coatings were burnt and cracked, fluorescence could be seen by eye but it was not possible to detect this fluorescence by a spectrometer.

^{xvii} See Figure 4-6 The spectrum of solid Ruby.

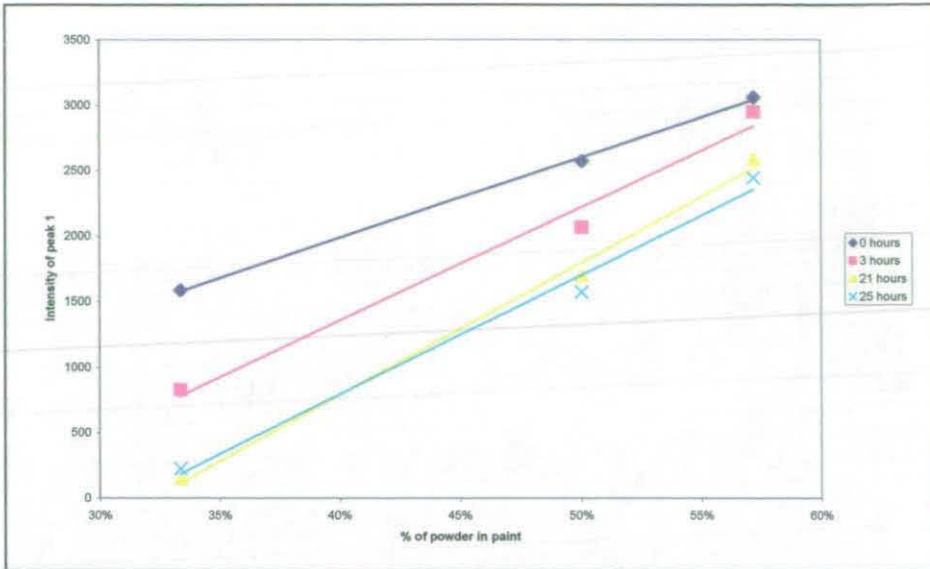


Figure 5-1 The affect of powder volume in paint mix on the intensity, before heating.

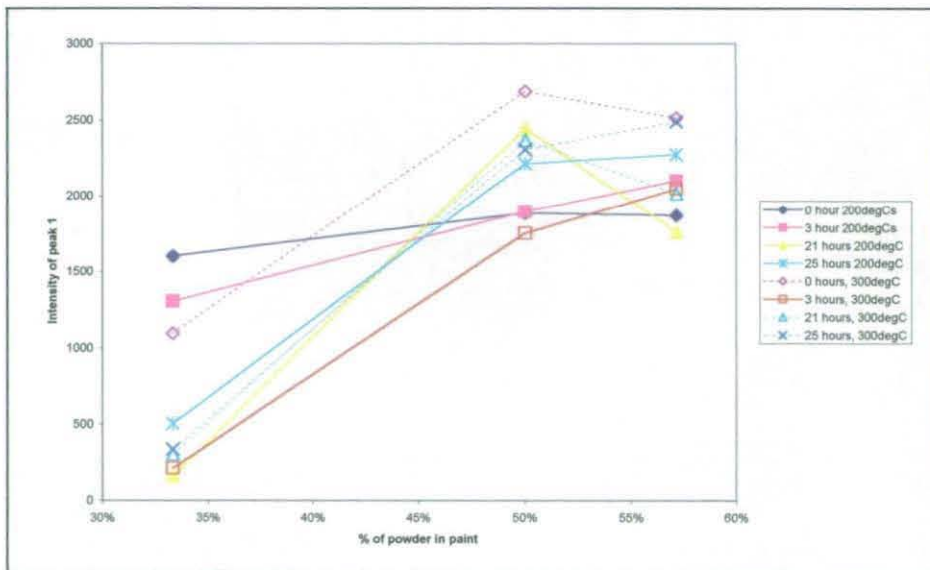


Figure 5-2 The affect of powder volume in paint mix on the intensity, after heating.

After heating the coatings the change in intensity between paints 1 and 2 was less noticeable, see Figure 5-2. It was also shown that in some cases the intensity increased. This shows that there is a dramatic decrease in intensity with paint 3. For paint 1 it is seen that if the coating is created immediately then heating will reduce the intensity of the coating. If the paint is left before heating then heating will increase the intensity of the coating, Figure 5-3.

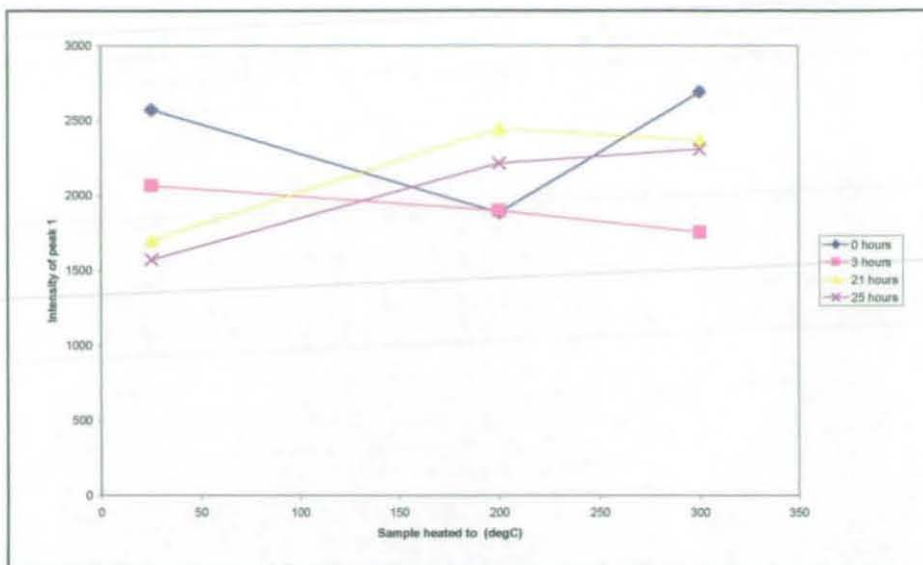


Figure 5-3 The affect of heating on the intensity of the fluorescence, for paint 1.

As the powder has to be achieved by grinding, the particle size is very small and spherical in shape. This means that the light reflects from the particles causing scattering. This is not a problem with the excitation wavelength as Ruby absorbs in a wide wavelength range. With the fluorescence this causes the light to be scattered over a wide range of wavelengths, and this means that the peaks are not as strong as they could be. The intensity that the paint gives is more than that given by the crystals but spread over a wider band of wavelengths and therefore the peaks are not as clear.

The use of an air gun was considered, as it was thought that this would produce an even coating through propelling the particles into the fine adhesive layer. This would also produce a coating that would resist the centrifugal forces present during the compressor operation. This technique was found to be unsuccessful, as the glue tended to set too quickly and only gave a very fine layer of powder on top of the glue rather than bedding into the glue. The amount of powder present was not enough to produce a strong fluorescent signal. For this to be used the particle diameter has to be increased, the air pressure increased, or an adhesive with a lower surface tension is required.

This shows that the creation of a Ruby paint using Mbond 600 can be used up to temperatures of 300°C. It will withstand the compressor running conditions and gives a strong signal at room temperature.

5.1.2 Plasma coating

A Plasma coated wheel has been tested optically and with a compressor. This withstood speeds of up to 80,000rpm for 1 hour. Four coatings were placed on the compressor wheel in the areas of most interest. After spin testing at Holset Engineering two coats remained fully intact with no signs of damage and two were damaged significantly though parts of the coat remained, from which a strong fluorescent signal could still be achieved. The problem here would be the synchronization of the laser with the small amount of remaining coating.

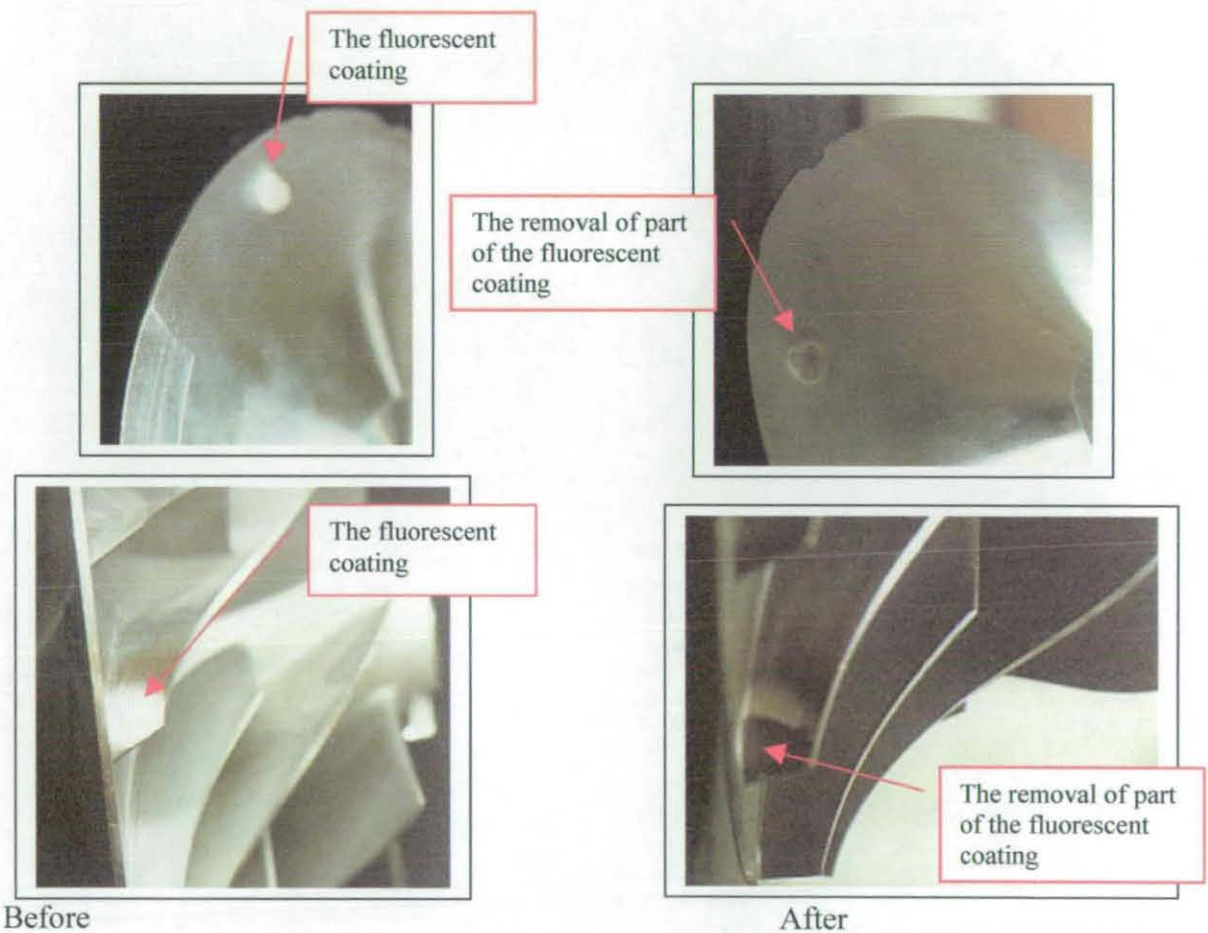


Figure 5-4 Plasma coatings affected by spinning.

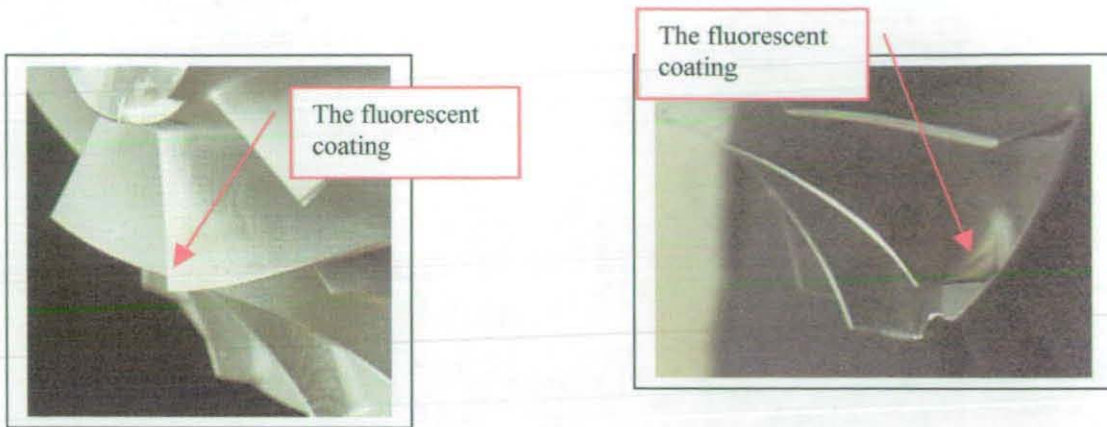


Figure 5-5 The plasma coatings unaffected by spinning

The coating produced is dependent upon a number of different factors in the arrangement. These factors include distance between the plate and the feeder, the outlet diameter of the feeder pipe, and feeder air pressure. The following section details how these were determined to achieve the best coating.

The work here is to produce a quality coating, a thin high density coating. A thin coating will have little affect on the air flow within the compressor creating a true to normal conditions as possible. A high density coating will produce a strong fluorescent signal which is essential for collection of the fluorescent signal at high speeds.

5.1.2.1 The creation of a plasma coating

The plasma coating was undertaken using Godwin P9 Air plasma to heat the Ruby powder. This creates an extremely hot arc that can be used for melting and projecting the Ruby particles onto the material to be coated. A powder feeding system was designed for feeding the powder into the plasma arc. The technique progressed from coating a single spot to creating an arc.

The factors to consider in the creating of the coating is air pressure in the plasma arc, the air pressure of the powder feeder, the distance between the plasma nozzle and the material, and time taken to create the coating.

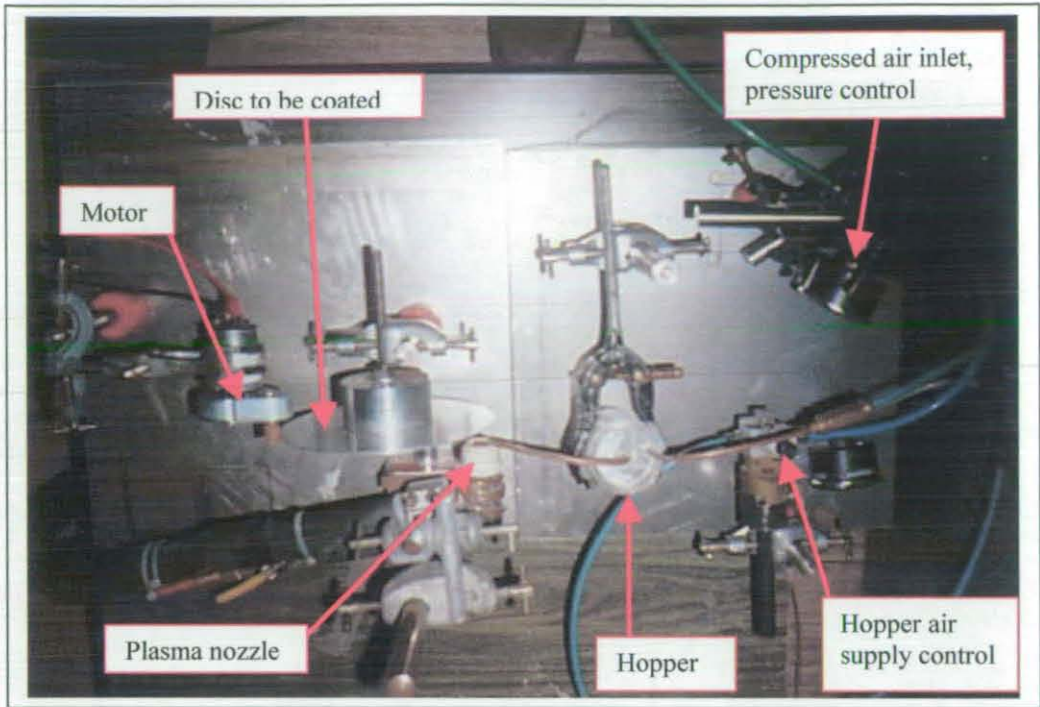


Figure 5-6 The plasma coating rig

The temperature of the arc has been measured at various points, the profile of which can be seen in Figure 5-8. The air temperature in front of the arc has also been measured. At a distance of 25mm from the arc a temperature of 450°C was recorded after 2 minutes. At a distance of 20mm a temperature of 790°C was reached after 3 minutes.

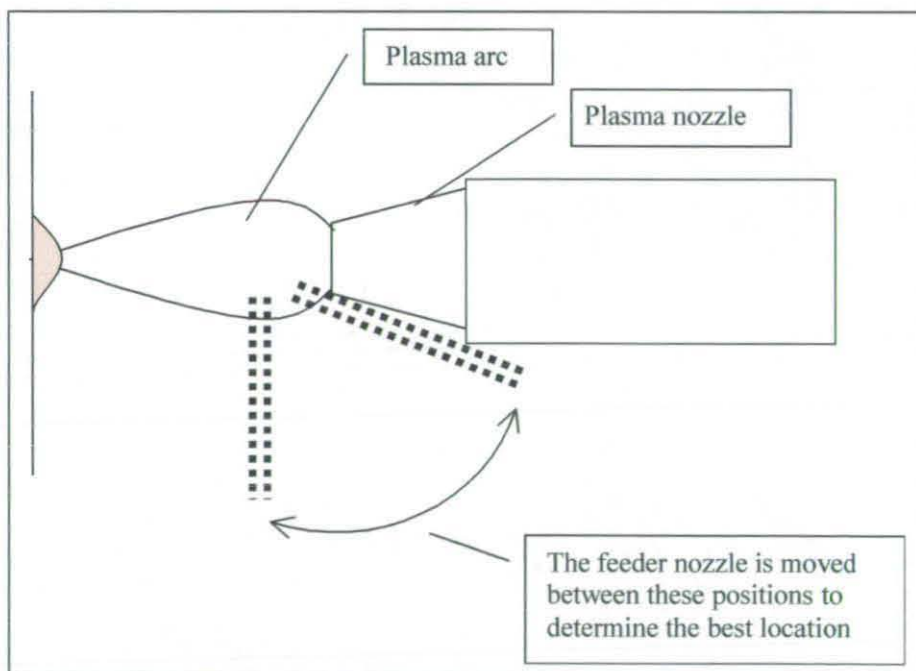


Figure 5-7 The plasma coating setup

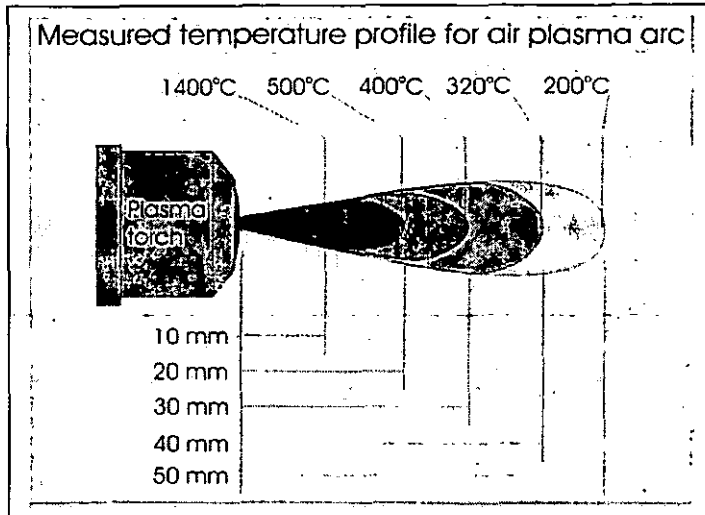


Figure 5-8 The temperature profile of the plasma arc¹¹⁷.

The distance between the plasma torch nozzle and the surface of the disc to be coated was changed and the quality of the coating compared. It was found that if the material was closer than 10mm it would be melted, as at this distance a temperature of above 1,400°C would be present, see Figure 5-8, a value way above the melting point of aluminium at 650°C. At a distance greater than 20mm a coating would not be produced. The ideal placement of the material is 15mm away from the plasma torch nozzle.

The position of the powder feed outlet was also moved within the space between the nozzle and the material. It was found that the best position was as close to the nozzle as possible without it touching, and for it to be just out of the actual arc. If the feeder nozzle is too close to the centre of the arc then the nozzle would melt. If the powder was not injected into the centre of the arc then very little of it would be melted and so a very poor low density coating would be produced.

The different coatings produced show that the spot size of the coating is dependent on the diameter of the feed tube. A small diameter feed tube gives a more intense coverage of Ruby over a small area, a larger diameter feed tube will give a larger coverage but less dense. If the diameter of the pipe is too large then the powder tends to disperse into the atmosphere rather than producing a coating. A diameter of about 0.5mm produces a coating of about 10mm in diameter.

The cleanliness of the material surface and that of the nozzle affects the quality of the coating, if these are not clean then the coating itself becomes contaminated. This reduces the fluorescence gained from the coating. The age of the plasma nozzle affects the efficiency of the plasma torch. After using the nozzle to produce a couple of coatings the nozzle becomes pitted, this affects the stability of the arc. This in turn reduces the quality of the coating significantly.

The time taken to create the coating contributes to the coating quality. If the system was running for too short a period then not enough material would be deposited, too long and the coating would be contaminated from the copper within the nozzle or would be burnt away from the aluminium.

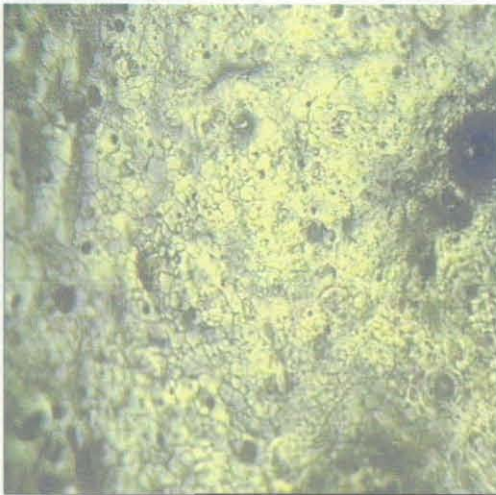
To enable the powder to be injected into the correct part of the plasma arc the Plasma arc pressure was set to 1bar and the feeder pressure set to 2bar. This enabled the powder to reach the arc position where it would be melted rather than being pulled into the air flow of the plasma arc. If the air pressure of the feeder was too high then the powder was blown either through the arc or into the centre of the arc and vaporises.

The plasma arc itself is dependent upon both the compressed air and electrical power supplies, and the stability of these supplies. The plasma will only create an arc if the correct power supply is present, small fluctuations can make the difference between achieving the arc or not. The air supply controls the stability of the arc. It was determined that a pressure of 1bar produced the most stable arc.

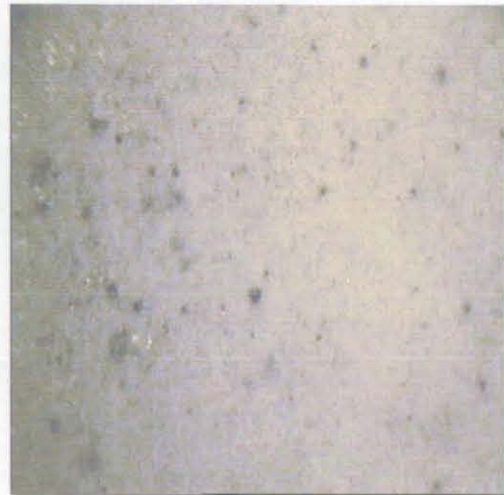
It was noted that the stronger fluorescence occurred at the areas of thicker coating, which would be expected as there would be a larger quantity of material here and therefore more fluorescence would be produced. As more material has been used to create the coating this would also mean that the coating itself would be denser. These areas of thicker coatings tended to be at the start of a section of coating. Reducing and increasing the pressure into the hopper would reproduce this affect. The change in air pressure gave a surge effect that stirred the powder and enabled more powder to be released from the hopper. When producing the thicker coatings there was a lot more powder present in the surrounding air, which indicated an inefficient method of coating.

The areas of thicker coating tended to be more brittle. The coating would start to break away from the disc after a short period. The exposed area of the disc had a fine coating and at the edges it would be seen that the layer that had broken off had not been fully attached to the disc. The coating had been formed as a blister with only the edges attached to the disc. Possible reasons for this is that the temperature difference between the disc and the heated powder caused the powder to set at a point before contact with the disc. Another possible explanation is that the density of the powder in the air at that moment caused the powder to bond together there rather than on the base material.

Vardelle et al¹¹⁸ determined that melted particles hitting the surface simulate a water droplet hitting a surface, though instead small droplets being formed and separated rapid cooling cause the droplet to solidify as one thin layer. This rapid cooling can cause air to be trapped between the particle and the substrate. It has been shown that increasing the torch power decreases the size of the pores present within the coating.



Fused, note the glossy appearance



Non-fused, note the powdery appearance

Figure 5-9 Comparing the fused and non-fused coatings.

This blister type forming is reducing the strength of the coating, work has therefore been undertaken to try to remove the blister affect. To reduce this temperature difference between the material and the coating material the disc was pre-heated using the plasma arc to temperatures of around 300°C. This was found to improve the bonding of the coating. The coating produced was also not as thick as previously, nor did it produce as strong a fluorescence.

To improve the quality of the coating further the heating of the powder was continued once it was attached to the disc using the plasma arc. This heats the Ruby powder sufficiently for it to fuse together, which produces a glassy finish and much stronger fluorescence from the same volume of powder. This post heating was done using the plasma arc for around 30seconds, this would equate to an increase in temperature of around 300°C. The melting point of Ruby is around 2,000°C so this increase in temperature would not be enough to melt the Ruby, but would cause an annealing affect. The difference between the fused and non-fused coatings at 10x magnification can be seen in Figure 5-9. The glassy finish is very distinctive compared to the dull white finish of the non-fused coating.

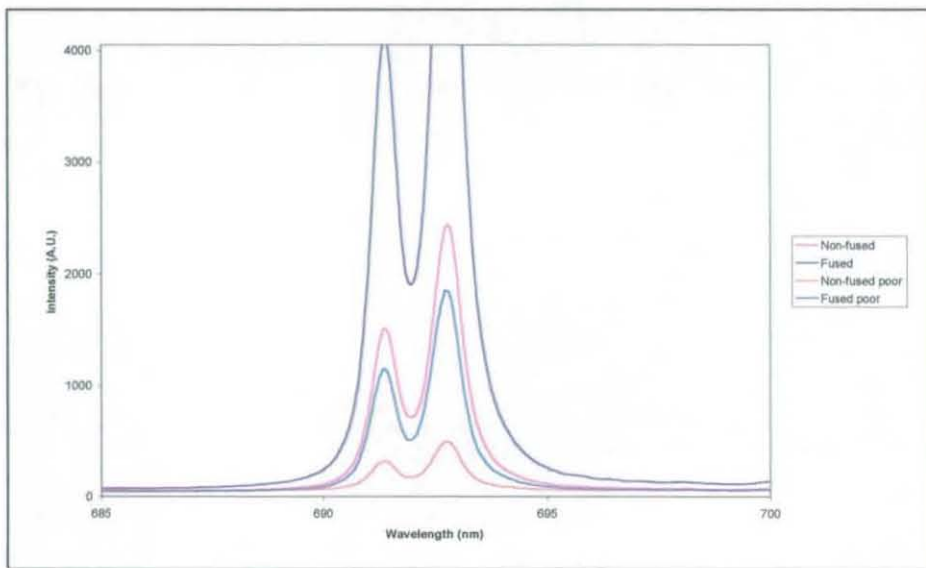


Figure 5-10 Comparing the difference in measured intensity between the fused and non-fused coatings.

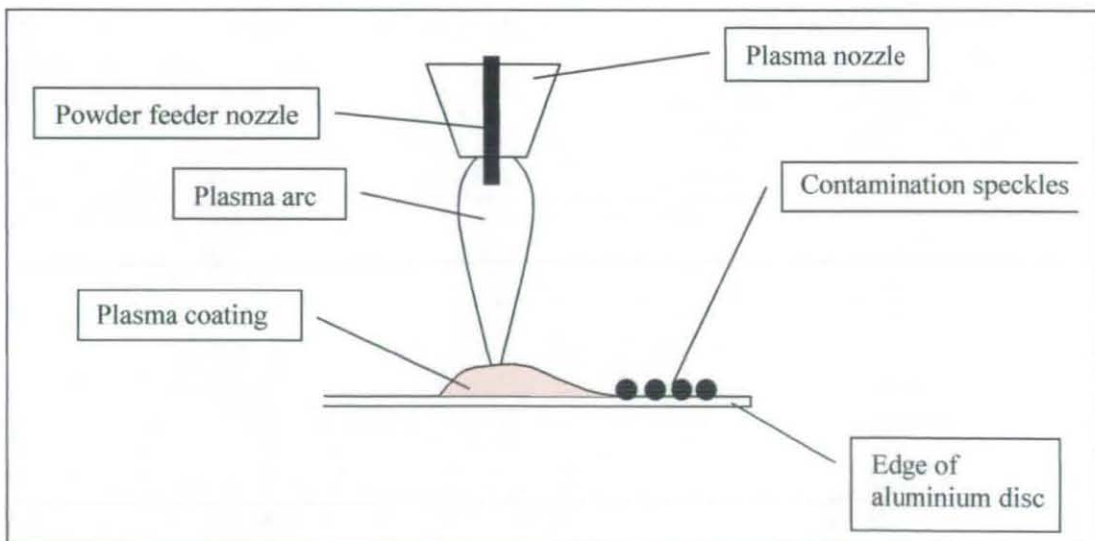


Figure 5-11 The side profile of a plasma coating

A number of tests were undertaken to create the glassy finish to the coating but it could not be reliably repeated. It was determined that only the coatings formed as a blister could be taken to this further stage. It is the surface of the powder coating that is fused together, underneath, the white powder coating still remains. This has been noted from studying the pieces of fused coatings that have come away from the base material. It is therefore only a small proportion of the coating that is giving the stronger fluorescence. The blister type coating is not strongly attached to the aluminium and is easily damaged so is not suitable for spinning. It is thought that the reason why this type of coating allows the fusing to occur is that the air pocket between the coating and aluminium reduces the heat transfer and this keeps the coating at a higher temperature, thus allowing it to become very close to its melting point.

A cross sectional diagram of the coating can be seen in Figure 5-11. This shows that the coating was pulled towards the edge of the disc along with the contamination. This indicates that the air flow from the arc and the powder feeder was pulled in that direction dropping the particle remaining in the air flow as it changed direction sharply.

5.1.2.1.1 Hopper design

To control the distribution of the powder, different hoppers were built and tested as well as feeding the powder directly into the plasma torch air feed. The later technique was found to block the nozzle area of the plasma torch, and therefore was not a possibility.

The different designs of hopper mainly involved changes in the placement of the air inlet feed. Three designs of hopper were tested, and are shown in Figure 5-12. With the first design the powder seemed to be compressed at the bottom of the hopper, the powder still flowed out of the hopper. The next design enabled the air to be inserted into the mass of powder. This would enable the air to agitate the powder and thus allowing it to flow through the outlet nozzle. Again the powder was compressed to the side of the hopper, but the powder did not flow out of the hopper. The third design put the outlet pipe on the side of the hopper. In the previous hopper designs the powder was pushed against the side, it was therefore decided to see what would be achieved by the placement of the

outlet pipe where the powder was being pushed to. The powder flow was an improvement on the second design but was not as good as the first. The first design produced the most consistent flow of powder from the hopper, and used low air pressure to do so.

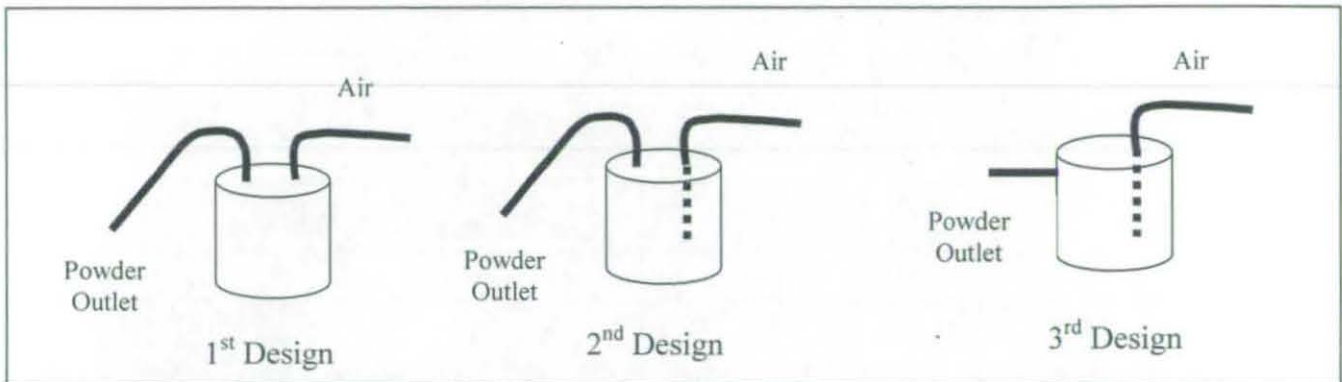


Figure 5-12 Hopper Designs

A powder feeder was tested but this also proved to be unsuccessful. The problem with the feeder was that it was an open hopper, this meant that the powder became air borne around the hopper. Sealing the hopper was tried but this could not be done successfully. The second problem was reducing the diameter of the outlet pipe down to a size that was acceptable for the feed of powder into the plasma torch. The change in bore diameter through the outlet pipe, and the low air pressures which were being used, meant that the powder remained in the pipe rather than flowing through. The next step within the hopper design would be to produce a stirring system into the hopper to help keep the powder air-borne within the hopper.

5.1.2.1.2 *Creating a circular coating*

To remove the need to pulse the laser in time with a spot coating from the experiment it was decided to coat a ring of Ruby around the disc, this is to be done using the plasma coating technique. The disc to be coated is spun slowly in front of the plasma arc by an electric motor. The Ruby powder is fed into the plasma arc from a hopper that is fed by compressed air. The plasma nozzle was placed at a distance of 15mm from the disc as this was found previously to be the best position. The disc was spun at different speeds and the amount of material in the coating was studied.

The disc shows the thicker coating at the start, point A, of the ring that has broken away from the disc, point B. The coating at position A can be seen to be coming away from the aluminium, Figure 5-14, Figure 5-16. At 10x magnification it can be seen that although the majority of the coating has peeled away there is still a fine layer of powder attached to the disc^{XVIII}.

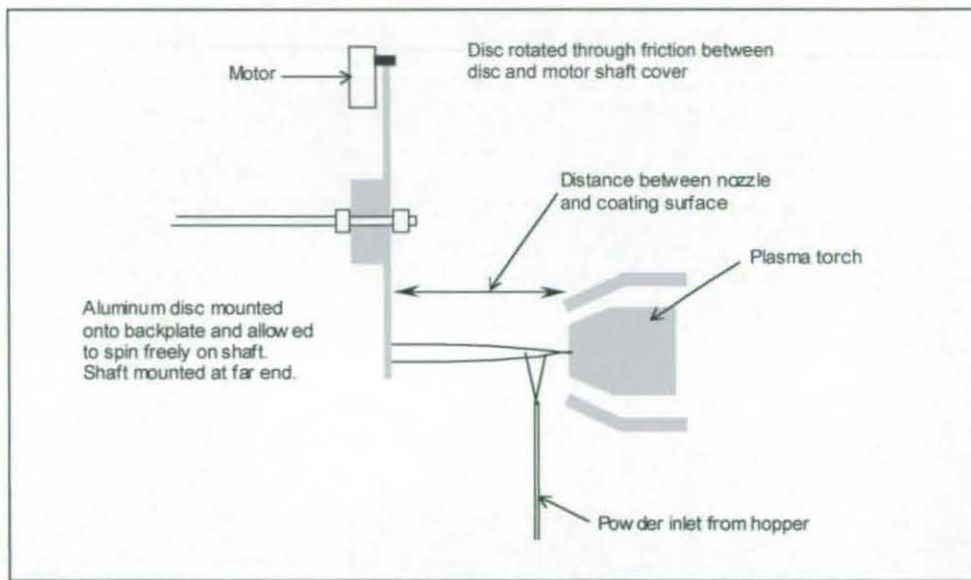


Figure 5-13 The arrangement to produce the circular coating, viewing from above.

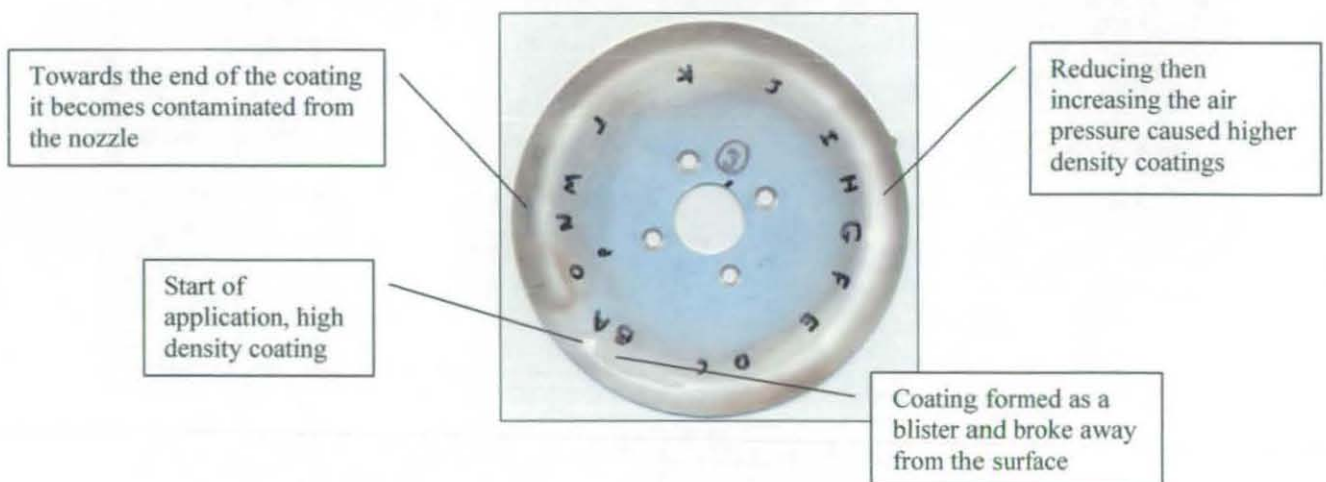


Figure 5-14 Ruby coated disc

^{XVIII} See Appendix - 9.4 Coatings

During the coating the air pressure was increased and decreased in the hopper. The affect of which can be seen in Figure 5-14, at points E through to H. Points E and G are showing increasing air pressure, and the coating becomes wider. At points F and H the air pressure is decreased, and the coating narrows.

As the coating comes to its end the plasma nozzle has collected contamination from the material being coated, the powder and the surrounding atmosphere. This is transferred to the disc and can be seen as the darker speckled areas, this is particularly noticeable at points M, N and O, this occurs all through the coating process.

The fluorescence spectra gained from the disc are shown in Figure 5-15, a pulsed laser beam of pulse energy $1.5\mu\text{J}$ and wavelength 532nm was used to produce the fluorescence. The spectra shows that the coating at position A gives a much stronger signal than any of the others. Followed by positions G and E with correspond to an increase in air pressure in the air feeder. As expected position B did not give any fluorescence signal. The fluorescent signal became weaker further as we moved around the disc. This is not surprising given that more contamination was deposited further into the coating and less powder was being fed into the plasma arc.

Plasma coating has been shown to be a very viable method for coating of fluorescent materials as it produces a hard wearing coating, proven to withstand the operating conditions in a compressor. The fluorescence achieved from the coating is strong and has not been altered through exposure to temperatures involved in melting the particles. It tended to be fragile though work showed that this could be improved through pre-heating of the disc with the plasma arc. This could be looked into further where the pre-heating is done using a furnace to heat the whole disc, to temperatures of around 300°C , rather than just the area to be coated. This could have the advantage of reducing the heat difference more significantly.

The air plasma used in the creation of the coating is not designed to run at the conditions that are required to produce the coating. This meant that parts degraded extremely quickly, hence the high amounts of contamination present on some of the coatings. The air plasma machine is designed for cutting of materials, this means that the arc comes in contact with the material being cut. The material being cut then disperses the heat in the

nozzle through the arc contact with the material. During the coating the arc does not come in contact with the material, this means that the heat builds up in the plasma nozzle, causing it to melt. The molten particles are then deposited onto the material being coated.

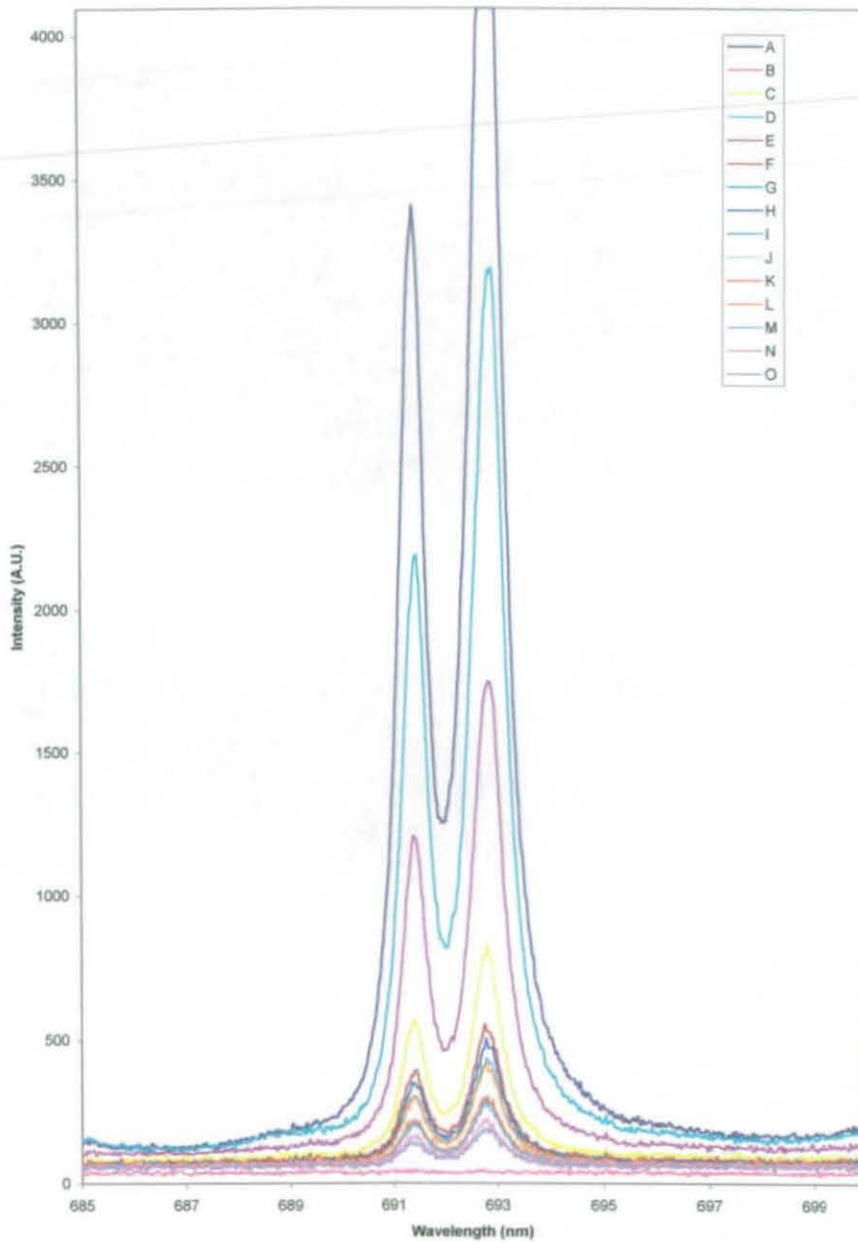


Figure 5-15 The fluorescent spectra gained from the different positions on the plasma coated disc, as seen in Figure 5-14.

This method has potential for the creating of highly luminescent temperature sensitive coatings, though for this work to be continued further it would require the correct

equipment for plasma coating. Issues to be studied would be the removal for the blister structure and the post-heating to create the fusing for the powder.

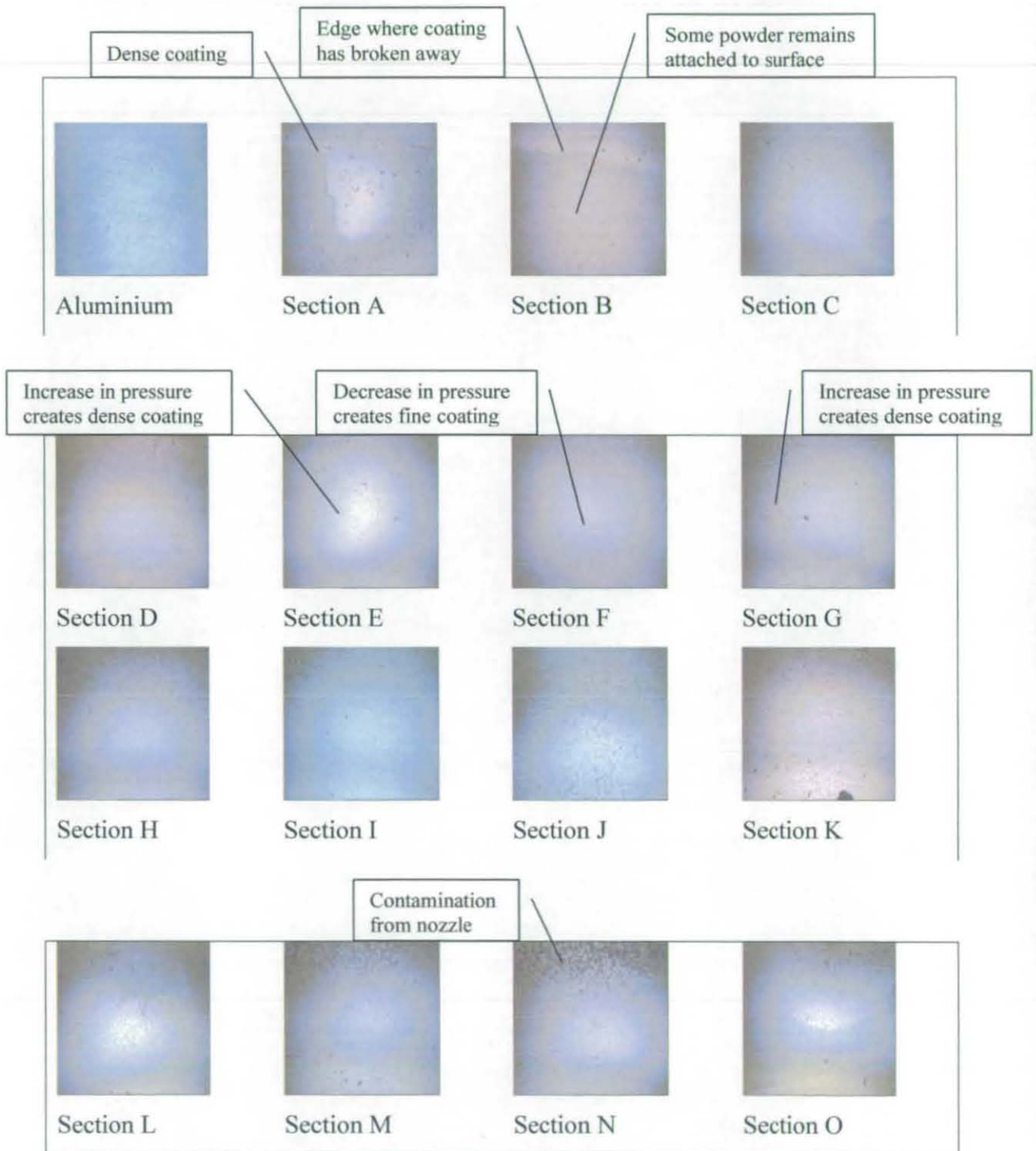


Figure 5-16 The difference in the quality of the coatings around the disc in Figure 5-14. Images taken at 1x magnification.

5.1.3 Comparing the Ruby coatings

The plasma coating has been compared optically with the Ruby rod, paint technique, and coarse powder technique, this can be seen in Figure 5-17. It can be seen that the paint causes light scattering of the Ruby to surrounding wavelengths, thus reducing the amount of intensity in the peaks. The intensity that the paint gives is more than that given by the crystals but spread over a wider wavelength band and therefore the peaks are not as clear.

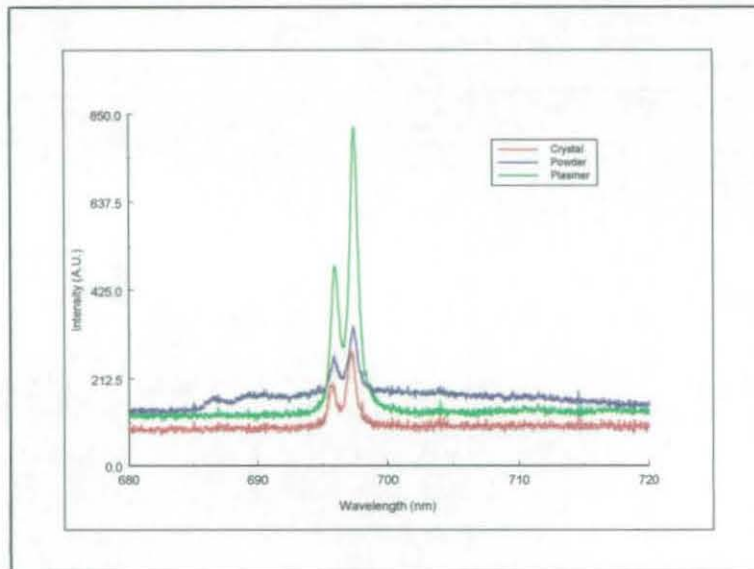


Figure 5-17 Comparing the spectra at room temperature for the different coatings

The plasma coating gives considerably more intense peaks from a significantly smaller excitation area. The plasma coating was tested for temperatures up to 325degC which shows it is still possible to clearly distinguish the two peaks, Figure 5-18.

The advantage of plasma coating is that it does not involve any other materials that cause scattering and absorption of the excitation wavelength and fluorescence. The coating is thin, and will only cover the area of interest. The testing undertaken shows that plasma coating gives good optical results, and that at temperatures up to 300°C fluorescence can be detected.

Disadvantages of this technique are that it is difficult to implement in hard to reach areas such as the inside edge of the blade on the compressor wheel. Specialist equipment is

required to produce the coating, which is expensive. During the coating process the surface temperature is close to the melting point of aluminium.

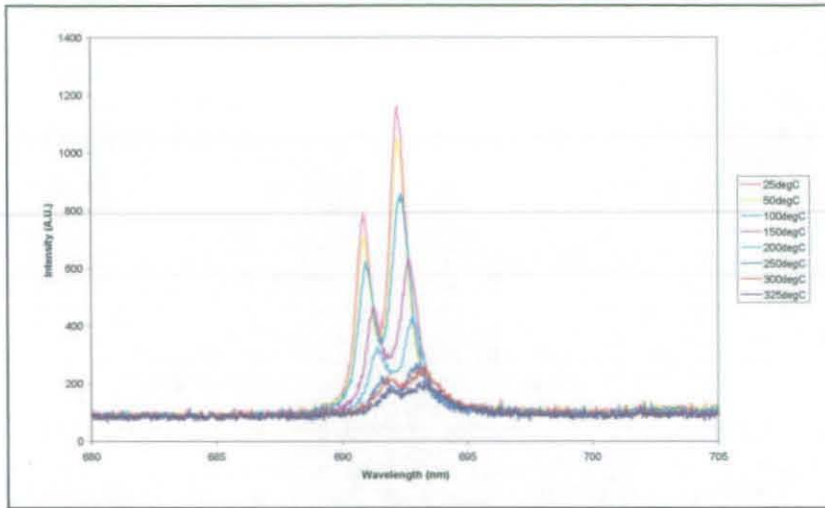


Figure 5-18 The spectra for plasma coated Ruby heated to 325°C.

Good quality coating can be formed but the equipment and knowledge available limit the repeatability of this. A complete circle of Ruby coating has been achieved. The quality of the coating varied immensely along the coating. It has been found that the quality of the coatings are dependent upon; distance from plasma nozzle to surface; plasma air pressure; plasma input power; cleanliness of the nozzle; surface temperature; flow of powder. The post heating of the coating is an interesting development that has further potential. To improve the bonding preheating of the base material may need to be studied further.

The ideal coating thickness and density would depend upon the laser intensity and spot size used to excite the material. If the material is too thin then the laser could saturate the material reducing the intensity, Figure 5-19. If a material becomes saturated then the ground state has enough electrons to be stimulated to a higher level and has to wait until luminescence occurs returning electrons to the ground state^{XIX}.

^{XIX} See Appendix 9.3 for theory of luminescence

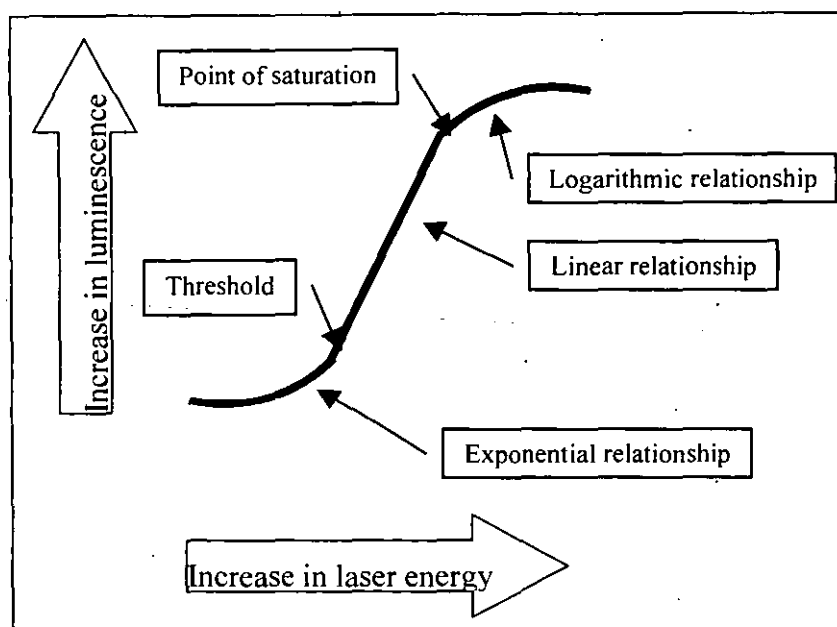


Figure 5-19 The relationship between laser energy and luminescence

5.2 Summary of coating techniques

A number of different coating techniques have been tested for use on a compressor wheel. Techniques used were bonding Ruby chips onto the wheel with a high temperature adhesive, creating a fluorescent paint using fine powder and plasma coating.

Of the techniques for Ruby the plasma coating showed the most potential, as it produced a strong fluorescent signal and adhered well to the compressor wheel. This technique involves the melting of a powder in an arc, the molten particles are then propelled onto the surface being coated by the air flow through the arc. A thin coating is produced which does not require any solvent, therefore scattering of light does not reduce the fluorescence signal. The disadvantage of this technique is that specialist equipment is required which can make it expensive.

The creating of a fluorescent paint involved the mixing of powder and adhesive to create a paint. This technique also showed good potential for creating coatings. The paint can be coated to the area of interest, more difficult places can be reached than by using the plasma technique. The coating produced withstands the conditions in the compressor housing. The fluorescent signal produced is about a third of the intensity of the plasma

coating. There was a lot of scattering to longer and shorter wavelengths, this scattering could be reduced by the use of a more viscous adhesive¹¹⁹, investigation into adhesive useable up to 300°C would be required. The main advantage of this technique is that no specialist equipment or personnel are required to produce the coating. The paint has been made up and stored for 3 days, with it still being useable.

At lower temperature the use of the fluorescent paint would be effective, at higher temperatures the peaks would become too low to be detected reliably. The plasma machine used in these experiments was not designed for working under the conditions required to produce the coating. With the correct equipment much more repeatable plasma coatings could be produced. It is possible that the plasma coating could be undertaken by an outside company, though this was looked into and no company could be sourced that would undertake the work mainly due to the small quantity required.

It is possible to create plasma coatings using a rod of material placed in the arc rather than the jet of powder. This technique has the advantage of being cleaner, and less wasteful than the powder technique. This technique has been tested using the equipment available but was unsuccessful, though with the correct equipment this could have potential.

In summary both plasma coating and the fluorescent paint technique have potential. The paint is easy to create and to apply even to difficult to reach places, cheap to create, and it also involves little wastage of material, its disadvantage is that compared to the plasma coating the signal is not as strong, and scattering occurs within the coating. The plasma coating technique produced highly fluorescent coatings, which were thinner than the paint technique, its disadvantage being that specialist equipment and personnel are required which makes the process expensive. For this work the plasma coating technique is favoured for Ruby as it produces a much stronger fluorescent signal. For Yttrium the paint technique is favoured because this gives a strong fluorescent signal and is easy to create.

6 Yttrium Oxysulphide Praseodymium doped

Praseodymium doped Yttrium Oxysulphide^{XX} (Y₂O₃S:Pr) has been tested for its temperature sensitivity. This phosphor has been chosen for this application because of its very short, 7μsec, lifetime, which will allow most of the fluorescence emitted after pulse excitation to be detected during the pass of the compressor wheel. When spinning at 80,000rpm a point on the wheel at 70mm from the centre would move a distance of 4mm during the fluorescence lifetime. The compressor wheel has a radius of 70mm. It also has a number of emission peaks, which allows for the possibility of self-referencing the reading.

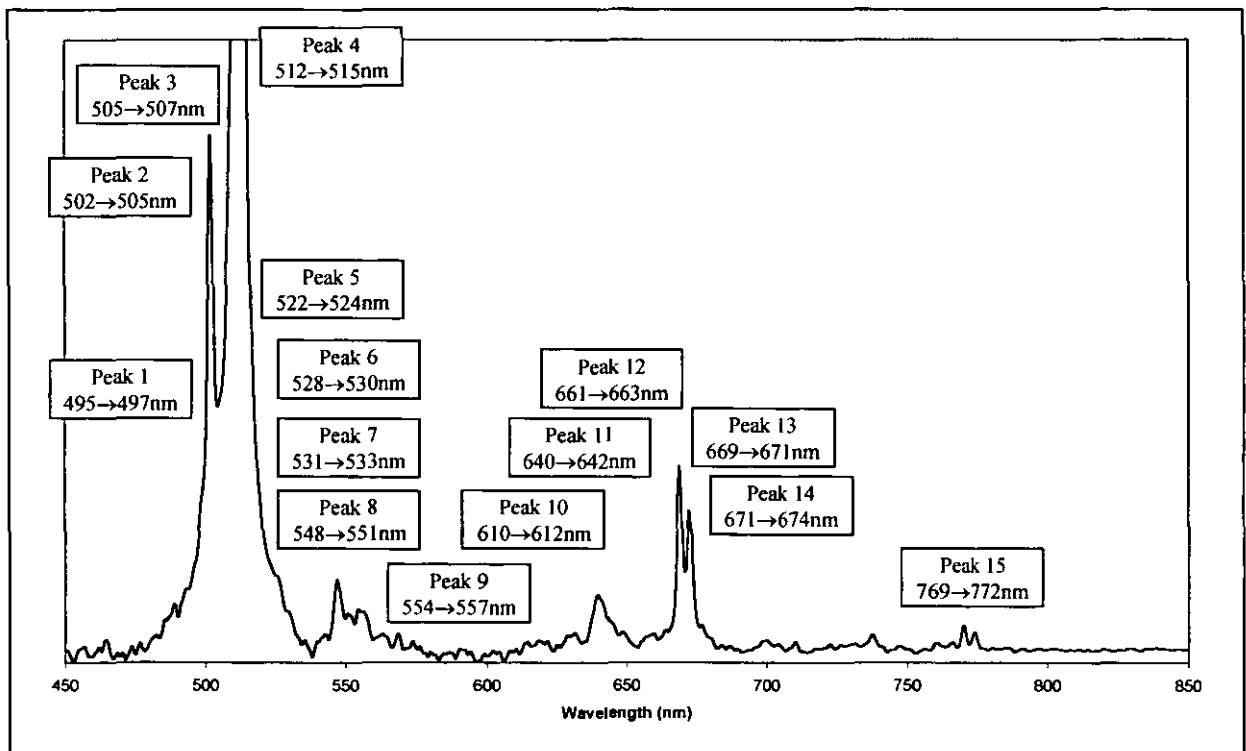


Figure 6-1 The spectrum of Y₂O₃S:Pr, with the peaks labelled.

^{XX} From Phosphor Technology

6.1 Y₂O₃S:Pr decay-time temperature relationship

It is known that the decay-time of thermoluminescent materials can have a strong, very reliable relationship with temperature. The decay time of Y₂O₃S:Pr has therefore been considered. The Y₂O₃S:Pr was obtained in powder form so it is in this form that it was first tested for temperature sensitivity. The Y₂O₃S:Pr powder was excited at 337nm using a nitrogen lamp, the decay time of which can be seen in Figure 6-2, and the decay time was recorded using Norland ino-tech 5300 multichannel analyser. The photon count was set to 4,000 which means that counting will occur until one channel reaches a total of 4,000 counts.

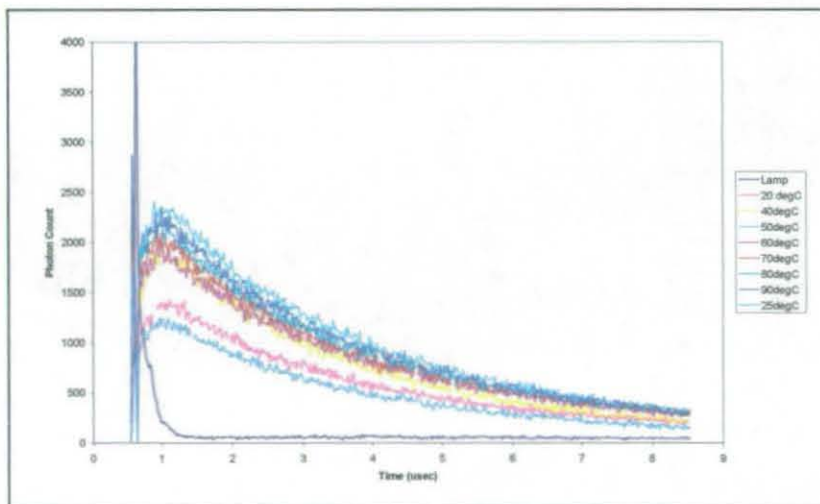


Figure 6-2 The recorded decay period of Y₂O₃S:Pr with the decay period of the lamp subtracted.

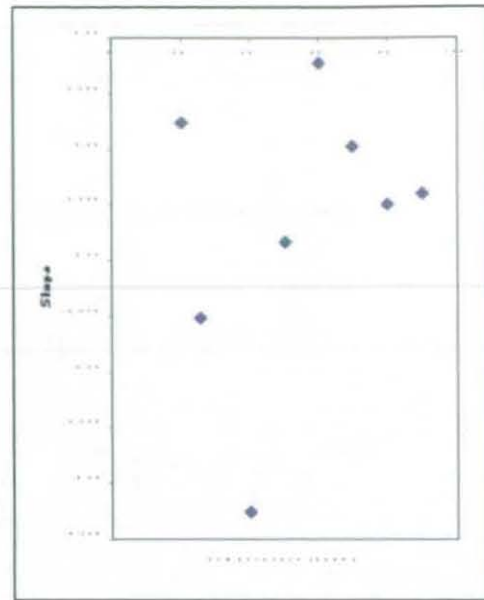
The powder was heated using an electrical heater mat due to the compact nature of the equipment. This meant that only temperatures of 90°C could be achieved due to the limited power in the heater mat trying to heat the sample and the material of the equipment. The raw data for the decay times is shown in Figure 6-2, which indicates that there is a slight change between room temperature decay time and heated decay time.

The actual decay profile was then determined through curve fitting the data after 1µsec to remove the influence of the lamp profile. This showed that there was no change in the actual decay curve with temperature, Table 6-1. This shows that the decay slope cannot

be used for temperature measurement, as the data does not follow a trend with temperature.

Temperature (degC)	Decay profile	R ²
20	$y = 1307.3e^{-0.2577x}$	0.98
40	$y = 1836.9e^{-0.2925x}$	0.99
50	$y = 2244e^{-0.2684x}$	0.99
60	$y = 1766.9e^{-0.2523x}$	0.99
70	$y = 1900.3e^{-0.2597x}$	0.99
80	$y = 1997.5e^{-0.2649x}$	0.99
90	$y = 2097.1e^{-0.2639x}$	0.99
25	$y = 1147.2e^{-0.2751x}$	0.99

Table 6-1 The decay curve of $Y_2O_3S:Pr$, non-normalise data



When normalising the data, to remove the lamp influence, over the temperature range 20°C to 90°C no change in decay period was noted with a change in temperature, see Figure 6-3. Though at higher temperatures changes may occur which is not possible to test for using the equipment available. This shows that the decay time of $Y_2O_3S:Pr$ cannot be used for temperature measurement over the temperature range 20°C to 90°C.

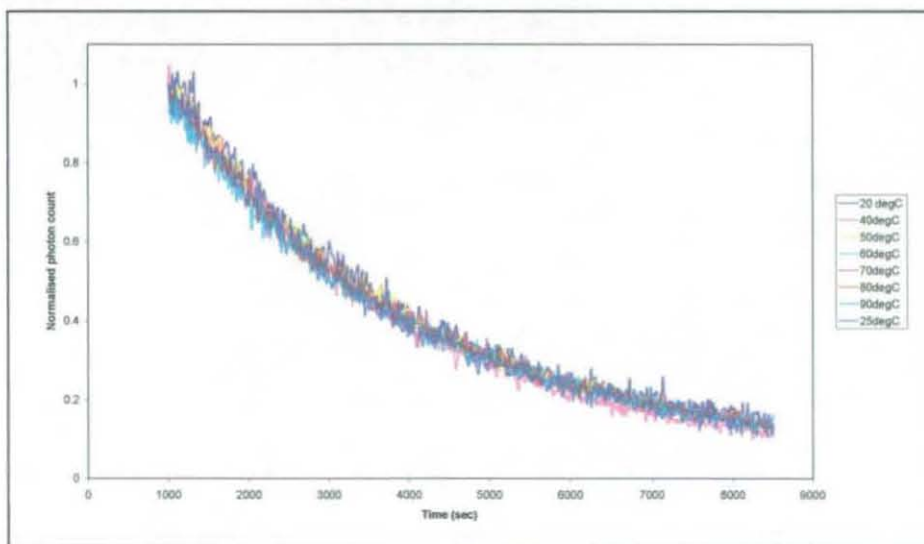


Figure 6-3 The normalised decay periods

6.2 Y₂O₃S:Pr spectrum temperature relationship

The fluorescence spectrum of Y₂O₃S:Pr is shown Figure 6-1, the peaks are labelled as to the system used in the calculations. The wavelength bands for each peak were calculated by using the 'peak find' routine in LabView to determine the peak positions, then by manually looking at three sets of data the range was determined for each peak. This was done through finding the most common minimum and maximum wavelengths that occurred for each peak, so that any stray peaks would be ignored in the future calculations.

The peaks positions and amplitudes are determined by a program written^{XXI} in LabView. The program looks for peaks above a certain level, the threshold value, and larger than a certain width. These values can be set in the program. The selection of the correct values is crucial, as setting too low a threshold will detect the noise as peaks, but too high will mean that the smaller fluorescence peaks will not be detected. The same is also true with the width values, too small a width and the noise will be detected as well as many peaks being shown rather than a single peak. If the peak is too large then the thinner peaks will not be detected. Careful selection of the threshold and widths will eliminate the need for processes such as smoothing which can affect the data.

The data was then entered into Excel and a macro^{XXI} written to organise the results from LabView into the peak ranges, if extra peaks were present then the set of data was deleted. This was done as if the width was too small then more than one peak would be present where there is only one peak, this would affect the results as it was unsure as to which peak was the true position of the peak. An Excel macro^{XXI} then determined the linear relationship between the temperature and peak position, peak intensity, separation of selected peaks and the intensity ratio of selected peaks. The R² value and fit equation was outputted into a table. For R² value greater than 0.7 the relationship was considered as a possible means of temperature measurement. This value was chosen as it would

^{XXI} See Appendix - 9.7 Programming

provide a range of possible relationships for further analysis without selecting those that would not be able to be used to give a reliable temperature measurement.

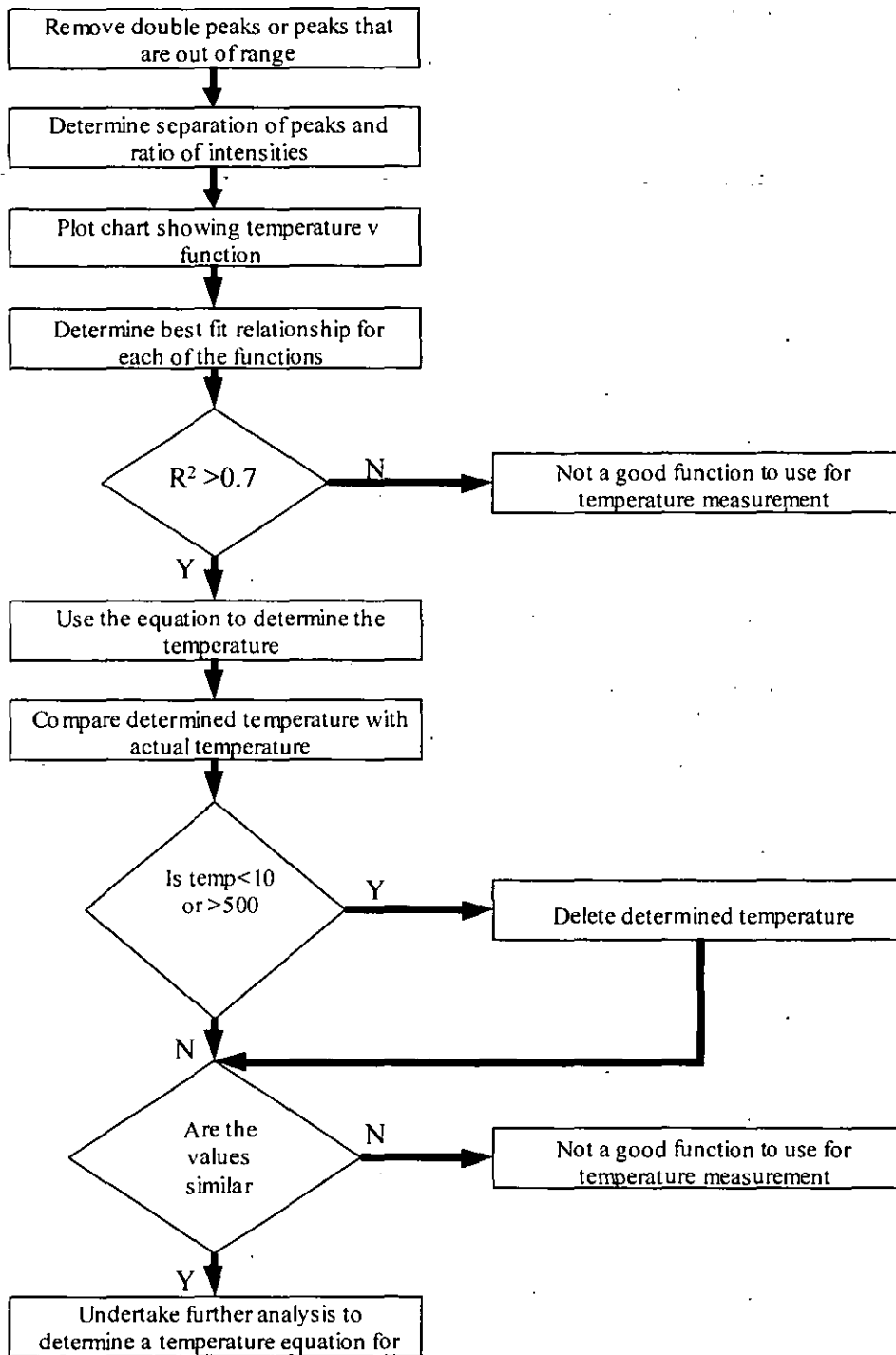


Figure 6-4 The processes involved with the data analysis.

Initial worked studied a range of different thresholds (values 0, 20, 50, 100, 150, 200) and widths (values 3 to 50) to determine the best values for use with this material. A number of peak find routines were run in Labview with different values for with and

threshold were selected. If the width value is too small then too many peaks will be located which masks the true peak position. If the width value is too large then the peaks will not be detected. When using the peak values determined from the different peak width settings to create a temperature relationship different reliability of fits were also noted. This showed that a value of 10 for the peak width was best as a large number of relationships gave a good fit at this setting. It was also noted that with the threshold value if this was set too high then some of the peaks would not be detected at higher temperatures, and if it was set too low then noise in the spectrum would be detected. The threshold value should be set at a value of 20 as the background level is low because background has been subtracted from the spectrum. Setting the background at 20 rather than 0 means that any slight fluctuations in the background are not detected.

6.3 Creating a fluorescent coating using Y₂O₃S:Pr

The fluorescent coatings for Yttrium were made using the paint technique. The disadvantage of the paint technique when using Ruby was the lack of fluorescence intensity, especially at higher temperatures. This has been tested for with Y₂O₃S:Pr and has been found to produce strong fluorescence with the paint technique. The paint technique was therefore used for creating coatings with Y₂O₃S:Pr. As the adhesive Mbond 600 used to create the Ruby coatings did not affect the fluorescent spectrum and worked well up to 330°C, the same adhesive is used here.

A set of coatings have been created with Mbond 600 as the adhesive, as this adhesive has been shown to work well under the compressor conditions with the work undertaken with Ruby. A summary of the coatings created is shown Table 6-2, a powder content of greater than 60%, by volume, meant that the paint would not bond to the aluminium. The thermocouples, which had an accuracy of $\pm 1^\circ\text{C}$, were attached to a 50mm square, 1mm thick aluminium plate using a high temperature silicone adhesive. The coating was applied once the adhesive for the thermocouple had dried. The coatings were then left to dry at room temperature and left overnight on a large steel table to allow for the temperature of the plates to stabilise. The temperature reading of the thermocouples was

then taken first thing the next morning while the temperature of the room was still stable. This shows thermocouples have a greater than $\pm 1^\circ C$ variation which needs to be considered when calibrating.

Sample	Powder:Glue ratio	Powder % by volume	Thermocouple reading
3	1:1	50%	17.1
4	1:1	50%	17.3
5	1:1	50%	17.1
6	1:1	50%	17.2
7	1:2	33%	20.5
8	3:2	60%	17.1
9	3:2	60%	19.9
10		>60%	17.1

Table 6-2 The coatings produced for comparison

6.3.1 *The relationship of the coating with temperature*

A selection of coatings were considered to determine which relationships between temperature and the fluorescent spectrum was present for the majority of the coatings. It was found that some relationships which showed a strong correlation with temperature for one coating would not be present in any of the other coatings. Selection of a relationship with temperature was undertaken under the guidelines laid out previously in Section 6.2.

	Sample 6	Sample 8a	Sample 8b	Sample 9	Sample 10
Pos 2	$Y = -0.0012x + 502.84$ $R^2=0.7376$		$Y = -0.0012x + 502.68$ $R^2=0.9095$	$Y = -0.0011x + 502.84$ $R^2=0.7517$	$Y = -0.0017x + 502.17$ $R^2=0.7200$
Pos 4			$Y = 0.0006x + 513.45$ $R^2=0.7798$		
Pos 8				$Y = 548.42e^{-0.000003x}$ $R^2=0.7048$	
Pos 13	$Y = 0.0022x + 670.05$ $R^2=0.9653$		$Y = 0.0018x + 669.98$ $R^2=0.9698$	$Y = 0.0025x + 670.05$ $R^2=0.9574$	$Y = 0.0025x + 669.93$ $R^2=0.8627$
Pos 14	$Y = 0.1773*\ln(x) + 673.01$ $R^2=0.9156$	$Y = 0.0014X + 673.68$ $R^2=0.9052$	$Y = 0.0011X + 673.57$ $R^2=0.8843$	$Y = 0.1401*\ln(x) + 673.24$ $R^2=0.8683$	$Y = 0.0009X + 673.61$ $R^2=0.7904$
Pos 15			$Y = 0.0019x + 770$ $R^2=0.9657$	$Y = 0.0014x + 770.04$ $R^2=0.7024$	

Table 6-3 The relationship between temperature and peak positions.

From the many possible relationships between temperature and the fluorescence spectrum the relationships which showed the most potential for a means of measuring temperature are shown in Table 6-3 through to Table 6-8. From these relationships the ones which show consistency over the different samples from each group will be selected to be studied further.

From the peak position relationships, Table 6-3, there are three peak positions that show potential. These are peak 2, peak 13 and peak 14 as they all show similar relationships with more than one coating, they also high R² values which show a strong correlation. The peak separation, Table 6-4, showed that there are four main possibilities for temperature determination P15-P2, P14-P2, P13-P2, and P8-P2. These four relationships showed consistency over four or more samples.

	Sample 6	Sample 8a	Sample 8b	Sample 9	Sample 10
P15-P14	Y = -0.0015x + 100.04 R ² =0.7107		Y = 0.0008x + 96.421 R ² =0.761		Y = 0.0016x + 96.37 R ² =0.7704
P15-P11			Y = 0.0018x + 129.29 R ² =0.722		Y = 0.0029x + 129.26 R ² =0.8256
P15-P4			Y = 0.0013x + 256.54 R ² =0.8886		Y = 0.0018x + 256.52 R ² =0.7222
P15-P2	Y = 0.0019x + 267.23 R ² =0.7687	Y = 0.0022x + 267.19 R ² =0.8094	Y = 0.0031x + 267.31 R ² =0.9801	Y = 0.0025x + 267.21 R ² =0.8751	Y = 0.0042x + 267.27 R ² =0.9484
P15-532			Y = 0.0014x + 238.38 R ² =0.7666		
P14-P2	Y = 0.0026x + 170.83 R ² =0.9345	Y = 0.0028x + 170.8 R ² =0.9433	Y = 0.0023x + 170.89 R ² =0.9614	Y = 0.0025x + 170.88 R ² =0.9244	Y = 0.0027x + 170.88 R ² =0.8832
P13-P2	Y = 0.0034x + 167.19 R ² =0.952	Y = 0.0034x + 167.18 R ² =0.757	Y = 0.0031x + 167.29 R ² =0.965	Y = 0.0036x + 167.21 R ² =0.9441	Y = 0.0042x + 167.23 R ² =0.8861
P13-P4			Y = 0.0013x + 156.52 R ² =0.8894		
P13-532			Y = 0.0016x + 138.32 R ² =0.8193		
P13-P9	Y = 0.0045x + 113.2 R ² =0.7097		Y = 0.0029x + 113.34 R ² =0.7283		
P8-P2	Y = 0.0027x + 45.568 R ² =0.8133	Y = 0.0029x + 45.561 R ² =0.7035	Y = 0.0023x + 45.489 R ² =0.778	Y = 0.0029x + 113.34 R ² =0.7283	
P4-P2			Y = 0.0018x + 10.766 R ² =0.9394		Y = 0.0024x + 10.731 R ² =0.7695
P15-P9					Y = 0.0031x + 213.39 R ² =0.7561
P14-P13	Y = 3.6511e ^{-0.0002x} R ² =0.7048				Y = -0.0041x + 3.6531 R ² =0.7060
P13-P11				Y = 0.0024x + 29.273 R ² =0.7853	

Table 6-4 The relationship between temperature and peak separation.

It is expected that the intensity will vary between the different samples, as this is dependent upon the coating, laser intensity and collection efficiency, so the peak height itself cannot be used. The reduction in intensity with heating should follow the same trend between the samples. Comparing the decay curve of the different samples it can be

seen that there is consistency and therefore it is possible to use the intensity change as a means of measuring temperature.

	Sample 6	Sample 8a	Sample 9
Int 2	$Y = 2617.6e^{-0.0145x}$ $R^2=0.8549$	$Y = 2243.8e^{-0.0139x}$ $R^2=0.8439$	$Y = 2533.7e^{-0.0139x}$ $R^2=0.8385$
Int 4	$Y = 6114.7e^{-0.015x}$ $R^2=0.8785$	$Y = 5263.8e^{-0.0139x}$ $R^2=0.833$	
Int 11	$Y = 331e^{-0.0078x}$ $R^2=0.8221$	$Y = 379.53e^{-0.0083x}$ $R^2=0.8264$	$Y = 424.36e^{-0.0083x}$ $R^2=0.8283$
Int 13	$Y = 1309e^{-0.0112x}$ $R^2=0.8746$	$Y = -3.6287x + 935.66$ $R^2=0.7763$	$Y = 1590.5e^{-0.0118x}$ $R^2=0.8603$
Int 14	$Y = 887.18e^{-0.0102x}$ $R^2=0.8685$	$Y = 946.95e^{-0.0101x}$ $R^2=0.8685$	$Y = 1081.4e^{-0.0106x}$ $R^2=0.8396$
Int 15	$Y = 197.89e^{-0.008x}$ $R^2=0.8398$	$Y = 236.36e^{-0.0086x}$ $R^2=0.8606$	$Y = 264.37e^{-0.0092x}$ $R^2=0.8365$

Table 6-5 The relationship between temperature and peak intensity.

	Sample 8b
14/1532	$Y = -7.1752*\ln(x) + 48.327$ $R^2=0.8372$
115/1532	$Y = -0.9599*\ln(x) + 6.2174$ $R^2=0.7694$

Table 6-6 The relationship between ratio of laser pulse and fluorescence spectrum with temperature

	Sample 6	Sample 8a	Sample 8b	Sample 9	Sample 10
114/110	$Y = 8.2067e^{-0.0102x}$ $R^2=0.8875$	$Y = 8.4051e^{-0.01x}$ $R^2=0.8459$		$Y = 10.21e^{-0.0114x}$ $R^2=0.8637$	$Y = 24.511e^{-0.007x}$ $R^2=0.938$
113/111	$Y = -0.0071x + 3.5367$ $R^2=0.907$	$Y = -0.0069x + 3.4876$ $R^2=0.8741$		$Y = -0.0073x + 3.5614$ $R^2=0.9288$	
114/111	$Y = -0.0046x + 2.5844$ $R^2=0.8947$	$Y = -0.0043x + 2.5474$ $R^2=0.8843$		$Y = -0.0047x + 2.5858$ $R^2=0.9269$	
114/19	$Y = -1.0827*\ln(x) + 7.0777$ $R^2=0.852$	$Y = -1.1224*\ln(x) + 7.2578$ $R^2=0.9733$		$Y = -1.2529*\ln(x) + 7.7721$ $R^2=0.9621$	$Y = -1.1559*\ln(x) + 7.2073$ $R^2=0.7401$
111/19		$Y = -0.2972*\ln(x) + 2.4059$ $R^2=0.778$	$Y = -0.517*\ln(x) + 3.5907$ $R^2=0.9352$	$Y = -0.3597*\ln(x) + 2.6336$ $R^2=0.8346$	$Y = -0.3619*\ln(x) + 2.4896$ $R^2=0.968$
19/18	$Y = 0.6943e^{0.0013x}$ $R^2=0.8892$	$Y = 0.7184e^{0.0011x}$ $R^2=0.8902$		$Y = 0.7001e^{0.0014x}$ $R^2=0.9309$	
19/12	$Y = 0.1163e^{0.0078x}$ $R^2=0.9769$	$Y = 0.1318e^{0.0073x}$ $R^2=0.9772$	$Y = 0.0009x + 0.1379$ $R^2=0.8938$	$Y = 0.1227e^{0.0041x}$ $R^2=0.9809$	$Y = 0.0018x + 0.0673$ $R^2=0.9795$
18/12	$Y = 0.1668e^{0.0063x}$ $R^2=0.9793$	$Y = 0.1839e^{0.0061x}$ $R^2=0.9794$	$Y = 0.0011x + 0.171$ $R^2=0.9723$	$Y = 0.1754e^{0.0067x}$ $R^2=0.9828$	$Y = 0.0018x + 0.1216$ $R^2=0.8729$
19/14	$Y = 0.0512e^{0.0076x}$ $R^2=0.976$	$Y = 0.0566e^{0.0076x}$ $R^2=0.9305$	$Y = 0.0405*\ln(x) - 0.0789$ $R^2=0.8703$	$Y = 0.0561e^{0.008x}$ $R^2=0.9693$	$Y = 0.0477e^{0.007x}$ $R^2=0.9734$
18/14	$Y = 0.074e^{0.0065x}$ $R^2=0.9809$	$Y = 0.0788e^{0.0064x}$ $R^2=0.924$	$Y = 0.0004x + 0.0883$ $R^2=0.9624$	$Y = 0.079e^{0.0067x}$ $R^2=0.9711$	$Y = 0.0009x + 0.0456$ $R^2=0.9672$
110/14	$Y = 0.0179e^{0.0118x}$ $R^2=0.9048$	$Y = 0.0224e^{0.0113x}$ $R^2=0.8491$		$Y = 0.0179e^{0.0132x}$ $R^2=0.8394$	$Y = 0.061e^{0.0011x}$ $R^2=0.8391$
110/12	$Y = 0.0416e^{0.0112x}$ $R^2=0.8897$	$Y = 0.0527e^{0.0113x}$ $R^2=0.8609$	$Y = 0.0182e^{0.0057x}$ $R^2=0.856$	$Y = 0.0427e^{0.0114x}$ $R^2=0.8783$	

Table 6-7 The strongest relationships between intensity ratio and temperature

It is thought that the fluctuations in intensity due to environmental and coating conditions could be eliminated through referencing the laser peak with the fluorescence peaks. Table

6-6 shows that there is not a strong relationship between temperature and the ratio of a peak with the laser peak, as only one data set gives two strong relationships. This could indicate that the laser energy is either just above the threshold level of Y₂O₃S:Pr or just below the peak fluorescence energy as at these points slight changes in the laser energy would put the relationship into a non-linear zone, and as such not creating a strong relationship.

	Sample 6	Sample 8a	Sample 8b	Sample 9	Sample 10
I13/I10	$Y = 11.825e^{-0.011x}$ $R^2=0.8993$		$Y = 55.746e^{-0.0055x}$ $R^2=0.8974$	$Y = 14.671e^{-0.0122x}$ $R^2=0.8886$	$Y = 31.906e^{-0.0068x}$ $R^2=0.877$
I11/I10	$Y = 3.0464e^{-0.0078x}$ $R^2=0.8609$		$Y = -5.0102*\ln(x) + 31.972$ $R^2=0.9472$	$Y = 3.9214e^{-0.0093x}$ $R^2=0.8536$	$Y = 10.717e^{-0.007x}$ $R^2=0.9568$
I15/I10	$Y = 1.8702e^{-0.0081x}$ $R^2=0.8481$	$Y = 2.0277e^{-0.0083x}$ $R^2=0.8565$		$Y = 2.541e^{-0.0102x}$ $R^2=0.841$	$Y = -0.0212x + 4.9601$ $R^2=0.8476$
I13/I10		$Y = 12.357e^{-0.0113x}$ $R^2=0.8459$			
I11/I10		$Y = 3.223e^{-0.0078x}$ $R^2=0.8459$			
I13/I9	$Y = -1.4792*\ln(x) + 9.6007$ $R^2=0.8645$	$Y = -1.4787*\ln(x) + 9.6124$ $R^2=0.9621$	$Y = -1.8108*\ln(x) + 12.81$ $R^2=0.9392$		
I13/I8	$Y = -0.8276*\ln(x) + 6.0156$ $R^2=0.7178$	$Y = -0.9582*\ln(x) + 6.7676$ $R^2=0.9307$	$Y = -1.3854*\ln(x) + 9.8631$ $R^2=0.9884$	$Y = -1.0698*\ln(x) + 7.0889$ $R^2=0.9552$	$Y = -0.0105x + 3.0667$ $R^2=0.9691$
I14/I8		$Y = -0.7369*\ln(x) + 5.0768$ $R^2=0.9544$		$Y = -0.7859*\ln(x) + 5.2237$ $R^2=0.947$	$Y = -0.6064*\ln(x) + 4.2602$ $R^2=0.9631$
I15/I9		$Y = -0.2276*\ln(x) + 1.6628$ $R^2=0.7259$	$Y = -0.484*\ln(x) + 3.32$ $R^2=0.947$	$Y = -0.309*\ln(x) + 1.9794$ $R^2=0.903$	$Y = -0.1744*\ln(x) + 1.2178$
I15/I11				$Y = 0.6698e^{-0.0014x}$ $R^2=0.7488$	
I13/I2					$Y = 0.4871e^{0.0021x}$ $R^2=0.8787$
I11/I8			$Y = -0.3875*\ln(x) + 2.7363$ $R^2=0.9634$		$Y = -0.2192*\ln(x) + 1.6531$ $R^2=0.9419$
I15/I8			$Y = -0.3647*\ln(x) + 2.5329$ $R^2=0.9856$	$Y = -0.1878*\ln(x) + 1.3113$ $R^2=0.8326$	$Y = -0.1372*\ln(x) + 0.9546$ $R^2=0.8374$
I14/I2					$Y = 0.353e^{0.0022x}$ $R^2=0.8784$
I13/I4	$Y = 0.204e^{0.0041x}$ $R^2=0.72$	$Y = 0.2667e^{0.0029x}$ $R^2=0.7004$			$Y = 0.2104e^{0.0021x}$ $R^2=0.8445$
I11/I2	$Y = 0.1324e^{0.0062x}$ $R^2=0.8138$	$Y = 0.1738e^{0.0051x}$ $R^2=0.8023$		$Y = 0.1675e^{0.0031x}$ $R^2=0.7938$	$Y = 0.1496e^{0.0026x}$ $R^2=0.7973$
I14/I4					$Y = 0.152e^{0.0023x}$ $R^2=0.8486$
I10/I8	$Y = 0.2597e^{0.0076x}$ $R^2=0.7399$		$Y = 0.0897e^{0.0022x}$ $R^2=0.7233$	$Y = 0.2435e^{0.0077x}$ $R^2=0.7079$	
I15/I2					$Y = 0.0003x + 0.0684$ $R^2=0.8598$
I15/I4					$Y = 0.0001x + 0.0291$ $R^2=0.835$
I11/I4	$Y = 0.056e^{0.0066x}$ $R^2=0.8356$	$Y = 0.074e^{0.0134x}$ $R^2=0.8609$		$Y = 0.0648e^{0.006x}$ $R^2=0.7532$	

Table 6-8 The relationships which showed possibility between intensity ratio and temperature

Using the ratio of the fluorescent peaks will also remove fluctuations in the peak intensity due to outside conditions. There are many ratios that showed potential for use as a means of measuring temperature, those which showed the strongest relationship are shown in Table 6-7, those which were not as consistent across the samples are shown in Table 6-8. Those that show the strongest relationship with temperature will be studied further.

With the selection of relationships for temperature reading those which showed the strongest and most consistent relationship across the samples will be considered first. If these prove to be unsuccessful during further analysis then the other relationships will be considered.

A reference value at 200°C has been set for each of the relationships and these have been used to make each of the relationships transferable between each of the samples. Each of the relationships, as well as the average of the slope of the relationship was then turned around to make temperature the “Y” value and applied to the data from each of the samples to determine the best relationship. Taking the relationship of position 2 with temperature the values for the equations used can be seen in Table 6-9, where the

equation is of the form; $Temp = \left(\frac{pos - Pref}{m} \right) + Tref$.

Derived from	Initial relationship	m	Tref (°C)	Pref (nm)
Sample 6	P = -0.0012T + 502.84	-0.0012	128.5	502.69
Sample 8a			125.5	502.72
Sample 8b	P = -0.0012T + 502.68	-0.0012	120	502.56
Sample 9	P = -0.0011T + 502.84	-0.0011	96.6	502.72
Sample 10	P = -0.0017T + 502.17	-0.0017	100.9	502.58
Average	P = -0.0013T + 502.63	-0.0013		

Table 6-9 The relationships tested with position of peak 2 for temperature measurement.

The error between the actual temperature and the determined temperature was calculated in percentage and the error distribution considered for four temperature ranges 20°C to 300°C, 20°C to 100°C, 100°C to 200°C and 200°C to 300°C. The error distribution was considered and for the relationships which had 50% of its data within an error range of 20% was considered further. Further analysis used a constant which would be used to shift the error to centre on zero, see Equation 6-1, see Appendix 9.6.4.3 for definition.

$$Temp = \left(\frac{100 + s}{100} \right) \left(\frac{x - Pref}{m} + Tref \right)$$

Equation 6-1

Where; s = constant for centring of error around zero
 x = peak position
 Pref = reference value (peak position, separation)
 Tref = reference temperature
 m = slope

Using Equation 6-1 the equations which gave 50% of its readings within ±10% of the actual reading were then considered to have a strong fluorescence temperature relationship. This analysis on the relationships of the fluorescence to temperature showed that the following relationships produced a strong relationship with temperature;

Position of peak 13 – Position of peak 2
Position of peak 14 – Position of peak 2

Intensity of peak 8 / Intensity of peak 4
Intensity of peak 9 / Intensity of peak 4
Intensity of peak 8 / Intensity of peak 2
Intensity of peak 13 / Intensity of peak 9
Intensity of peak 14 / Intensity of peak 9
Intensity of peak 15 / Intensity of peak 9
Intensity of peak 14 / Intensity of peak 8

The decrease in intensity of the spectrum with temperature was seen to differ for each peak, the decrease in intensity from 20°C to 200°C can be see in Table 6-10.

	Decrease for coatings			Average
	s3c	s7c	s7cc	
Peak 2		0.17	0.24	0.20
Peak 4		0.16	0.19	0.18
Peak 7		0.25	0.89	0.57
Peak 8	0.30	0.62	0.76	0.56
Peak 9	0.36	1.02	1.29	0.88
Peak 10	0.55			0.55
Peak 11	0.15	0.47	0.58	0.40
Peak 13	0.16	0.31	0.31	0.27
Peak 14	0.21	0.31	0.32	0.28
Peak 15	0.18	0.47		0.33

Table 6-10 The decrease in intensity for each of the peaks from 20°C to 200°C.

6.3.1.1 Coating reliability

Coating 3 was tested for repeated heating and cooling, see Table 6-2. It is shown below that the peak positions and peak separations showed no change between the experiments. The intensity and the intensity ratios showed large changes between each of the experiments. As would be expected from the results gained from the powder only. The separation of the peaks was also found to be a reliable technique when considering different coatings. It can be seen that there is a difference in relationship for some of the coatings below 50°C, but as this is not within the temperature range of interest it is not a concern here.

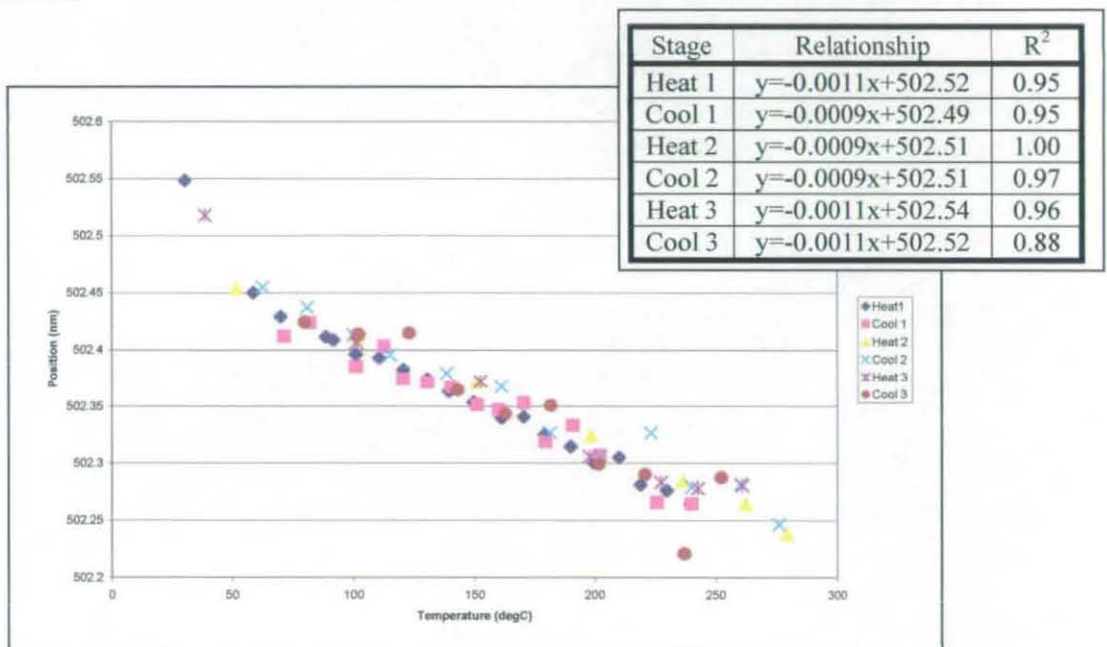


Figure 6-5 The affect of repeated heating and cooling on the position of Peak 2^{XXII} of Y₂O₃S:Pr.

The peak positions and separations are not affected through repeated heating and cooling. This shows that the relationships determined for temperature are due to an affect of temperature on the crystal fields associated with the luminescent centres rather than an affect of temperature on the coating. This shows that the peak position and separation produce a relationship with temperature that is consistent from one experiment to another, and that the same coating can be used repeatedly.

^{XXII} See Figure 6-1 page 138

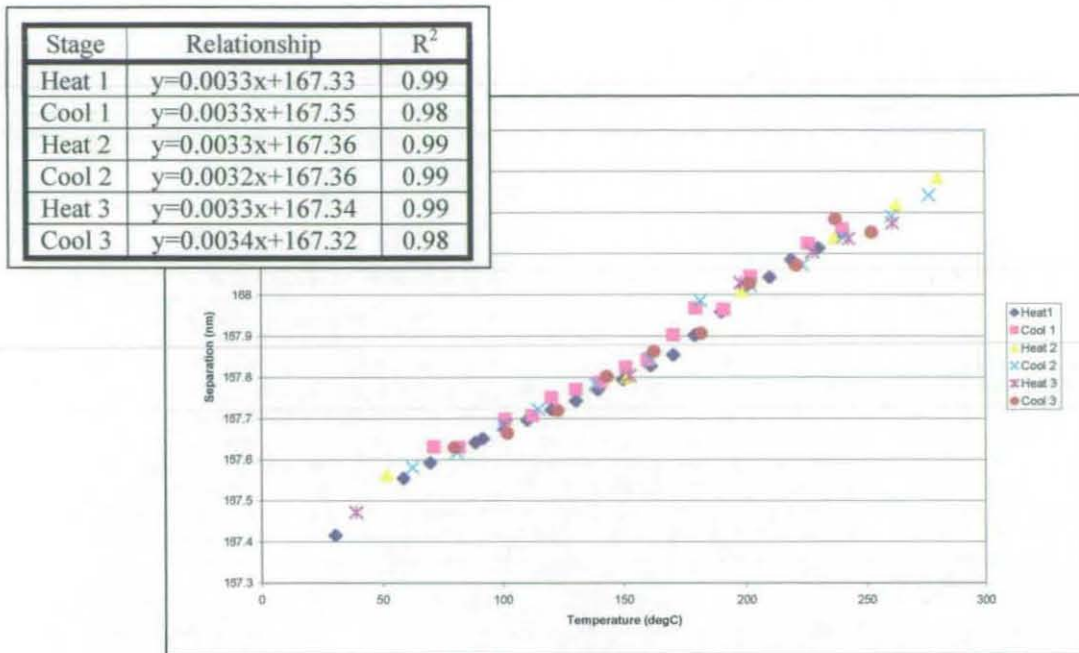


Figure 6-6 The affect of repeated heating and cooling on the separation of Peak 13 and Peak 2.

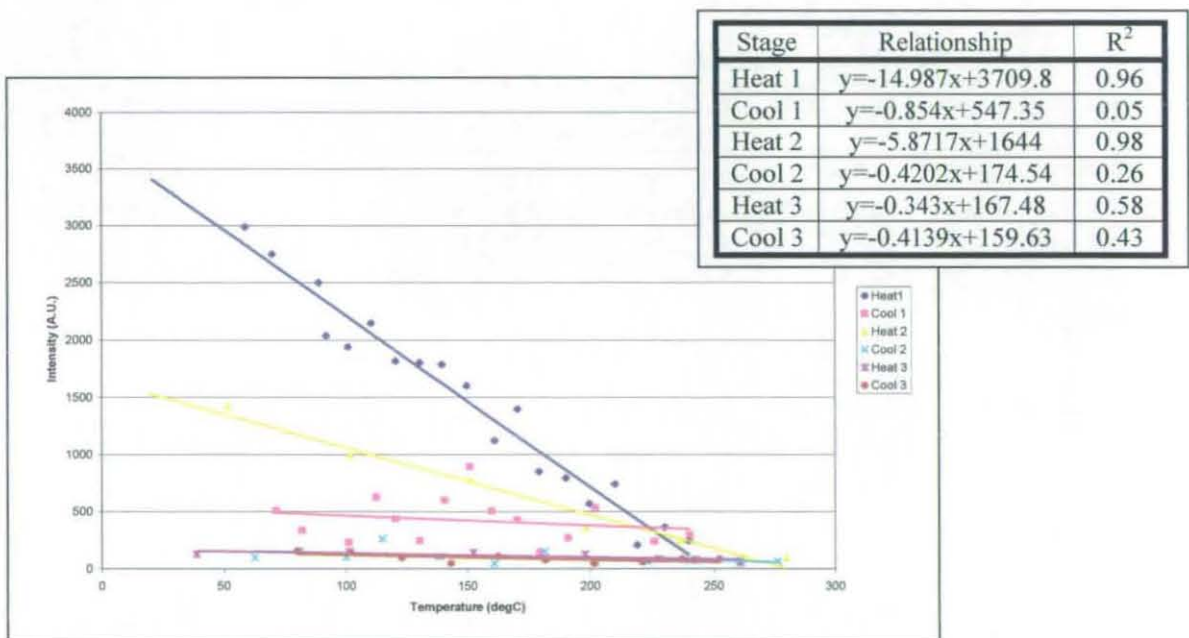


Figure 6-7 The affect of repeated heating and cooling on the intensity of peak2.

As with the powder only data, the intensity ratio did not produce a reliable relationship with temperature, see Figure 6-8. This relationship with temperatures shows a linear trend rather than the exponential trend of the powder, Figure 6-14, showing that the adhesive has an affect on the intensity ratio of the paint.

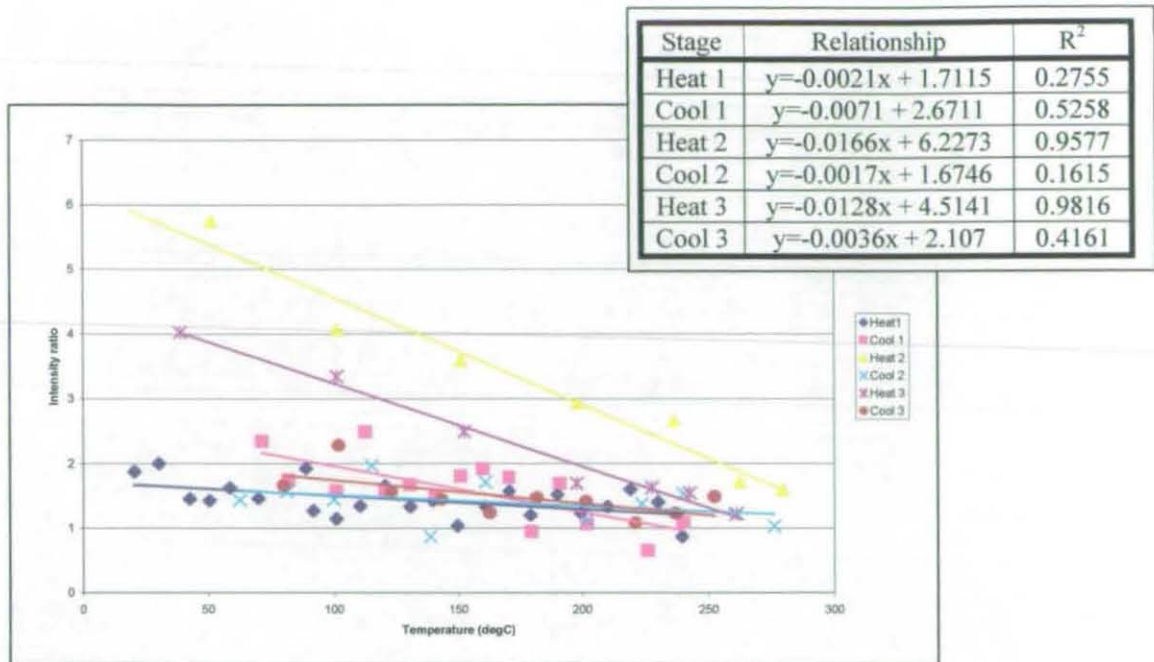


Figure 6-8 The affect of repeated heating and cooling on the ratio of Peak 13 to Peak 9.

As with the powder this shows that the peak positions produce a much more reliable method of measuring temperature than using the intensity. The decrease in the intensity causes concern in the fact that the signal may become too weak that the peaks cannot be detected reliably from the background.

6.3.1.2 *Affect of powder quantity on the fluorescent spectrum*

Using the best fits determined from the powder data, the affect of powder content on the fluorescent spectrum was studied. The peak position and peak separation is expected to show a stable relationship with temperature with different coatings as the wavelength is due to the molecular structure of the material which should not be affected by volume. As the peak intensity and ratio of peaks does not show a constant relationship with temperature it is not expected to show consistency with change in powder content, though a decrease in intensity with powder content would be expected.

The peak position is seen to differ from one paint sample to another, Figure 6-9, a difference of 0.41nm is noted, this difference can be equated to 1¼ pixels and can therefore be contributed to accuracy in the peak fitting routine in LabView rather than an affect of powder content.

It is noted that the separation of the peaks also varies with coating, Figure 6-10, this difference equates to a difference of ½ a pixel. The use of the separation of the peaks reduces the error in the reading between different coatings, though the difference in peak position could be removed by taking a reference reading for each of the coatings and using this value in the equation to determine temperature. A difference in the slope of the relationship is noted for both the peak position and separation of the peaks. As this difference does not show a relationship with powder content it is thought to be an error introduced in the peak fitting routine.

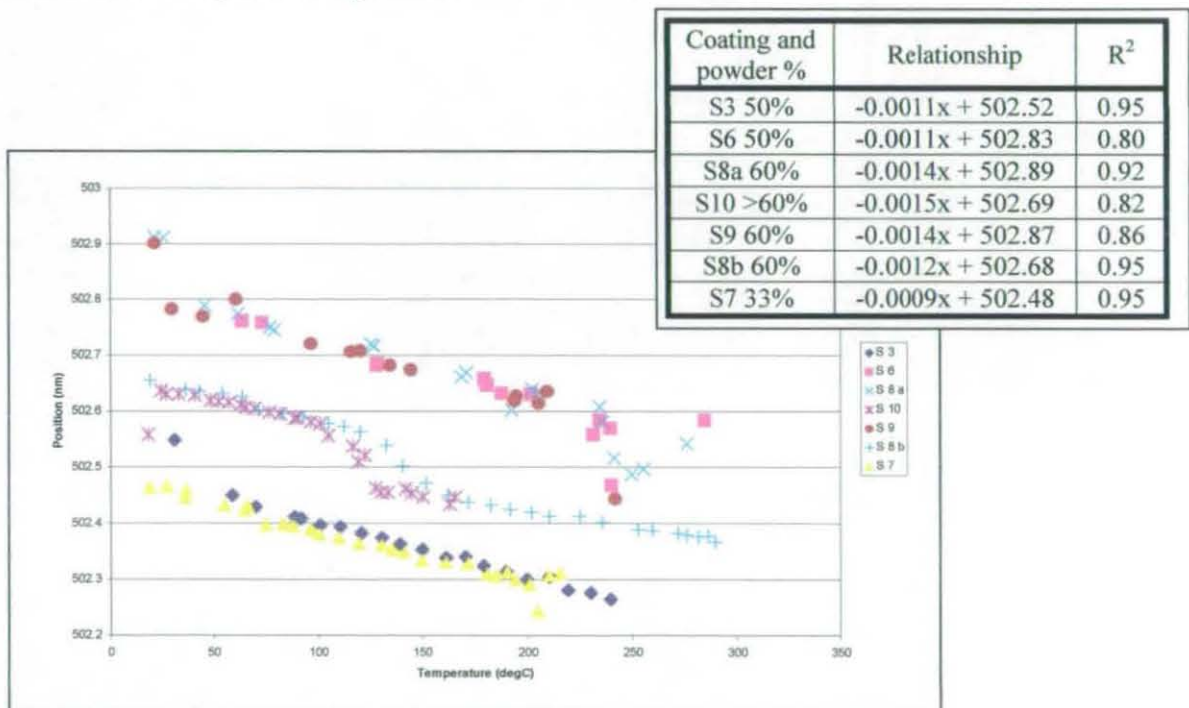


Figure 6-9 The difference in the position of Peak 2 with different powder content.

The change in the intensity of Peak 2 with powder content, Figure 6-11, shows that there is more than the powder volume which affects intensity as the value of 'c' in the relationship $y=m*\ln(x)+c$ cannot be related to powder volume. It is known that the laser pulse energy affects the intensity and so the change in intensity here can be contributed to laser pulse energy as well as the powder volume of the paint.

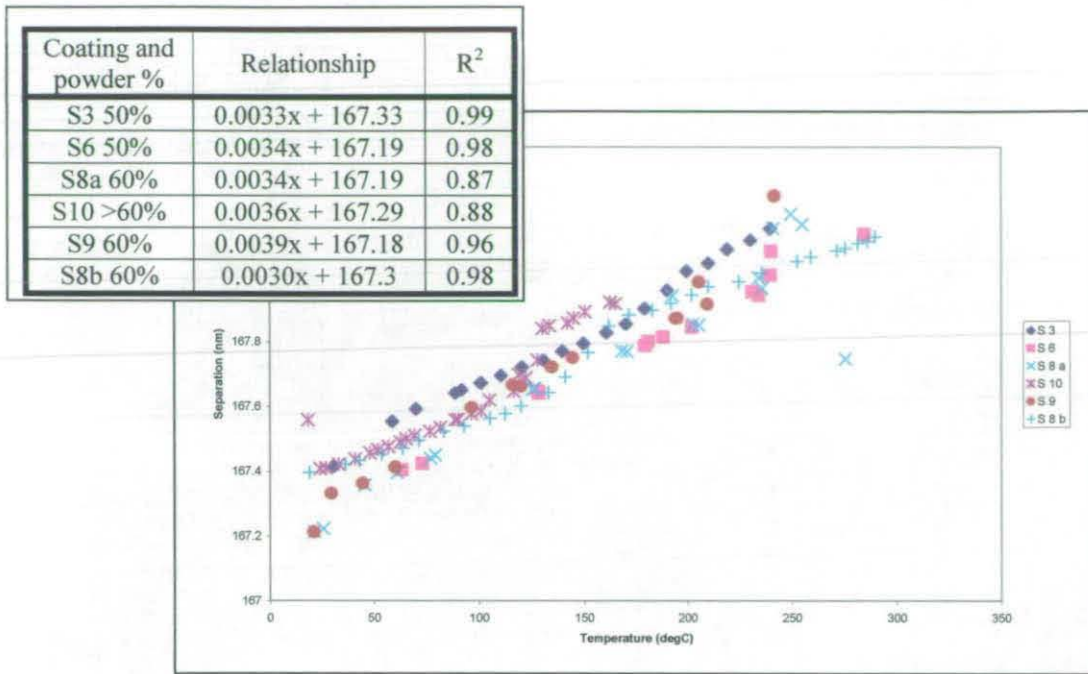


Figure 6-10 The difference in the separation of Peak 13 and Peak 2 different powder content.

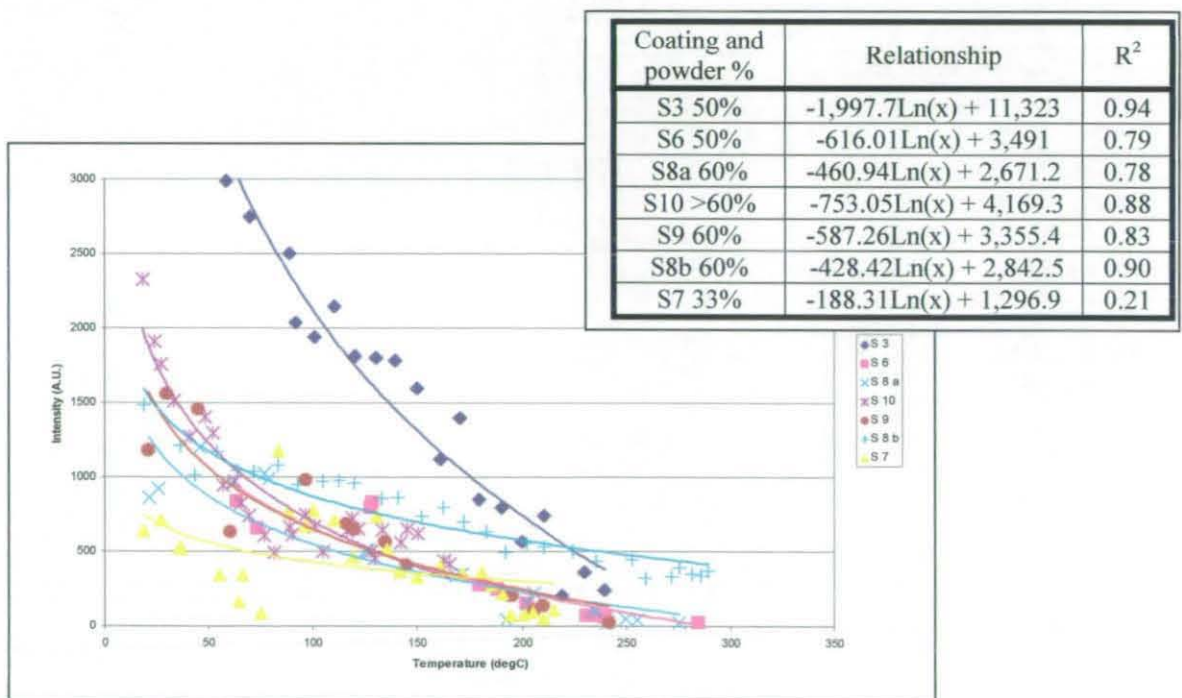


Figure 6-11 The affect of powder content on the intensity of Peak 2

6.3.1.2.1 Summary of Y₂O₃S:Pr coating

It is shown that the Y₂O₃S:Pr coating gives a strong relationship with temperature. The peak properties that show a strong reliability are shown in Table 6-11 with Equation 6-2 showing the relationship with temperature for these properties.

$$Temp = \left(\frac{100 + s}{100} \right) \left(\frac{x - Pref}{m} + Tref \right)$$

Equation 6-2

Where; s = constant for centring of error around zero
 x = peak position
 Pref = reference value (peak position, separation)
 Tref = reference temperature
 m = slope

The work shows that there is little difference in the accuracy of the fits between 50% and 60% volume powder content, also there is no affect on the peak position and peak separation. A coating with between 50% and 60% powder volume should therefore be used.

Relationship	m	s	Temp range	% of data within			
				4%	6%	8%	10%
P2	-0.0012	3	20→300°C	25	37	47	55
			20→100°C	30	40	60	80
			100→200°C	36	49	62	72
			200→300°C	27	41	54	64
P13	0.0025	3	20→300°C	27	39	50	60
			20→100°C	78	93	100	100
			100→200°C	43	59	70	81
			200→300°C	18	31	51	69
P14	0.0012	6	20→300°C	29	42	53	63
			20→100°C	No data			
			100→200°C	32	46	58	73
			200→300°C	19	38	47	57
P13-P2	0.0028	3	20→300°C	35	47	56	61
			20→100°C	28	39	51	56
			100→200°C	59	76	85	91
			200→300°C	36	44	50	58
P14-P2	0.0020	2	20→300°C	35	54	65	75
			20→100°C	39	56	64	83
			100→200°C	45	63	73	80
			200→300°C	27	43	52	61

Table 6-11 The relationship between the coating and temperature

6.4 Y₂O₃S:Pr powder temperature sensitivity

As the decay period of Y₂O₃S:Pr did not show a relationship with temperature the spectrum itself was studied for temperature sensitivity, Figure 6-12. Each possible relationship for peak position, separation of peak, peak intensity and ratio of peak intensity was considered. To determine which peaks, if any, showed a relationship with temperature. Initial work showed that the peaks intensities and ratio of peak intensities showed the most promising for a temperature relationship.

These relationships were then tested for stability through repeated heating and cooling. The intensity and the intensity ratio was shown to change with repeated heating Figure 6-13 and Figure 6-14. This shows that the peak intensities cannot be used as a means of temperature measurement. It also shows that above 100°C there is little change in intensity and of intensity ratio with temperature so this would also mean that the intensity ratio of Y₂O₃S:Pr could not be used for high temperature measurement.

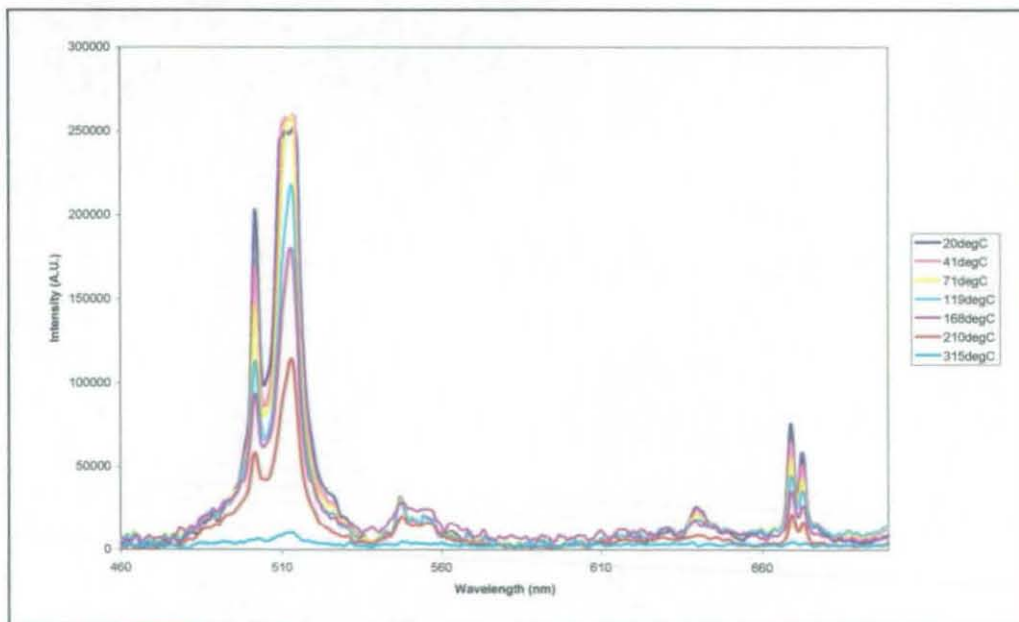


Figure 6-12 The relationship between temperature and the fluorescence spectrum of Y₂O₃S:Pr.

The peak position and peak separation showed a stable relationship with temperature, Figure 6-15 and Figure 6-16. The peak position shows a strong relationship with

temperature up to 200°C whereas the peak separation shows a strong relationship with temperature up to 300°C, the maximum temperature that could be reached using the hot plate technique of heating. For the peak position and peak separation the important factor for consistency is the slope of the graph as changes in the offset can be accounted for by taking a reference value at a known temperature at the start of the experiment. For peak position the change in the offset for the equation is 0.02nm, and for peak separation it is 0.03nm, which accounts for less than a tenth of a pixel, this difference can be accounted for by the method used to determine peak position.

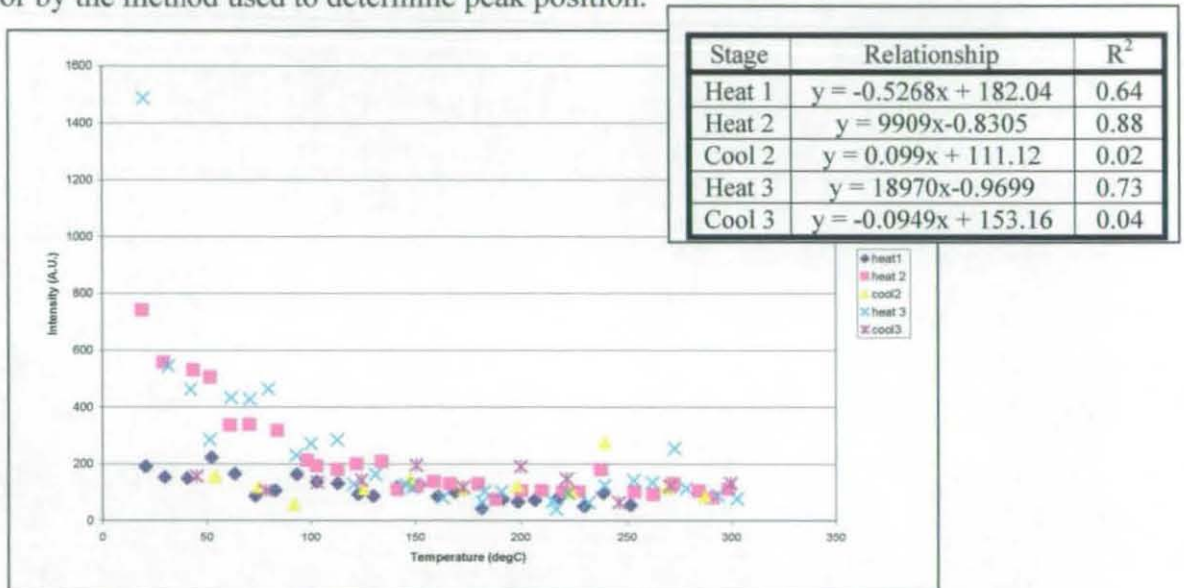


Figure 6-13 The relationship of the intensity of Peak 2 with temperature

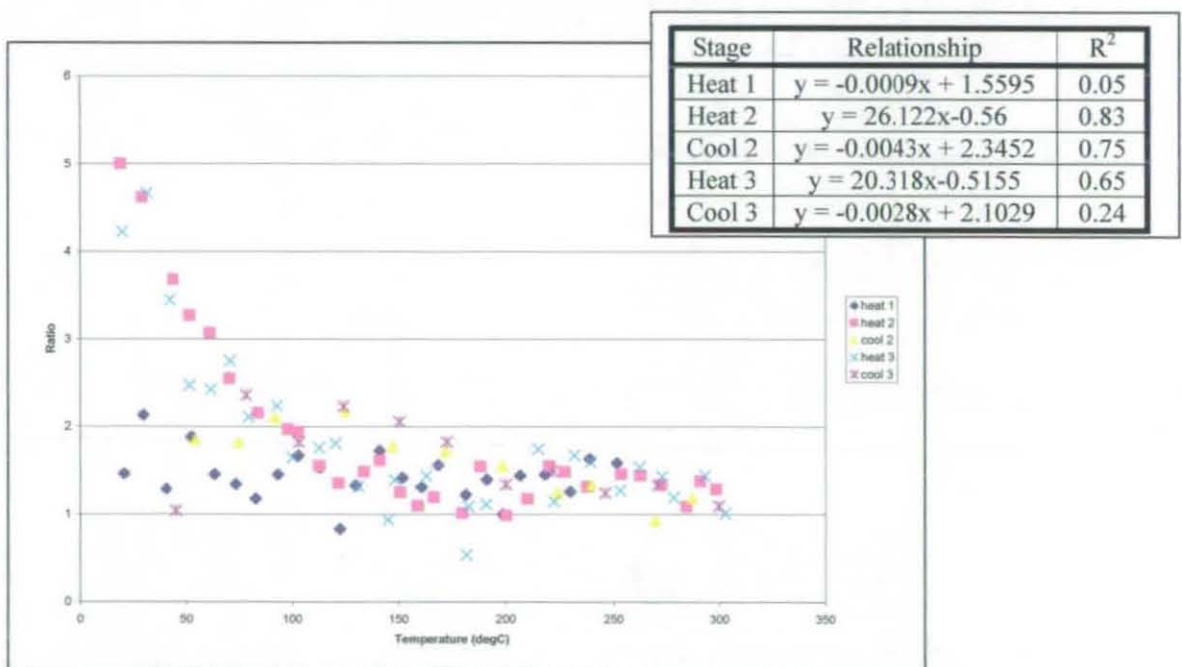


Figure 6-14 The relationship of ratio of intensities of Peak 13 and Peak 9 with temperature

Given the stability of the relationship of peak separation, temperatures greater than 300°C could probably be reached if a stronger fluorescent signal could be achieved. It would be the lack in intensity that would mean the peaks could not be detected and therefore not used for temperature prediction.

During the experiments undertaken it was noted that the laser energy seemed to decrease with time. This was therefore looked at as a possible reason for the unstable intensity, and intensity ratio with temperature. Using a reflected 532nm beam from the laser the intensity of the laser beam can be monitored using the spectrometer at the same time as the fluorescence reading. This cannot be used as a measure of laser intensity but can be used as a reference for the change in laser energy. It is shown in Figure 6-17 that the laser pulse intensity decreases by half over a period of an hour. This would affect the peak intensity relationship with temperature. Through taking the ratio of the peak intensities any difference in the laser pulse intensity should be removed if each peak emission has the same relationship with input intensity.

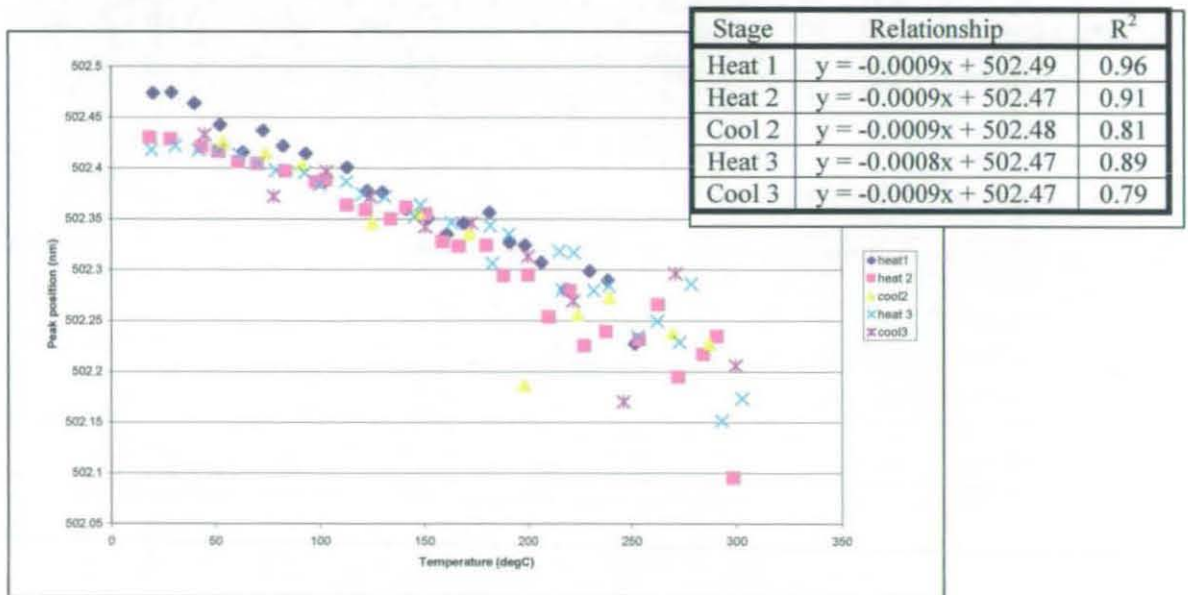


Figure 6-15 The relationship of the position of Peak 2 with temperature

It is thought that by taking the ratio of the peak intensities would count for any change in laser energy. It is shown that each of the emission peak intensities has a different relationship with laser intensity (int7), Figure 6-18, for this data the sample was kept at

room temperature. This shows that the ratio of the peaks cannot be used as a method of calibration for laser intensity change as the relationship between intensity ratio and input power does not produce an accurate relationship. Figure 6-19 shows that there is not a linear relationship between laser energy and fluorescence intensity. This indicates that the $Y_2O_3S:Pr$ coating is not being excited at its most favourable energy, the exponential relationship seen in Figure 6-19 suggests that the material is being excited just above its threshold limit, see Figure 5-19, and as such increasing the laser energy would create a more stable relationship as this would move the laser energy luminescence relationship into the linear region.

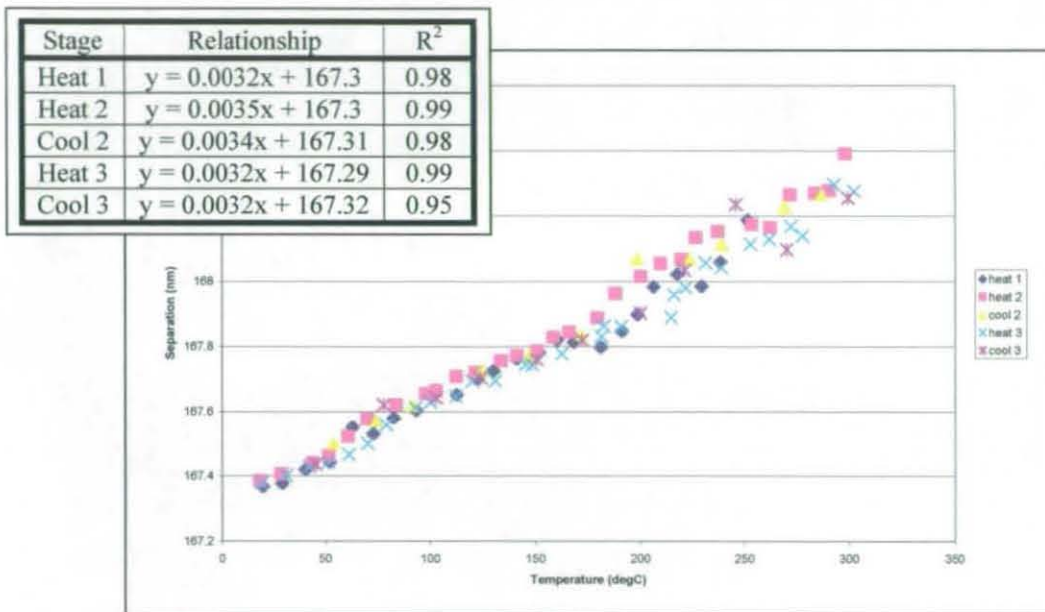


Figure 6-16 The relationship of separation of Peak 13 and Peak 2 with temperature

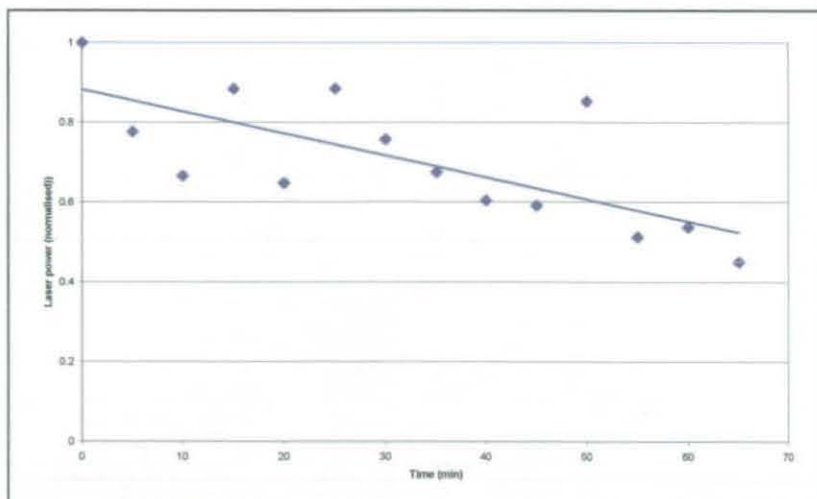


Figure 6-17 The affect of time on the laser pulse intensity.

Ratio of peak with laser intensity	Slope of fit	R ²
Int 2 / Int 7	0.0102	0.26
Int 4 / Int 7	0.0104	0.16
Int 8 / Int 7	0.0009	0.09
Int 9 / Int 7	-0.0003	0.01
Int 11 / Int 7	0.0017	0.23
Int 12 / Int 7	-0.0002	0.02
Int 13 / Int 7	0.0058	0.23
Int 14 / Int 7	0.004	0.24
Int 15 / Int 7	-0.0011	0.08

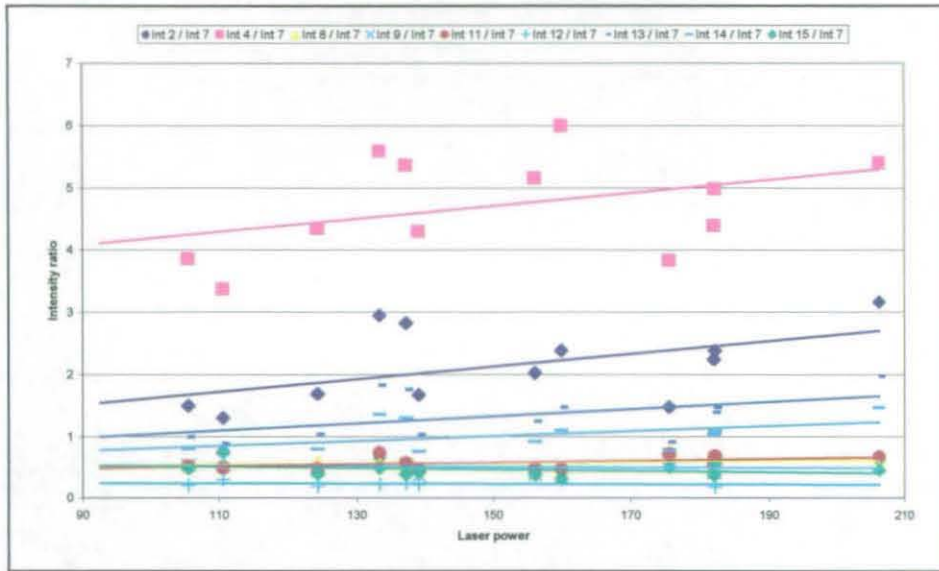


Figure 6-18 The affect of the laser pulse intensity on the peak intensity ratio.

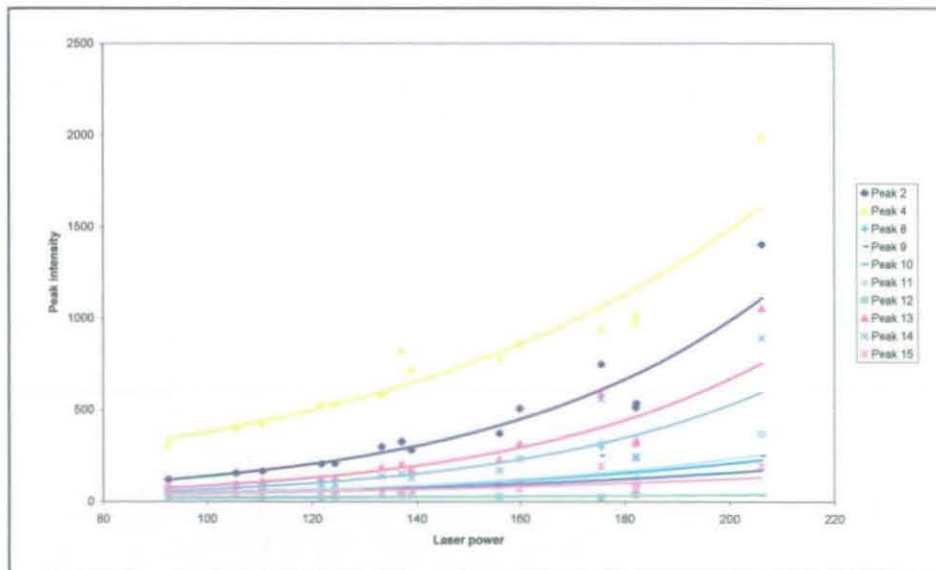


Figure 6-19 The relationship between laser energy and peak intensity

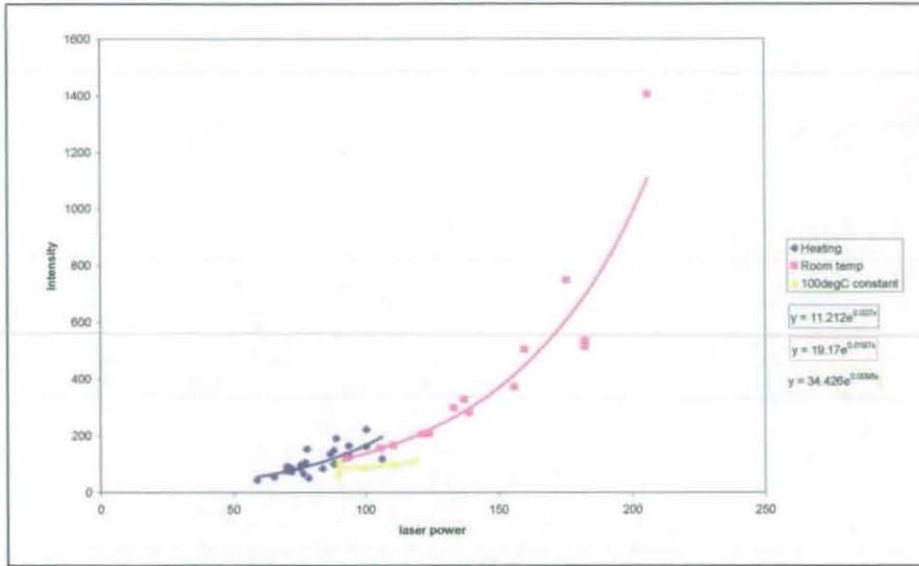


Figure 6-20 The affect of time and laser energy on the intensity of peak 2

When comparing the change in intensity with time it is noted that the readings taken at room temperature, and those that are taken while heating the powder give a very similar trend, Figure 6-21. As laser intensity decreases with time, Figure 6-17, this shows that the change in intensity noted with temperature is a factor due to the intensity of the laser rather than the affect of heating the material. The affect of time on intensity ratio can be seen in Figure 6-22, this shows that there is minimum difference between the room temperature ratio and that of the sample being heated from room temperature up to 250°C. It is therefore considered that the peak intensity or ratio of peak intensity cannot be used reliably for temperature measurement under these conditions as the laser energy has such a large affect on the peak intensity. If the laser energy was increased so that the coating is excited in the linear region of the energy luminescence relationship then the intensity relationship may become more stable and this can then be used for temperature measurement.

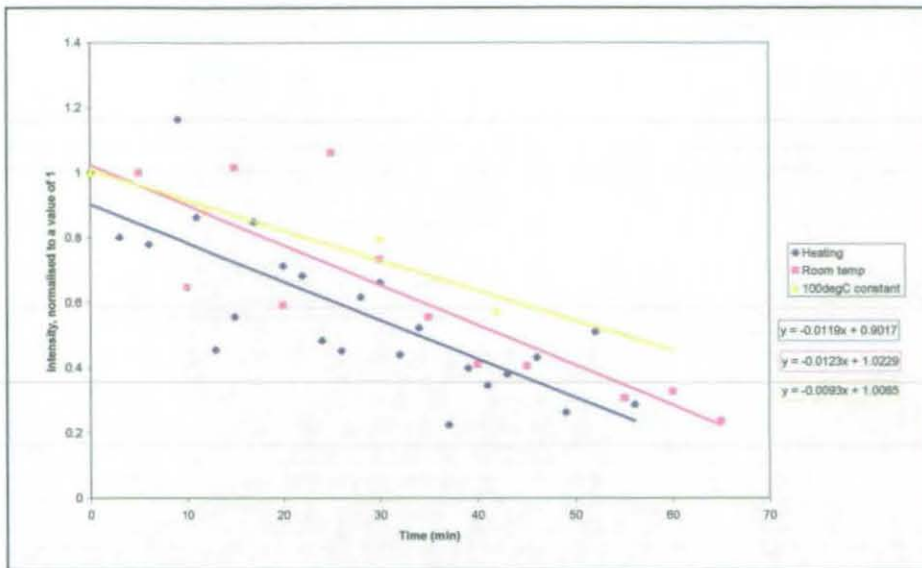


Figure 6-21 The affect of time and laser energy on the normalised intensity of peak 2

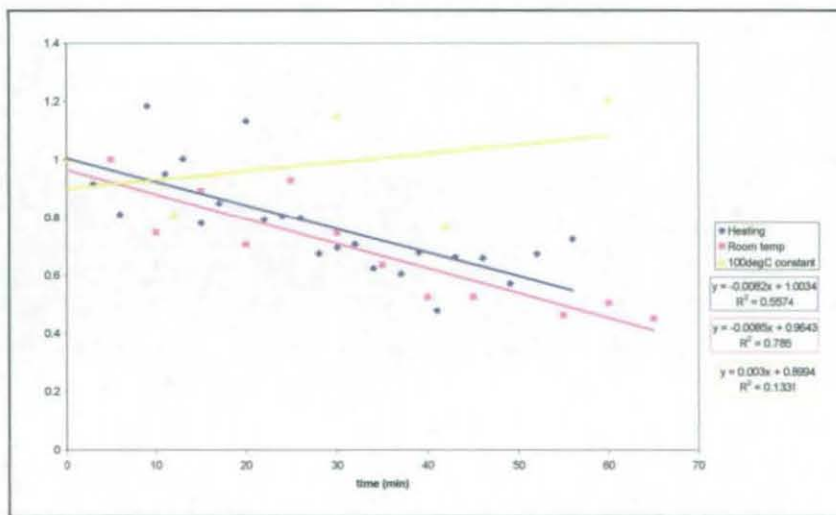


Figure 6-22 The affect of time and laser energy on the ratio of the intensities of peak 13 and peak 7.

Each possible relationship between the peaks were considered, from this data the best of the relationships between temperature and the peak positions and the peak separation can be seen in Table 6-12 and Table 6-13.

Peak	R ²
p13	0.90
p2	0.88
p4	0.88
p14	0.86
p8	0.75

Table 6-12 The relationship between temperature and the peak position.

Separation	R ²
p13-p2	0.94
p14-p2	0.92
p15-p2	0.91
p15-p10	0.90
p13-p532	0.89
p4-p2	0.89
p14-p9	0.87
p15-p9	0.87
p8-p2	0.87
p13-p11	0.86
p13-p10	0.85
p13-p9	0.85
p13-p4	0.84
p10-p8	0.83
p14-p11	0.83
p15-p11	0.82
p15-p4	0.82
p11-p8	0.81
p15-p14	0.81
p15-p532	0.80
p14-p13	0.78

Table 6-13 The relationship between temperature and the peak separation.

The equations produced were then changed to enable temperature to be determined from the peak position. These equations were then tested with the data recorded to determine the accuracy of the equations, this was undertaken using a macro^{XXI} written in Excel. Using this data to produce a relationship between the peak position or peak separation and temperature, shows that not all of these relationships can be used. Although the data shows a strong relationship when used in reverse to create a relationship between peak and temperature, large errors in the calculated temperature occurred. Of the relationships the ones which produced the strongest relationship between peak and temperature are shown in Table 6-14. These were chosen due their high percentage rate of temperature value falling within $\pm 10\%$ of the actual temperature reading.

Each of the relationships were studied for four temperature ranges room temperature to 300°C, room temperature to 100°C, 100°C to 200°C, and 200°C to 300°C. For each of the temperature ranges the accuracy of the relationship was considered by looking at the percentage of the predicted results fell within a certain percentage of the actual temperature reading, Table 6-14.

Peak	a ^{xxiii}	m ^{xxiii}	Temperature range	% of data within			
				4%	6%	8%	10%
P14-P2	17	0.0028	20°C to 100°C	45	62	77	81
			100°C to 200°C	45	65	78	86
			200°C to 300°C	23	35	46	55
P13-P2	2	0.0028	20°C to 300°C	37	49	56	61
			100°C to 200°C	59	76	85	91
P13 a	2	0.0022	20°C to 300°C	28	40	52	64
			100°C to 200°C	40	61	76	86
			200°C to 300°C	14	28	47	67
P13 b	2	0.0020	20°C to 300°C	39	50	59	63
			100°C to 200°C	50	69	83	88
P13 c	-5	0.0025	100°C to 200°C	30	50	64	71
			200°C to 300°C	50	64	76	80

Table 6-14 The relationship between peak and temperature.

The equation used to determine temperature from the spectrum was of the following form.

$$T = \left(\frac{100 + a}{100 \times m} \right) \times (P - Pref + (m \times Tref))$$

Equation 6-3

where;

a = constant

m = slope

P = Peak value, position or separation

Pref = Peak value at known temperature

Tref = Temperature at reference reading

The reference values calibrate the coating to enable the most accurate temperature reading to be obtained. The constant m represents the slope of the relationship between temperature and peak, and a is a calibration function, see Table 6-14 for the values, which were determined through curve fitting of the data. The reference values are determined by taking the peak position or peak separation value, Pref, at a known temperature, Tref.

^{xxiii} See Equation 6-3

6.5 Summary

This shows that Yttrium Oxysulphide Praseodymium doped can be used to measure temperature to an accuracy of $\pm 10\%$ given the current system. The use of the LabView peak find routine means that the accuracy of the peak position is determined by the resolution of the spectrometer used as this uses the pixel position. The use of a higher resolution spectrometer would increase the accuracy of the peak position value. This would in turn create a greater accuracy in the temperature measurement. The use of a curve fitting routine will also increase the accuracy of the determination of the peak position, thus increasing the accuracy of the temperature reading. A curve fitting routine can predict the shape of the peak between the given positions thus allowing the whole range of positions to be available rather than the pixel steps used in the peak find routine of LabView.

The frequency quadrupled Nd:YAG laser used had a very unreliable pulse energy due to problems with its electronic circuitry. Improvements to the system can be made by upgrading the laser to one which has a much more stable Q-switch and would give much more intense pulses than the one used in the experimentation. This caused problems at high temperatures as when a low intensity pulse the fluorescent signal achieved was not high enough above the background to be used. At high temperatures only about 1 in 6 pulses produced a fluorescent signal that was strong enough to be detected.

7 Spin Testing

The Ruby and Yttrium coating have been tested for fluorescence collection when spinning, as it is a concern that when spinning at high speeds there will not be enough fluorescence available for temperature measurement. To enable the laser to be pulsed in time with the spinning blade an electronic triggering system is required that will use a signal from the spinning wheel to trigger the laser and the detector.

Doppler shift is a technique which is used to measure vibration through the reflection of laser beams. It is a concern that this may also cause an affect on the fluorescence spectrum of the coating. The exact effect can be determined by experimentation and calibrated into the curve fitting technique. This should be able to be determined by taking stationary measurements of the spectrum at a controlled temperature and then rotating the compressor wheel, controlling the temperature, and taking measurements. This will also require an understanding of the pressure fluctuations that are expected around the compressor wheel during spinning.

7.1 High speed detection

At speeds of 79,000rpm the edge of the compressor wheel will move a distance of 4mm during laser excitation, the fluorescence delay period and the fluorescence decay period for $Y_2O_3S:Pr$. This is a distance that is well within the field of view^{xxiv} of the fibre, which is 6mm for a 2mm diameter fiber with a collection distance of 10mm. This field of view can increase further through the use of a collection optic. At lower speeds the edge of the compressor wheel will move even less thus the collection area of the fibre is even less of a concern.

Consider the time that it takes one spot to pass through the field of view of the collection fiber. The collection availability of the Ruby coating would be 2% when spinning at

^{xxiv} See Appendix 9.6.5 for calculation

speeds of 40,000rpm compared to that for the $Y_2O_3S:Pr$ coating which would have a fluorescence availability of 100%^{xxv}.

	Ruby plasma				$Y_2O_3S:Pr$ paint		
	532nm	max	532nm	max	266nm	max	
Input energy							
excitation wavelength	532	532	532	532	266	266	nm
input energy	0.0015	0.0015	6	6	6	6	mJ
photon energy	3.74E-19	3.74E-19	3.74E-19	3.74E-19	7.48E-19	7.48E-19	J
number of photons per pulse	4.01E+12	4.01E+12	1.60E+16	1.60E+16	8.02E+15	8.02E+15	
Volume							
Molecular weight	257.95	257.95	257.95	257.95	382.784	382.784	
molecules per gram	2.33E+21	2.33E+21	2.33E+21	2.33E+21	1.57E+21	1.57E+21	
density	3.99	3.99	3.99	3.99	4.1	4.1	g/cm ³
molecules per cm ³	9.31E+21	9.31E+21	9.31E+21	9.31E+21	6.45E+21	6.45E+21	
length	0.01	0.01	0.01	0.01	0.01	0.01	cm
volume	0.0079	0.0079	0.0079	0.0079	0.0039	0.0039	cm ³
weight	0.0313	0.0313	0.0313	0.0313	0.0161	0.0161	g
number of molecules	7.31E+19	7.31E+19	7.31E+19	7.31E+19	2.53E+19	2.53E+19	
Absorption							
absorption coefficient ^{xxvi}	10000	250000	10000	250000	10000	250000	dm ³ /(mol*cm)
concentration	0.1215	0.1215	0.1215	0.1215	0.0421	0.0421	moles/liter
Absorption value	12.15	303.72	12.15	303.72	4.21	105.16	
absorption efficiency	1	1	1	1	0.9999378	1	
photons absorbed	4.01E+12	4.01E+12	1.60E+16	1.60E+16	8.02E+15	8.02E+15	
Emission							
Quantum efficiency	1	1	1	1	0.14	0.14	
photons emitted	4.01E+12	4.01E+12	1.60E+16	1.60E+16	1.12E+15	1.12E+15	
availability	0.02	0.02	0.02	0.02	1	1	
Photons available for collection	8.02E+10	8.02E+10	3.21E+14	3.21E+14	1.12E+15	1.12E+15	photons

Ratio of $Y_2O_3S:Pr$: Ruby output Given current experimental setup 13999.13
 assuming a laser energy input for Ruby the same as that 3.50
 being used for $Y_2O_3S:Pr$

Table 7-1 Energy calculation for Ruby and $Y_2O_3S:Pr$

The optical efficiency of the Ruby coating to that of the $Y_2O_3S:Pr$ coating has been considered, see Table 7-1. The amount of energy available on each pulse, the density and molecular weight and quantum efficiency of the materials. This showed that the Yttrium coating has the potential for 14,000 times more intensity being available for collection. This energy would be distributed between the numerous emission peaks of $Y_2O_3S:Pr$, rather than the two peaks of Ruby, so this would not be indicated by a peak intensity

^{xxv} See Appendix 9.6 Calculations for exact calculations

^{xxvi} 10,000 is the minimum absorption value possible, 250,000 is the maximum absorption value possible

increase of 14,000 times. This indicates that the $Y_2O_3S:Pr$ coating has much greater potential for use on high speed objects.

7.2 Ruby

The plasma coating was initially simulated spinning at 80,000rpm by spinning a disc over the coating. This showed that collecting the fluorescence from 260 pulses a strong fluorescence signal can be achieved. This was then tested at a high speed test facility at Holset Engineering which proved to be unsuccessful.

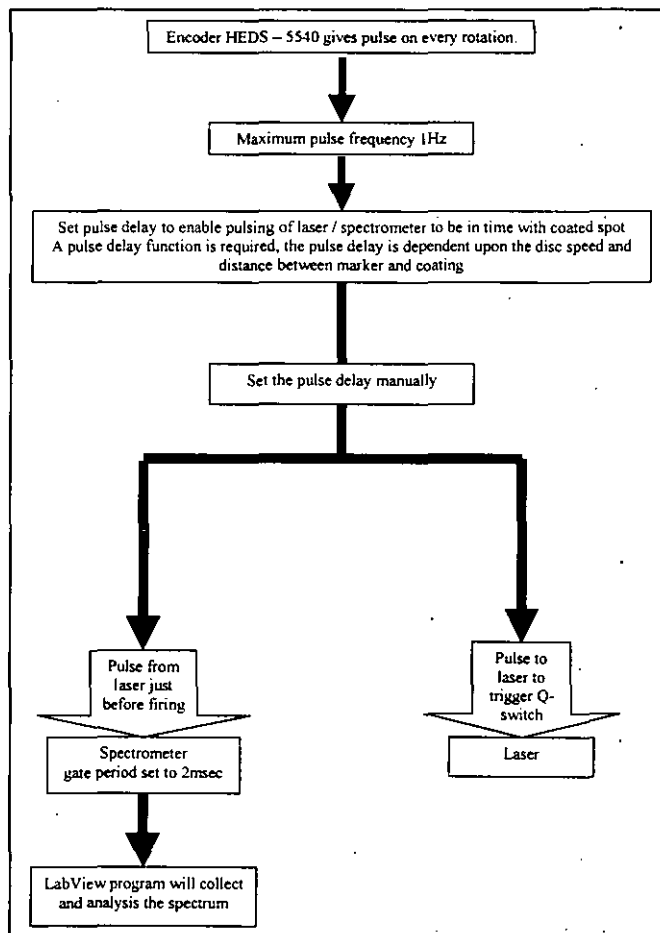


Figure 7-1 The electronic pulsing circuit for the Ruby system

The illumination of the coating with more than one laser pulse during one rotation has been considered to increase the intensity output. This is not possible because the minimum delay between pulses is not small enough to allow the coating to be excited twice, though this could be achieved with the use of two lasers. A higher energy laser

would also increase the intensity output, pulse energies of over 150mJ per pulse are easily available^{XXVII}.

When the object is spinning a pulse from the object is required to enable the pulsing of the laser and the spectrometer to be in time with the coating. A circuit flowchart showing the process required is shown in Figure 7-1.

7.2.1 *Simulation of 80,000rpm*

Initial consideration involved the simulation of the 80,000rpm speed by keeping the Ruby plasma coating stationary and spinning a slotted disc over the sample. The disc was spun at a speed of 5,000rpm, and has 16 slots placed in it to simulate the pulsing at 80,000rpm. The spectrum achieved was then divided by 16 to reduce the intensity to a value which would be seen at 16 times the speed.

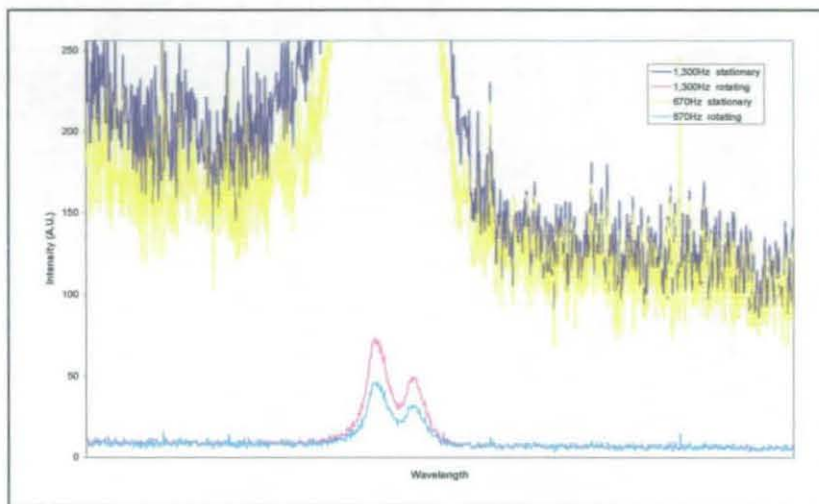


Figure 7-2 The simulation of spinning at 80,000rpm.

The data was collected over a period of 200msec, the reduction in intensity of the lower speed was due to the fewer number of laser pulses occurring during the gate period. The peak positions were not found to shift when spinning. This shows that Doppler shifting

^{XXVII} <http://www.bigskylaser.com/lablasers.html#yg980>

does not affect the peak position because the signal is generated from the spinning object rather than a reflection.

The ratio of the peak intensities also did not change with spinning. This shows that the Ruby plasma coating can be used reliably when rotating. It also indicates that there will be enough fluorescence intensity available for measurements to be taken when spinning at speeds between 40,000rpm and 80,000rpm.

This requires the fluorescence spectra to be summed over a time period of at least 200msec. A reduction in intensity of 98% is expected between the intensity of the peaks when stationary and when spinning. Considering the reduction in intensity is also due to temperature this would indicate that temperatures up to 200°C would be possible to be measured using this technique. An increase in the gate period would allow more fluorescence to be collected and thus higher temperatures can be reached.

7.2.2 *Low speed testing*

With a disc coated with a circular plasma coating and spinning at speeds between 3,000rpm and 12,600rpm a fluorescence signal could be detected when the laser is pulsed at a frequency of 2kHz. The circular coating meant that the laser did not have to be timed to the disc. The quality of the coating varied around the disc and this affected the strength of the signal, as this depended on whether a good or bad section of the coating was excited. The average of 10 laser pulses is shown in Figure 7-3. This shows that the quality of the coating has a big influence on the reduction in the intensity, as well as the speed.

Considering the reduction in the intensity due to heating the peaks will still be able to detected at 300°C at these speeds.

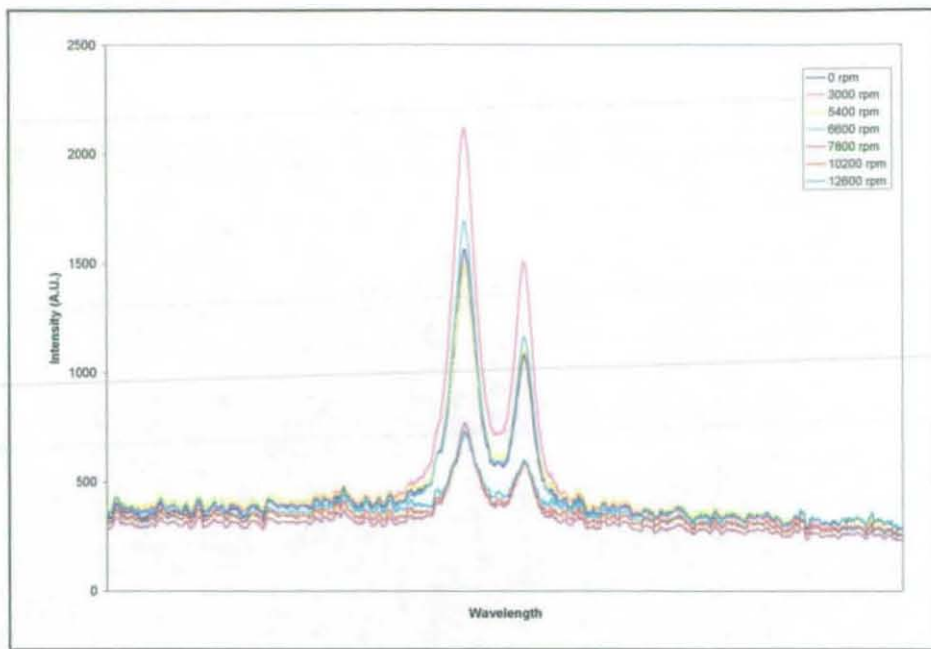


Figure 7-3 The affect of spinning on the fluorescence recorded.

7.2.3 *High speed test using Ruby coating*

Both the Ruby paint and the plasma coating have been tested for being able to withstand the conditions within the compressor. Both were able to withstand the conditions very well with little damage to the coatings. This test did not produce a successful result, as no fluorescence could be detected. There are a number of thoughts as to why this did not provide successful. These are discussed below.

The optical window became dirty during the testing and did not allow the light to pass through. This was tested for optical transmission after the high speed test before and after cleaning and it was found that this was not a concern.

The alignment of the optics was checked and it was shown that they are not located in the ideal position. This would mean that less intensity could be collected than from an ideally aligned system, showing that careful alignment is required. The use of a lens to collect the fluorescence and focus it into the fibre would mean that a larger diameter area can be viewed and such careful alignment would not be required.

There is not enough energy present to produce a strong enough signal that can be detected during the time the fluorescence passes in front of the detector. A higher energy pulse laser would increase the intensity emitted from the Ruby. A material with a much shorter decay time would also mean that more intensity would be present during the time in which the coating passes the detector.

The production of a pulse from the spinning compressor wheel was done by Holset Engineering, they were unable to tell us the time between the triggering pulse obtained from the wheel and the passing of the coating. It was therefore not certain if the laser pulse is actually hitting the required spot and therefore not actually producing the fluorescence. The use of a high-speed video camera located in the test cell would enable this to be seen. This would require the use of a filter to remove the laser light to enable the fluorescence to be seen. An electronic circuit needs to be designed to enable the delay period between the trigger and the laser pulse to be set easily. This led to the design of our own system by our electronics workshop. This allowed us to collect a signal from the back of a spinning disc which is then used to trigger the firing of our laser and spectrometer. The time between receiving the signal and outputting a signal to the laser and spectrometer was set through changing the angle. This would then use the speed of the disc to determine the time delay.

This test produced unsuccessful results and showed that the long decay period of Ruby is not ideal for high speed rotation measurements. An increase in the intensity available for collection can be achieved through increasing the laser energy. Consideration of the absorption efficiency of Ruby showed that changing the excitation wavelength, and thus the absorption efficiency, would have little affect on the overall emission due to the high molecular concentration.

7.3 Yttrium Oxysulphide Praseodymium doped

Yttrium oxysulphide doped with Praseodymium has been chosen for its short decay period making it ideal for use at high speeds. At a speed of 80,000rpm and at a radius of 70mm the material will only travel 4mm during its decay period. The fluorescent spectrum has been successfully collected at speeds of 23,000rpm (380Hz) and temperatures of 160°C. It is shown that this technique, with this laser power, can be feasibly used both at temperatures up to 200°C and speeds of 80,000rpm. With an increase in the laser much faster speeds and higher temperatures could be achieved.

7.3.1 Experimental arrangement

This required the use of a Nd:YAG laser emitting at 266nm, a spectrometer, a LabView program to collect and analyse the spectrum from the spectrometer, and a router with a speed range of 9,000rpm to 28,000rpm which spins an aluminium disc of 140mm in diameter. A schematic of the experimental set up can be seen in Figure 7-4, and a photograph of the arrangement in Figure 7-5.

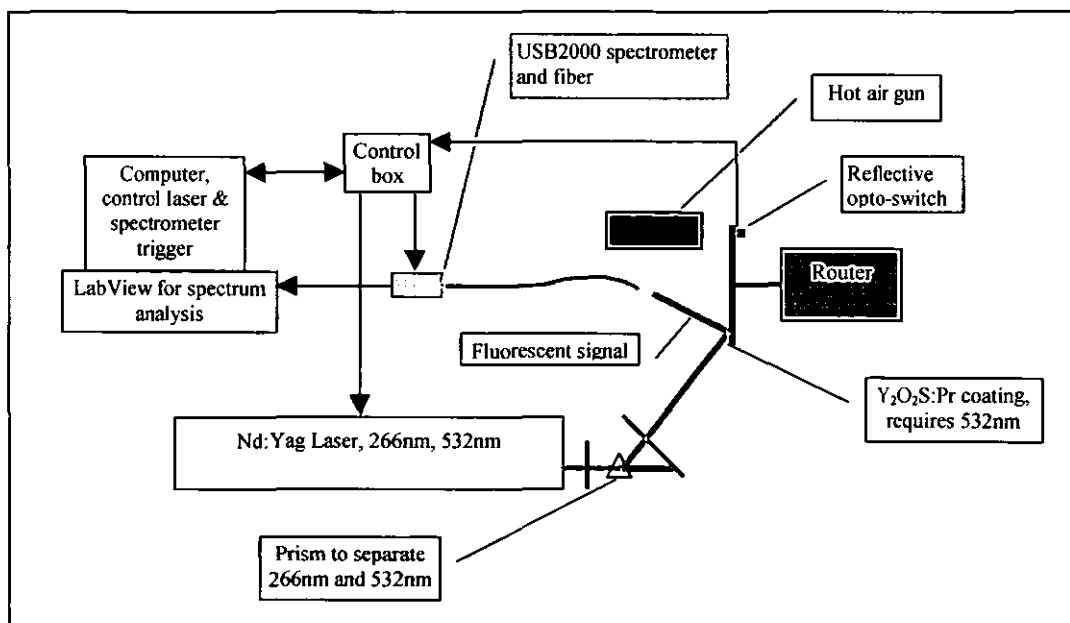


Figure 7-4 The experimental arrangement for measurements from a spinning, heated disc

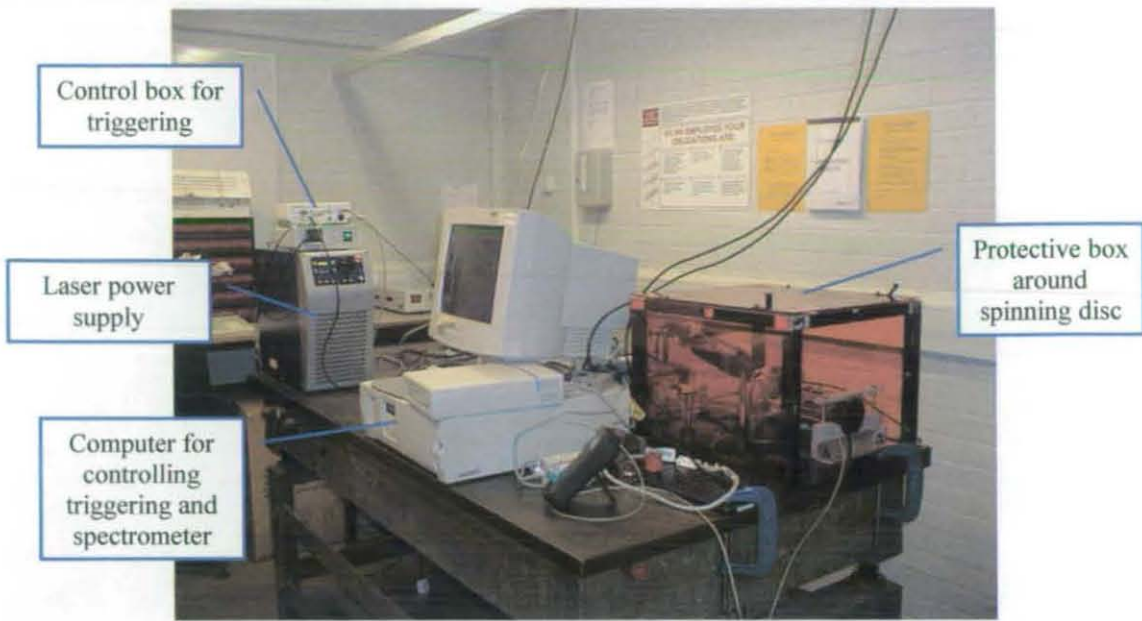


Figure 7-5 A general view of the rig

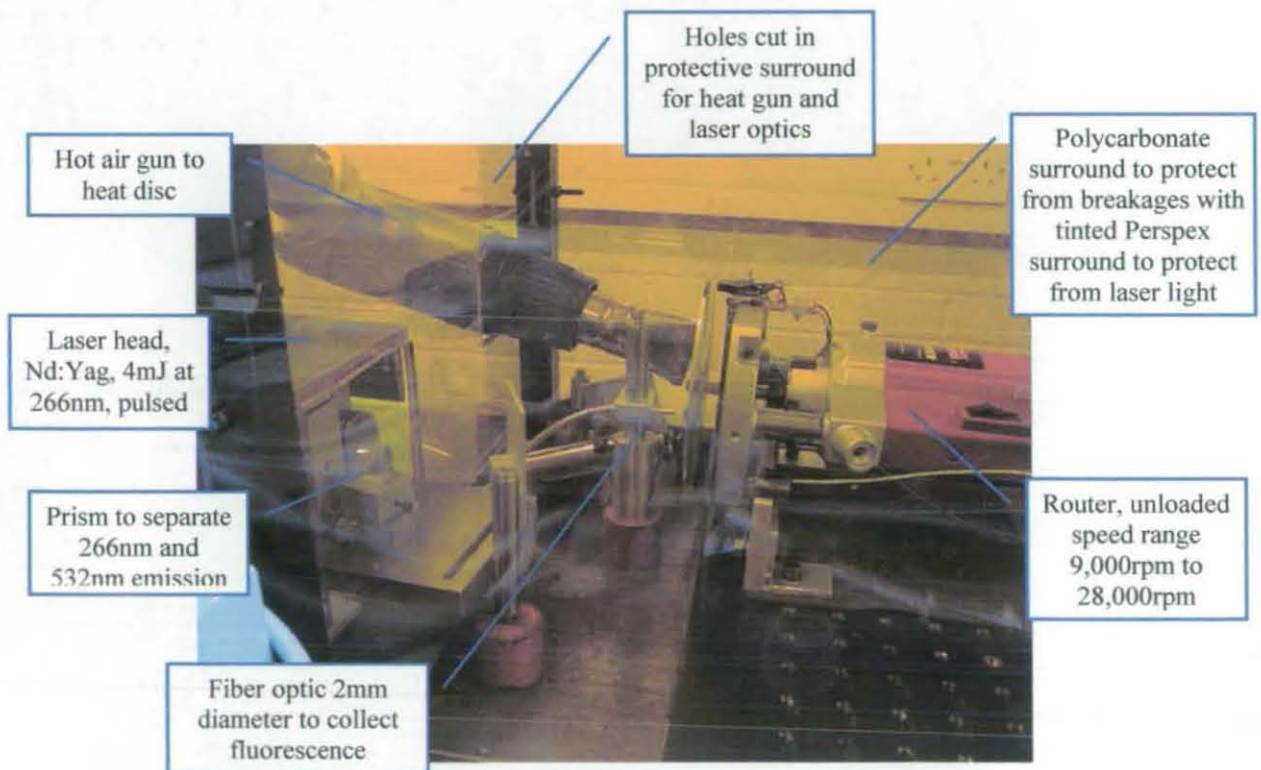


Figure 7-6 The experimental arrangement.

The experimental arrangement can be seen in Figure 7-6. The air flow from a hot air gun is directed at the disc, to heat the disc as it rotates, this enables temperatures of 160°C to be reached. The laser light is aimed directly at the disc to enable as high an energy pulse

as possible to excite the material as the laser pulse is only 4mJ. The fluorescent coating is a paint made from $Y_2O_3S:Pr$, powder, and Mbond 600, adhesive, with a 50% volume powder. The signal is collected by a spectrometer and analysed in real time.

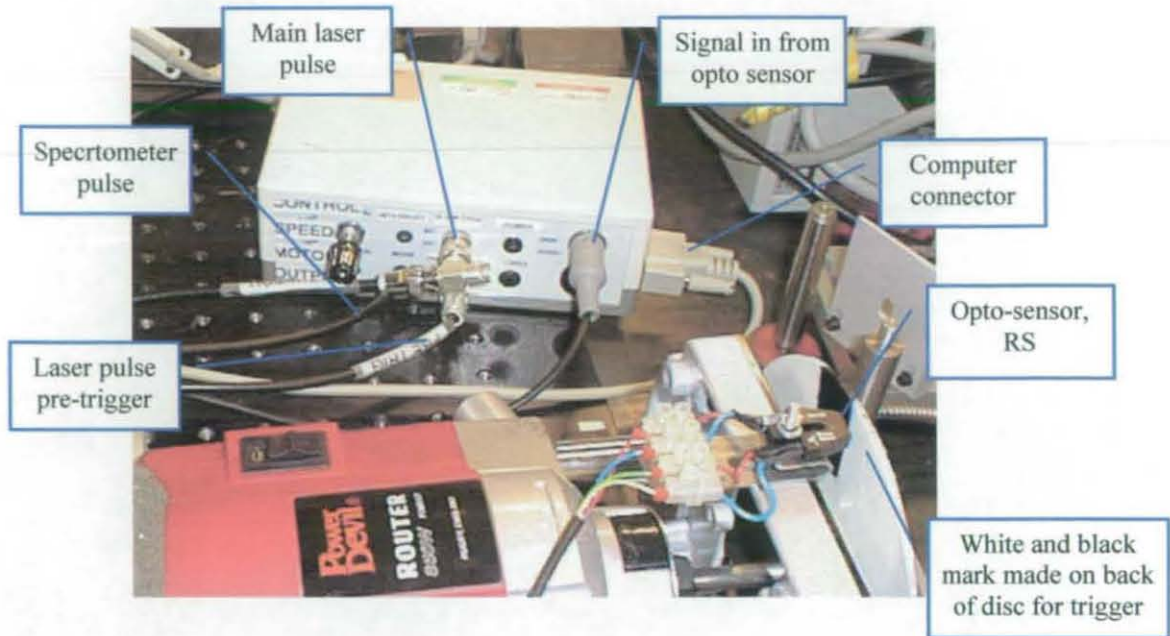


Figure 7-7 The triggering system

To control the pulsing of the laser and spectrometer in synchronisation with the spinning disc, an electronic circuit, and control program has been developed by our electronics workshop. A reflective opto-switch is used to detect a mark on the back of the disc, this signal is used to both trigger the laser and determine the speed of the disc. The angle between the trigger point and the coating can be altered to enable the laser to hit the correct spot on the disc and so it will automatically update the time between the receiving of the pulse and the triggering of the laser dependent upon speed. This also means that measurements can also be made at different radiuses. This set up can be seen in Figure 7-7.

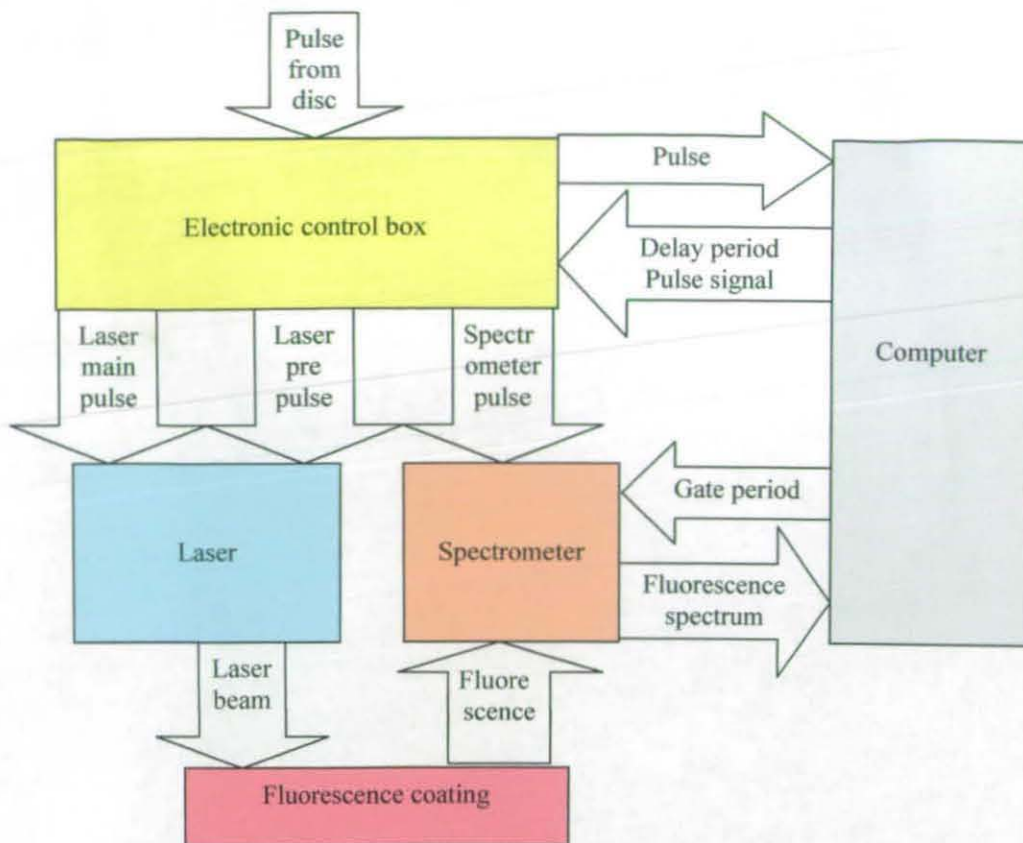


Figure 7-8 Diagram showing the triggering system

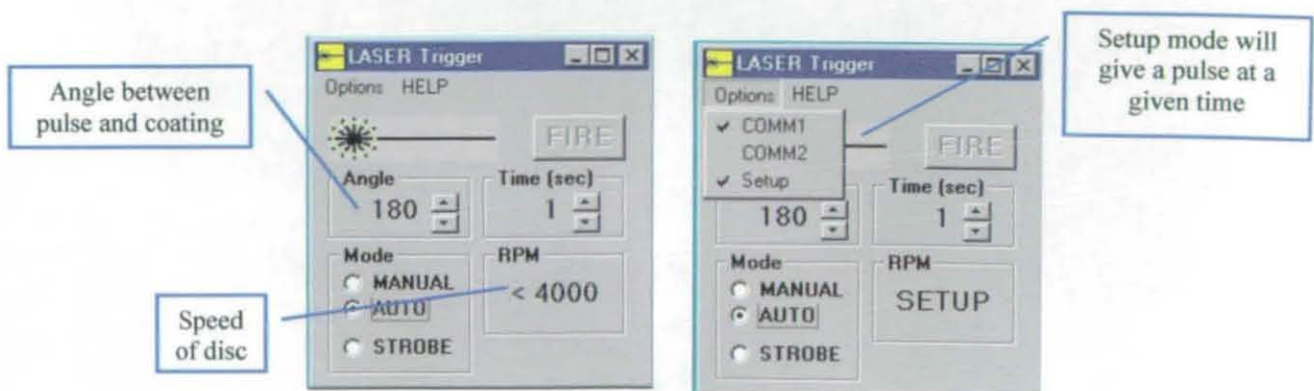


Figure 7-9 The triggering system control program

The fluorescence from the coating is collected using a 2mm diameter fiber optic and received by a USB2000 spectrometer, made by Ocean Optics. The spectrometer used has a spectral range of 350nm to 1000nm over 2048 pixels (0.32nm dispersion) and a resolution of 1nm. The spectrum is analysed by a LabView program to enable the temperature to be determined in real time. This program has been modified from a

standard LabView program supplied by Ocean Optics for collection of data from the spectrometer^{XXVIII}. The fluorescence obtained from the coating can be seen in the Figure 7-12.

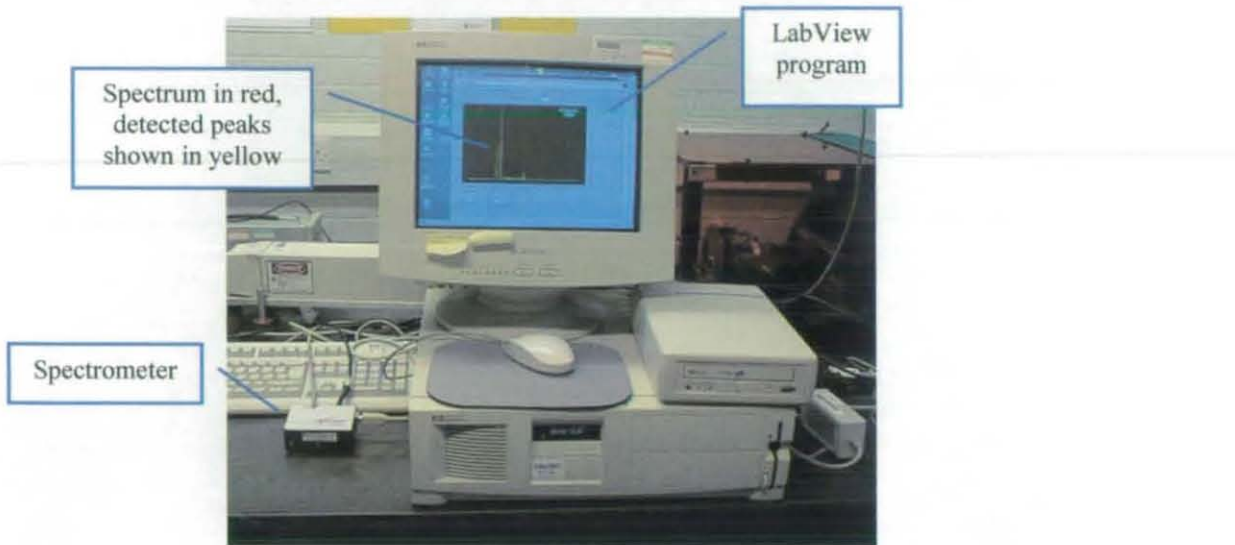


Figure 7-10 The spectrometer and software

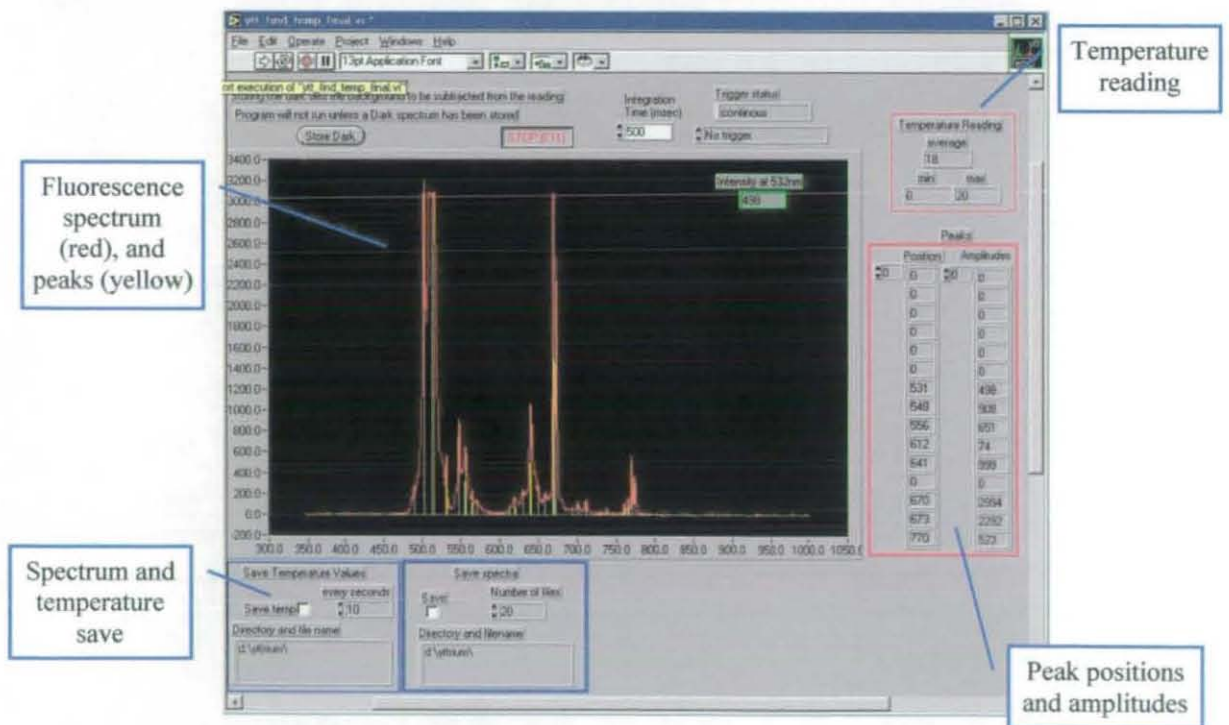


Figure 7-11 The LabView control program screen

^{XXVIII} See Appendix - 9.7 Programming

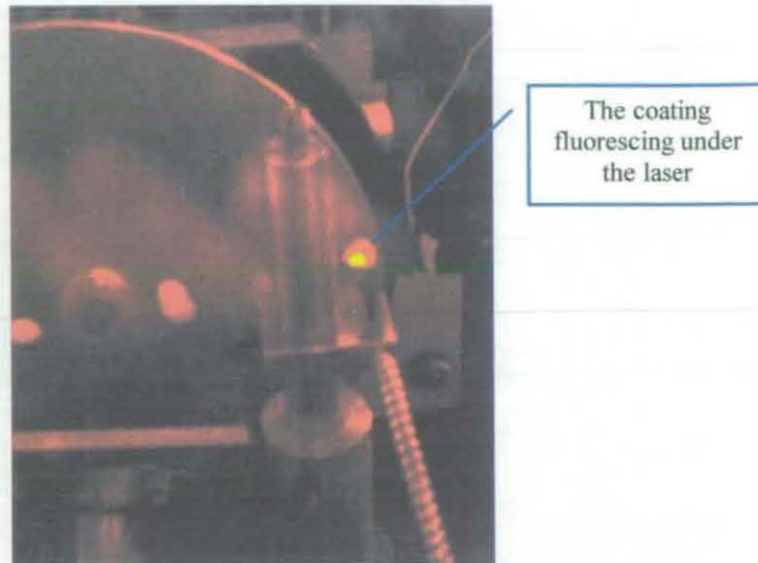


Figure 7-12 The $Y_2O_3S:Pr$ coating luminescing under the laser excitation

7.3.2 *Experimental results*

The disc has been at speeds of up to 23,000rpm (380Hz, or 170m/sec) which is the maximum speed obtainable from the router and it is seen that a strong fluorescent signal can still be achieved at this speed, Figure 7-13. It has been shown that the relationships; difference in position between peak 14 and peak 2, difference in position between peak 13 and peak 2, and position of peak 13 showed strong relationship with temperature. Given the relationship between intensity of peak 13 with speed and temperature it is estimated that speeds of up to 80,000rpm and temperatures of 200°C can be achieved, when considering peak 13. This intensity could be increase by the use of higher pulse energy, pulse energy of the laser used here is 4mJ, and stable beam position^{XXIX}.

^{XXIX} The output angle of the beam from the laser fluctuates due the problems with the ageing of the laser head meaning that the laser does not always hit all of the coating, nor is in best alignment for the fiber.

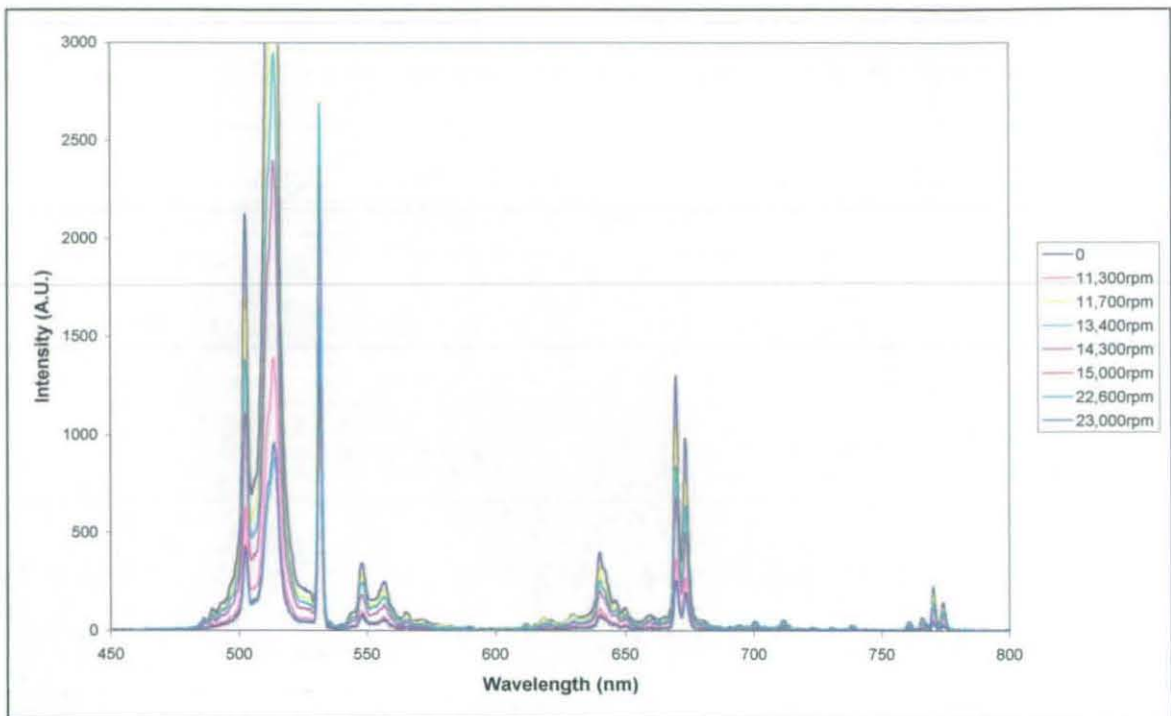


Figure 7-13 The affect of spinning on the spectrum, taken at room temperature.

	Rate of decrease with speed
Peak 2	$y = -0.0083x + 920.99$
Peak 4	$y = -0.0092x + 1928.3$
Peak 8	$y = -0.0003x + 147.97$
Peak 9	$y = -0.0005x + 110.72$
Peak 11	$y = -0.0018x + 179.16$
Peak 13	$y = -0.0046x + 548.61$
Peak 14	$y = -0.003x + 400.66$
Peak 15	$y = -0.0007x + 91.584$

Table 7-2 The decrease in peak intensity with speed, at 20°C, where x = speed

Considering the rate of decrease in intensity with temperature, Table 6-10, and that with speed, Table 7-2, its is seen that temperatures of 200°C can be measured at speeds of 80,000rpm given the current system, Figure 7-14 Table 7-3.

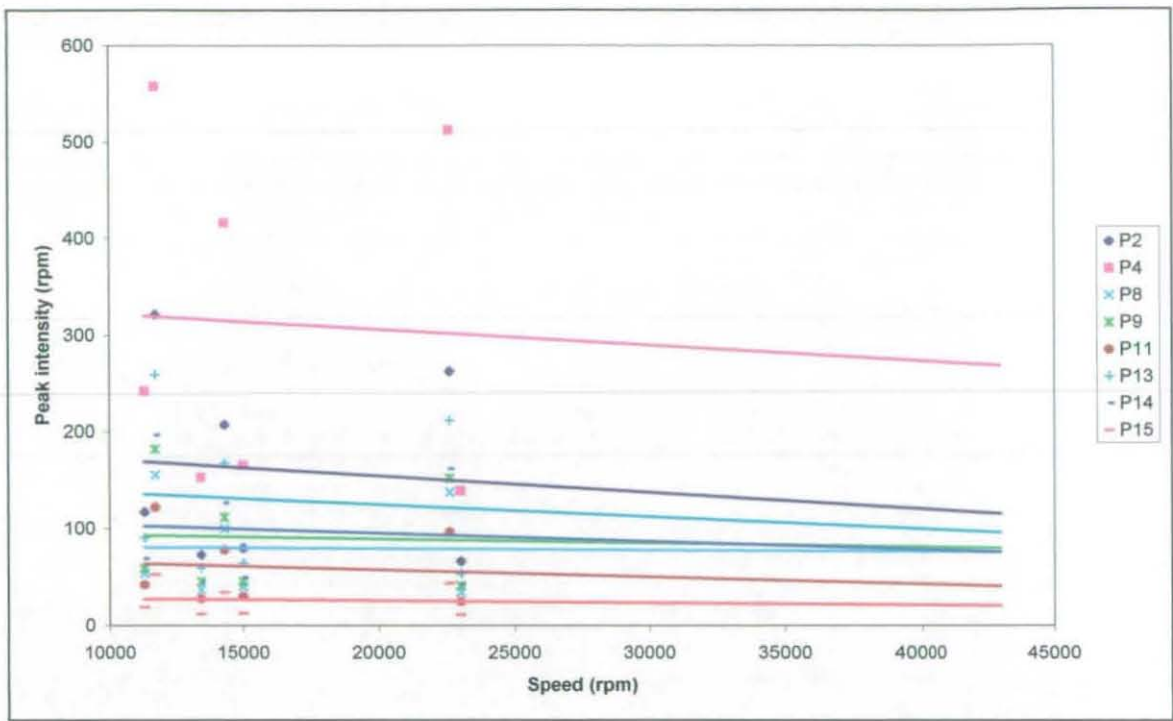


Figure 7-14 The decrease in peak intensities with speed, at 200°C, predicted to 40,000rpm.

	Rate of change of intensity with speed	Expected intensity at	
		40,000rpm	80,000rpm
Peak 2	$y = -0.0017x + 188.28$	120	52
Peak 4	$y = -0.0016x + 337.94$	273	209
Peak 8	$y = -0.0002x + 82.428$	76	70
Peak 9	$y = -0.0004x + 97.787$	81	64
Peak 11	$y = -0.0007x + 71.881$	43	14
Peak 13	$y = -0.0012x + 149.22$	100	50
Peak 14	$y = -0.0008x + 112.16$	78	44
Peak 15	$y = -0.0002x + 29.939$	21	12

Table 7-3 The expected peak heights, in intensity units as per Figure 7-13, at 200°C and given speeds.

It is seen that each of the peaks intensities decreases differently with speed. This indicates that although a decay time of $7\mu\text{sec}$ is quoted for the material each of the peaks has a different decay period. If the decay periods were all the same the decrease in intensity with speed would be expected to be the same. Peaks 2 and 4 have the largest decrease with speed and therefore it is thought that these would have the longest decay period of $7\mu\text{sec}$. The difference in the rate of change with temperature could also be due to the stimulation of the bands which is associated with each of the emission wavelengths, Figure 5-19.

The disc was spun at 11,000rpm and heated by the hot air gun. Using the relationships in Table 6-11 the temperature of the disc was determined, the relationships P2, P13, P13-P2, and P14-P2 all gave similar temperature readings, Figure 7-15. From this it determined that a temperature of 160°C was reached and that the relationships P2, P13, P13-P2, and P14-P2 could be used for measuring temperatures.

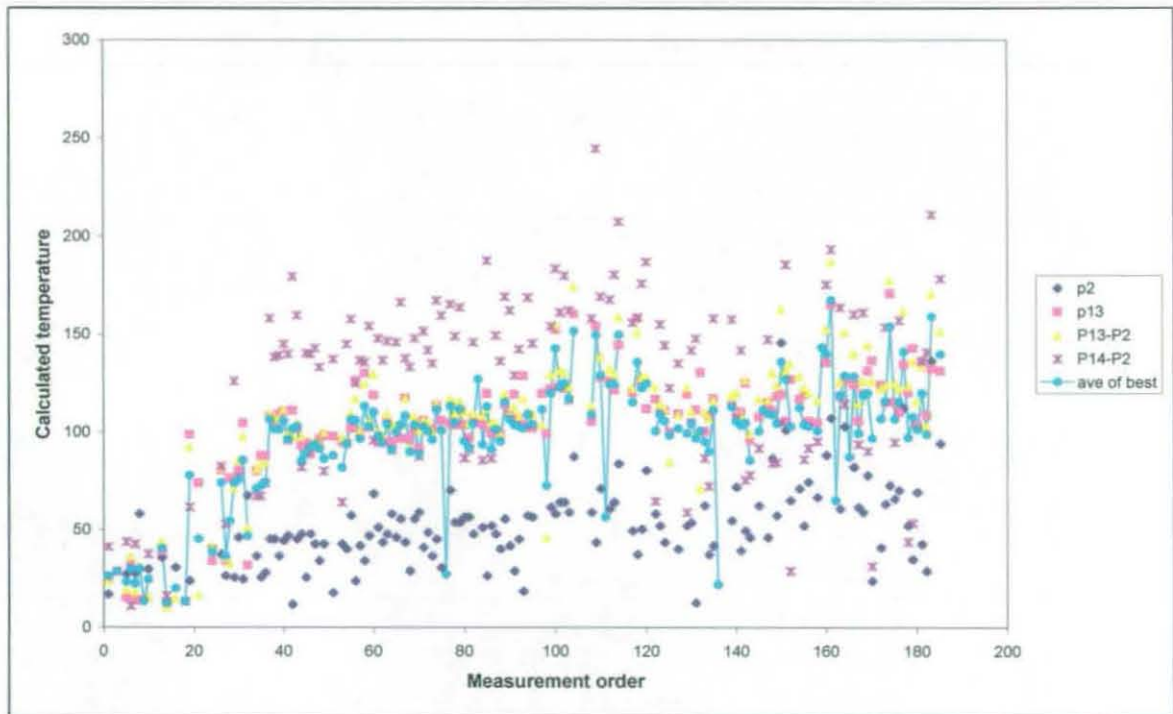


Figure 7-15 The measurement of temperature from a spinning disc.

7.3.3 Conclusion on spinning $Y_2O_3S:Pr$

It has been shown that a strong fluorescent signal can be collected from the $Y_2O_3S:Pr$ coating on the edge of a 140mm diameter disc spinning at speeds of up to 23,000rpm (380Hz), the equivalent to moving at 170m/sec. It is shown that the movement of the coating does not affect the spectrum obtained and that with the laser system used speeds of up to 80,000rpm and temperatures of 200°C should easily be capable of being measured.

The decrease in intensity with speed and temperature is different for each peak, see Table 6-10, Table 7-2, and Figure 7-14. This can be improved using a higher pulse energy as the present system is only emitting a 4mJ pulse which is exciting the material just above its threshold level.

It has been shown that using the 4mJ the coating is being excited just above its threshold, Figure 5-19, it is therefore possible to increase the laser energy and thus increase the fluorescent energy collected.

With further investigation into the analysis of the spectrum this material can be used for high speed remote temperature measurement.

7.4 Summary of spinning

Work undertaken with the Ruby coating showed that this had potential for measurements at high speed. Fluorescence measurements were taken at speeds of up to 12,600rpm where luminescence could be detected. Extrapolating the data from the spectrum showed that the luminescence peaks could be detected up to 300°C. At high speed testing, 40,000rpm and above a fluorescence spectrum could not be detected. There are a number of thoughts as to why this happened; the pulsing of the laser was not accurate enough to hit the coating, the fibres, the input power of the laser was not strong enough to create a strong fluorescence signal which could be detected at these speeds.

Yttrium oxysulphide doped with praseodymium shows good potential for high speed testing with its short decay period meaning that most of the fluorescence emitted from the material can be collected. It is shown that speeds of up to 80,000 rpm at 200°C can be achieved using this set up, but with increased laser energy, and stability of the laser output position this speed can be increased significantly. Due to equipment limitations speeds of up to 23,000rpm and temperatures of 160°C have been proved to be successfully measured from the edge of a 140mm diameter disc.

Yttrium oxysulphide praseodymium doped can be used for measuring temperatures of up to 200°C and at speeds greater than 80,000rpm. Further work is required to improve the accuracy of the measurement.

To be able to spin the disc faster and to increase the temperature of the disc when being spun, a redesign of the rig is required. The disc itself needs to be enclosed in a much smaller area so that the air temperature and, thus the disc temperature can be increased. A means of spinning the disc faster is required as the router has a top speed of 23,000rpm, when loaded with the disc.

8 Conclusion

The creation of a method of measuring temperature in the range 100°C to 250°C remotely from a compressor wheel spinning of speeds of up to 80,000rpm using thermoluminescent techniques required a number of points to be considered. They are the selection of a suitable thermoluminescent material, creation of a coating, the collection of the luminescent signal and the analysis of the luminescence to produce a reliable temperature relationship.

Looking at materials already in use as thermoluminescent sensor over 80 materials were considered^{xxx}. None proved to be an ideal candidate for this application. An ideal material would meet the following criteria;

- known to be temperature sensitive in required temperature range
- peak shape/position used for temperature measurement previously
- excited in the visible wavelength
- emit in the visible wavelength
- easy to obtain
- emits fluorescence at more than one wavelength
- emits fluorescence at two wavelengths to enable maximum detection
- has a short decay period

From the materials considered three materials showed possibility; Acridine Yellow, Ruby, and Sapphire which were considered further. Three other materials previously untested for temperature sensitivity were also tested these were; Brilliant Sulphoflavine, Panacryl Brilliant Flavine and Yttrium Oxysulphide Praseodymium doped ($Y_2O_3S:Pr$). The material $Y_2O_3S:Pr$ was of particular interest as this material had a short decay time of 7 μ sec which would allow most of the luminescence to be collected when spinning at 80,000rpm.

Previous work with Acridine Yellow has only studied the temperature sensitivity of the decay period. The work here has shown that the peak intensity, position, and width are all temperature sensitive, though as the material only emits one peak other materials were still considered.

^{xxx} See Appendix – 9.5 Luminescent Materials for a list of materials considered

Brilliant Sulphoflavine, previously untested for temperature sensitivity, showed that its luminescent spectrum could be used for temperature measurement as its peak position, intensity, and width were all related to temperature. Again as this material only emitted a single peak other materials were still considered.

Panacryl Brilliant Flavine, previously untested for temperature sensitivity, this material did not have such a strong relationship with temperature as Brilliant Sulphoflavine and Acridine Yellow so this material was not considered further.

The use of Sapphire previously has been using the decay time. The work undertaken here looked at the relationship of peak with temperature. Sapphire did not show a stable relationship with temperature as the peak intensity was seen to rise before falling when being heated from room temperature. It was therefore chosen not to continue with Sapphire.

Ruby has mainly been used for pressure sensitivity previously and a small amount of work has considered its temperature sensitivity, see Table 8-1. Using data analysis techniques the work here has improved the accuracy of the temperature prediction from the luminescent spectrum.

Undertaken by	Using	Temperature range	Accuracy
M ^c Cumber & Sturge	Linewidth Position shift	-186°C → 87°C	Not stated
Powell et al	Linewidth Position shift	-250°C → 187°C	±10%
Grattan et al 1987	Ratio of peaks	30°C → 170°C	±2%
Huang et al	Width	-253°C → 37°C	Not stated
Jmison & Imbush	Intensity	-163°C → -249°C	Not stated
Munro et al	Peak shape	20°C → 300°C	±10%
This work	Peak position	25°C → 270°C	±4%

Table 8-1 Temperature relationships with the luminescent spectrum of Ruby.

To enable a thin coating to be achieved the Ruby is required to be in a fine powder form, crushing and grinding of fluorescent materials can affect the crystal structure of the material due to the stress caused²⁵. Previous work has shown that Ruby emits strong fluorescence even when used in a crushed form¹²⁰. The work here has shown that at a

much smaller diameter of 10 μ m Ruby still emits a strong twin peak fluorescence that is temperature sensitive within the required range.

The most widely used technique for creating a fluorescent coating is mixing the luminescent material with an epoxy to create the paint. This technique is easy, quick and cheap to use and can also be used on difficult to reach areas. The maximum temperature that can be measured may be dependent upon the epoxy used. It is shown in this work that the epoxy can produce scattering, thus reducing the intensity of the luminescent signal. At high speeds the reduction in intensity could be significant enough to move the luminescent signal into the background noise thus not allowing this technique to be used for temperature measurement at high speeds.

This work shows that the paint technique although the easiest method to use is not the best. Plasma coating has shown to work well for the creation of coating for use at high speeds as this produced a strong fluorescent signal for Ruby. This signal could be detected at much higher speeds than the paint coating, it also produced a much more stable emission that produced a much more reliable temperature sensor. Although the coating techniques used created strong luminescent signals Ruby proved to be unsuccessful at high speed spinning tests, this was due to its long decay period and as such a material with a shorter decay period was sought.

Praseodymium doped Yttrium oxysulphide has not been considered for temperature measurement previously, though it has been noted by Okuno et al ¹²¹ that its peak width is affected by temperature. The reason why this material has been chosen for temperature measurement is its short pulse length, 7 μ sec, enabling the whole of the fluorescence to be collected during one pass. Y₂O₃S:Pr shows a strong relationship with temperature in particular its peak separation, which was also shown to be very reliable between coatings and after continuous heating and cooling.

The decay time of Y₂O₃S:Pr as well as all the combinations of peak separation, ratio of peak intensities have been considered for temperature sensitivity. The decay time was found not to be sensitive to temperature for temperatures up to 100°C. From the emission spectrum it is shown that; Peak14–Peak2, Peak13–Peak2 and the position of Peak13 can be used to determine the temperature reliably.

It is determined that using the equations determined for $Y_2O_3S:Pr$ an accuracy of 10% can be achieved over the temperature range 20°C to 300°C. Within the temperature range 100°C to 200°C this accuracy increases to 8%.

The ratio of the intensities of the peaks initially showed to have great potential for temperature measurement. Further investigation showed that the intensity of the luminescent peaks were not all related to the input power of the laser in the same way which meant that the ratio was also dependent upon laser energy. The intensity ratio was also found to be affected by repeated heating and cooling when the material is mixed in to Mbond 600 to create a paint.

A $Y_2O_3S:Pr$ coating has been spun at speeds of up to 23,000rpm, and at temperatures of up to 160°C. No change in the spectrum was noted due to the spinning of the coating. This work gave an indication that speeds of up to 60,000rpm at 300°C could be reached with the current set up. The pulse energy used of 4mJ is exciting the $Y_2O_3S:Pr$ coating just above its threshold limit. Increasing the pulse energy, would enable faster speeds to be obtained, possibly higher temperatures and more stable peak intensities of the fluorescence.

A LabView program has been written using the temperature relationships determined for $Y_2O_3S:Pr$ to enable a temperature reading to be made in real time. An electronic circuit and control program has been developed by the electronics workshop to enable pulses to be obtained from a mark on the back of a spinning disc at speeds of up to 100,000rpm. This circuit triggers both the laser and the spectrometer enables the offset between trigger and laser pulse to be set. The LabView receives the spectrum from the spectrometer, determines the peak positions and peak intensities and then uses this information to create a temperature reading. The program also enable the temperature readings and the spectrum to be saved.

8.1 Further Work

Although Praseodymium doped Yttrium Oxysulphide meets many of the criteria for an ideal material, it emits at many wavelengths meaning the peaks used for temperature determination. Which means that it is not as efficient as it could be and the emission energy is spread over many peaks rather than the ones used for temperature measurement.

To improve the accuracy of the temperature relationship from $Y_2O_3S:Pr$ a high resolution detector (or more than one) could be used to determine the peak position more accurately before data analysis. The use of a grating giving a 400 to 800nm range would half the wavelength range over one pixel, thus making the detection of the peak position much more accurate. The LabView values used were optimised for the initial peak relationships, these need to be reconsidered which may also improve the detection of the peak positions and amplitudes. The intensity, and intensity ratios may also wish to be studied further to see if a reliable relationship with temperature can be determined, through data analysis and consideration of the laser intensity on each of the peaks. The use of a more stable and higher pulse energy laser would improve the consistency of the data obtained, thus improving the analysis of the data.

Consideration of other materials of similar decay time, but fewer emission lines would also be required as although $Y_2O_3S:Pr$ has shown potential a more suitable, material could be available, a list of possibilities are shown in Table 8-2 .

Material	Decay time	No of emission peaks	Type
$Y_2O_3S:Pr$	7 μ s	14	Rare earth
CsI:TI	5 μ s	2	Band gap
Anthracene	32ns	4	Organic
$YVO_4:Tm$	220 μ s	2	Rare earth
$BaMg_2Al_{16}O_{27}:Eu,Mn$	0.8 μ s	2	Band gap
$Zn_{0.4}Cd_{0.6}S:Ag$	80 μ s	2	Band gap
$Gd_2O_2S:pr,Ce,F$	7 μ s	10	Rare earth
$Gd_2O_2S:Pr$	7 μ s	6	Rare earth

Table 8-2 Other materials which maybe suitable for remote high speed temperature measurement

To enable higher speeds and higher temperature readings to be obtained the rig needs to be redesigned. The disc should be enclosed in a small insulated housing to enable the air temperature and thus the disc temperature to be increased. The method of spinning the disc should also be considered as the router can only obtain speeds of up to 23,000rpm.

The Mbond 600 coating worked well for the ruby coatings but with the $Y_2O_3S:Pr$ it was noted that the intensity of the spectrum began to decrease with repeated usage. The method of attachment of the $Y_2O_3S:Pr$ powder to the surface needs further consideration. Either in terms of the selection of a different adhesive, see Table 8-3, or by looking into other suitable coating techniques such as plasma coating, or sputtering techniques. The use of the plasma coating technique has shown great potential even without the correct coating equipment. This should therefore be considered further using the correct coating equipment to create consistent coatings. The techniques of pre-heating and post-heating also require further investigation for improvement of coating quality.

Adhesive	Company	Temperature range	Other properties
RTV382	Intek Adhesives Ltd	-55 → 260°C	40,000 hours
Thermasil	Intek Adhesives Ltd	-55 → 260°C	Thermally conductive
114	Envirograft	1400°C	
4460	Duralco	370°C	
TRTV-02	Saveguard	-25°C → 300°C	
IP1009	Indestructible paint Ltd	600°C	100 hours very smooth aluminium coating

Table 8-3 Possible adhesives for a luminescent paint

9 Appendix

9.1 Equipment specification

9.1.1 General

Item	Manufacture and model	Specification	
Glue	Measurements Group UK Ltd M-Bond 600	Max temperature	370°C
Router	Power Devil PDW5027	No load speed	9,000 to 28,000 rpm

9.1.2 For ruby experimentation

Item	Manufacture and model	Specification	
Laser	Laser Compact LCS-DTL-112QT	Wavelength	532nm used 1064nm also available
		Pulse energy	532nm >1μJ 1064nm >2μJ
		Repetition rate	external 0 to 2kHz internal 2kHz
		Pulse length	<15nsec
		Beam diameter	<1mm
Spectrometer	Solar T II S-3801	Wavelength range	200 to 600nm
		Diffraction grating	1200 grooves/mm 700nm blaze λ 40% efficiency
		Spectral resolution	0.1nm
		Entrance slit	10mm height 0 to 0.4mm width
Fibers	Laser 2000	Diameter	Fiber bundle 5mm diam
		NA	0.22

9.1.3 For $Y_2O_3S:Pr$ experimentation

Item	Manufacture and model	Specification	
Laser	Spectron	Wavelength	355nm used 532nm, 1064nm available
		Pulse energy	300mJ max 9mJ @ 355nm
		Repetition rate	1 to Hz
		Pulse length	6 – 9 nsec
		Beam diameter	5mm
		Wavelength range	350 to 850nm
Spectrometer	Avantes USB2000	Diffraction grating	600 lines/mm
		Spectral resolution	4.2 pixels 1.03nm
		Entrance slit	25 μ m
		Detector	Sony ILX511 CCD
		Intergration time	3msec to 60 sec
		Diameter	2mm
Fibers	Laser 2000	NA	0.22

9.2 Material Specification

	Aluminum	Ruby	Sapphire	Ytrium	Praseodymium	
Chemical formula	Al	Al ₂ O ₃ :Cr ³⁺	Al ₂ O ₃ :Cr ³⁺	Y	Pr	Y ₂ O ₃ S:Pr
Melting point	660°C 940°K	2320°K	2320°K	1800°K		
Specific heat	900 JK ⁻¹ kg ⁻¹ @25°C	750 JK ⁻¹ kg ⁻¹ @300°K	750 JK ⁻¹ kg ⁻¹ @ 300°K	300 JK ⁻¹ kg ⁻¹ @300°K	190 JK ⁻¹ kg ⁻¹ @300°K	
Thermal conductivity	237 Wm ⁻¹ K ⁻¹ @100°C	40 Wm ⁻¹ K ⁻¹ @300°K ^{xxxI}	40 Wm ⁻¹ K ⁻¹ @ 300°K	17 Wm ⁻¹ K ⁻¹	13 Wm ⁻¹ K ⁻¹	
Thermal expansion	25*10 ⁻⁶ K ⁻¹	5.4*10 ⁻⁶ K ⁻¹	5.4*10 ⁻⁶ K ⁻¹	10*10 ⁻⁶ K ⁻¹	56.7*10 ⁻⁶ K ⁻¹	
Density	2.7 g/cm ³	3.99 g/cm ³	3.99 g/cm ³	4472 kg/m ³		4.1 g/cm ³
Mohs hardness	2.8	9	9			
Young's Moduls	70 GPa	4400 Gpa @ 300°K	4400 GPa @ 300°K	64 GPa	37 GPa	
Tensile strength	Upto 195 MPa	190 MPa @300°K	180 MPa @300°K	Upto 455 MPa	110 MPa	
Refractive index		1.76 @ 0.65μm	1.76 @ 0.65μm			
Decay time		3.5msec				7μsec

^{xxxI} Different values are quoted for thermal expansion by different sources, below are some other quoted values

5.4*10⁻⁶ °K⁻¹ perpendicular to the c-axis, 6.2*10⁻⁶ K⁻¹ parallel to c-axis

-30°C to +70°C 7.1*10⁻⁶ °C⁻¹, 20°C to 3,00°C 8.3*10⁻⁶ °C⁻¹

9.3 Theory

9.3.1 Radiation

The movements in the electronic, molecular and atomic structure of a material give rise to the emission of energy in the form of electromagnetic radiation. The rate of emission is related to the internal energy and hence the temperature of the matter. The separation and amplitude of the emitted wavelengths are also temperature dependent. Emission can be reabsorbed within a body before it is actually emitted or internally reflected at the surface. A black body emits all of the radiation, this is given an emissivity value of unity.

Plank's Law, Equation 9-1, defines the rate of emission by a perfect emitter, a black body. The closer the emissivity is to the blackbody state and the higher the temperature the more accurate the measurement. Black body radiation is used for temperatures greater than 400°C though fluorescence based correction techniques can be used.

$$L_{\lambda} = \frac{C_1}{\lambda^5 \exp\left(\frac{C_2}{\lambda T}\right)}$$

Equation 9-1 Planks Law

where;

- L_{λ} = spectral radiance of the body
- λ = wavelength
- T = absolute temperature
- C_1 & C_2 are constants

9.3.2 Luminescence

Luminescence emission occurs through radiation energy being absorbed by the electrons of the solid. The electrons move from ground level state, G, to an excited state, F²⁵.

If the electron is trapped at a metastable state, M, it will stay there until it has gained enough energy to return to level F, this could be thermal or optical energy. It will then return to the ground level state as phosphorescence which is temperature dependent. As temperature increases from room temperature the intensity will initially increase as the electrons escape from the metastable state, but as this state becomes empty the intensity decreases as the temperature continues to rise.

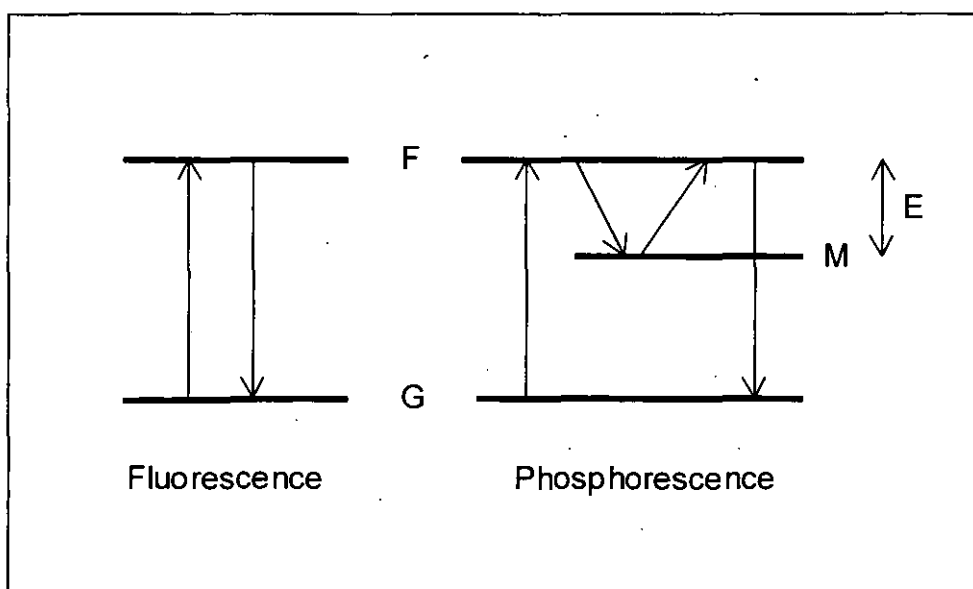


Figure 9-1 The difference in electron movement in fluorescence and phosphorescence

When a photon is absorbed a molecule from the ground state rises to the singlet state this is then released as fluorescence. A molecule can convert to an excited triplet state without the emission of radiation. When this energy is released it does so phosphorescence. It is possible that the singlet and triplet states can be deactivated through quenching. This can come in the form of thermal quenching or oxygen quenching. Which gives us the possibility of temperature and pressure measurement.

It is the crystal structure of the material that is effected by changes in temperature and pressure. The change in temperature and pressure cause strains within the structure, which in turn alter the energy levels of a particular ion³⁵. It is the variation in the energy of a given state that causes strain broadening. The stress occurs when the outside of the crystal is at a different temperature or pressure than the inside. The thermal stress increases as the thermal conductivity decreases¹²². As the temperature is increased the nonradiative transition rate increases, decreasing the fluorescence intensity.

Stresses can build up during crushing and grinding processes. At low temperatures the luminescence is independent of absorption. Changes in paint thickness, lighting and fluorophore concentration of the paint do not affect the fluorescence¹²³. Background emission from surroundings components can interfere with the luminescence of the material of interest. This often determines the lower limit of concentration.

It is possible that self-illumination of the luminescent coating can occur, this can lead to measurement errors. The magnitude of this error depends upon the geometry of the sample³⁴. This is of main concern when more than one surface is coated in fluorescent paint when they are in close proximity optically.

If monochromatic light is scattered from a substance very weak bands of light at different wavelengths can be seen. The separation between the side bands and the incident wavelength is dependent upon the material.

The angle of incidence of the emission wavelength onto a filter is important, because if this angle is increased the peak wavelength shifts to shorter wavelengths. An increase in temperature causes a shift to longer wavelengths, this shift is dependent upon temperature and the filter. This implies that care has to be taken in the arrangement and that the repeatability of a set of readings will not be able to be repeated accurately. The greatness of the affect of these changes on the final results needs to be considered.

To improve the luminescence reading it was noted by Hubner et al¹²⁴ that a base coat of white primer could be used. This increases the reflection of the emission from the object. The optical response time of a material on a moving target has to be less than the time required for the material to pass through the line of site.

For any given emitting state, both radiative and nonradiative transitions are possible. In the majority of cases as the temperature increases the nonradiative transition rate also increases, this decreases the fluorescence intensity⁴⁰.

Through comparison of different dopants within a base material it can be seen that it is the dopant that effect he fluorescencent spectrum¹²⁵.

The heating rate of a material can effect the fluorescence spectrum, with intensities decreasing and peaks shifting to higher wavelengths¹²⁵. Heating a sample and then leaving it to cool can also affect the spectrum. Samples that are heated and left to cool slowly have lower intensity than those that were heated and then quenched¹²⁵. There is an advantage to slow cooling in that it can enhance the low temperature signals. During slow cooling the defects and impurities have a tendency to stabilise into pairs or clusters. It is thought that in this case the material was at its optimum before quenching and therefore quenching did not have any affect. In general multiple ion sites reduce the efficiency of the dopant. When a sample is doped by more than one dopant it was found that when quenched it has a higher intensity than when left untreated or slowly cooled. This could imply that clustering was already present and the quenching has broken these clusters.

It is not only the UV, visible and infrared regions of the electromagnetic scale that can be used to stimulate phosphors. Electronic beams used in scanning electron microscopes have also been used. This has enable individual particles to be stimulated, by focusing the beam¹²⁶. A beam pulse of 1.5msec repeated every 50msec produced acceptable results, increasing the frequency of period was thought to produce electron beam heating of the particle.

9.3.3 Ruby

Ruby absorbs in both the green, at 555nm, and violet, at 410nm, areas of the spectrum. As it absorbs at the two different wavelengths it must be a 3-level system^{127,128}, with the terminal level being the ground state. It is very nearly an ideal 3-level system due to its

broad absorption bands, has a long lifetime, and its fluorescence quantum efficiency is very close to unity. The 3-level system means that the material is inefficient unless cooled below 10°C or by pumping the laser so hard that nearly all the electrons are in the upper lasing level. Both of these techniques work in by depopulating the ground state. At least half of the electrons have to be pumped to higher levels before fluorescence occurs⁵⁰. The 3-level energy system is as shown in Figure 9-2.

Emission occurs in both the red, at 694.3nm, 692.8nm, 688.8nm and 659.3nm, and blue bands, at 476.8nm, 475.3nm, and 468.7nm. The highest peaks occur at 694.3nm (R₁) and 692.8nm (R₂) and are the ones that have been used extensively for thermoluminescence. It is the Cr³⁺ ion that is responsible for the absorption. As the chromium concentration increases extra peaks are formed¹²⁹, as seen in Figure 9-4.

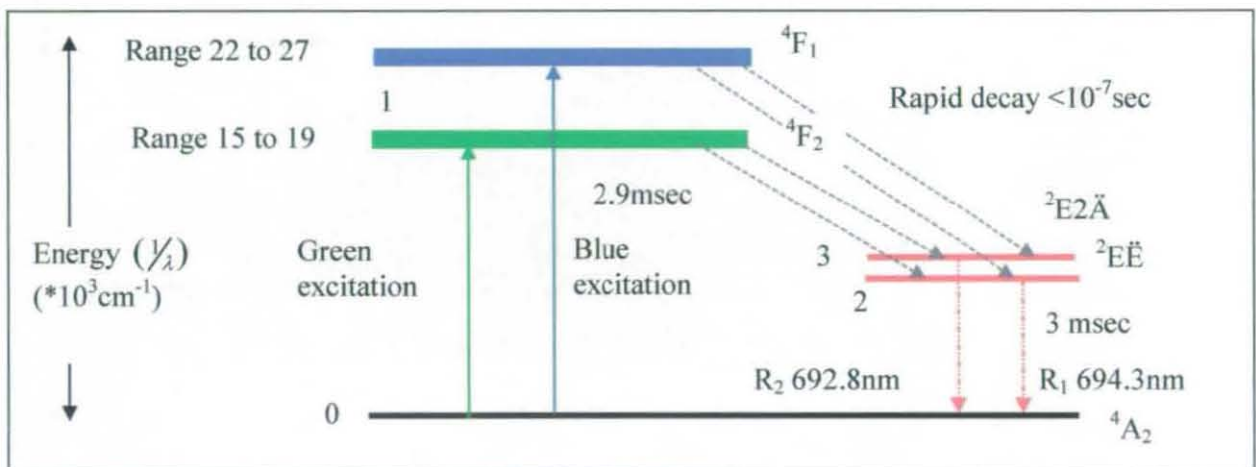


Figure 9-2 The energy-levels of ruby.

The absorption spectrum of ruby is shown in the lower diagram in Figure 9-3. The area of dark indicates the regions of light that has been absorbed by the ruby. It is interesting to note that absorption also occurs at around 700nm. This will be at the point of fluorescence as it is known that the wavelength at which a material fluoresce they also absorb.

Initially more than half the atoms in the ground state must be pumped into the upper laser level before any inversion is obtained. An electron is allowed to pass from one level to another by gaining or losing energy it is not allowed to have an amount of energy would put it between two levels. Green excitation takes the atoms into the $4F_2$ level while blue

excitation takes the atoms up to the 4F_1 level. From Figure 9-2 it can be seen that a minimum energy of $15,000\text{cm}^{-1}$ is required to move one photon from the ground state to the higher level when pumping with green light. As there are 10^{19} photons per cm^3 the total amount of energy that is required is 2.9Jcm^{-3} .^{XXXII} Atoms absorbed into the 4F_2 and 4F_1 bands will relax very rapidly with close to 100% quantum efficiency down to the 2E levels.

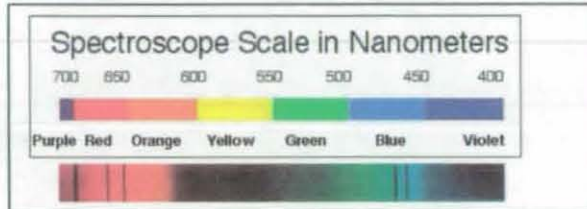


Figure 9-3 The absorption spectrum of Ruby¹³⁰.

An alternative explanation can be found in the paper by Maiman et al¹³¹. They stated that when the fluorescence lifetime was long compared to the excitation pulse the energy requirement per unit area is;

$$J = \frac{\left(1 + e^{-h\nu_p/kT}\right)^{h\nu_p}}{4\sigma_p}$$

Equation 9-2

Which for ruby gives $J \approx 1.67\text{joules/cm}^2$. Below the threshold energy the ruby will not fluoresce.

The quantum efficiency is defined as the ratio of the number of fluorescent photons emitted to the number of exciting photons absorbed. As the temperature increases the lifetime of the fluorescence decreases, this is due to thermal relaxation which will reduce the quantum efficiency to a maximum of 70%¹³². The fluorescence time at room temperature of ruby is 2.9msec for R_1 and 3msec for R_2 . This will decrease with temperature.

Previous work by other authors, such as Munro et al, has shown that the two peaks do not follow standard Gaussian or Lorentzian trends but a mixture of the two, producing what

^{XXXII} See Appendix - 9.6.2 Ruby energy calculations

is known as a Voigt function. Gaussian and Lorentzian functions can be used to represent the basic trend of the emission from ruby, though as the temperature increases the representation becomes less and less similar to the actual trend. The Gaussian trend is due to strain broadening due to the random crystal field distortion, and generally can be taken to be temperature independent. The Lorentzian contribution is from two phonon relaxation and thermal broadening.

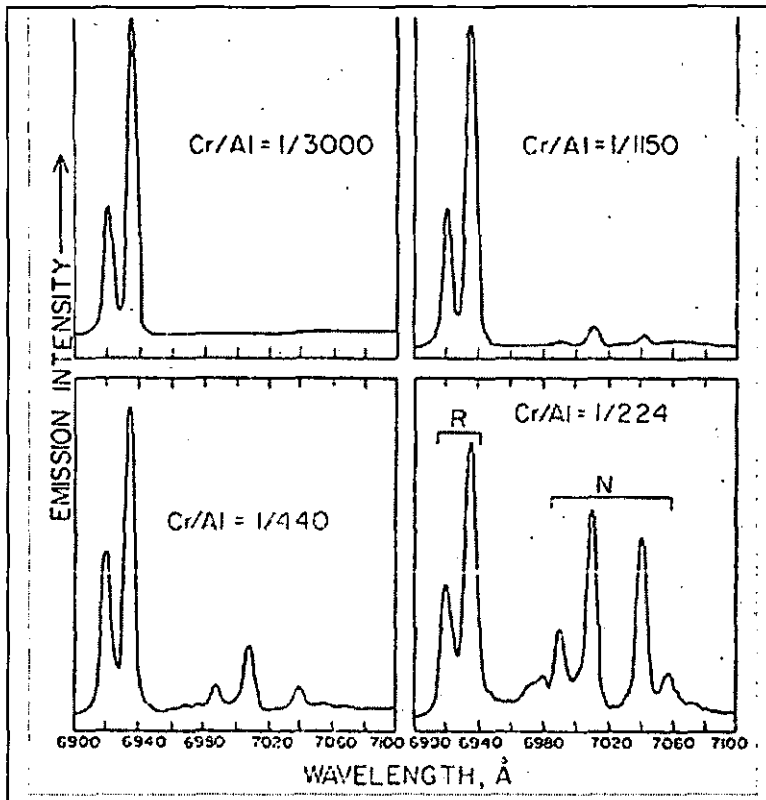


Figure 9-4 The emission spectrum of Ruby ¹³³

9.4 Coatings

9.4.1 Safety

The use of powders has many regulations that need to be considered. The main points to consider are with the dust produced¹³⁴. Protection against dust inhalation and contact with the skin, as it can cause skin dermatitis, is required. The systems used require regular cleaning to reduce the amount of dust in the atmosphere, stop blockages and

prevent a dust explosion. A dust explosion will occur when the concentration of the dust in air falls within the explosive limits when there is a source of ignition.

9.4.2 Plasma coatings

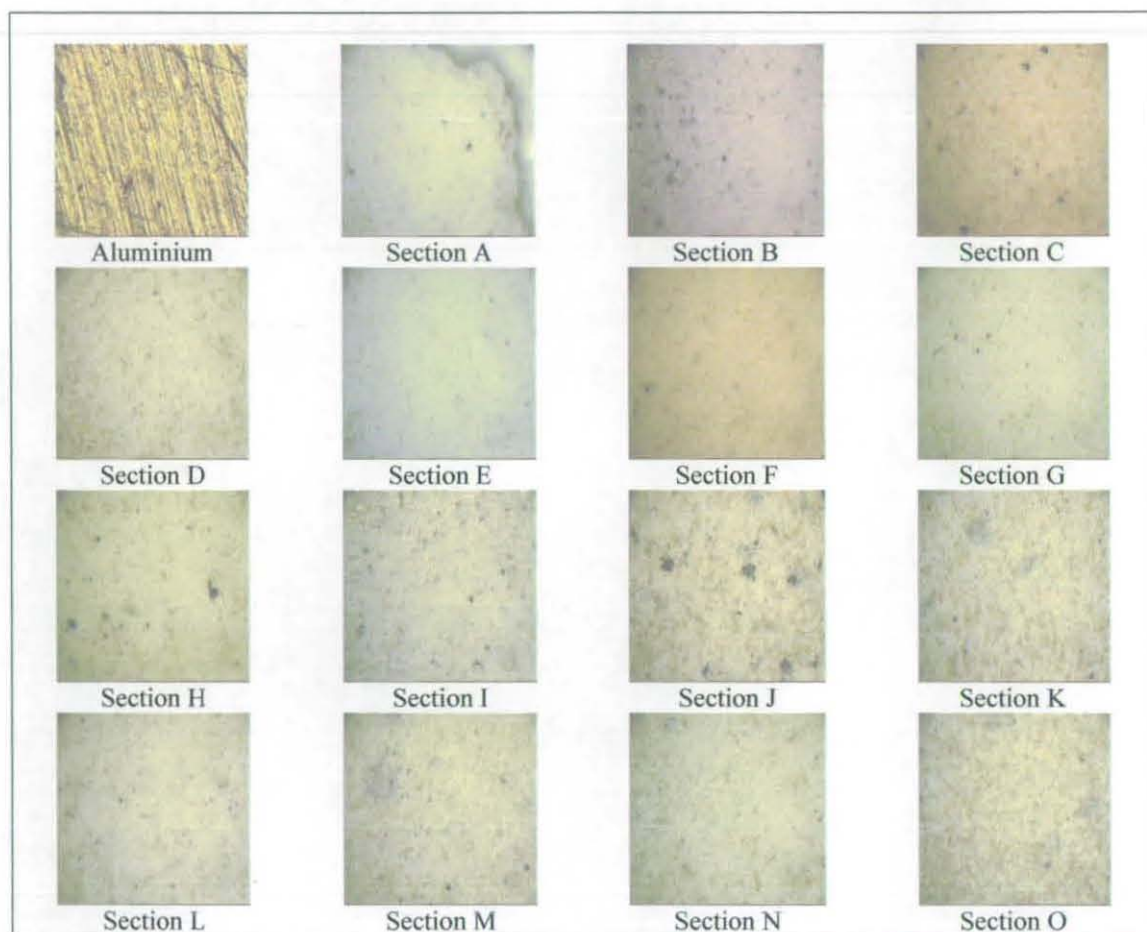


Figure 9-5 The difference in the quality of the coatings around the disc. At 10x magnification.

9.5 Luminescent Materials

Material	Technique	Temp (°C) & pressure range	Accuracy	How used	Decay time @ room temp	Excitation wavelength	Emission wavelength	Binder	Ref
Acridine yellow	decay time	-70 → 23°C	2%			Xenon, 75nm band center 410nm	>550nm		21
Acridine yellow	intensity	-50 → 50°C	4.5%			Xenon, 75nm band center 410nm	500nm, 580nm		21
Acridine yellow	intensity					Xenon, 75nm band center 410nm ~ 100mJ/cm ²			39
Alexandrite	Decay time	20 → 150°C	±2°C @ extremes ±1°C	Fiber optic temperature sensor		Green LED		EPOTECK epoxy	135
Alexandrite	Intensity decay time	20 → 700°C	0.3%/°C ⁻¹ @ 300°C			380 – 680nm	685nm		
Alexandrite	Lifetime	20 → 700°C				669nm Absorption range 380 → 680nm			136
Au-passivated porous silicon (ps)						325nm He-Cd laser	Red photoluminescence 1.9eV		137
BaClF:Sm ²⁺	decay time	25 → 200°C				417nm	687.7nm		138
BaMgAl ₁₀ O ₁₇ :Eu	Wavelength	20 → 280°C		Particle flow measurements		UV	Blue, 447nm		23
BTBP	Wavelength Intensity	15 → 70°C	±2°C			480nm	490→545nm 490→530nm		139
CaSO ₄ :Dy	Intensity	25°C → 400°C	±8°C			532nm ~130mJ/pulse 266nm ~20mJ/pulse	480nm 580nm		140
CaSO ₄ :Dy:Tm	Intensity	25°C → 400°C	±8°C			532nm ~130mJ/pulse 266nm ~20mJ/pulse	340nm 360nm 455nm 480nm 580nm		140
CaSO ₄ :Tm	Intensity	25°C → 400°C	±8°C			532nm ~130mJ/pulse 266nm ~20mJ/pulse	340nm 360nm 455nm		140
CdS single crystals	Absorption change Intensity	27°C	±0.3°C			514.5nm 520.8nm 530.9nm			141
Cerium							Blue		142

Material	Technique	Temp (°C) & pressure range	Accuracy	How used	Decay time @ room temp	Excitation wavelength	Emission wavelength	Binder	Ref
Chlorpromazine sulphoxide	Absorption Intensity	5 → 45				335nm	380nm		143
Chlorpromazine sulphoxide	Absorption Intensity	5 → 45				335nm	380nm		144
Chlorpromazine sulphoxide	Absorption Intensity	5 → 45				335nm	380nm		145
Chromium						359.35nm 425.43nm	278.1nm, 298.6nm, 301.5nm, 357.9nm, 425.4nm, 427.5nm, 429.0nm		
CoS ₂		130kbar							146
Coumarin		20 → 100				UV		PMMA	42, 147
CuOEP		-180 → 20				480 → 515nm		GP-197	42, 148
dEuFOD	Phase shift	30 → 60°C	±1°C						149
DL-β-Phenylalanine	Absorption Intensity	5 → 45				258nm	284nm		143
DL-Tryptophan	Absorption Intensity	5 → 45				281nm	358nm		143
Dy:YAG	Intensity	27 → 1427°C		surface		355nm	Variable 467nm variable >237°C 514nm fixed 496nm		
Dy:YAG	Intensity ratio	27 → 1427°C					496nm constant 467nm 512nm Yellow		29
Dysprosium									142
Emetine hydrochloride	Absorption Intensity	5 → 45				282nm	318nm		143
Emetine hydrochloride	Absorption Intensity	5 → 45				282nm	318nm		145
Erbium							Infrared		142
Europium							Red		142
EuTTA		-20 → 80			500 μsec	350nm	612nm	Dope	42, 150
EuTTA		20°C → 50°C	±0.5						123
EuTTA		19°C → 50°C 55 → 150kpa	-2.2%/deg ⁻¹						151
EuTTA	Intensity		0.08°C		0.2 msec	365nm			152
EuTTA	Phase shift	30 → 60°C	±1°C	surface			620nm		149
FeS ₂		130kbar							146
Fluorescein sodium	Absorption Intensity	5 → 45				487nm	512nm		143

Material	Technique	Temp (°C) & pressure range	Accuracy	How used	Decay time @ room temp	Excitation wavelength	Emission wavelength	Binder	Ref
Ga						403.4nm	245 to 300nm		153
Ga		1877°C	±727°K						153
Gadolinium							UV		142
Guaiphenesium	Absorption Intensity	5 → 45				274nm	310nm		143
Guaiphenesium	Absorption Intensity	5 → 45				274nm	310nm		145
InAs/Al _{0.1} Ga _{0.9} As		10 → 290K					0.8 → 1.1µm		154
InAs/GaAs									155
La _{0.9} F _{0.1} :Dy ³⁺	Decay time, intensity	-70 → 60	±10.3°C	Spinning 2,000rpm					71
La ₂ O ₂ S:Eu		100 → 200			100 µsec	337nm	537nm		42, 156
La ₂ O ₂ S:Eu	Decay time	20 → 90C				337nm	514nm		74
La ₂ O ₂ S:Eu	Decay time	20 → 200				337nm	537nm		74
La ₂ O ₂ S:Eu	Decay time	100°C → 260°C		Turbine wheel Spinning 13,200rpm	0.02 → 0.12 msec	337nm	537nm		73
La ₂ O ₂ S:Eu	Decay time			Emission line with constant lifetime					40
La ₂ O ₂ S:Eu	Decay time	300°C	0.3°C	Spinning 700rpm					31
La ₂ O ₂ S:Eu ³⁺			±0.5°C	Spinning					71
La ₂ O ₂ S:Eu ³⁺	Intensity	19 → 60	±0.5%			355nm	512nm 620nm		34
La ₂ O ₂ S:Eu ³⁺	Intensity	24°C → 55°C	±1.2°C	Curved surface					8
Liquid crystal		-30°C → -20°C 20°C → 25°C							9
Liquid crystal				Spinning 7,500rpm					91
Liquid crystals		-30 → 200°C							9
L-Tyrosine	Absorption Intensity	5 → 45				275nm	304nm		143
LuPO ₄ :Dy(1%)Eu(2%)	Intensity, emission linewidth, decay time	20 → 350°C				353nm 390nm	453nm, 484nm, 575nm 484nm, 575nm, 595nm		52
Magnesium fluorogermanate	Decay time	-200 → 400°C	±1°C						22

Material	Technique	Temp (°C) & pressure range	Accuracy	How used	Decay time @ room temp	Excitation wavelength	Emission wavelength	Binder	Ref
Magnesium fluorogermanate activated with manganese $Mg_2(F)GeO_6:Mn$	Decay time	-200 → 450°C	±2°C	Surface		Electron beam from scanning electron microscope (SEM)	658nm	diluted adhesive solution	157
Magnesium fluorogermanate activated with tetravalent manganese	Decay time	-200°C → -400°C	±1°C	Environment, surface, remote		Blue		binder – water based silicates	22
M ^c Donnell Douglas TSP		-5 → 90				340 → 500nm	>500nm		42, 158
Mg, Ti TLD-100		74°C → 424°C							159
$Mg_2(F)GeO_6:Mn$	Decay time	450°C → 730°C		Turbine wheel Spinning 13,200rpm	3 msec	337nm	656nm		73
NASA-Ames (Uni of Washington) TSP		0 → 50				UV			42 160
Nd:YAG	Blackbody, fluorescence lifetime	900°C		Environment measurement		810nm	1064nm infrared		
Nd:Yag	Lifetime Blackbody	50 → 900°C	±3°C 100→600°C ±2°C 750→900°C ±1°C @ 850°C			810nm	1064nm	Cement	161
Ne(2p ³ 3s ³ P ₂)						588.2nm, Rh6G dye laser pumped with Ar ⁺ ion laser	616.4nm		162
Neodymium	Absorption	-60 → 200°C							20
NiS ₂		130kbar							146
NO				Turbine flow		225.786nm	240 → 300nm		163
NO	Wavelength shift	-123 → 22°C		Flame temperature measurement		225.9nm	225 → 330nm		164
OH				Turbine flow		284.458nm	306 → 340nm		165
Perylene		0 → 100			5 nsec	330 → 450nm	430 → 580nm	Dope	42, 148
Perylenedicarboximide		50 → 100				480 → 515nm		PMMA	42, 147
Phenol	Absorption Intensity	5 → 45				270nm	299nm		143
Phenol	Absorption Intensity	5 → 45				270nm	299nm		145

Material	Technique	Temp (°C) & pressure range	Accuracy	How used	Decay time @ room temp	Excitation wavelength	Emission wavelength	Binder	Ref
PtOEP&EuTTA		20 → 50°C 1 ~30psia							45
PtOEP&MgOEP		20 → 50°C 1 ~30psia							45
PtOEP&PtT(PEP) P		20 → 50°C 1 ~30psia							45
PtTFPP					20μsec	532nm			166
Pyronin B		50 → 100				460 → 580nm		PMMA	42, 147
Pyronin Y		0 → 100				460 → 580nm		Dope	42, 147
Quinine sulphate	Absorption Intensity	5 → 45				350nm	450nm		143
Radiation	Infrared	27 → 877		Two colour pulsed					12
Radiation	blackbody	1,227°C – 3,227°C							167
Radiation	blackbody		0.2-2°K						168
Radiation	infrared		±10°C						169
Rhodamine B		0 → 80			4 nsec	460 → 590nm	550 → 590nm	Dope	42, 170
Ru(bpy)		0 → 90			5 μsec	320nm, 452nm	588nm	Shellac	42, 150,
Ru(bpy)/Zeolite		-20 → 80				320nm, 452nm	588nm	Poly Vinyl Alcohol	42, 148
Ru(trpy)		-170 → -50				310nm, 475nm	620nm	GP-197	42, 147
Ru(trpy)/Zeolite		-180 → 80				310nm, 475nm	620nm	Poly Vinyl Alcohol	42, 148
Ruby					4.3 msec				50
Ruby		→ 156 Gpa							62
Ruby							Strongest 694.2nm 692.8nm Weakest 669.0nm 659.2nm Strong 476.5nm 475.0nm 468.5nm		171
Ruby		20 → 160	High temps ±0.04°C Low temps ±0.2°C						53
Ruby		20 → 170	155 → 160 ±0.04°C 40 → 45 +0.18°C						172
Ruby						Green LED			38

Material	Technique	Temp (°C) & pressure range	Accuracy	How used	Decay time @ room temp	Excitation wavelength	Emission wavelength	Binder	Ref
Ruby		263 → 27							57
Ruby					R ₁ =2.9 msec R ₂ =3 msec				173
Ruby					3 msec				131
Ruby	Curve fitting	20 → 300	5 → 10%						6
Ruby	Decay time intensity	40 → 100°C 100 → 200°C	±0.04°C ±0.2°C	Environment measurement		Green LED	695nm		
Ruby	Fluorescence decay	600°C		Environment measurement		Green LED	695nm		38
Ruby	Peak position	-180 → 210							56
Ruby	Peak position								174
Ruby	Peak separation	2 → 12GPa							175
Salicylic acid	Absorption Intensity	5 → 45				269nm	410nm		143
ScPO ₄ :Eu	Decay time	300 → 600		Found to have low fluorescence		355nm			81
Semiconductor	Absorption shift		0.1°C						176
Sm:YAG	Frequency shift	700°C 100kbar	±2.5kbar						86
Sr ₁ Al ₄ O ₂₃ :Eu	Wavelength	20 → 280°C		Particle flow measurements		UV	Green, 488nm		23
Terbium							Green		142
Various	Phase changing Melting point	38 → 13371	1%						177
Y ₂ O ₂ :Eu		510 → 1000			1.4msec	266nm	611nm		42, 178
Y ₂ O ₂ :Eu		700 → 1000				254nm (Hg)			76
Y ₂ O ₂ :Eu	Decay time	650 → 1200		Spinning 10,568rpm		355nm not as good as 467nm & 538nm	611nm		81
Y ₂ O ₂ S:Eu		60°C - 150							80
Y ₂ O ₂ S:Eu	Lifetime								84
Y ₂ O ₂ S:Tb	Decay time	250 → 550				337nm	545nm		74
Y ₂ O ₃ :Eu				Coating testing, turbine wheel					86
Y ₂ O ₃ :Eu	Decay time	500 → 930				337nm	612nm		74
Y ₂ O ₃ :Eu	Decay time	500 → 1,200		Flame environment Spinning 5Hz	497 μsec	337nm	611nm		82
Y ₂ O ₃ :Eu	Decay time	600 → 1,200		Coating testing, dopant ratios		325nm 355nm	611nm		78
Y ₂ O ₃ :Gd	Decay time	48 → 465				337nm			74

Material	Technique	Temp (°C) & pressure range	Accuracy	How used	Decay time @ room temp	Excitation wavelength	Emission wavelength	Binder	Ref
Yag:Tb				Coating testing, turbine wheel					87
YVO ₄ :Dy		290°C → 450		Turbine wheel Spinning 13,200rpm	0.02 → 0.15 msec	337nm	574nm		73
YVO ₄ :Eu							272nm broadband, 615nm		88
YVO ₄ :Eu	Decay time	387 → 527		Coating testing, turbine wheel		337nm	620nm		87
YVO ₄ :Eu	Decay time	500 → 700		Flame environment Spinning 5Hz	503 μsec	337nm	618nm		82
YVO ₄ :Eu	Decay time	300 → 600		Spinning 10,568rpm		355nm	618nm		81
ZnTPP						532nm 1.9mJ/pulse	550 → 700nm delayed fluorescence >730nm phosphorescence		29
ZnTPP:Cd:La									28
?		1,227 – 5,727°C							179
?		149 - 677°C	±4%	Spinning					73
?		-196 - -93°C		Turbine blades					83
?		-273 – 1,627°C							32
?		-50°C → 3,000°C	±0.1%						32
?			±15°C						180
?	Intensity ratio			spinning					43

9.6 Calculations

9.6.1 Thermodynamic calculations

The heating rate of the material can be determined²⁵ from Equation 9-3 below.

$$\Delta T = \beta d^2 c \frac{\rho}{k}$$

Equation 9-3

Where;

d = sample thickness

β = heating rate

k = thermal conductivity

ρ = density

9.6.2 Ruby energy calculations

Calculation for minimal input energy required to move one photon from the ground state;

$$E_s = hvN_2$$

It is known that;

$$N_2 = 10^{19} \text{ cm}^{-3}$$

$$hv = 2.9 \times 10^{-19} \text{ J}$$

Which gives;

$$E_s = 2.9 \text{ Jcm}^{-3}$$

9.6.3 *Ruby timing calculations*

Laser pulse length = 10nsec
Minimum time between pulses = 0.5msec
Delay period = 0.1msec
Fluorescence lifetime = 3.5msec
Fiber collection diameter = 5mm

9.6.3.1 *Running at 79,000rpm*

Speed at edge of wheel = 579,100mm/sec
Distance moved during laser pulse = 0.0058mm
Distance moved between laser pulses = 290mm
Distance moved during delay period = 0.058mm
Time available for fluorescence collection = 8.63×10^{-6} sec = 8.63 μ sec
% of available fluorescence collected during this time = 1%
Number of rotations during which fluorescence is still present = 5

9.6.3.2 *Running at 40,000rpm*

Speed at edge of wheel = 293,200mm/sec
Distance moved during laser pulse = 0.0029mm
Distance moved between pulses = 147mm
Distance moved during delay period = 0.029mm
Time available for fluorescence collection = 17.1×10^{-6} sec = 17.1 μ sec
% of available fluorescence collected during this time = 2%
Number of rotations during which fluorescence is still present = 3

9.6.4 *Y₂O₃S:Pr timing calculations*

Laser pulse length = 6nsec
Minimum time between pulses = 0.5msec
Delay period = 20psec
Fluorescence lifetime = 7 μ sec
Fiber collection diameter = 5mm

9.6.4.1 *Running at 79,000rpm*

Speed at edge of wheel = 579,100mm/sec

Distance moved during laser pulse = 0.0035mm

Distance moved between laser pulses = 290mm

Distance moved during delay period = 0.006mm

Time available for fluorescence collection = 8.63×10^{-6} sec = 8.63 μ sec

% of available fluorescence collected during this time = 100%

Number of rotations during which fluorescence is still present = 1

9.6.4.2 *Running at 40,000rpm*

Speed at edge of wheel = 293,200mm/sec

Distance moved during laser pulse = 0.0018mm

Distance moved between pulses = 147mm

Distance moved during delay period = 0.003mm

Time available for fluorescence collection = 17.1×10^{-6} sec = 17.1 μ sec

% of available fluorescence collected during this time = 100%

Number of rotations during which fluorescence is still present = 1

9.6.4.3 *$Y_2O_3S:Pr$ relationship*

$$Temp = \left[\left(\frac{x - Pref}{m} \right) + Tref \right] + \left[\frac{s}{100} \left[\left(\frac{x - Pref}{m} \right) + Tref \right] \right]$$

$$Temp = \left(\frac{100}{100} \right) \left[\left(\frac{x - Pref}{m} \right) + Tref \right] + \left(\frac{s}{100} \right) \left[\left(\frac{x - Pref}{m} \right) + Tref \right]$$

$$Temp = \left(\frac{100 + s}{100} \right) \left(\frac{x - Pref}{m} + Tref \right)$$

Equation 9-4

Where; s = constant for centring of error around zero
 x = peak position
 Pref = reference value (peak position, separation)
 Tref = reference temperature
 m = slope

9.6.5 Fiber optic

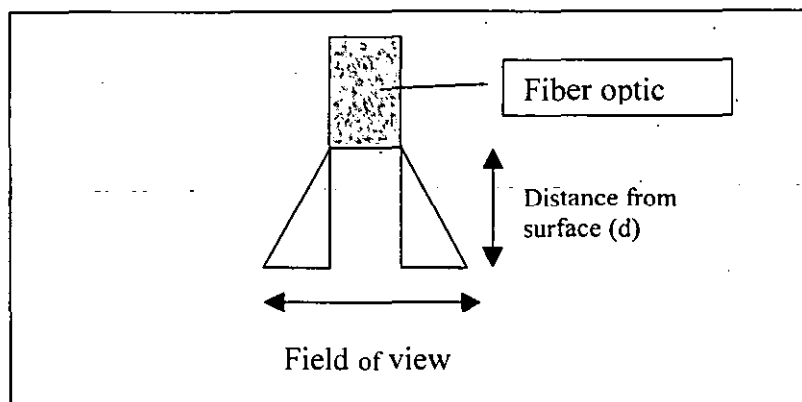


Figure 9-6 the calculation of the field of view

$$\text{field of view} = 2 \times d \tan \left(\sin^{-1} \left(\frac{\text{NA}}{n} \right) \right) + \text{diameter}$$

$$\begin{aligned} \text{NA} &= 0.22 \\ n &= 1 \end{aligned}$$

distance from surface (mm)	diameter (mm)		
	0.05	1	2
	field of view (mm)		
1	0.50	1.45	2.45
2	0.95	1.90	2.90
3	1.40	2.35	3.35
4	1.85	2.80	3.80
5	2.31	3.26	4.26
6	2.76	3.71	4.71
7	3.21	4.16	5.16
8	3.66	4.61	5.61
9	4.11	5.06	6.06
10	4.56	5.51	6.51

9.7 Programming

Sorting the LabView data into peaks and removing double peaks

This program was written in excel and was used to sort the peaks determined by LabView into the peaks of interest and redundant peaks. Sets of data with double peaks

within the peaks range are removed. The average of the peaks values for each temperature range are determined.

9.7.1 *Determining the reliability of the equations*

This program uses the equations determined to find the temperature from the given peak data. It removes data that is out of range, and then determines the error between the actual temperature and the determined temperature.

```

Sub Doall_sheets()

Dim count As Integer
Dim s_name As String
Dim c As Integer ' number of columns per set
Dim climit As Integer 'the maximum acceptable temperature reading
Dim plimit As Integer 'the maximum acceptable percentage range
Dim minwavelength As Integer
Dim maxwavelength As Integer
Dim maxseparation As Integer
Dim rowcounter As Integer
Dim columncount As Integer

'rowcounter is the number of rows down that the data is recorded on sheets ("data")
rowcounter = 1

c = 3
climit = 500
plimit = 500

Sheets("T50").Select
numpeaks = Range("d1") / 2
'clear the above threshold data
totalrows = Range("b1")
For y = 1 To totalrows
    For p = 1 To numpeaks
        If Range("b2").Offset(y, p + 15) > 3000 Then
            Range("b2").Offset(y, p + 15) = ""
            Range("b2").Offset(y, p) = ""
        End If
    Next p
Next y
'determine the maximum possible separation
maxseparation = Sheets("t50").Range("J1").Value
Sheets("Cp50").Select
' Range("b3").Select
' Selection.CurrentRegion.Select
' columncount = Selection.Columns.count - 1

```

```

' Range("b3").Resize(1, columncount).Select
' Selection.AutoFill Destination:=Range("b3").Resize(totalrows, columncount), Type:=xlFillDefault
' Call clear_nonwavelengths2(maxseparation) 'call the program to clear the sheet of junk
'Sheets("Ci50").Select
'Call clear_text 'call the program to clear the sheet of junk

Sheets("fit").Select
count = Range("d10").Value
Range("a5").Select
Selection.CurrentRegion.Select
hist = Selection.Rows.count + 2

For n = 1 To count
  Sheets("fit").Select
  Range("a5").Select
  Selection.CurrentRegion.Copy
  s_name = Range("D11").Offset(n, 0)
  Sheets(s_name).Select
  Range("a5").PasteSpecial

  Range("b6").Select
  Selection.CurrentRegion.Select
  columncount = Selection.Columns.count - 1
  Range("b6").Resize(1, columncount).Select
  Selection.AutoFill Destination:=Range("b6").Resize(totalrows, columncount), Type:=xlFillDefault

  Call clear_crap3(c, climit, plimit)
  Call temp_range(s_name, c, hist, rowcounter)
  ActiveWorkbook.Save
Next n
End Sub

```

```

Sub temp_range(s_name, c, hist, rowcounter)
' creates histograms given the histogram range of values
' three histograms are created for different temp range
' these are setup above the data

```

```

Dim x As Integer
Dim h As Integer
Dim diff As Variant
Dim y As Integer
Dim numcolumns As Integer
Dim numrows As Integer
Dim temp1 As Integer
Dim temp2 As Integer
Dim temp3 As Integer
Dim t As Integer
Dim rangend As Integer
Dim rangestart As Integer
Dim rowcount As Integer
Dim end1 As Integer
Dim end2 As Integer
Dim start4 As Integer
Dim percentloopy As Integer
Dim percentvalue As Integer
Dim checkpercent As Integer
Dim totalpercent As Variant

```

```

temp1 = 100
temp2 = 200

```

```
temp3 = 300
```

```
rowcount = 0
```

```
end1 = 0
```

```
end2 = 0
```

```
Range("b2").Select
```

```
Selection.CurrentRegion.Select
```

```
numrows = Selection.Rows.count - 5
```

```
numcolumns = (Selection.Columns.count - 2) / c
```

```
rangestart = 1
```

```
rangend = numrows
```

```
For s = 1 To numrows
```

```
  If Range("b5").Offset(s, 0) < temp1 Then
```

```
    end1 = end1 + 1
```

```
  Else
```

```
    If Range("b5").Offset(s, 0) < temp2 Then end2 = end2 + 1
```

```
  End If
```

```
  If Range("b5").Offset(s, 0) < temp3 Then start4 = start4 + 1
```

```
Next s
```

```
For t = 1 To 3
```

```
  Sheets(s_name).Select
```

```
  If t = 2 Then rangestart = 1
```

```
  If t = 2 Then rangend = end1
```

```
  If t = 3 Then rangestart = rangend
```

```
  If t = 3 Then rangend = end2 + end1
```

```
  If t = 4 Then rangestart = rangend
```

```
  If t = 4 Then rangend = numrows
```

```
Rows("1:" & hist).Select
```

```
Selection.Insert Shift:=xlDown
```

```
Range("a" & (hist * t) + 5 & ":a" & (hist * t) + hist + 2).Copy
```

```
Range("b2").PasteSpecial
```

```
Range("c1") = " temp range " & t
```

```
For y = 1 To numcolumns
```

```
  Range("b2").Offset(0, y * c) = Range("b2").Offset((hist * t) + 3, y * c)
```

```
  Range("b1").Offset(0, y * c).Select
```

```
  ActiveCell.FormulaR1C1 = "=sum(R3C:R" & hist - 1 & "C)"
```

```
  Range("c1").Offset(0, y * c).Select
```

```
  ActiveCell.FormulaR1C1 = "=sum(R3C:R" & hist - 1 & "C)"
```

```
  For x = rangestart To rangend
```

```
    Range("b5").Offset((hist * t) + x, y * c).Select
```

```
    diff = Range("b5").Offset((hist * t) + x, y * c)
```

```
    For h = 1 To hist - 3
```

```
      If diff <> "" Then
```

```
        If h = hist - 3 Then
```

```
          If diff > Range("b2").Offset(h, 0).Value Then
```

```
            Range("b2").Offset(h, y * c) = Range("b2").Offset(h, y * c) + 1
```

```
          End If
```

```
        End If
```

```
        If diff < Range("b2").Offset(h, 0).Value Then
```

```
          Range("b2").Offset(h, y * c) = Range("b2").Offset(h, y * c) + 1
```

```
          h = hist - 3
```

```
        End If
```

```
      Else
```

```
        h = hist - 3
```

```
      End If
```

```
    Next h
```

```
  Next x
```

```

Range("c3").Offset(0, y * c).Select
ActiveCell.FormulaR1C1 = "=RC[-1]/SUM(R3C[-1]:R" & hist - 1 & "C[-1])*100"
Range("c3").Offset(0, y * c).Select
Selection.AutoFill Destination:=Range("c3:c" & hist - 1).Offset(0, y * c), Type:=xlFillDefault

Sheets(s_name).Select
Sheets("data").Range("B1").Offset(rowcounter, 0) = Sheets(s_name).Range("C1")
Sheets("Data").Range("A1").Offset(rowcounter, 0) = Sheets(s_name).Range("B1").Offset(1, y * c)

For percentloopy = 1 To 4
    percentvalue = percentloopy * 2 + 2
    totalpercent = 0

    'this loop goes down the list of histogram setup and checks if the values fit within the percentage
error
    For checkpercent = 1 To hist - 3
        If Range("B2").Offset(checkpercent, (y * c) + 1).Text = "#DIV/0!" _
            Or Range("B2").Offset(checkpercent, (y * c) + 1).Text = "#NUM!" _
            Or Range("B2").Offset(checkpercent, (y * c) + 1).Text = "#VALUE!" _
            Or Range("B2").Offset(checkpercent, (y * c) + 1).Text = "" Then
            Range("B2").Offset(checkpercent, (y * c) + 1).ClearContents
        End If

        If Range("B2").Offset(checkpercent, 0) > (percentvalue * -1) And
Range("B2").Offset(checkpercent, 0) <= percentvalue Then
            totalpercent = totalpercent + Range("B2").Offset(checkpercent, (y * c) + 1)
        End If
    Next checkpercent
    Sheets("data").Range("B1").Offset(rowcounter, percentloopy) = totalpercent

Next percentloopy
rowcounter = rowcounter + 1

Next y

Sheets(s_name).Select
' Call graph_xheadings(hist)
' Call graph_create(hist, s_name, t, numcolumns, c)
Next t
'
End Sub

```

```

Sub graph_xheadings(hist)

```

```

    Range("A3").Select
    ActiveCell.FormulaR1C1 = ""less than "" & RC[1]"
    Range("A3").Select
    Selection.AutoFill Destination:=Range("A3:A" & hist - 2), Type:=xlFillDefault
    Range("A3:A" & hist - 2).Select
    Range("A" & hist - 1).Select
    ActiveCell.FormulaR1C1 = ""more than "" & RC[1]"

```

```

End Sub

```

```

Sub graph_create(hist, s_name, t, numcolumns, c)

```

```

Dim x_values As Range
Dim y_values As Range
Dim graphdata As Range
Dim c_name As String

```

```

Dim c_title As String
Dim g As Integer
Dim r_name As String

Range("A3:A" & hist - 1).Select
Set x_values = Selection
Range("c3:c" & hist - 1).Offset(0, c).Select
Set y_values = Selection
Set graphdata = Union(x_values, y_values)
c_name = s_name & "c" & t
c_title = s_name & " Temperature range " & t
r_name = Range("c2").Offset(0, c - 1)

Charts.Add
ActiveChart.ChartType = xlColumnClustered
ActiveChart.SetSourceData Source:=graphdata, PlotBy:=xlColumns
ActiveChart.SeriesCollection(1).name = r_name
ActiveChart.Location Where:=xlLocationAsNewSheet, name:=c_name
With ActiveChart
    .HasTitle = True
    .ChartTitle.Characters.Text = c_title
    .Axes(xlCategory, xlPrimary).HasTitle = True
    .Axes(xlCategory, xlPrimary).AxisTitle.Characters.Text = "Percentage error"
    .Axes(xlValue, xlPrimary).HasTitle = True
    .Axes(xlValue, xlPrimary).AxisTitle.Characters.Text = "Percentage"
End With

For g = 2 To numcolumns
    Sheets(s_name).Select
    Range("c3:c" & hist - 1).Offset(0, c * g).Select
    Set y_values = Selection
    r_name = Range("b2").Offset(0, c * g)

    Sheets(c_name).Select
    ActiveChart.PlotArea.Select
    ActiveChart.SeriesCollection.NewSeries
    ActiveChart.SeriesCollection(g).Values = y_values
    ActiveChart.SeriesCollection(g).name = r_name
Next g
End Sub

Sub clear_crap4(c)
' for use with the error determination sheets
'this subroutine removes the error message from cells
'clears the cells of error values

Dim x As Integer
Dim y As Integer
Dim totalrows As Double
Dim totalcolumns As Double
Dim limit As Integer

limit = 30

Range("a1").Select
Selection.CurrentRegion.Select
totalrows = (Selection.Rows.count) - 5
totalcolumns = ((Selection.Columns.count) - 2) / c
'autoformat width
Cells.Select
Cells.EntireColumn.AutoFit
Range("a1").Select

```



```

For y = 1 To totalrows
  For x = 1 To totalcolumns
    Range("e5").Offset(y, (x - 1) * c).Select
    If Range("e5").Offset(y, (x - 1) * c).Value < -limit _
    Or Range("e5").Offset(y, (x - 1) * c).Value > limit Then
      For z = 1 To c
        Range("e5").Offset(y, (x - 1) * c + (1 - z)).ClearContents
      Next z
    End If
  Next x
Next y

End Sub

```

```

Sub clear_nonwavelengths2(maxseparation)
' autoformats cell width so that #### doesnot cause a problem
' removes values equal to or less than zero,
'   greater than maximum sepatation of peaks,
'   and #div/0!
' number of rows and colums in the sheet are counted and used for the loop

```

```

Dim num_rows As Integer
Dim num_columns As Integer
Dim x As Integer
Dim y As Integer

```

```

num_rows = Range("b1").Value
num_columns = Range("d1").Value

```

```

'autoformat width
Cells.Select
Cells.EntireColumn.AutoFit
Range("b2").Select

```

```

' removes crap
For y = 1 To num_rows
  For x = 1 To num_columns
    If Range("b2").Offset(y, x).Text = "#DIV/0!" Then Range("b2").Offset(y, x).ClearContents
    If Range("b2").Offset(y, x).Value <= 0 Then Range("b2").Offset(y, x).ClearContents
    If x < (num_columns / 2) + 1 And Range("b2").Offset(y, x).Value > maxseparation Then
      Range("b2").Offset(y, x).ClearContents
    Next x
  Next y
End Sub

```

```

Sub clear_text()
' for use with the error determination sheets
' this subroutine removes the error message from cells
' clears the cells of error values

```

```

Dim x As Integer
Dim y As Integer
Dim totalrows As Double
Dim totalcolumns As Double

```

```

Range("a1").Select
Selection.CurrentRegion.Select
totalrows = (Selection.Rows.count) - 2
totalcolumns = ((Selection.Columns.count) - 2)

```

```

'autoformat width
Cells.Select
Cells.EntireColumn.AutoFit
Range("a1").Select

For y = 1 To totalrows
  For x = 1 To totalcolumns
    If Range("b2").Offset(y, x).Text = "#DIV/0!" _
      Or Range("b2").Offset(y, x).Text = "#NUM!" _
      Or Range("b2").Offset(y, x).Text = "#VALUE!" _
      Or Range("b2").Offset(y, x).Text = "" Then
      Range("b2").Offset(y, x).ClearContents
    End If
  Next x
Next y

End Sub

```

9.7.2 *Summing the spectrum and finding the average*

This program was written in excel and was used to add a number of spectrum together to determine if a reliable average could be determined from a summation of spectrum over a wide temperature range.

```

Sub find_average()
'
Dim reading(1 To 2050) As Variant
Dim back(1 To 2050) As Variant
Dim filenumber As String
Dim tempset As String
Dim minfile As Integer
Dim maxfile As Integer
Dim sheetcounter As Integer
Dim filecount As Integer
Dim sheetnumber As Integer
Dim sheetname As String
Dim setnumber As Integer
Dim setcounter As Integer
Dim myfilename As String
Dim x As Double
Dim opencount As Integer
Dim intave As Integer
Dim maxmin As Integer

Sheets("start").Select
sheetnumber = Range("A2")

'copies sheets

```

```

For x = 1 To sheetnumber
    sheetname = Range("A2").Offset(x, 0)
    Sheets(sheetname).Select
    Sheets(sheetname).Copy Before:=Sheets(1)
    Sheets(sheetname & " (2)").Select
    Sheets(sheetname & " (2)").Name = sheetname & "-back"
    Sheets("start").Select
Next x

For sheetcounter = 1 To sheetnumber
    Sheets("start").Select

    sheetname = Range("A2").Offset(sheetcounter, 0)
    Sheets(sheetname).Select
    Range("B2").CurrentRegion.Select
    setnumber = Selection.Columns.Count - 1

    For setcounter = 1 To setnumber

        For x = 1 To 2050
            reading(x) = 0
        Next x

        filecount = Range("B1").Offset(0, setcounter)

        For groupcount = 1 To filecount

            tempset = Range("B3").Offset(groupcount * 5 - 5, setcounter)
            minfile = Range("B4").Offset(groupcount * 5 - 5, setcounter)
            maxfile = Range("B5").Offset(groupcount * 5 - 5, setcounter)

            For opencount = minfile To maxfile

                If opencount < 10 Then myfilename = "C:\my Documents\alison\h data\H" & tempset & "R0" &
opencount
                If opencount > 9 Then myfilename = "C:\my Documents\alison\h data\H" & tempset & "R" &
opencount

                Workbooks.OpenText filename:=myfilename, Origin _
:=xlWindows, StartRow:=1, DataType:=xlDelimited, TextQualifier:= _
xlDoubleQuote, ConsecutiveDelimiter:=False, Tab:=True, Semicolon:=False, _
Comma:=False, Space:=False, Other:=False, FieldInfo:=Array(1, 1)

                For x = 1 To 2050
                    reading(x) = reading(x) + Range("A2").Offset(x, 0)
                Next x
                ActiveWorkbook.Close

            Next opencount

        Next groupcount
        maxmin = (maxfile - minfile) + 1
        For x = 1 To 2050
            Range("B39").Offset(x, setcounter) = reading(x) / maxmin
        Next x
        intave = Int(Range("B37").Offset(0, setcounter))

        Workbooks.Open "C:\My Documents\Alison\h data\blanksheet"
        For x = 1 To 2050
            Range("A2").Offset(x, setcounter) = reading(x) / maxmin

```

```

Next x

Application.DisplayAlerts = False

ActiveWorkbook.SaveAs filename:="C:\My Documents\Alison\h data\h" & sheetname & "R" &
intave, _
    FileFormat:=xlText, CreateBackup:=False
ActiveWorkbook.Close

'sorts out background reading
For x = 1 To 2050
    back(x) = 0
Next x

For groupcount = 1 To filecount

    tempset = Range("B3").Offset(groupcount * 5 - 5, setcounter)

    For y = 1 To 2

        If y = 1 Then minfile = 1
        If y = 1 Then maxfile = 5
        If y = 2 Then minfile = 11
        If y = 2 Then maxfile = 15

        For opencount = minfile To maxfile

            If opencount < 10 And tempset < 210 Then myfilename = "C:\my Documents\alison\h data\H"
& tempset & "BA0" & opencount
            If opencount < 10 And tempset > 210 Then myfilename = "C:\my Documents\alison\h data\H"
& tempset & "B0" & opencount
            If opencount > 10 And tempset < 210 Then myfilename = "C:\my Documents\alison\h data\H"
& tempset & "BA" & opencount
            If opencount > 10 And tempset > 210 Then myfilename = "C:\my Documents\alison\h data\H"
& tempset & "B" & opencount

            Workbooks.OpenText filename:=myfilename, Origin _
:=xlWindows, StartRow:=1, DataType:=xlDelimited, TextQualifier:= _
xlDoubleQuote, ConsecutiveDelimiter:=False, Tab:=True, Semicolon:=False, _
Comma:=False, Space:=False, Other:=False, FieldInfo:=Array(1, 1)

            For x = 1 To 2050
                back(x) = back(x) + Range("A2").Offset(x, 0)
            Next x
            ActiveWorkbook.Close

        Next opencount
    Next y
Next groupcount

'copies reading - background into sheet

Sheets(sheetname & "-back").Select
For x = 1 To 2050
    Range("B39").Offset(x, setcounter) = (reading(x) / maxmin) - (back(x) / 10)
Next x

'creates a text file of just the background
Workbooks.Open "C:\My Documents\Alison\h data\blanksheet"
For x = 1 To 2050

```

```
    Range("A2").Offset(x, setcounter) = back(x) / 10
Next x

Application.DisplayAlerts = False
ActiveWorkbook.SaveAs filename:="C:\My Documents\Alison\h data\h" & sheetname & "B" &
intave, _
    FileFormat:=xlText, CreateBackup:=False
ActiveWorkbook.Close

'creates a text file of the reading - background
Workbooks.Open "C:\My Documents\Alison\h data\blanksheet"
For x = 1 To 2050
    Range("A2").Offset(x, setcounter) = (reading(x) / maxmin) - (back(x) / 10)
Next x

Application.DisplayAlerts = False
ActiveWorkbook.SaveAs filename:="C:\My Documents\Alison\h data\h" & sheetname & "RB" &
intave, _
    FileFormat:=xlText, CreateBackup:=False
ActiveWorkbook.Close

Next setcounter

Next sheetcounter
End Sub
```

9.7.3 LabView program to determine temperature from spectrum in real time

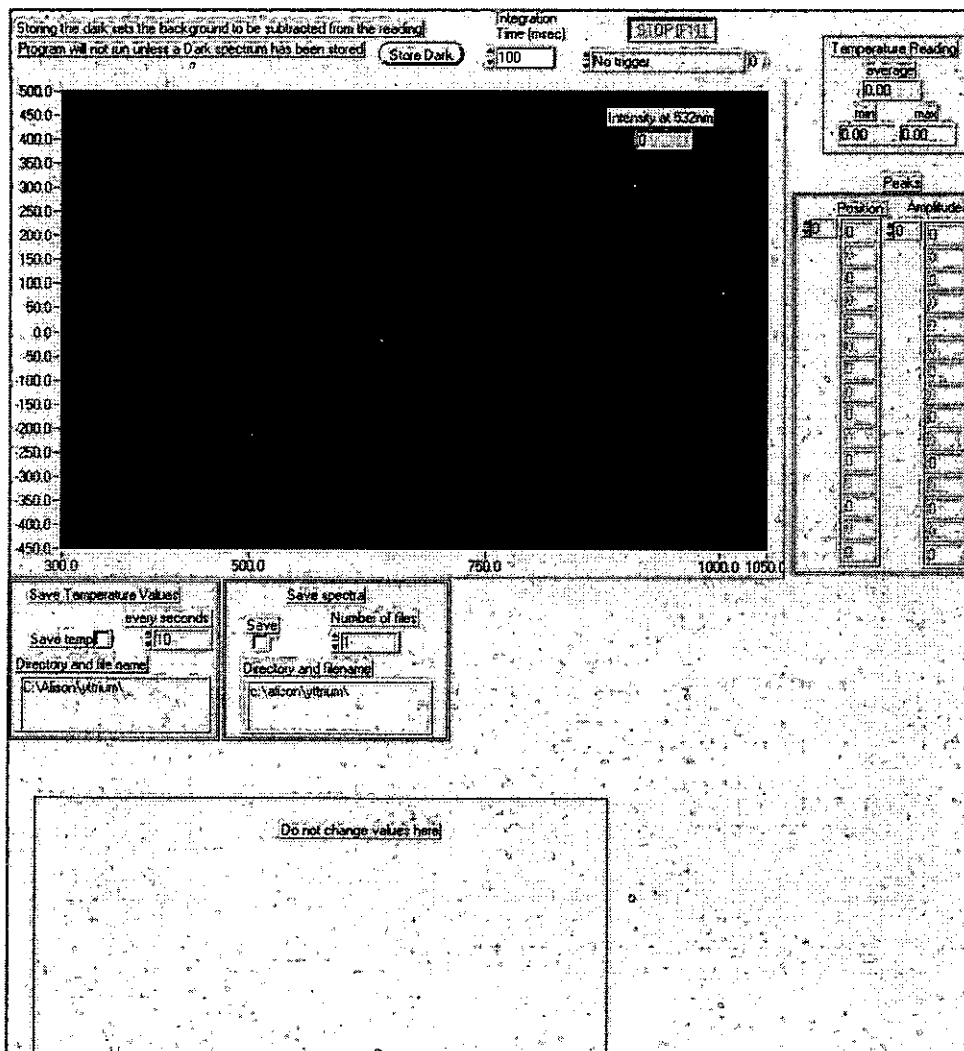
The part of the program which communicates with the spectrometer is software developed by the spectrometer company. I have added to this to produce the collection of data from the spectrum which could then be used to determine the temperature. I have also added functions to enable the spectrum and the temperature reading to be saved.

9.7.3.1 ytt_find_temp.vi

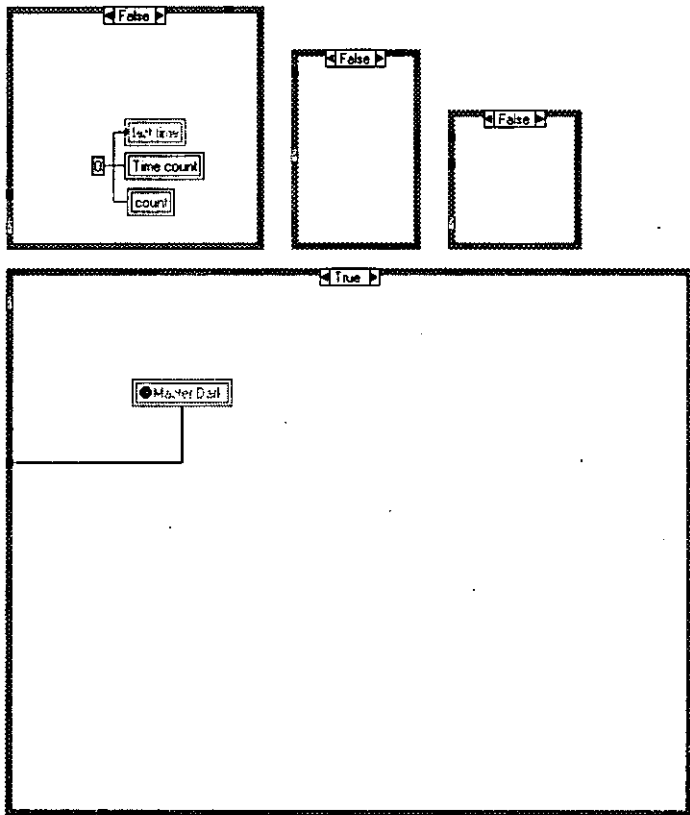
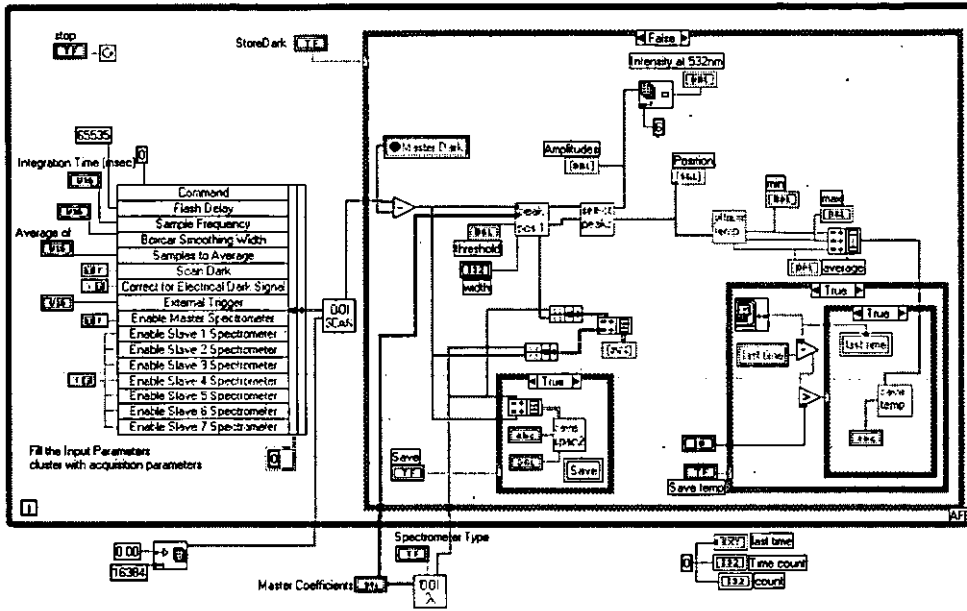
Connector Pane



Front Panel



Block Diagram

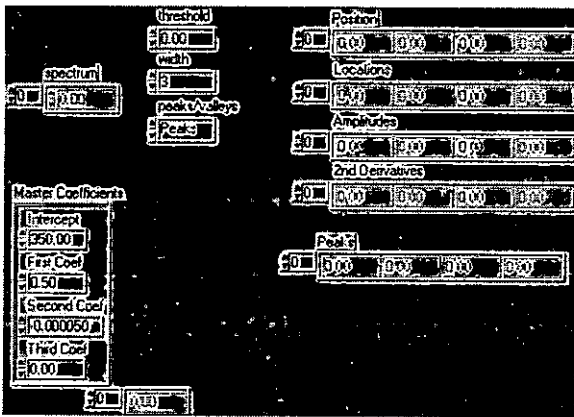


9.7.3.2 peakfind.vi

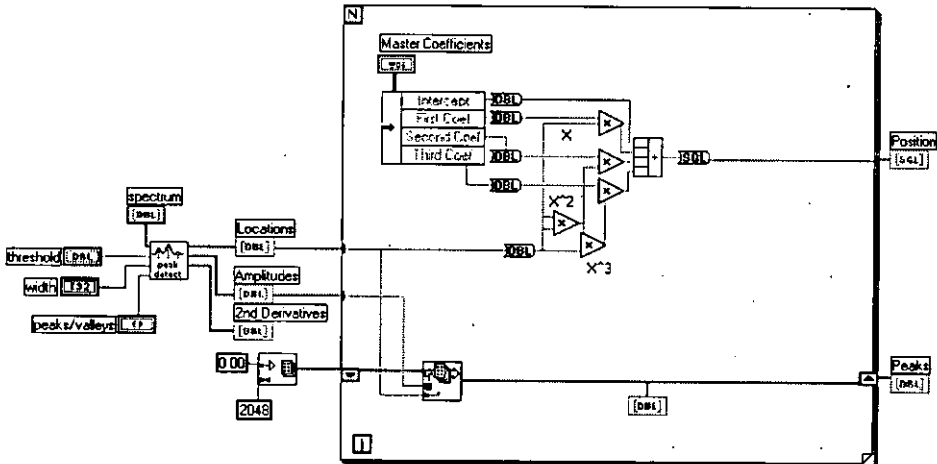
Connector Pane



Front Panel



Block Diagram



9.7.3.3 *MinMaxAve.vi*

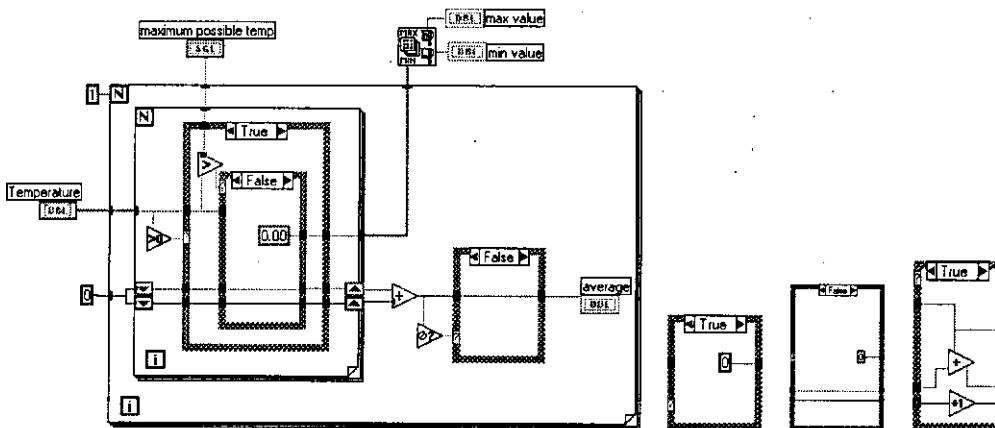
Connector Pane



Front Panel

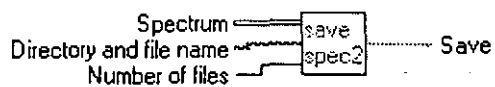


Block Diagram

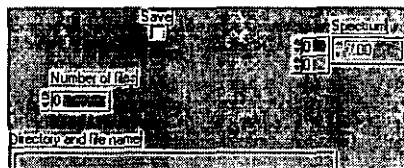


9.7.3.4 save spectra 2.vi

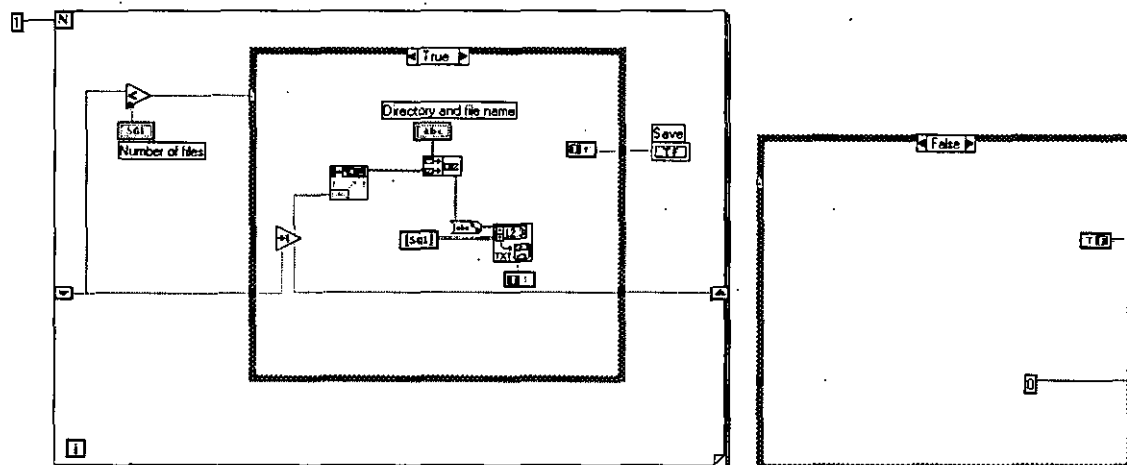
Connector Pane



Front Panel

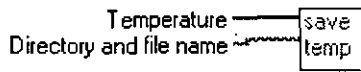


Block Diagram



9.7.3.5 *save temp.vi*

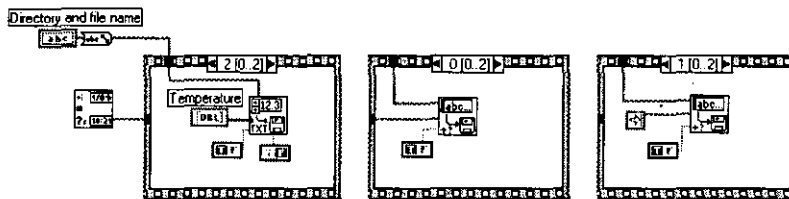
Connector Pane



Front Panel

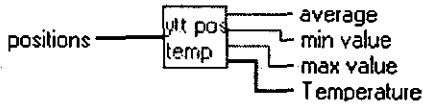


Block Diagram

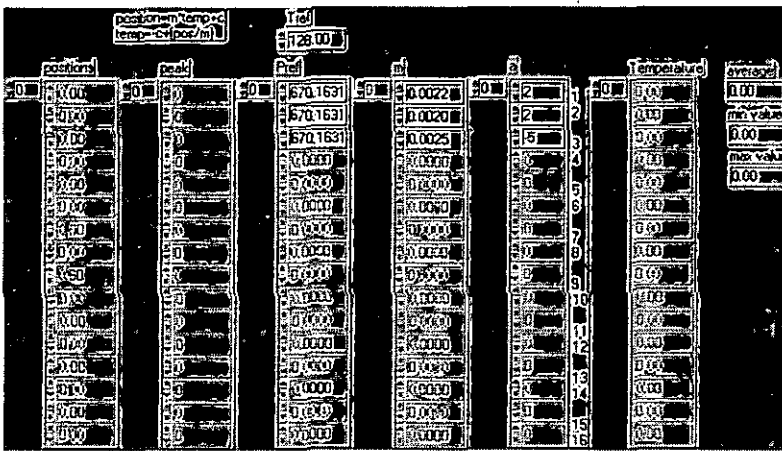


9.7.3.6 ytt_pos_temp.vi

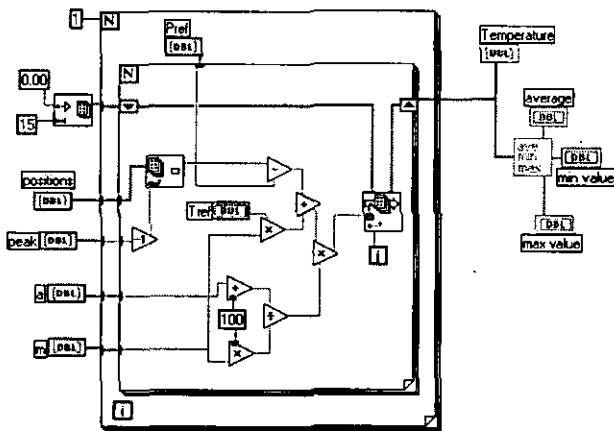
Connector Pane



Front Panel

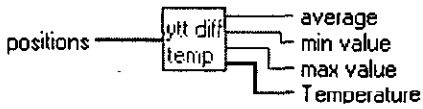


Block Diagram

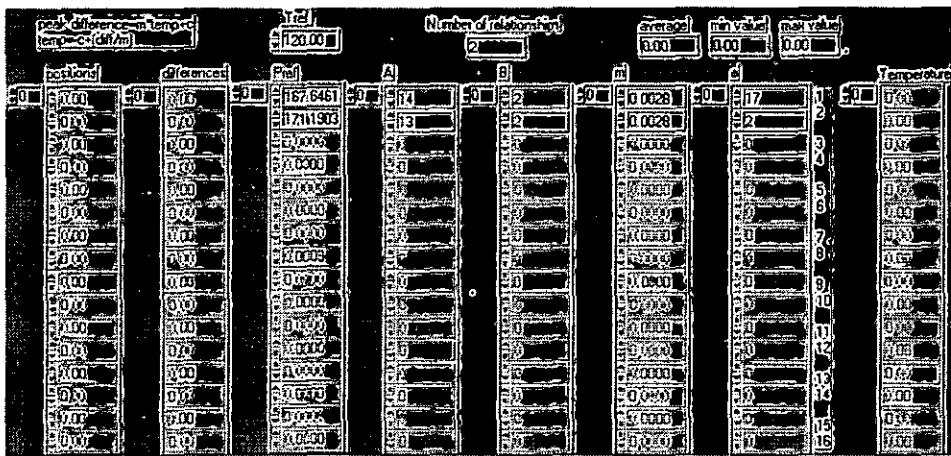


9.7.3.7 ytt_posdiff_temp_v2.vi

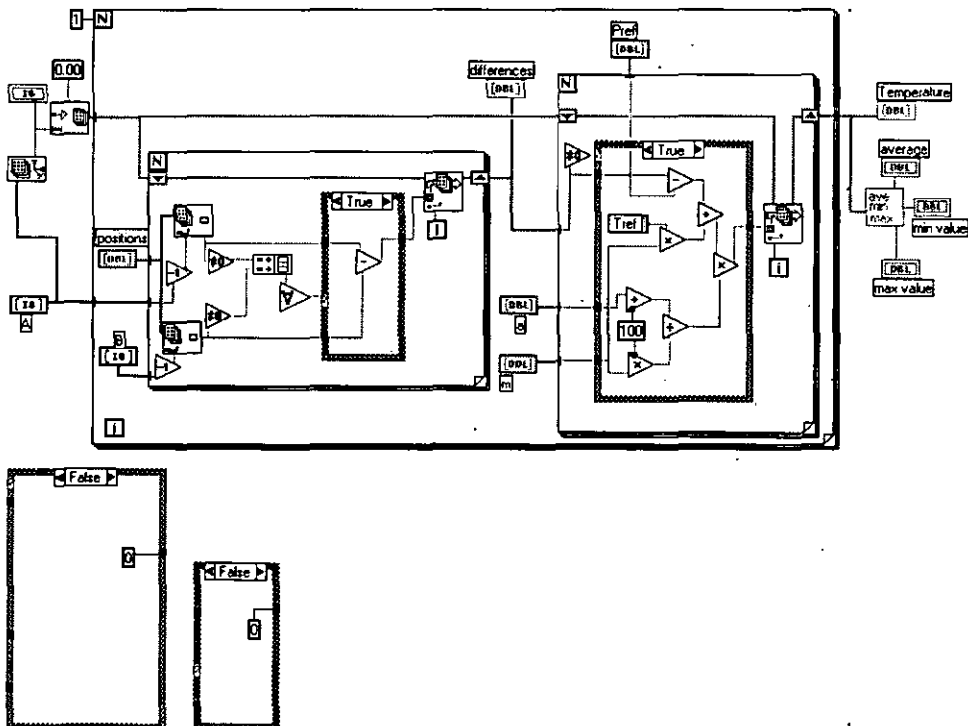
Connector Pane



Front Panel

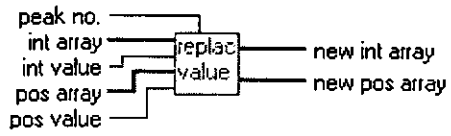


Block Diagram

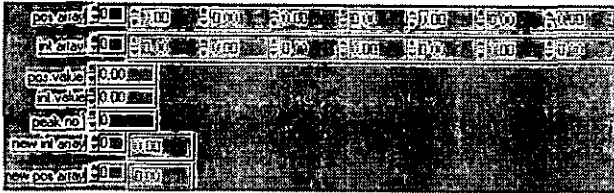


9.7.3.8 *ytt_posint_replace.vi*

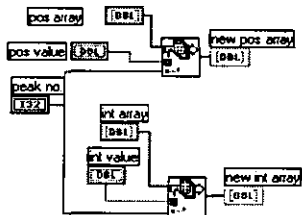
Connector Pane



Front Panel



Block Diagram

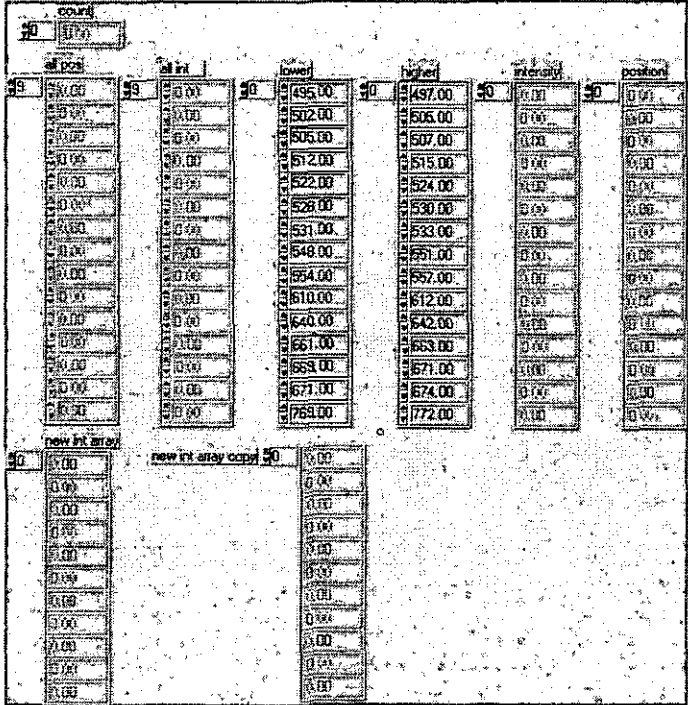


9.7.3.9 ytt_posint_v5.vi

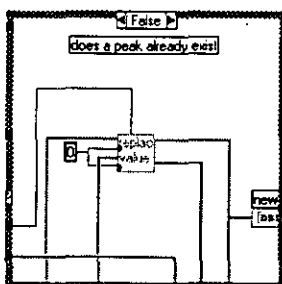
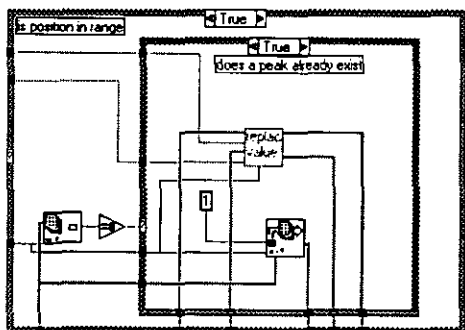
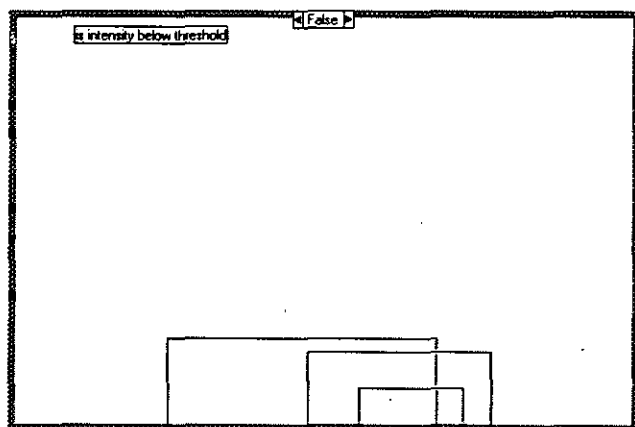
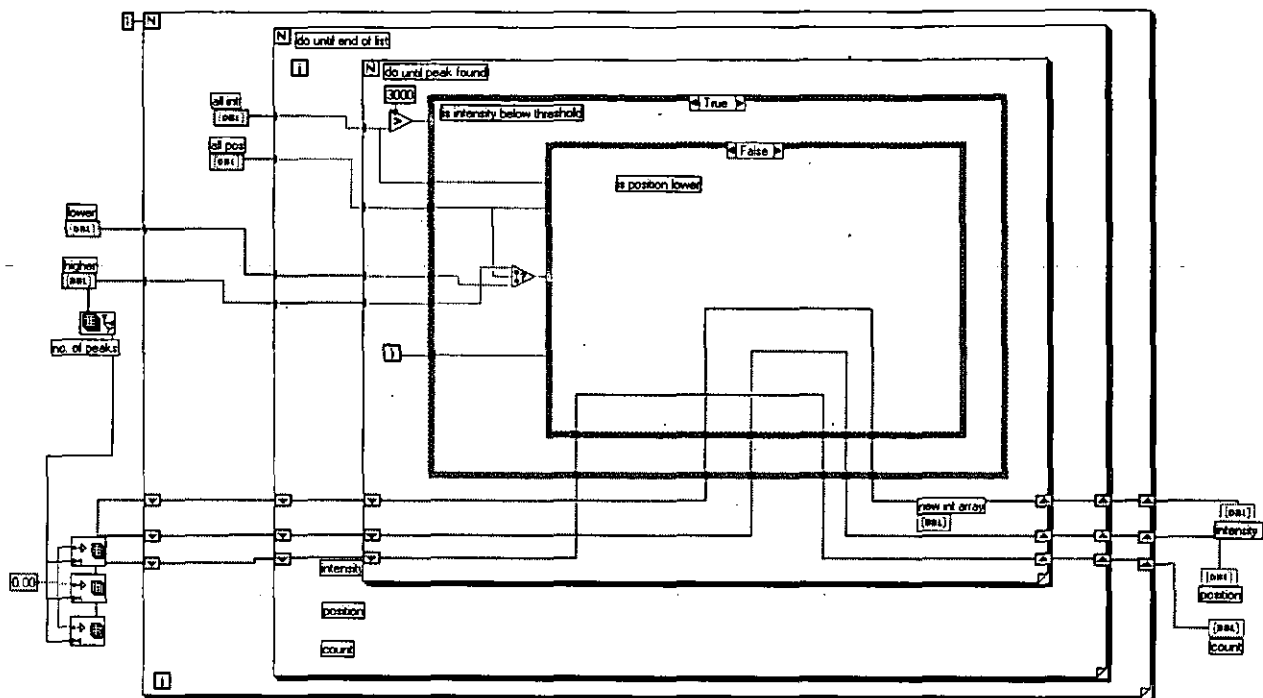
Connector Pane



Front Panel

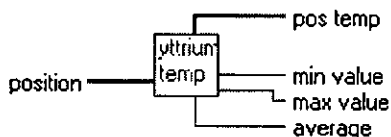


Block Diagram

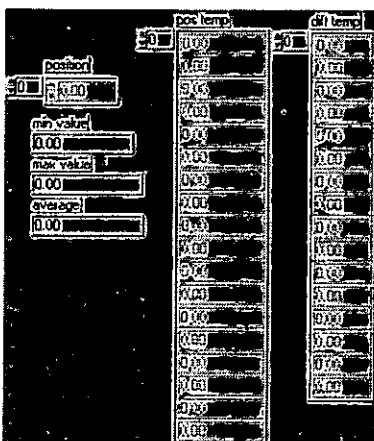


9.7.3.10 ytt_temp_v2.vi

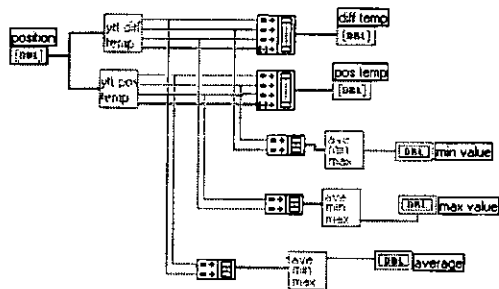
Connector Pane



Front Panel



Block Diagram



9.8 Equations

9.8.1 Lorentzian¹⁸¹

$$Y = \frac{A}{1 + \left(\frac{x-C}{W}\right)^2}$$

where;

A = Amplitude

C = Center

W = full width at half maximum (FWHM)

9.8.2 Gaussian¹⁸¹

$$Y = A \times \exp\left(-\frac{1}{2}\left(\frac{x-C}{W}\right)^2\right)$$

where;

A = Amplitude

C = Center

W = full width at half maximum (FWHM)

9.8.3 Voight¹⁸¹

$$y = \frac{\gamma_L}{\gamma_G} A_L \sqrt{\pi \ln 2} V\left(\frac{2(x-c)\sqrt{\ln 2}}{\gamma_G}, \frac{\gamma_L \sqrt{\ln 2}}{\gamma_G}\right)$$

where;

A_L = Lorentzian amplitude

γ_G = Gaussian width

γ_L = Lorentzian width

C = Center

$$V(X, Y) = \frac{Y}{\pi} \int_{-\infty}^{+\infty} \frac{e^{-z^2}}{Y^2 + (X-z)^2} dz$$

9.8.4 Pearson VII¹⁸¹

$$y = \frac{A}{\left(1 + 4\left(\frac{x-C}{W}\right)^2 \left(2^{1/s} - 1\right)\right)^s}$$

where

A = amplitude

C = centre

W = full width at half maximum (FWHM)

9.8.5 Munro⁶

$$R(x) = c_1 R_1(x) + c_2 R_2(x) + \rho(x)$$

where;

R(x) = net intensity at the position x

c₁ & c₂ = amplitude factors for the R₁ & R₂ peaks

ρ(x) = background factor

$$R_k(x) = C_L(k)L(A_k, B_k, x) + (1 - C_L(k))G(A_k, B_k, x)$$

where;

C_L(k) = relative amplitude factor

0 ≤ C_L(k) ≤ 1

$$L(A, B, x) = \frac{B^2}{B^2 + 4(A-x)^2}$$

$$G(A, B, x) = \exp\left(\frac{\ln(1/2)(A-x)^2}{(B/2)^2}\right)$$

where;

A_k = peak position for peak R_k

B_k = full width at half maximum (FWHM) for the Lorentzian contribution

B_k = full width at half maximum (FWHM) for the Gaussian contribution

9.8.6 Stern-Volmer

The relationship between luminescence output and oxygen partial pressure is given by the Stern-Volmer equation below.

$$\text{Stern-Volmer equation } \frac{I_0}{I} = 1 + K_{sv} P_{O_2} = \frac{\tau_0}{\tau} \quad \text{Equation 9-5}$$

$$\frac{I_{REF}}{I} = 1 + K_{sv} \frac{P}{P_{REF}} \quad \text{Equation 9-6}$$

$$K_{sv} = \tau_0 k_{sv} \quad \text{Equation 9-7}$$

P = the partial pressure of oxygen

I_0 = the luminescence output at zero oxygen pressure (unquenched)

I = the luminescence output at some oxygen pressure P

K_{sv} = the Stern-Volmer constant

τ_0 = the lifetime of the luminescence at zero oxygen content (unquenched)

τ = the lifetime of the luminescence at some oxygen content

I_{REF} = the intensity reference value of a particular point

P_{REF} = the pressure reference value of a particular point

k_{sv} = the bimolecular collisional quenching rate

9.9 References

- ¹ Private communication, Alan Parks Holset Engineering
- ² Alfred, *The properties of aluminium and its alloys*. 1993
- ³ *The development of gas turbine materials*. G.W. Meetham 1981.
- ⁴ *Reciprocating and Rotary Compressors*. V. Chlumsky, 1965.
- ⁵ *The centrifugal Compressor Stage*. T.B. Fergusson. 1963.
- ⁶ Munro R.G., Piermarini G.J., Block S., Holzapfel W.B., *Model line-shape analysis for the Ruby R lines used for pressure measurement*. J. Appl. Phys. Vol;57, No;2, pp165-169, Jan. 1985
- ⁷ Guthrie J.D., Sparr B.J., *Infrared study of factors affecting the emissivity of aluminium*. Applied spectroscopy, Vol;45, No;4, pp;588-596, 1991.
- ⁸ Ervin J., Murrawski C., MacArthur C., Chyu M., Bizzak D., 1995. *Temperature measurement of a curved surface using thermographic phosphors*. *Experimental thermal and fluid science*. Vol:11, pp:387-394
- ⁹ Bize D., Lempereur C., Mathe J.M., Mignosi A., Seraudie A., Serrot G., *Surface temperature mapping using liquid crystals applied to identifying the laminar – turbulent transition*. Instrumentation in aerospace simulation facilities ICIASF conf. Pacific Grove, California: IEEE, 1997, pp:66
- ¹⁰ Oglesby D.M., Upchurch B.T., Sealey B.S., Leighty D.D., Burkett C.G., Jalali A., 1997. *Development of temperature sensitive paints for the detection of small temperature differences*. Instrumentation in the aerospace industry. 43rd int. instrumentation sympos. pp:329-337.
- ¹¹ Colour-Therm Ltd. Burdon Lane, Cheam, Surrey.
- ¹² Loarer T., Greffet J.-J., Huetz-Aubert M., 1990. *Noncontact surface temperature measurement by means of a modulated photothermal effect*. Applied optics Vol:27, No:7, pp:979-987.
- ¹³ Zhang Z., Grattan K.T.V., Palmer A.W., 1992. *Fibre optic temperature sensor based on the cross referencing between blackbody radiation and fluorescence lifetime*. Rev. Sci. Instruments 63(5).
- ¹⁴ Dixon J., 1987. *Industrial radiation thermometry*. Measurement and control Vol:20, July, pp:11-16.
- ¹⁵ Valenti M., *Infrared sensors, hands off temperature measurement*. Mechanical Engineering pp;40-45, Oct. 1991
- ¹⁶ Zhao H., Collings N., Ma T., *The cylinder head temperature measurement by thermal imaging technique*.
- ¹⁷ Guthrie J.D., Sparr B.J., *Infrared study of factors affecting the emissivity of aluminium*. Applied spectroscopy, Vol;45, No;4, pp;588-596, 1991.
- ¹⁸ Allison S.W., Cates M.R., Gillies G.T., Noel B.W., *Fiber optic pulsed laser delivery for remote measurements*. Optical engineering, Vol;26, No;6, 1987,
- ¹⁹ Hu Y.L., Zhang Z.Y., Grattan K.T.V., Palmer A.W., Meggitt B.T., *Ruby-based decay-time thermometry: effect of probe size on extended measurement range (77-800K)*. Sensors and actuators A, Vol;63, pp;85-90, 1997.
- ²⁰ Grattan K.T.V., Selli R.K., Palmer A.W., 1986. *Fibre-optic absorption temperature sensor using fluorescence reference channel*. Rev. Sci. Instruments 57(6) pp:1175-1178.

- ²¹ Fister J.C., Rank D., Harris J.M.. 1995. *Delayed fluorescence optical thermometry*. Analytical Chemistry Vol. 67 No. 23
- ²² Wickersheim J., Sun M., 1985. *Phosphors and fibre optics remove doubt from difficult temperature measurements*. Research & development, Nov., pp:114-119.
- ²³ Wagenaar B.M., Meijer R., Kuipers J.A.M., van Swaaij W.P.M., 1995. *Novel method for noncontact measurement of particle temperatures*. AIChE Journal Vol:41, No:4, pp:773-781.
- ²⁴ Guthrie J.D., Sparr B.J., *Infrared study of factors affecting the emissivity of aluminium*. Applied spectroscopy, Vol:45, No:4, pp:588-596, 1991.
- ²⁵ *Thermoluminescent Materials*. D.R.Vij. PTR Prentice Hall, 1993.
- ²⁶ Solntsev M.K., Ekobena H.P.F., Karavaev V.A., Yurina T.P. *Dynamics of the action of various physical and chemical factors on the thermoluminescence of photosynthetic systems*. Journal of luminescence. 1998 Vol:76&77, pp:349-353.
- ²⁷ Schrum K.F., Williams A.M., Haerther S.A., Ben-Amtoz D.. 1994. *Molecular fluorescence thermometry*. Analytical Chemistry, Vol 66 No17.
- ²⁸ Morishima Y., Saegusa K., Kamachi M., *Photophysical behavior of Zinc(II) tetraphenylporphyrin in Highly constraining microenvironments. Anomalously long-lived excited-triplet in the hydrophobic clusters of amphiphilic polysulfonates*. J. Phys. Chem. 1995, Vol:99, pp:4512-4517.
- ²⁹ Goss L.P., Smith A.A., Post M.E.. 1989. *Surface thermometry by laser-induced fluorescence*. Rev. Sci. Instruments 60(12), pp:3702-3706.
- ³⁰ Grattan K.T.V., Selli R.K., Palmer A.W.. 1987. *Ruby fluorescence wavelength division fibre-optic temperature sensor*. Rev. Sci. Instruments 58(7).
- ³¹ Allison S.W., Cates M.R., Noel B.W., Gilles G.T.. 1988. *Monitoring permanent magnet motor heating with phosphor thermometry*. IEEE Transactions on instrumentation and measurement. Vol.37 No.4
- ³² Noel B.W., Turley W.D., Allison S.W., *Thermographic-phosphor temperature measurements: Commercial and defense-related applications*. ISA 1994 – paper #94-1003
- ³³ Allison S.W., Beshears D.L., Cates M.R., Noel B.W., Turley W.D. *Taking an engine's temperature*. Mechanical engineering. Jan 1997, pp:72-74.
- ³⁴ Chyu M.K., Bizzack D.J. *Surface temperature measurement using a laser-induced fluorescence thermal imaging system*. Journal of heat transfer. Feb 1994. Vol:116, pp:263-266
- ³⁵ Kiel A., *Temperature dependent linewidth of excited states in crystals. I. line broadening due to adiabatic variation of the local fields*. Physical review, 1962, Vol:126, No:4, pp:1992- 1297.
- ³⁶ Dixon G.J., *Time resolved spectroscopy defines biological molecules*. Laser focus world, Oct. 1997, pp:115-122.
- ³⁷ Grattan K.T.V., Palmer W.A.. 1996. *Infrared fluorescence "Decay-Time" temperature sensor*. Rev. Sci. Instruments 56(9)
- ³⁸ Grattan K.T.V., Palmer A.W., Zhang Z., *Development of a high-temperature fibre-optic thermometer probe using fluorescent decay*. Rev. Sci. Instrum., Vol:62, No:5, May 1991.
- ³⁹ Fister J.C., Harris J.M.. 1996. *Time and wavelength resolved delayed-fluorescence emission from acridine yellow in an inhomogeneous saccharide glass*. Analytical Chemistry Vol. 68 No. 4
- ⁴⁰ Allison S.W., Boatner L.A., Gilles G.T.. 1995. *Characterisation of high temperature thermographic phosphors: Spectral properties of LuPO₄:Dy(1%),Eu(2%)*. Applied Optics Vol.34 No.25.

-
- ⁴¹ Morris M.J. Dr. 1995. *Use of pressure sensitive paints in low speed flows*. Int. congress on instrumentation in Aerospace Simulation Facilities. July
- ⁴² Liu T., Campbell B.T., Burns S.P., Sullivan J.P.. 1997. *Temperature and pressure sensitive luminescent paints in aerodynamics*. Appl. Mech. Rev. Vol.50 No.4
- ⁴³ Burns S.P., Sullivan J.P. 1995. *The use of pressure sensitive paints on rotating machinery*. Int. congress on instrumentation in Aerospace Simulation Facilities. July
- ⁴⁴ Borovoy V., Bykov A., Orlov A., Radchenko V., Phonov S.. *Pressure sensitive paint application in shock wind tunnel*. Int. congress on instrumentation in Aerospace Simulation Facilities. July 1995.
- ⁴⁵ Oglesby D.M., Upchuch B.T., Leighty D.D., Simmons K.A., Demandate C.G.. *Pressure sensitive paint with internal temperature sensing luminophore*. International Instrumentation Symposium 42nd symposium. San Diego 1996. Pp:205
- ⁴⁶ Davies A.G., Bedwell D., Dunleavy M., Brownjohn N.. *Pressure sensitive paint limitations and solutions*. Instrumentation in aerospace simulation facilities ICIASF conf. Sept 1997.
- ⁴⁷ Carroll B.F., Winslow A., Abbitt J., Schanze K., Morris M.. *Pressure sensitive paint: Application to a sinusoidal pressure fluctuation*. Int. congress on instrumentation in Aerospace Simulation Facilities. July 1995.
- ⁴⁸ Mori N., Takahashi H., 1987. *Raman and reflection spectra of pyrite system under high pressure*. High pressure reaserach in mineral physics. pp:341-345.
- ⁴⁹ <http://omlc.ogi.edu/spectra/PhotochemCAD/html/acrdineyellow.html>
- ⁵⁰ Siegman A.E., *Lasers*. 1986
- ⁵¹ Lengyel B.A. 1966. *Introduction to laser physics*.
- ⁵² Grattan K.T.V., Palmer A.W., Zhang Z., *Development of a high temperature fibre optic thermometer probe using fluorescent decay*. Rev. Sci. Instrum., Vol:62, No:5, May 1991.
- ⁵³ Ghassemlooy Z., Grattan K.T.V., Lynch D. 1989. *Probe design aspects of Ruby decay-time fluorescent sensors*. Rev. Sci. Instrum. Vol.60.
- ⁵⁴ Gibson K.S. *The effect of temperature upon the absorption spectrum of a synthetic Ruby*. Phys. Rev. 1916, Vol. VIII No.1
- ⁵⁵ Imbusch G.F., *Energy transfer in heavily-doped Ruby*. *Journal of luminscence*, Vol;53, pp;465-467, 1992
- ⁵⁶ Abella and Cummins, *Lasers – Generation of light by stimulated emission*. B.A. Lenyal 1962
- ⁵⁷ Kuo C.T. et al. *Ruby Spectral Band-pofile analysis for temperature sensing*. J Anal Phys Vol. 75
- ⁵⁸ Powell R.C., Dibartoo B., Birang B., Naiman C.S. 1966. *Temperature dependance of the widths and positions of the R and N lines in heavily doped Ruby*. J. Appl. Phys. Vol. 37, December
- ⁵⁹ Chai M., Brown J.M., *Effects of static non-hydrostatic stress on the R lines of Ruby single crystals*. Geophysical research letters; Vol;23, No;24, pp;3539-3542. Dec. 1996.
- ⁶⁰ Okai B., Shimomura O., Fujishiro I., *Physica. B*, Vol;139&140, pp;799-802, 1986
- ⁶¹ Gupta Y.M., Shen X.A., *Potential use of the Ruby R₂ line shift for static high presure calibration*. Appl. Phys. Lett. Vol;58, No;6, pp;583-585, Feb. 1991.
- ⁶² Eggert j.H., Goettel K.A., Silvera I.F., *Ruby at high pressure. I. Optical line shifts to 156GPa*. Physical review B., Vol;40, No;8, pp;5724-5731, Sep.1989.
- ⁶³ Feher et al 1968
- ⁶⁴ Piermarini G.J., Block S., Barnett J.D., *Hydrostatic limits in liquids and solids to 100kbar*. J. App. Phys., Vol;44, No;12, Dec 1973.
-

- ⁶⁵ Piermarini G.J., Block S., Barnett J.D., Forman R.A., *Calibration of the pressure dependence of the R₁ Ruby fluorescence line to 195kbar*. J. App. Phys., Vol;46, No;6, June 1975.
- ⁶⁶ Shen Y. et al, *Sensors and actuators*; A. Physical, Vol;71, pp;70-73, 1998
- ⁶⁷ Shen Y. Tong L., Wang Y., Ye L., *Sapphire fibre thermometer ranging from 20 to 1800 °C*. Applied optics, Vol;38, No;7. Pp;1139-1143, March 1999
- ⁶⁸ Orbis Technologies Ltd. www.orbitech.co.uk/luxprobes.html
- ⁶⁹ Optical Microscopy Division of the National High Magnetic Field Laboratory. <http://micro.magnet.fsu.edu/primer/java/lasers/tsunami/>
- ⁷⁰ Web Elements <http://www.webelements.com/webelements/elements/text/La/key.html>
- ⁷¹ Chyu M.K., Bizzak D.J., *Two dimensional imaging of OH laser induced fluorescence in a flame*. Opt. Lett. Vol;7, pp;382-384, 1993
- ⁷² Fonger W.H., Struck C.W., *Eu^{+3,5}D resonance quenching to the charge transfer states in Y₂O₂S, La₂O₂S, and LaOCL*. J. Chem. Physics, Vol;52, pp;6364-6372 1970
- ⁷³ Lutz S.S., Turley W.D., Borella H.M., Noel B.W., Cates M.R., Probert M.R., *Remote temperature measurement instrumentation for a heated rotating turbine disk*. ISA 1988, paper #88-0725.
- ⁷⁴ Noel B.W., Borella H.M., Franks L.A., Marshall B.R., Allison S.W., Cates M.R., Stange W.A., *Proposed laser induced fluorescence method for remote thermometry in turbine engines*. J. Propulsion, Vol;2, No;6, pp;565-568, 1986.
- ⁷⁵ Choy K.L., Feist J.P., Heyes A.L., Su B., *Eu doped Y₂O₃ phosphor films produced by electrostatic-assisted chemical vapour deposition*. J. Mater. Res. Vol;14, No;7, July 1999
- ⁷⁶ Pelova V., Kynev K., Piperov T., *Luminescence of Y₂O₃:Eu and Gd₂O₃:Eu depending on precursor and activation temperature*. Cryst. Res. Technol. 1998. Vol;33 pp125-128
- ⁷⁷ Delgado da Vila L., Stucchi E.B., Davolos M.R., *Preparation and characterization of uniform, spherical particle of Y₂O₂S and Y₂O₂S:Eu*. J. Mater. Chem., Vol;7, No;10, pp;2113-2116, 1997.
- ⁷⁸ Ranson R.M., Thomas C.B., Craven M.R., *A thin film coating for phosphor thermography*. Meas. Sci. Technol., Vol;9, pp;1947-1950, 1998.
- ⁷⁹ Harazono T., Adachi R., Kijima N., Watanabe T., *¹Y MASNMR in red phosphor, Eu-Doped Y₂O₂S. Assignment of peaks shifted by paramagnetic Eu³⁺, spin lattice relaxation time, and Eu distribution*. Bull. Chem. Soc. Jpn., Vol;72, pp;2655-2664, 1999.
- ⁸⁰ Mannik L., Brown S.K., Campbell S.R., *Phosphor based thermometry of rotating surfaces*. Applied optics, Vol;26, No;18, Sept. 1987.
- ⁸¹ Noel B.W., Borella H.M., Lewis W., Turley W.D., Beshers D.L., Capps G.J., Cates M.R., Muhs J.D., Tobin K.W., *Evaluating thermographic phosphors in an operating turbine engine*. Journal of engineering for gas turbines and power. Vol;113, pp;242-245, April 1991.
- ⁸² Tobin K.W., Allison S.W., Cates G.J., Capps G.J., Beshers D.L., Cyr M., Noel B.W., *High temperature phosphor thermometry of rotating turbine blades*. AIAA Journal Vol;28, No;8, pp;1485-1490, Aug. 1990.
- ⁸³ Noel B.W., Turley W.D., Lewis W., Tobin K.W., Beshers D.L., *Phosphor thermometry on turbine-engine blades and vanes*. Temperature: Its measurement and control in science and industry. Vol;6, No;2, pp;1249-1254, 1992
- ⁸⁴ Dowell L.J., Gillies G.T., Allison S.W., *Measurements of lateral offset power losses in step-index optical fibres scanning point sources*. Optical engineering, Vol;26, No;6, pp;257-551, 1987.
- ⁸⁵ Okuno T., Tanaka K., Koyama K., Namiki M., Suemoto T., *Homogeneous line width of Praseodymium ions in various inorganic materials*. Journal of Luminescence, 1994, Vol;58, pp;184-187

- ⁸⁶ Hess N.J., Schifer D., *Pressure and temperature dependence of laser induced fluorescence of Sm:YAG to 100 kbar and 700 °C and an empirical model*. J. Appl. Phys., Vol:68, No:5, Sept 1990.
- ⁸⁷ McClean I.P., Simons A.J., Thomas C.B., Mutton J.E., *Comparison between thin film and bonded powder phosphors for thermographic sensing in gas turbine engines*. IEEE Transactions on instrumentation and measurement, Vol:49, No:1, Feb. 2000.
- ⁸⁸ Huignard A., Gacoin T., Boilot J.P., *Synthesis and Luminescence properties of colloidal YVO₄:Eu phosphors*. Chem. Mater. Vol:12, pp:1090-1094, 2000.
- ⁸⁹ Allied Scintillation Technologies. www.appscintech.com
- ⁹⁰ Allison S.W., Beshers D.L., Cates M.R., Noel B.W., Turley W.D., *Phosphor thermometry of gas turbine surfaces*. Presented at the international gas turbine and aeroengine congress and exposition, Houston, Texas, June 1995.
- ⁹¹ Camci C., Glezer G., Owen J.M., Pilbow R.G., Syson B.J., *Application of thermographic liquid crystal to rotating surfaces*. Presented at the international gas turbine and aeroengine congress and exposition, Birmingham, UK, June 1996.
- ⁹² AGEMA infrared systems, *Material development using infra-red thermography*. Metallurgia, pp:407-408, Dec. 1995.
- ⁹³ Chyu M.K., Bizzak, D.J., *Two dimensional laser induced fluorescence temperature measurement on a rotating surface*. Visualization of heat transfer processes, Vol:252, 1993.
- ⁹⁴ Goldschmidt R.E., Miller P.C., *Means for achieving accuracy and validity in gas turbine temperature measurement*. ISA paper~94-3026,1994
- ⁹⁵ Sabroske K.R., Gord J.R., *Surface coatings for optical pressure measurements*.
- ⁹⁶ T.A. Misesy, *Powder coatings chemistry and technology*. 1991
- ⁹⁷ Avimo Thin Film Technologies Ltd
- ⁹⁸ Smart R.F., Catherall J.A., *Plasma spraying*. 1972.
- ⁹⁹ D.L. Ruckle, *Thin Solid Films*, 73(1980) 455.
- ¹⁰⁰ McPherson R., *A review of microstructure and properties of plasma sprayed ceramic coatings*. Surface and coating technology, Vol:39/40, pp:173-181, 1989.
- ¹⁰¹ Aihua W., Beidi Z., Zengyi T., Xianyao M., Shijun D., Xudong C., *Thermal shock behaviour of plasma sprayed Al₂O₃-13wt.%TiO₂ coatings on Al-Si alloy influenced by laser remelting*. Surface and coating technology, Vol:57, pp:169-172, 1993.
- ¹⁰² Chuanxian D., Zatorski R.A., Herman H., Ott D., *Oxide powders for plasma spraying – The relationship between powder characteristics and coating properties*. Paper presented at the international conference on metallurgical coatings, San Diego, CA, USA. April 1984.
- ¹⁰³ Meyer P., Muehlberger S., *Historical review and update to the state of the art of automation for plasma coating processes*. Thin solid films, Vol:118, pp:445-456, 1984.
- ¹⁰⁴ Private discussion with Dr. T. Hodges of the mathematical support team at Loughborough University
- ¹⁰⁵ Vandeginste B.G.M., De Galan L., *Critical evaluation of curve fitting in infrared spectrometry*. Analytical Chemistry, Vol:47, No:13, Nov. 1975.
- ¹⁰⁶ Beacham J.R., Andrew K.L., J. Opt. Soc. Am. Vol:61, pp:231, 1971.
- ¹⁰⁷ Pitha J., Jones R.N., Can. J. Chem., Vol:44, pp:3031, 1966
- ¹⁰⁸ Jones R.N. et al., Nat. Res. Counc. Can. Bull. No:11 (1968), No:12 (1968), No:13 (1969)
- ¹⁰⁹ Maddams W.F., *The Scope and Limitations of Curve fitting*. Applied Spectroscopy. Vol:34 No:4, 1980 pp; 245
- ¹¹⁰ Jones R.N., in Infrared, Correlation and Fourier transform spectroscopy. Vol:7 of Computers in chemistry and instrumentation.

- ¹¹¹ Hult T.P., Svensson S.P., Anderson T.G., *A spectrum data processing system*. Computer physics communications, Vol;25, pp;417-431, 1982.
- ¹¹² Akkila T., Lindbald T., Lund-Jean B., Szekely G., Eide A., *A hardware implementation of an analog neural network for gaussian peak fitting*. Nuclear instruments and methods in physics research A327, pp;573-579, 1993.
- ¹¹³ Kakanis P.K., Katsanos A.A., *A computer program for background and multiple peak fitting*. Nuclear instruments and methods in physics research B.3; pp;311-314, 1984.
- ¹¹⁴ Blass, *Luminescent Materials*. 1984
- ¹¹⁵ Pesce, Rosen, Pasby, *Fluorescence Spectroscopy*. 1997
- ¹¹⁶ Jamison S.P., Imbusch G.F., *Temperature dependence of the luminescence from heavily doped Ruby*. Journal of Luminescence, Vol;75, pp;143-147. 1997.
- ¹¹⁷ Andrew Murry, Loughborough University.
- ¹¹⁸ M. Vardelle and J.L. Besson, *Ceram. Int.*, 7(1981) 48.
- ¹¹⁹ UV spectroscopy group, *UV Spectroscopy*, 1993
- ¹²⁰ Ghassemlooy Z., Grattan K.T.V., Lynch D. 1989. Probe design aspects of Ruby decay-time fluorescent sensors. *Rev. Sci. Instrum.* Vol.60.
- ¹²¹ Okuno T., Tanaka K., Koyama K., Namiki M., Suemoto T., Homogeneous line width of Praseodymium ions in various inorganic materials. *Journal of Luminescence*, 1994, Vol;58, pp;184-187
- ¹²² Tiller W.A., *The science of crystallization. Microscopic phenomena and defect generation*. 1991.
- ¹²³ Liu T., Campbell B.T., Sullivan J.P., *Fluorescent paint for measurement of heat transfer in shock – turbulent boundary layer interaction*. Experimental thermal and fluid science, 1995, Vol:10, pp:101-112.
- ¹²⁴ Huber J.P., Carroll B.F., Schanze K.S., Feng Ji H., *Techniques for using pressure sensitive paint in shock tunnel facilities*. Instrumentation in aerospace simulation facilities ICIASF conference, Pacific Grove, California: IEEE, 30, 1997.
- ¹²⁵ Karali T., Rowlands A.P., Townsend P.D., Prokic M., Olivares J. *Spectral comparison of Dy, Tm and Dy/Tm in CaSo₄ thermoluminescent dosimeters*. *Journal physics D:App. Phys.* 31, 1998, pp:754-765.
- ¹²⁶ Izaguirre f., Csanky G., Hawkins G.F. *Temperature measurements with micrometer spatial resolution*. *Rev. Sci. Instrum.* 62(8) Aug 1991. Pp:1916-1920.
- ¹²⁷ Ross D., *Laser light and amplifiers and oscillators*. 1969
- ¹²⁸ Hawkes J.F.B., Wilson J., *Laser principles and applications*. 1995,
- ¹²⁹ Wellesley college Chemistry Department web page
www.wellesley.edu/Chemistry.html
- ¹³⁰ Pictures taken from Your Gemologist web page
<http://www.yourgemologist.com/Spectroscope/spectroscope.html>
- ¹³¹ Maiman T.H., Hosins R.H., Haenens I.J., Asawa C.K., Evtuhov V., *Stimulated optical emission in fluorescent solids. II. Spectroscopy and stimulated emission in ruby*. *Phys. Rev.* Vol;123, pp1151-1157, Aug 1961.
- ¹³² Birnbaum M., Fincher C.L., Machan J., Bass M., *Radiative trapping effects in ruby: 77 to 300 K*. *J. Opt. Soc. Am. B* Vol;3, No;12, Dec 1986.
- ¹³³ picture taken from Wellesley college Chemistry Department web page,
www.wellesley.edu/Chemistry/amanda4b.html
- ¹³⁴ Code of safe practice application of powder coatings by electrostatic spraying, 1980.
- ¹³⁵ Augousti A.T., Grattan K.T.V., Palmer A.W., *Visible-LED Pumped fiber-optic temperature sensor*. *IEEE Transactions on instrumentataion and measurement*. Vol;37, No;3 pp;471. 1988

- ¹³⁶ Zhang Z., Grattan K.T.V., Palmer A.W., *Thermal Characteristics of alexandrite fluorescence decay at high temperatures, induced by a visible laser diode emission*. Journal of applied physics. Vol;73, No;7 pp;3493, 1993
- ¹³⁷ Chen C.H., Chen Y.F., *Strong and stable visible luminescence from Au passivated porous silicon*. Applied physics letters. Vol;75, No;17, pp;2560, 1999.
- ¹³⁸ M^cCormack J.S., *Remote optical measurement of temperature using luminescent materials*. Electronics letters, Vol;17, No;18, pp;630. 1981.
- ¹³⁹ Schrum K.F., Williams A.M., Haerther S.A., Ben-Amtoz D.. 1994. *Molecular fluorescence thermometry*. Analytical Chemistry, Vol-66 No17.
- ¹⁴⁰ Karali T., Rowlands A.P., Townsend P.D., Prokic M., Olivares J. *Spectral comparison of Dy, Tm and Dy/Tm in CaSO₄ thermoluminescent dosimeters*. Journal physics D:App. Phys. 31, 1998, pp:754-765.
- ¹⁴¹ Kobayashi T., Klemn W., Shockey D.A., *Development of a high-resolution thermoprobe*. Proceedings of the 29th international instrumentation symposium, Albuquerque, USA. May 1983.
- ¹⁴² Bell J., *Organic groups excite rare-earth emissions*. OLE pp;21-24 March 1999
- ¹⁴³ Davidson A.G., Fadiran E.O., *Effect of variation of temperature on second-derivative fluorescence spectra, Part 1*. Analyst. April 1988, Vol;113 pp;533.
- ¹⁴⁴ Davidson A.G., Fadiran E.O., *Effect of variation of temperature on second-derivative fluorescence spectra, Part 2*. Analyst. April 1988, Vol;113 pp;537.
- ¹⁴⁵ Davidson A.G., Fadiran E.O., *Effect of variation of temperature on second-derivative fluorescence spectra, Part 3*. Analyst. April 1988, Vol;113 pp;543.
- ¹⁴⁶ Mori N., Takahashi H., 1987. *Raman and reflection spectra of pyrite system under high pressure*. High pressure reaserach in mineral physics. pp:341-345.
- ¹⁴⁷ Campbell B., *Temperature sensitive fluorescent paints for aerodynamics applications*, MS Thesis, Purdue Uni, W Lafayette IN. 1993
- ¹⁴⁸ Campbell B., Liu T., Sullivan J., *Temperature sensitive fluorescent paint systems*. AIAA paper 94-2483. 1994
- ¹⁴⁹ Kolodner P., Katzir A., Hartsough N., *Non-contact surface temperature measurement during reactive-ion etching using fluorescent polymer films*. Appl. Phys. Lett. Vol;42, No;8, pp;749, April 1983
- ¹⁵⁰ Liu T., *Applications of temperature-sensitive luminescent paints in aerodynamics*. PhD Thesis Purdue Uni, W Lafayette IN. 1996
- ¹⁵¹ Asai K., Kunimasu T., Iijima Y., *Visulation of the quiet test region in a supersonic wind tunnel using luminescent paint*. Instrumentation in Aerospace simulation facilities ICIASF conf. Pacific Grove, California: IEEE 1997.
- ¹⁵² Kolodner P., Tyson J.A., *Remote thermal imaging with 07 μ m spatial resolution using temperature-dependent fluorescent thin films*. Appl. Phys. Lett. Vol;42, No;1, pp;117, Jan 1983
- ¹⁵³ Jokilk R.G., Horvath J.J., Semerjian H.G., *Temperature measurements in flames using thermally assisted laser induced fluorescence of GA*. Applied optics Vol;30, No;12, pp;1497 1991.
- ¹⁵⁴ Polimeni A., Patane A., henini M., Eaves L., Main P.C., *Temperature dependence of the optical properties of InAs?Al_yGa_{1-y}As self organized quantum dots*. Physcial review B. Vol;59, No;7, pp;5064, 1999.
- ¹⁵⁵ Patane A., Henini M., Polimeni A., Eaves L., Main P.C., Al-Khafaji M., Cullis A.G., *Luminescence tuning of InAs/GaAs quantum dots grown on high-index planes*. Superlattices and Microstructures, Vol;25, No;1/2, 1999.
- ¹⁵⁶ Noel B.W., et al. *Proposed method for remote thermometry in turbine engines*. AIAA paper 85-1468. 1985

- ¹⁵⁷ Izaguirre f., Csanky G., Hawkins G.F. *Temperature measurements with micrometer spatial resolution*. Rev. Sci. Instrum. 62(8) Aug 1991. Pp:1916-1920.
- ¹⁵⁸ Cattafesta & Moore. *Uncertainty estimates for luminescent temperature sensitive paint intensity measurements*. AIAA paper 95-2193. 1995
- ¹⁵⁹ Mahould A.G., Arafah D-E., Sharabati H., *Characterization of TL-glow curves resulting from sensitized TLD-100*. J. Phys. D: Appl. Phys. Vol;31, pp;224, 1998.
- ¹⁶⁰ M^cLachlan B.G., Bell J.H., Gallery J., Gouterman M., Callis J.. *Boundary layer transition detection by luminescent imaging*. AIAA paper 93-0177. 1993
- ¹⁶¹ Zhang Z., Grattan K.T.V., Palmer A.W., 1992. *Fiber optic temperature sensor based on the cross referencing between blackbody radiation and fluorescence lifetime*. Rev. Sci. Instruments 63(5).
- ¹⁶² Fischer S., Hanne G.F., Bartschat K., Zeman V., Srivastava R., *Study of electron-impact excitation of metastable Ne(2p⁵3s³P₂) substrates using laser induced fluorescence*. J. Phys. B:At. Mol. Opt. Phys. Vol;32, pp;4447, 1999.
- ¹⁶³ Margalith E., Deguchi Y., Nihida H., Hanson R.K., *Laser induced fluorescence fires up engine research*. Photonic spectra, pp;94, March 1997.
- ¹⁶⁴ Goss K.P., M^cKenzie R.L., *Measurements of Fluctuating temperatures in a supersonic turbulent flow using laser induced fluorescence*. AIAA Vol;23., No;12, pp;1932, 1985
- ¹⁶⁵ Margalith E., Deguchi Y., Nihida H., Hanson R.K., *Laser induced fluorescence fires up engine research*. Photonic spectra, pp;94, March 1997.
- ¹⁶⁶ Dale G., Baron A., Tyler C., Mastrocola V., *Global luminescent lifetime measurements on a body in free fall*. Instrumentation in aerospace simulation facilities ICIASF conf. Pacific Grove, California: IEEE 1997.
- ¹⁶⁷ Bassett W.A., Weathers M.S., *Temperature measurement in a laser heated diamond cell. High pressure research in mineral physics*. pp;129-133. 1987
- ¹⁶⁸ Clausen S., Morgenstjerne A., R athmann O., *Measurement of surface temperature and emissivity by a multitemperature method for a fourier transform infrared spectrometers*. Applied Optics Vol;35, No;28, pp;5683, 1996.
- ¹⁶⁹ Zhao H. Collings N., Ma T., *Two dimensional temperature distributions of combustion chamber surfaces in a firing spark ignition engine*. Proceedings of the insitution of mechanical engineers. Part D: Journal of automobile engineering. Vol;208 pp;99, 1994.
- ¹⁷⁰ Sullivan J.P., *Surface temperature measurement using fluorescent molecules* 1991 from refernce 42
- ¹⁷¹ Pringsheim, *Fluorescence and phosphorescence*. 1965
- ¹⁷² Grattan K.T.V., Selli R.K., Palmer A.W., *Ruby fluorescence wavelength division fiber optic temperature sensor*. Review of scientific instruments Vol;59, No;2, pp;256, 1988.
- ¹⁷³ Ross D., *Laser light and amplifiers and oscillators*. 1969
- ¹⁷⁴ Foreman R.A., Piermarini G.J., Barnett J.D., *Pressure measurement made by the utilization of ruby-sharp line luminescence*. Science Vol;176, pp;284, 1972
- ¹⁷⁵ Chai M., Brown J.M., *Effects of static non-hydrostatic stress on the R lines of ruby single crystals*. Geophysical research letters, Vol;23, No;24, pp;3539-3542. Dec. 1996.
- ¹⁷⁶ Wieder H., *Thermal profile measurements with submicrometer resolution*. Laser focus, May 1975.
- ¹⁷⁷ Flury A., *Measuring surface temperature with phase change devices*. Machine design, Aug 1995.
- ¹⁷⁸ Alaruri et al. *Development of a fiber optic probe for termographic phosphor measurements in turbine engines*. Optics and lasers in eng Vol;22, pp17-31. 1995

¹⁷⁹ Heinz D.L., Jean Loz R., 1987. *Temperature measurements in the Laser-heated diamond cell*. High-pressure research in mineral physics. pp:113-127

¹⁸⁰ Trojanowski A., Macdougall D., Harding J., *An improved technique for the experimental measurement of specimen surface temperature during hopkinson bar tests*. Meas, Sci. Technol. Vol;9 1998.

¹⁸¹ PeakAlyze User guide

